SEA-LEVEL CHANGE AND DELTA GROWTH: FRASER DELTA, BRITISH COLUMBIA

by

Harry F. L. Williams
B.Sc (HONS) Plymouth Polytechnic 1980
M.Sc University of British Columbia 1983

THESIS SUBMITTED IN PARTIAL FULFILLMENT OF
THE REQUIREMENTS FOR THE DEGREE OF
DOCTOR OF PHILOSOPHY
in the Department
of
Geography

SIMON FRASER UNIVERSITY
July 1988

APPROVAL

Name: Harry F. L. Williams

Degree: Ph.D Geography

Title of thesis: Sea-Level Change And Delta Growth: Fraser Delta, British Columbia

Examining Committee:

Chairman: Dr. L. Evenden

Dr. M. C. Roberts
Senior Supervisor

Dr. E. J. Hickin

Dr. I. Hutchinson

Dr. J. L. Luternauer
Geological Survey of Canada

Dr. J. D'Auria
Department of Chemistry

Dr. D. Smith
External Examiner
Department of Geography
University of Calgary

Date Approved: July 7, 1988

PARTIAL COPYRIGHT LICENSE

I hereby grant to Simon Fraser University the right to lend my thesis, project or extended essay (the title of which is shown below) to users of the Simon Fraser University Library, and to make partial or single copies only for such users or in response to a request from the library of any other university, or other educational institution, on its own behalf or for one of its users. I further agree that permission for multiple copying of this work for scholarly purposes may be granted by me or the Dean of Graduate Studies. It is understood that copying or publication of this work for financial gain shall not be allowed without my written permission.

Title of Thesis/Project/Extended Essay

Sea-Level Change and Delta Growth: Fraser River Delta, British Columbia

Author: _____
(signature)

Harry Frederick Leonard Williams
(name)

July 13, 1988
(date)

ABSTRACT

The depositional framework of the northern part of the Fraser Delta (Lulu Island) was investigated using a series of drill cores, in order to determine the manner in which aggradation occurred on the delta in response to a mid-Holocene rise in sea-level.

Selected contemporary depositional environments on Lulu Island were characterised in terms of their lithology, pollen spectra and microfossil content, in order to establish a comparative framework for the paleoenvironmental interpretation of subsurface facies. A chronology of the evolution of Lulu Island was developed, based on C dating, the identification of tephra layers encountered in drill cores and stratigraphic correlation.

The response of the deltaic system to the rise in sea-level was found to have taken the form of a depositional regression, rather than a marine transgression. Deposition was sufficient to maintain seaward progradation, even during the period of rising sea-level. At the same time, rising base level triggered aggradation of the delta and the adjoining Fraser River floodplain. Facies incorporated into the structure of the delta during this stage of its growth are of the same internal character and vertical order as their modern analogues, but may be of considerably greater vertical extent.

Former sea-levels were established within the body of the

delta by a lithologic transition from organic-rich silt of tidal marsh origin, to silts and sands of intertidal origin. This method of identifying former sea-levels, combined with the chronological control provided by this study, enabled a revised sea-level curve to be developed for the Fraser Lowland. The revised curve contains a hitherto unknown stillstand occurring at 6000 yr BP and indicates that the sea did not stabilize at its present level until 2250 yr BP.

Details of the Fraser Delta's Holocene progradation rates and vertical accretion rates calculated in this study, are used to estimate the Fraser River's sediment discharge rates during the last 9000 years. The estimate, although only a first approximation, suggests that the Fraser River's sediment discharge has been stable for the last 6000 years and was higher in the early Holocene, which is in accordance with the paraglacial concept.

The results from the Fraser Delta serve as a model for the depositional regression style of coastal aggradation.

DEDICATION

This work is dedicated to my wife, Kathy, for her moral support, limitless encouragement and divine patience.

ACKNOWLEDGEMENTS

I would like to thank my senior supervisor, Mike Roberts, for guidance, encouragement and for always willing to "give it our best try". John Luternauer provided valuable advice and assistance throughout the course of this study. I extend my thanks to my other committee members, Ted Hickin and Ian Hutchinson, for their helpful reviews of this thesis. The study would not have been possible without the hard work of my field assistants and drill crew volunteers - Greg Gjerdalen, Nick Kiniski, John White, Nancy Hori, Harry Jol, Bill Ophoff, Butch Morningstar, Valerie Cameron and Cliff Roberts. Bruce Cameron, Richard Hebda and Geoff Quickfall are thanked for their help with the paleontological studies. John Clague offered many useful comments as the work progressed. John D'Auria, Mike Cackett and Karen Moore provided guidance in the XES study. Bryan Kern and Bob Gerath are thanked for their assistance in obtaining Dept. of Highways materials. The study was funded by an Energy, Mines and Resources research grant awarded to Dr. M. C. Roberts and a Geological Society of America dissertation grant awarded to the author.

TABLE OF CONTENTS

LIST OF TABLES

LIST OF FIGURES

SECTION ONE

INTRODUCTORY MATERIAL

CHAPTER ONE

INTRODUCTION

1.1 INTRODUCTION

The main goal of this study is to determine the manner in which aggradation occurred on part of the Fraser Delta in response to a mid-Holocene rise in sea level. Particular emphasis will be given to changes in the location of the delta's topset depositional environments and the nature of the resulting stratigraphic record.

1.2 DELTAS: DEPOSITIONAL RESPONSE TO CHANGING SEA LEVEL

Attempts to model the sedimentary framework of deltas have progressed from the pioneering work of Gilbert's (1890) classical 3-tier depositional system (Fig. 1.1), to the more detailed three dimensional arrangement of facies in the modern Mississippi "bird's foot" delta (e.g. Fig. 1.2), which became the standard for comparison during the 1950's and 60's.

However, with increasing knowledge of deltaic deposits resulting from the rapid expansion of subsurface investigations in the 1950's, it became apparent that considerable variability existed in both the overall morphology of deltas and in the nature and arrangement of their constituent facies (Frazier, 1967; Wright and Coleman, 1973; Galloway, 1975). It was

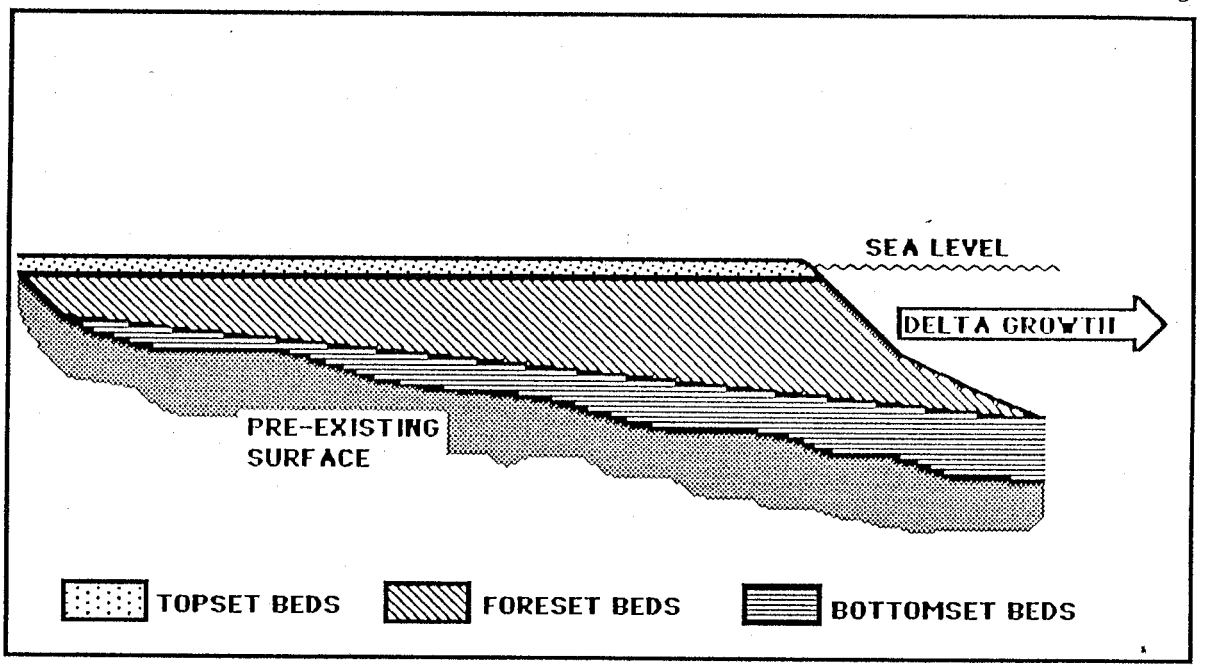

Figure 1.1 The Gilbert-type 3-tier deltaic depositional system (modified from Gilbert, 1890)

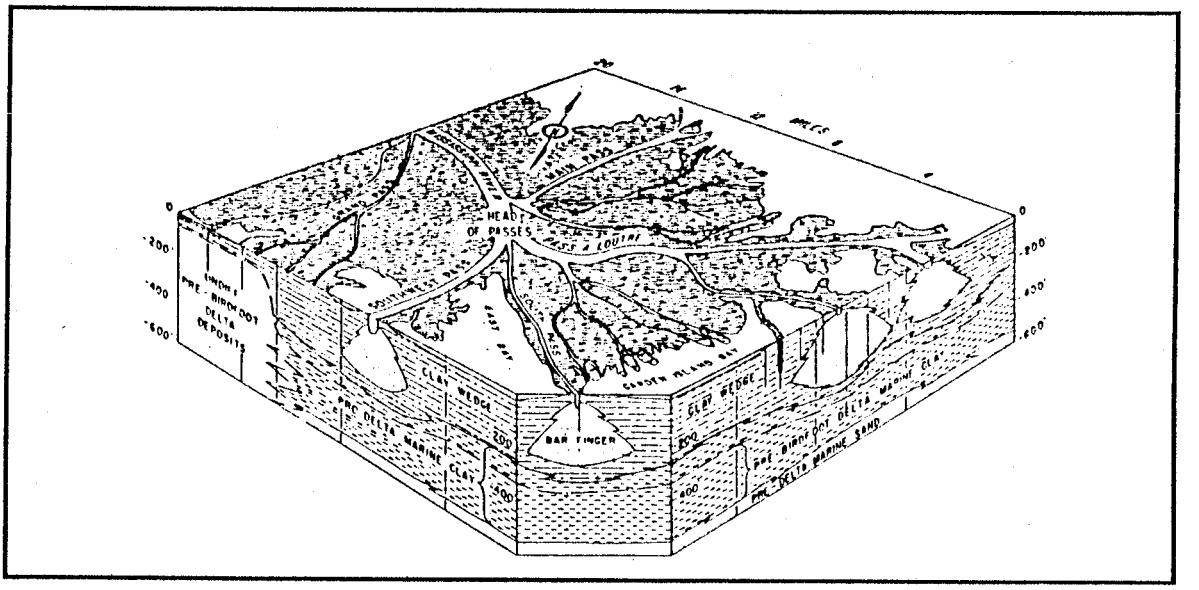

Figure 1.2 Sedimentary framework of the modern Mississippi Delta (after Fisk et al., 1954)

recognized that the "Gilbert" and "Mississippi" models were just two examples of a broader spectrum of deltaic depositional styles.

Consequently, much of the recent research concerning deltaic systems has focused on attempts to classify deltas in terms of the various factors which influence their morphology and depositional framework, in order to develop a comprehensive range of delta models (Coleman and Wright, 1977).

A consistent theme in deltaic modelling has been the relative magnitude of fluvial and marine processes. Models have been developed that reflect wave, tide or river dominance, in terms of the morphology of deltaic sand bodies (Coleman and Wright, 1971; 1973; 1975); the kind and abundance of specific process-linked facies (Scott and Fisher, 1969; Galloway, 1975); and, characteristic vertical facies sequences (Scott and Fisher, 1969; Coleman and Wright, 1975; Miall, 1984a).

A fundamental and unifying feature of deltaic depositional models is that the spatial arrangement of depositional environments on the deltaic plain is essentially controlled by the position of the delta's shorezone, where much of the interaction of fluvial and marine processes takes place.

The deltaic plain can be subdivided into three physiographic regions on the basis of shorezone location (Fig. 1.3): the subaerial upper deltaic plain, above the area of significant marine influence and consequently dominated by fluvial depositional environments; the lower deltaic plain, or intertidal zone, where fluvial sediment is subject to wave and

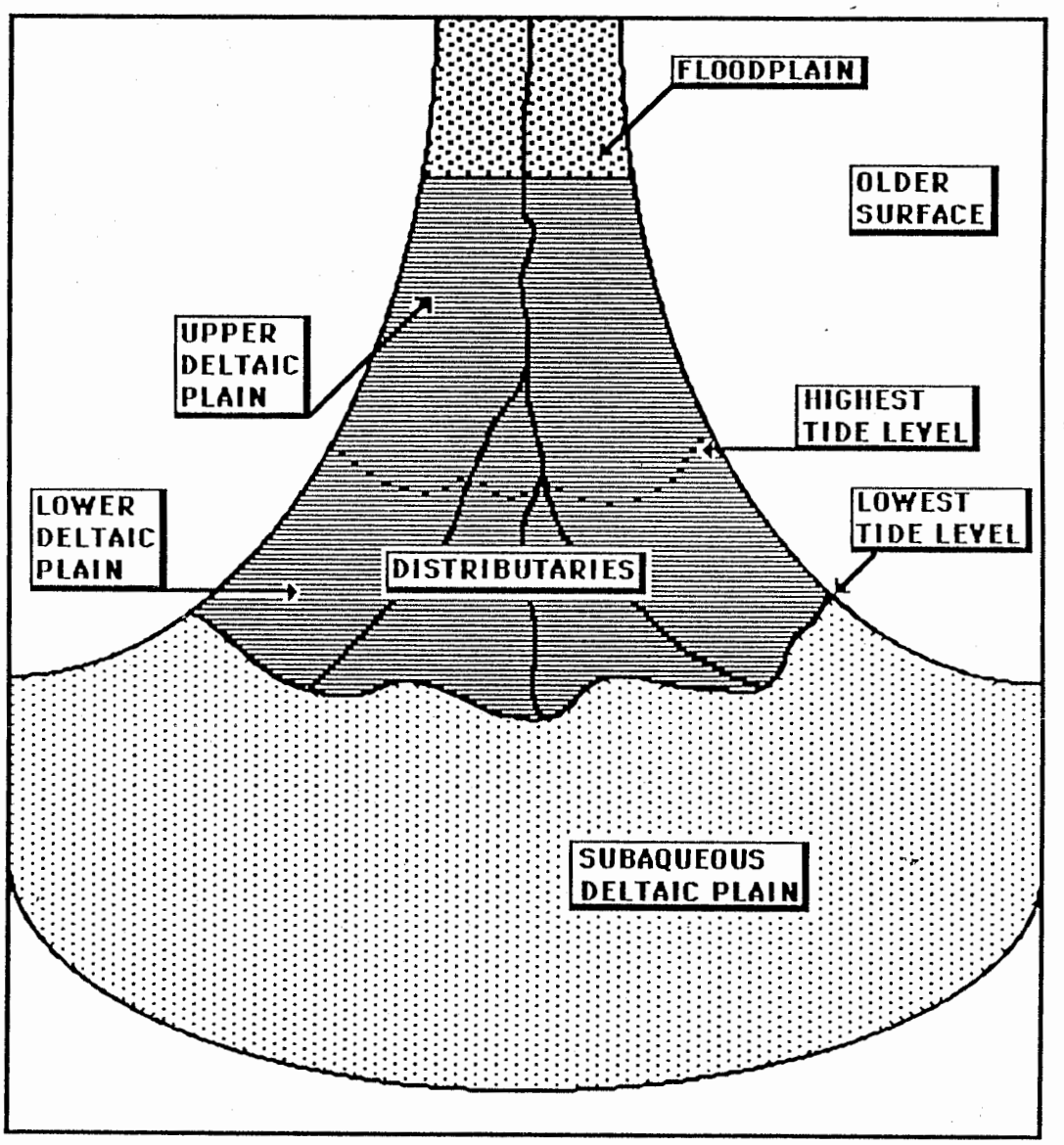

Figure 1.3 Components of the deltaic plain
(modified from Coleman and Prior, 1982)

tide modification; and the subaqueous deltaic plain, below lowest normal tide level and dominated by marine environments of deposition (Coleman and Prior, 1982).

An important consequence of this zonation of deltaic geomorphology is that changes in shoreline location are accompanied by the migration of the delta's depositional environments. In an actively prograding delta, there is a seaward migration of the shoreline, with the result that deposits of the lateral succession of depositional environments are incorporated into a vertical gradational sequence of facies (Fig. 1.4).

Landward migration of a shoreline during a marine transgression may generate more complex facies sequences than those resulting from seaward progradation. Scruton (1960) and van Straaten (1960) proposed that repeated progradation, abandonment, subsidence and reactivation of a deltaic lobe, would result in repetition of the deltaic facies sequence in vertical profile, with each cycle unconformably overlying the one below (Fig. 1.5).

Curray (1964), Curtis (1970) and Vail et al. (1977) produced hypothetical models of the depositional response of deltas to a relative rise in sea level. The basis of these models is the relative balance between the rate of deltaic deposition and the rate of sea level rise. It is this balance which determines whether the delta's depositional environments move landward in a marine transgression, remain geographically stationary, or move seaward in a depositional regression

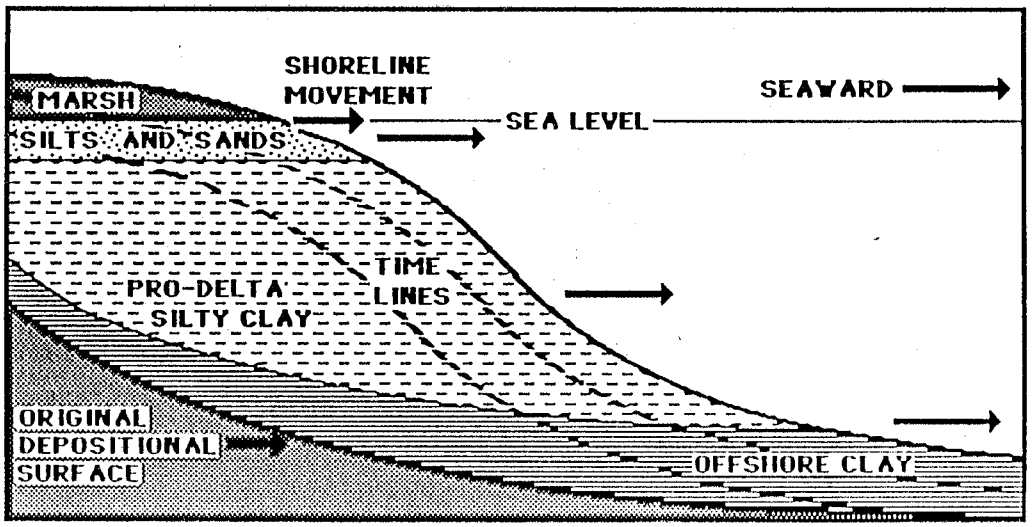

Figure 1.4 Seaward migration of depositional environments in a prograding delta (modified from Scruton, 1960)

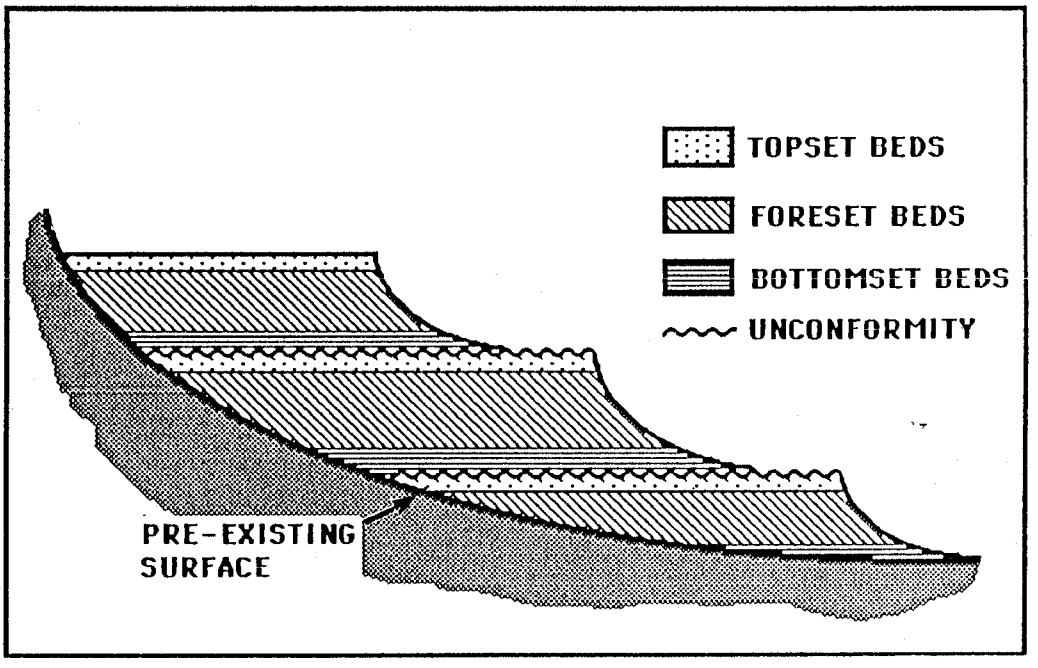

Figure 1.5 Cyclic deltaic sedimentation (modified from van Straaten, 1960)

(Curray, 1964). In each case, a distinctive vertical facies sequence is produced, in which the vertical order, extent and nature of contact between facies reflects the depositional response to the rise in sea level (Fig. 1.6).

Thus, by the mechanisms of shoreline regression or transgression, deposits formed in the delta's various depositional environments may be superimposed one on top of another, building up a vertical facies sequence which is incorporated into the sedimentary framework and serves as a record of the depositional history of the deltaic system.

Consequently, examination of a delta's sedimentary structure, in terms of the type of facies present, the order of facies in the vertical profile and the nature of contact between successive facies, may provide valuable insights into the depositional evolution of the deltaic system.

1.3 RATIONALE AND BASIS OF THE RESEARCH

The identification of facies and the use of facies models is now one of the most active areas in the general field of sedimentology (Walker, 1984; Miall, 1984b). A considerable amount of research has centered on the development of facies models in the form of idealized vertical sequences of facies, characteristic of specific depositional systems (Coleman and Wright, 1975; Cant and Walker, 1976; Miall, 1978).

Attempts to model the vertical facies succession in deltas began with Gilbert's (1890) 3-tier depositional system (Fig. 1.1). Although based on the coarse-textured, pro-glacial deltas

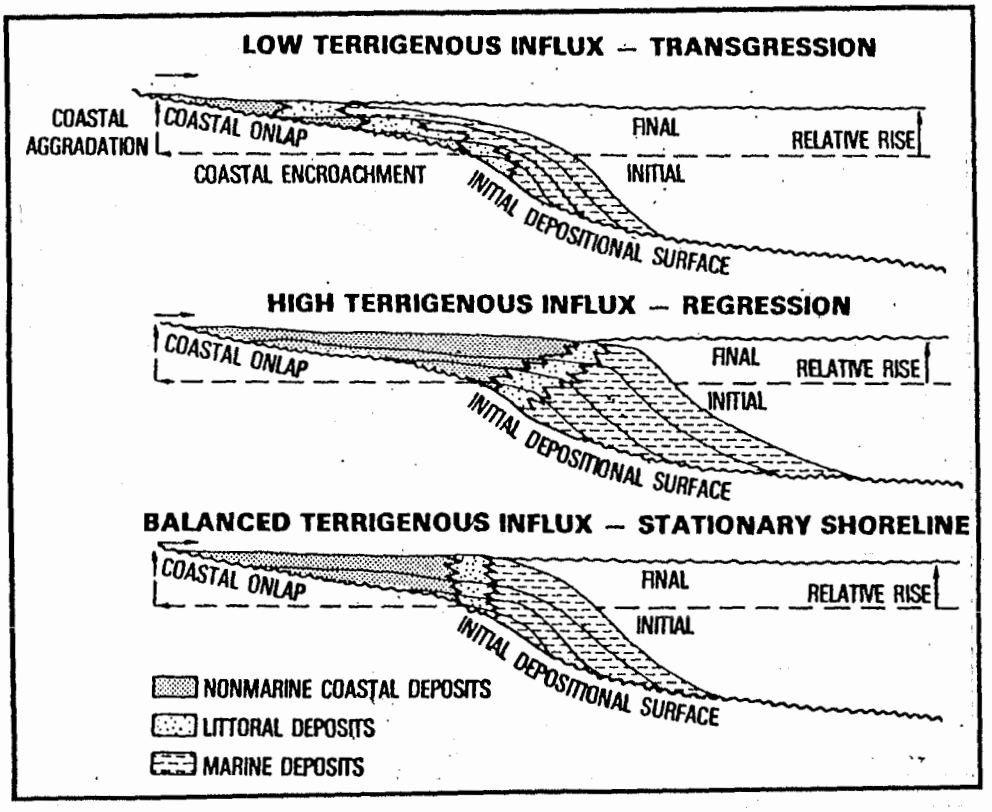

Figure 1.6 Stratigraphic response of deltas to a rise in sea level (after Vail et al., 1977)

of Lake Bonneville, the generalized features of this model are still widely applicable today to many deltaic systems. In general, the model consists of a gradational vertical succession of facies, from progressively shallower marine deposits, through intertidal sediments and culminating in a cap of terrestrial deposits.

The generalized "Gilbert" model serves to illustrate two important and interrelated principles of delta construction; firstly, the model conforms to Walther's (1894) law of facies superimposition, wherein laterally adjacent facies are superimposed vertically as the delta progrades seaward; and, secondly, sea level is shown to be the major control on the vertical positioning of facies within the body of the delta.

It follows that changes in sea level are accompanied by a consequent displacement of the facies sequence within the stratigraphic record. During a relative rise in sea level, the direction of such a displacement and nature of the resulting facies sequence will be dependent on the balance between the rate of sea level rise and the rate of deltaic deposition (Curray, 1960; Curtis, 1970; Vail et al., 1977) (Fig. 1.6).

To illustrate how deltaic development might be affected by changes in the relative balance between sea level rise and deltaic deposition, three contrasting hypothetical models have been developed and are described below;

1) The rate of sea level rise exceeds the rate of deposition (Fig. 1.7a).

A rapid marine transgression occurs, accompanied by the landward migration of depositional environments. As a result, the facies sequence will be repeated in a cyclic fashion, lying unconformably on the older surface below.

2) Deposition and sea level rise occur at the same rate (Fig. 1.7b).

A lateral migration of the shoreline does not occur. Each depositional environment aggrades vertically. Facies incorporated into the stratigraphic record during this period attain a greater thickness, than would be acquired during deltaic progradation under stable sea level conditions.

3) Deposition occurs more rapidly than the rate of sea level rise (Fig. 1.7c).

The shoreline and the delta's depositional environments migrate seaward in a depositional regression. Each depositional environment aggrades vertically and progrades seaward at the same time. The resultant stratigraphic record will show a vertical shift of the facies sequence over a horizontal distance determined by the deltaic progradation rate during the period of rising sea level.

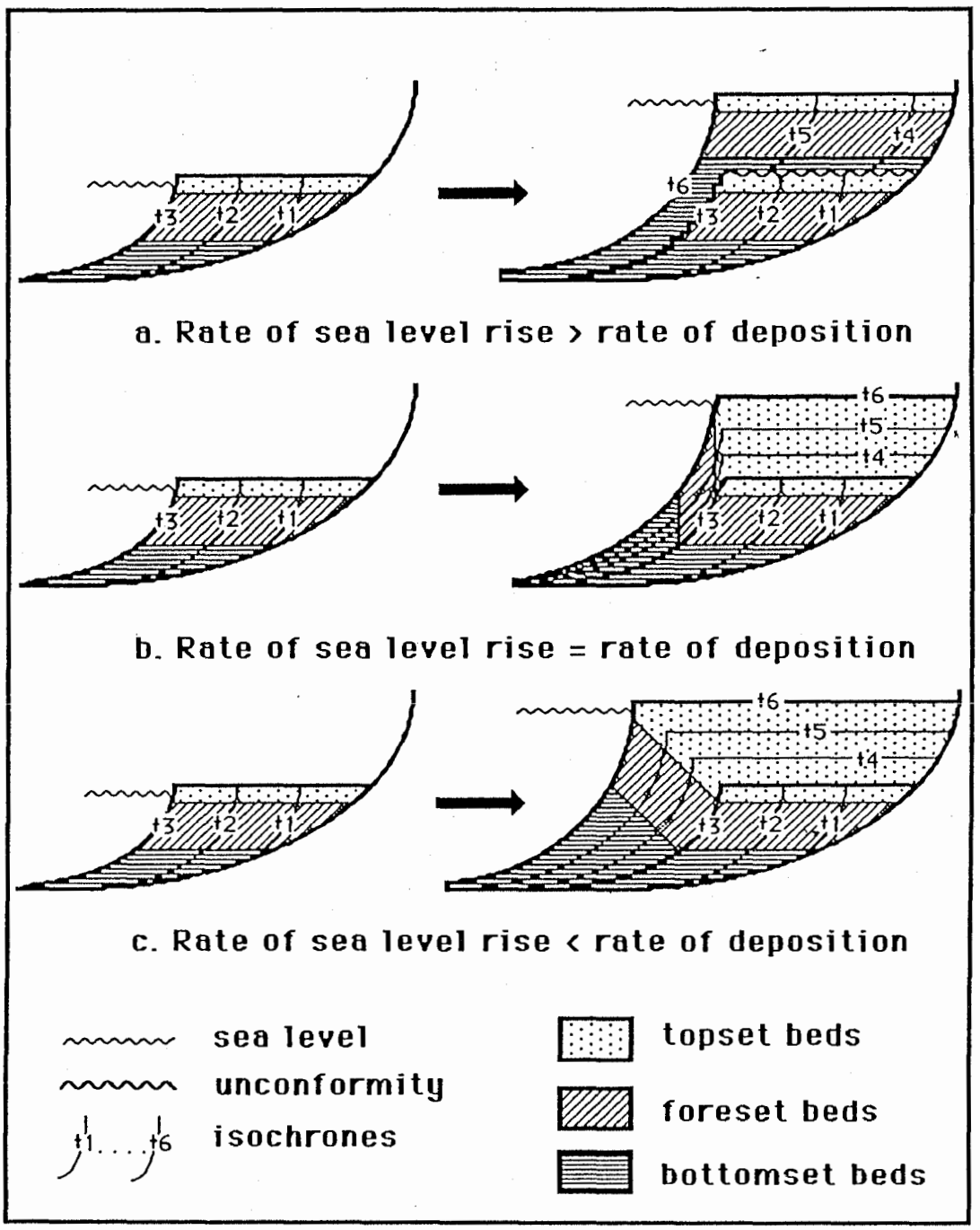

Figure 1.7 Hypothetical models of delta development during a period of rising sea level (modified from Curtis, 1970; Vail et al, 1977)

The Fraser Delta, on the southwest coast of British Columbia, provides an opportunity to study the relationship between Holocene sea-level fluctuations and the depositional response of a delta. Coastal British Columbia has a history of complex sea level changes during the Holocene period (Mathews et al., 1970; Clague, 1981; Clague et al., 1982). Many of these changes were associated with isostatic adjustments following retreat of ice sheets at the end of the late Wisconsinan Fraser Glaciation (Clague, 1983).

The Fraser Lowland region is known to have experienced a sea level rise of approximately 12 metres during early to mid Holocene time (Clague et al., 1983). At the commencement of this period, the Fraser River floodplain was in place to the east of New Westminster and growth of the Fraser Delta westward into the Strait of Georgia was underway (Mathews and Shepard, 1962).

The delta aggraded in response to the rise in sea level. However, the manner by which aggradation occurred, whether by renewed deltaic progradation following a marine transgression (Fig. 1.7a), by vertical accretion about a geographically stable shoreline (Fig. 1.7b), or by vertical and lateral accretion in a depositional regression (Fig. 1.7c), remains unknown.

1.4 OBJECTIVES OF THE STUDY

The purpose of this research is to determine the manner in which aggradation occurred over part of the Fraser Delta in response to the mid-Holocene rise in sea level. This will be achieved by establishing the depositional environments and

chronology of deposits underlying Lulu Island (the northern portion of the delta).

It is anticipated that interpretation of the delta's depositional evolution in terms of the hypothetical framework in Figure 1.7, will not only provide information on the delta itself, but also information of a wider, regional significance. This includes:

(i) a better understanding of the depositional evolution of the Fraser Delta and the adjoining Fraser River floodplain.

(ii) details of the Fraser Delta's vertical sedimentation and lateral progradation rates during the Holocene.

(iii) a more precise and detailed Holocene sea level curve for the Fraser Lowland region.

(iv) some insights into the Fraser River's post-glacial sediment discharge rates.

1.5 METHODOLOGICAL APPROACH

In order to achieve the primary objective of this research it will be necessary to establish paleoenvironmental interpretations for the facies present in the subsurface of Lulu Island. Facies are sedimentary units distinguished by their lithologic, structural and organic characteristics. The paleoenvironmental interpretation of a subsurface facies is based on a comparison of the external relations and internal character of the facies with those of a deposit of a known environment, particularly contemporary depositional environments

(DeRaff, et al., 1965).

Selected characteristics of contemporary depositional environments, usually some combination of lithologic and biologic attributes, can be used to construct an interpretive framework (Middleton, 1978; Miall, 1984).

The use of a range of attributes, both lithologic and biologic, has the advantage of providing a broad basis for the interpretive framework. This approach ensures a greater confidence in paleoenvironmental interpretations applied to subsurface facies. It also reduces the chance of misinterpretation through overreliance on a particular aspect of the subsurface deposit, which may not be unique to one particular environment of deposition (Walker, 1984).

In this study, both lithologic and biologic attributes of contemporary depositional environments will be used to construct an interpretive framework. The lithologic attributes of mean grain size and sorting, sedimentary structures and organic matter content were selected on the basis of their ease of recognition, both in contemporary environments and core samples.

In addition to these lithologic characteristics, two types of microfossil were selected for incorporation into the interpretative framework - pollen grains and foraminifera tests. Both have previously been successfully applied to the interpretation of depositional environments within drill cores. Hebda (1977) used pollen analysis of core samples in a study of the paleoecology of a raised peat bog on the Fraser Delta. Foraminifera tests have been used to identify tidal marsh

deposits and to locate former sea levels in drill cores from coastal deposits in California (Scott, 1977) and Atlantic Canada (Scott and Medioli, 1980a). Foraminifera tests have also been found in drill cores from the southern Fraser Delta (Roberts et al., 1985).

Consequently, the research is divided into three main areas;

1) the biosedimentological characterisation of contemporary topset depositional environments on Lulu Island. These data will be used on a comparative basis to interpret facies encountered in drill cores.
2) the establishment of the sedimentary framework of Lulu Island on the basis of vertical facies sequences encountered in drill cores.
3) the establishment of a chronology for the subsurface deposits. This will be based on radiocarbon dating of selected organic samples and the identification of tephra layers encountered in drill cores.

1.6 ORGANIZATION OF THE TEXT

The text is organized into four sections containing nine chapters, as follows (Fig. 1.8):

SECTION ONE: INTRODUCTORY MATERIAL

CHAPTER 1: INTRODUCTION. This chapter will provide a general introduction to the topic and objectives of the research.

CHAPTER 2: THE STUDY AREA. A description of the study area will be presented and previous work on the structure and evolution of

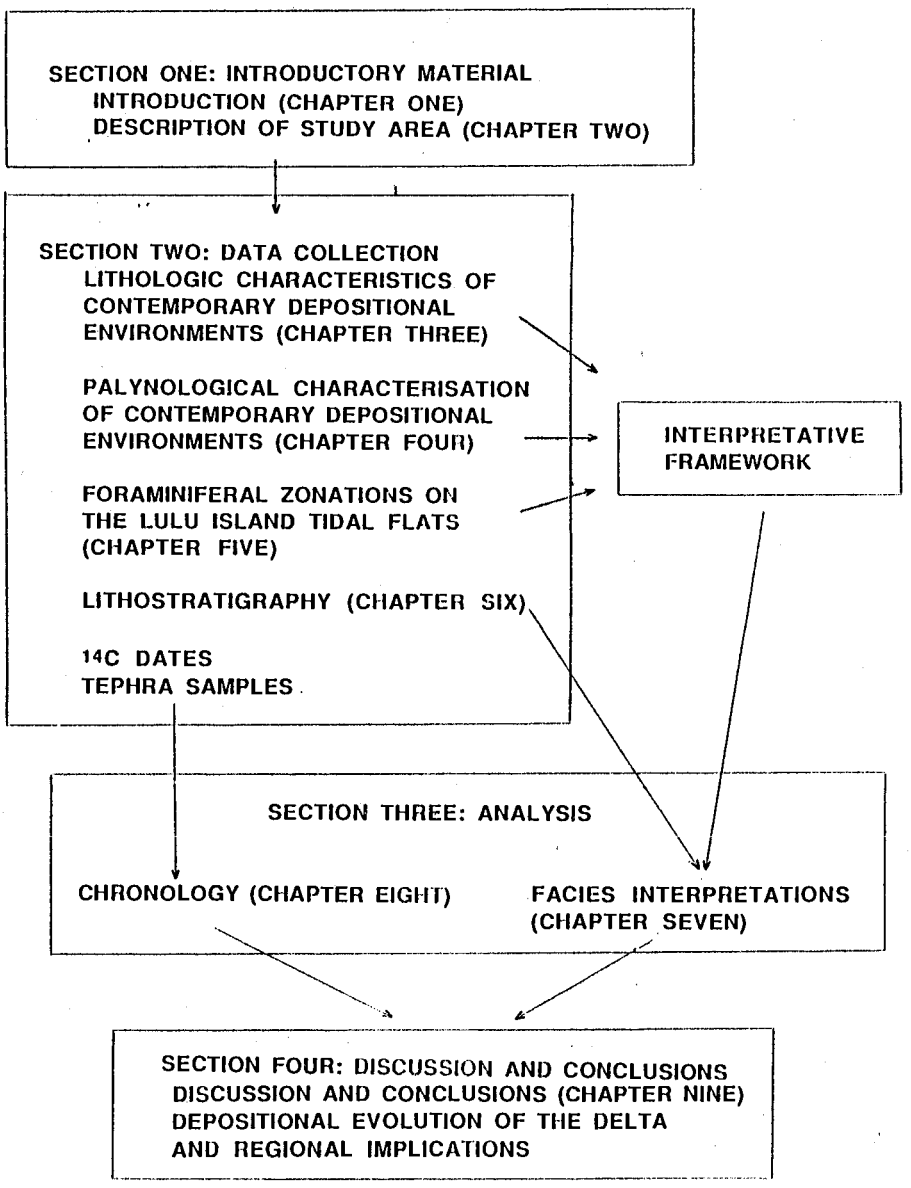

Figure 1.8 Flowchart outlining organization of the research and text

the Fraser Delta will be reviewed.

SECTION TWO: CONSTRUCTION OF INTERPRETATIVE FRAMEWORK AND SUBSURFACE DATA COLLECTION

This section covers all aspects of field data collection. The section begins with the characterisation of contemporary depositional environments in order to a develop a comparative framework for the interpretation of subsurface facies. This consists of:

CHAPTER 3: LITHOLOGIC CHARACTERISTICS OF CONTEMPORARY DEPOSITIONAL ENVIRONMENTS.

CHAPTER 4: PALYNOLOGICAL CHARACTERISATION OF CONTEMPORARY DEPOSITIONAL ENVIRONMENTS.

CHAPTER 5: FORAMINIFERAL ZONATIONS ON THE LULU ISLAND TIDAL FLATS.

The remainder of section two concerns the collection of subsurface data to establish the lithostratigraphy of Lulu Island and to obtain samples for ^{14}C dating, tephra, grain size, palynological and microfossil analyses. This is covered by:

CHAPTER 6: SUBSURFACE DATA COLLECTION.

SECTION THREE: ANALYSIS

This section concerns the environmental interpretation of the subsurface deposits established in Chapter 6, on the basis of the interpretive framework developed in section two (based on the characteristics of contemporary depositional environments

established in chapters 3, 4 and 5). This is covered in:

CHAPTER 7: FACIES INTERPRETATIONS

This section also concerns the development of a chronology for Lulu Island, based on ^{14}C dating and identification of tephra encountered in drill cores using XES analysis. This is presented in:

CHAPTER 8: CHRONOLOGY.

SECTION FOUR: DISCUSSION AND CONCLUSIONS

CHAPTER 9: DISCUSSION AND CONCLUSIONS. In this chapter, the depositional response of the delta to the rise in sea level will be examined and regional implications will be discussed. The major findings of the study will be summarized at the end of the chapter.

CHAPTER TWO

THE STUDY AREA

This chapter presents a description of the physiographic setting of the Fraser Delta and the nature and extent of its contemporary depositional environments. Previous work on late Quaternary sea-level fluctuations in the study area and on the structure and evolution of the delta, is briefly reviewed.

2.1 PHYSIOGRAPHY

The Fraser Delta is located at the western edge of the Fraser Lowland where the Fraser River enters the Strait of Georgia, a semi-enclosed marine basin lying between Vancouver Island and mainland British Columbia (Fig. 2.1).

The subaerial portion of the delta covers some 400 km^2 and extends from its apex in the vicinity of New Westminster 15-23 km west and south to meet the sea along a perimeter approximately 40 km in length.

The delta's four main distributary channels all discharge into the Strait of Georgia across the western delta front. The southern delta front has remained relatively inactive since the delta joined up to the former island of Point Roberts and cut off the supply of Fraser River sediment entering Boundary Bay.

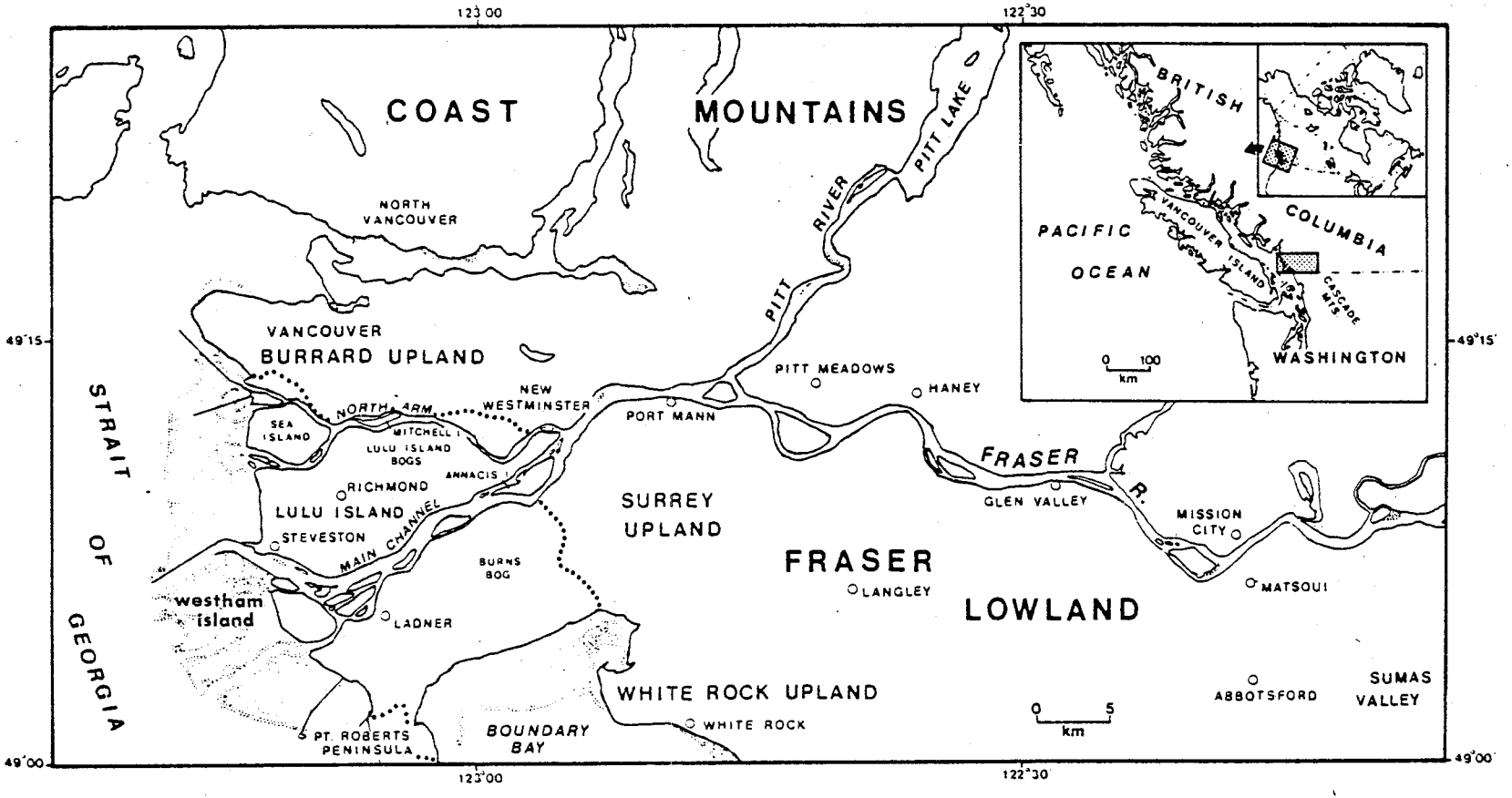

Figure 2.1 Location map: Fraser Delta and vicinity
(dotted line encloses delta)
(after Clague et al., 1983)

The delta is fringed by extensive tidal flats, which, on the western side of Lulu Island, extend some 6 km seaward to the lower low water level. The tidal flats form part of a gently sloping platform (ca. 0.05^{0}) which meets the delta's foreslope at a pronounced break in slope approximately 7 km offshore at a depth of about 9 metres below lowest normal tide level (Luternauer and Murray, 1973).

The foreslope typically slopes at about 1.5^{0} to meet the floor of the Strait at a depth of approximately 300 m, some 17 km seaward of the subaerial delta (Mathews and Shepard, 1962). In its upper reaches, where it is cut by gullies, the foreslope can be inclined up to 23^{0} (Luternauer, 1980).

Sediment is suppied to the delta by the Fraser River, which, with a total length of more than 1200 km and a drainage area in excess of 230000 km^2, is the largest river reaching the west coast of Canada (Mathews and Shepard, 1962). The river has a pronounced freshet in late spring and early summer when flows range up to 15000 $m^3\ s^{-1}$ and average more than 4000 $m^3\ s^{-1}$. Flows are generally below 1500 $m^3\ s^{-1}$ during the rest of the year. About 80 - 85% of river flow passes through the Main Arm (Fig. 2.1), with the remainder fairly evenly distributed between the other three distributary channels (Luternauer and Murray, 1973).

Approximately 80% of the annual sediment load of 12 to 30 million tonnes is discharged during the freshet period. The sediment is markedly sandy, with sand accounting for more than 30% of the annual sediment discharge passing Port Mann near the

apex of the delta (Milliman, 1980).

Much of this sand is initially deposited on the distributary channel floors, though it continues moving seaward as bedload during high flows (Kostaschuk, 1986). Some 4 million tonnes of this sediment is now dredged annually from the North Arm and Main Channel. This material is dumped on the channel margins and in deeper water offshore, removing it from estuarine circulation (Luternauer, 1980).

Dyking has been carried out along distributary channels and the landward edge of the tidal flats since the late 1800's. The dykes, in preventing flooding of the delta's terrestrial surface due to extreme high tides or river discharges, have also prevented the continuation of natural overbank sedimentation (Clague and Luternauer, 1983).

The dykes, together with extensive drainage ditch networks, have resulted in the general lowering of water tables and a reduction in the area of bogs and marshes on the delta surface (North et al., 1984).

Natural sedimentation at the delta front has also been modified by the construction of jetties (Fig. 2.1), which interrupt longshore transport and increase resuspension of sand in the outer estuary by channelizing flow (Milliman, 1980; Kostaschuk and Luternauer, 1987).

Sediment arriving at the delta front is subject to wave and tide reworking. Tides are of the mixed semi-diurnal type. The range of spring tides approaches 5 metres at the mouth of the Main Channel (Ages and Woollard, 1976). The strongest winds

generally blow from a westerly direction, generating waves over the delta foreslope that average 0.6 metres in height and range up to a maximum significant wave height of about 1.5 metres (Hoos and Packman, 1974).

2.2 CONTEMPORARY DEPOSITIONAL ENVIRONMENTS

The distribution of surficial sediments on Lulu Island has been studied in considerable detail (Johnston, 1921; Armstrong, 1956, 1957; Armstrong and Hicock, 1980a, 1980b; Medley and Luternauer, 1976; Luternauer, 1980). On the basis of these studies, and combining observations made in this study, a map was produced of contemporary sedimentary environments associated with the prodelta (foreslope) and intradelta (subaqueous platform, tidal flats, floodplain, peat bog and river channels) regions (Fig. 2.2).

The following sections contain a brief review of the nature and extent of contemporary depositional environments on the delta, based on the findings of the studies listed above. Details of the biosedimentological characterization of selected contemporary depositional environments carried out for this study, will be presented in later chapters.

2.2.1 FORESLOPE

Off Lulu Island, foreslope sediments generally become progressively finer with increasing water depth (Johnston, 1921; Mathews and Shepard, 1962; Luternauer and Murray, 1973; Pharo

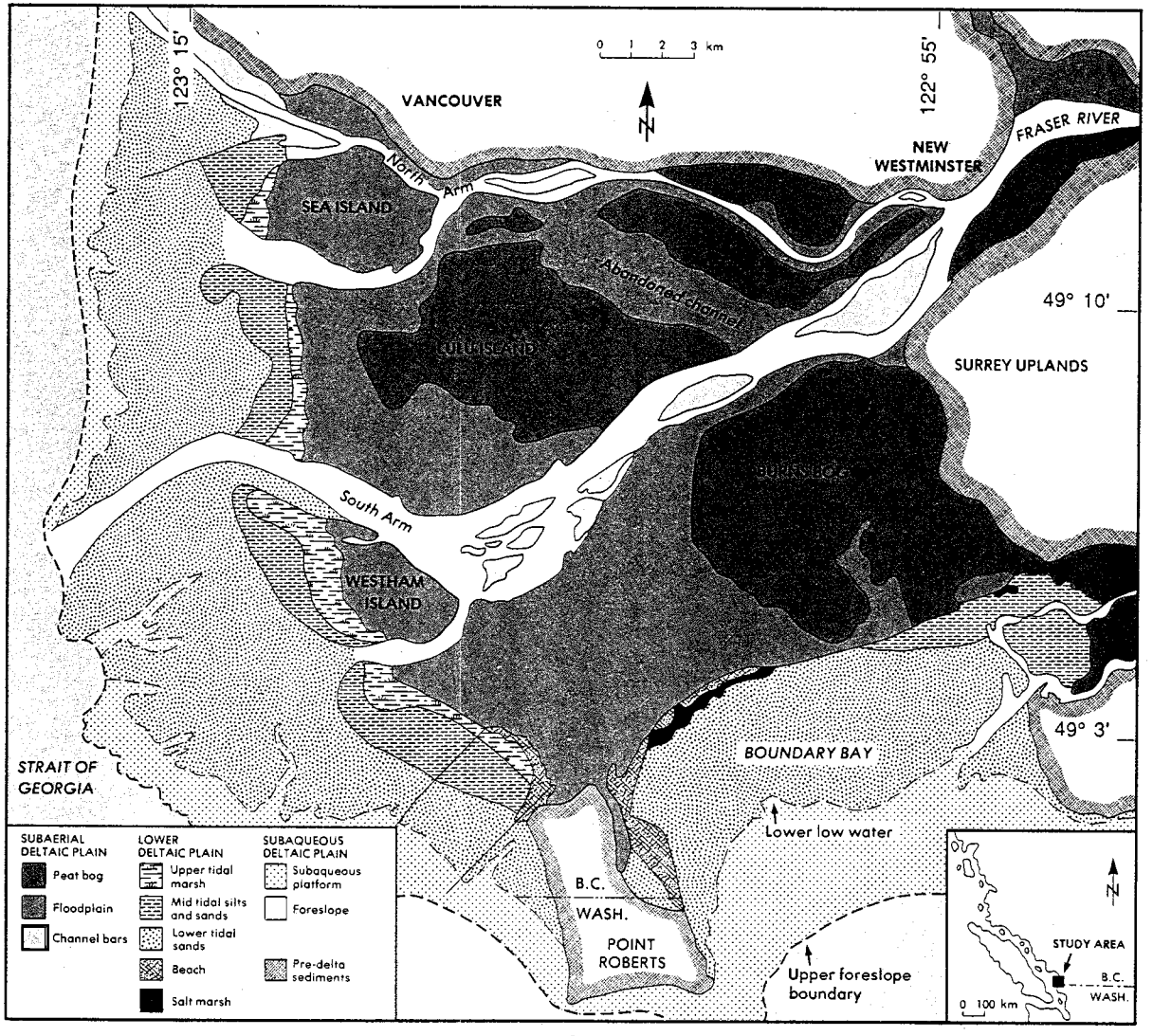

Sources: Luternauer & Murray, 1977; Armstrong, 1981; Clague et al., 1983

Figure 2.2 Contemporary depositional environments on the Fraser Delta

and Barnes, 1976).

Foreslope environments in the immediate vicinity of the Main Channel are characterized by silty fine sand, having a mean grain size of the order 0.125 - 0.25 mm. North of the Main Channel, upper foreslope sediments are somewhat finer, consisting of sandy silt and silty sand, with mean grain sizes in the range 0.031 - 0.125 mm. Foreslope samples from a water depth of about 100 m have yielded mean grain sizes of the order 0.01 mm (Luternauer and Murray, 1973).

Sand content is generally less than 5% below 100 m water depth. Sediments at the base of the foreslope, at a water depth of about 300 m, are characterized by clayey silt (Mathews and Shepard, 1962).

The foreslope sediments are inclined parallel to the submarine slope and, in places, consist of poorly developed and irregular laminations of fine sand and sandy to clayey silt (Johnston, 1921; Mathews and Shepard, 1962; Luternauer et al., 1986).

In the vicinity of distributary channel mouths, the foreslope is cut by gullies formed by mass wasting or turbidity currents (Mathews and Shepard, 1962; Luternauer, 1980). Mass movements of sediment down these gullies contribute to the redistribution of deposits on the delta slope and are responsible for localized deformation of foreslope sediments (Mathews and Shepard, 1962; Clague and Luternauer, 1983; Luternauer and Finn, 1983; McKenna and Luternauer, 1987).

2.2.2 SUBAQUEOUS PLATFORM

The subaqueous platform (Fig. 2.2) consists of gently inclined deposits (ca. 0.5^{o}) lying between lowest normal tide level and the break in slope 9 m below lowest normal tide level. This break in slope marks the beginning of the delta's foreslope and also coincides with the maximum depth of vigorous wave and current turbulence (Luternauer and Murray, 1973). Physiographically, the subaqueous platform is the seaward extension of the delta's tidal flats (Fig. 2.2) and, in the terminology of Gilbert (1890), forms the base of the delta's "topset" deposits.

Sediments of this zone consist of well-sorted 0.125 - 0.35 mm sand. Sand in this size range is discharged through the distributary channels during periods of high flow. This sediment is presumably distributed along the delta front by longshore drift (Luternauer and Murray, 1973).

2.2.3 TIDAL FLATS

Landward of lowest normal tide level, the subaqueous platform merges with laterally extensive tidal flat deposits. The tidal flats form a very gently inclined (ca. 0.05^{o}) 6 km wide platform fringing the subaerial delta (Fig. 2.2).

The lower tidal flats area consists of a 4 km wide zone of sandy deposits, which rise up to 1.8 m above lowest normal tide level on their landward edge. This zone is sedimentologically similar to the subaqueous platform. The deposits consist of

well-sorted fine to medium sand (0.125 - 0.35 mm), generally lacking any vegetation (Luternauer and Murray, 1973). Hydrodynamic structures are common, ranging from widespread small wave and current ripples, to patches of low (< 0.5 m), long wavelength (50 - 100 m) sand swells, apparently formed by wave action (Luternauer, 1980).

The lower tidal flat sands grade landward into a 1 - 2 km wide zone of silts, sands and sandy silts, containing isolated patches of eelgrass (Zostera sp.) and bulrush (Scirpus sp.) vegetation (Medley and Luternauer, 1976). Mud pools (silt accumulations in excess of 0.6 m thick) and dendritic drainage networks of tidal channels are found in this area (Luternauer, 1980). The landward boundary of these deposits coincides approximately with mean sea level (about 2.8 m above lowest normal tide level - Swan Wooster Engineering Ltd., 1967), giving this zone a vertical extent of about 1 m.

The upper tidal flats, a zone 1 - 1.5 km wide west of the dyke, consists of tidal marsh (Fig. 2.2). This zone contains abundant vegetation, mainly sedges and rushes. Species density and diversity generally increases landward. Sediments consist of organic-rich clayey to fine sandy silt. The mean grain size of these deposits generally decreases landward, reflecting reduced wave and tidal energy at higher marsh surface elevations (Hutchinson, 1982). The marsh extends up to the base of the dyke at an elevation of about 4.4 m above lowest normal tide level, giving the marsh zone a vertical extent of about 1.6 m.

2.2.4 FLOODPLAIN

Floodplain deposits are found within the dyked portion of the delta (Fig. 2.2). These sediments are flat lying to very gently inclined (< 1^{o}) and generally extend up to 1 - 2 m above mean sea level (Clague and Luternauer, 1983). The deposits consist of organic-rich sandy to clayey silts of overbank origin (Armstrong and Hicock, 1980a, 1980b). These sediments accumulated in fresh and brackish water marshes and swamps during periodic flooding by the Fraser River (Clague et al., 1983).

The floodplain sediments overlie, and grade into, tidal marsh deposits. Although similar sedimentologically, the two can be distinguished on the basis of their organic content; floodplain deposits, for example, commonly contain small amounts of pollen and spores from fresh water plants, including water plantain (Alisma plantago-aquatica), scouring rush (Equisetum sp.), skunk cabbage (Lysichiton americanum) and buckbean (Menyanthes trifoliata). Pollen of these freshwater species is rare or absent in tidal flat sediments (Clague and Luternauer, 1983).

2.2.5 PEAT BOG

Much of the eastern part of Lulu Island is covered by peat bogs (Fig. 2.2). Peat began to accumulate when the floodplain of Lulu Island was built high enough to avoid regular flooding by the river and the sea (Clague et al., 1983). These organic

accumulations are typically 2 - 3 m thick and, in places, have a surface elevation in excess of 3 m above sea level (Styan, 1981; Styan and Bustin, 1984).

The bogs have a marked vertical successional sequence beginning with a basal layer of sedge-grass peat, followed by sedge-sphagnum peat and, finally, ericaceous and pure sphagnum peats, representing the climax biofacies. This sequence represents the change from brackish to fresh water conditions, accompanying the progressive elevation of the bog surface above sea level (Clague et al., 1983; Styan, 1981; Styan and Bustin, 1984; Hebda, 1977).

2.2.6 RIVER CHANNELS

The principal distributary channels of the delta are scoured to depths of up to 22 m below sea level. They are floored by medium to coarse sand, containing scattered pebbles and gravel lenses (Mathews and Shepard, 1962).

An abandoned distributary, comparable in size to the present Main Channel, cuts across the peat deposits on eastern Lulu Island (Fig. 2.2). The channel fill deposits consist of fine to medium sand, overlain by about 2 m of organic-rich silt. The channel sands contain characteristic fluvial structures, including fining-upward sequences, erosional contacts and gravel lag layers (Roberts et al, 1985).

The fact that peat has not yet covered this former distributary suggests that it was abandoned fairly recently, probably within the last 5000 years (Mathews and Shepard, 1962;

Clague and Luternauer, 1982). The abandoned distributary forms the only gap in the peat deposits not now occupied by an active channel, attesting to the stability of the delta's distributaries during late Holocene time (Clague et al., 1983).

2.3 LATE QUATERNARY SEA LEVEL FLUCTUATIONS IN THE FRASER LOWLAND REGION

The Fraser Glaciation (late Wisconsinan) reached its maximum extent during the Vashon Stade, approximately 15000 yr BP (Mullineaux et al., 1965; Heusser, 1973). At this time, the Fraser Lowland was completely covered by a lobe of the Cordilleran Ice Sheet, which extended a further 280 km to the south (Clague, 1983).

Evidence provided by glacial erratics and glaciated surfaces in the southern Coast Mountains, suggests that the Vashon Ice Sheet attained a thickness of at least 1800 m in the Fraser Lowland area (Mathews et al., 1970). The weight of the ice caused isostatic depression of this region of at least 275 m, which more than compensated for the eustatic lowering of sea level of about 75 m (Mathews et al., 1970; Clague, 1983).

Consequently, during and immediately following retreat of the Vashon Ice about 13000 yr BP (Fulton, 1971), the sea invaded the Fraser Lowland region up tc an elevation of at least 200 m above present sea level (Armstrong, 1981).

Isostatic rebound proceeded rapidly following removal of the ice load. Raised glacio-deltaic deposits in the Fraser Lowland suggest that sea level fell to about 40 m elevation by

around 11500 yr BP (Clague and Luternauer, 1983) and reached its present level between 11000 and 10000 yr BP (Clague, 1981).

Emergence of the Fraser Lowland continued, causing the sea to drop below its present level. Widespread terrestrial organic deposits occur 10 to 11 m below present sea level beneath the floodplain of the Fraser River and its tributaries (Mathews et al., 1970). Radiocarbon dates on these deposits range from 7300 ± 120 yr BP (S-99) to 8360 ± 170 yr BP (GSC-225) (Clague, 1980). These deposits are interpreted as peat accumulations on a former alluvial surface, graded to a sea level in the Strait of Georgia about 12 m lower than at present (Clague et al., 1982, 1983).

The low stand of the sea in the early Holocene, resulting from isostatic rebound, was followed by a relative rise in sea level which continued until at least mid-Holocene time. This rise in sea-level was apparently eustatic in nature, as it conforms to the general pattern of global eustatic sea-level curves (Mathews et al., 1970). Contrasting sea-level histories have been reported from other parts of British Columbia (e.g. Queen Charlotte Islands, western Vancouver Island), suggesting that tectonic movements have also played an important role in some areas (Clague et al., 1982).

The base of peat bogs on the Fraser Delta, lying 0 - 2 m below present sea level, have been dated at 4650 ± 80 yr BP (GSC-3045) to 5510 ± 80 yr BP (GSC-3066). This suggests that the sea was within 2 m below its present level by about 5000 years ago (Clague et al., 1983).

A buried peat bed, 1.5 m below high tide level at Boundary

Bay (Fig. 2.1), has been radiocarbon dated at 4350 ± 100 yr BP (GX-0781). This evidence indicates that sea level was about 1.8 m lower than at present at that time (Kellerhals and Murray, 1969; Mathews et al., 1970; Clague et al., 1982).

Palynological analysis of peat deposits on the Fraser Delta has shown that terrestrial organic sedimentation has continued without interruption for approximately the last 5000 years, precluding a rise in sea level of more than 1 to 2 m during this period (Hebda, 1977; Clague et al., 1982). This evidence, and the widespread occurence of intertidal silts and sands (reported from engineering excavations) a few metres beneath the western part of the Fraser Delta, suggests that sea level has remained comparatively stable during the latter half of the Holocene period (Clague et al., 1982).

In summary, post-glacial sea level history in the Fraser Lowland region is characterised by rapid emergence of the land following de-glaciation; a low stand of about -12 m during the early Holocene; a relative rise in sea level up to about its present position by mid-Holocene time; and, a comparatively stable sea level during the last 5000 years (Clague et al., 1982 - Fig. 2.3).

2.4 PREVIOUS WORK ON THE STRUCTURE AND EVOLUTION OF THE FRASER DELTA

2.4.1 STRUCTURE OF THE DELTA

Knowledge of the subsurface of the delta is fairly limited.

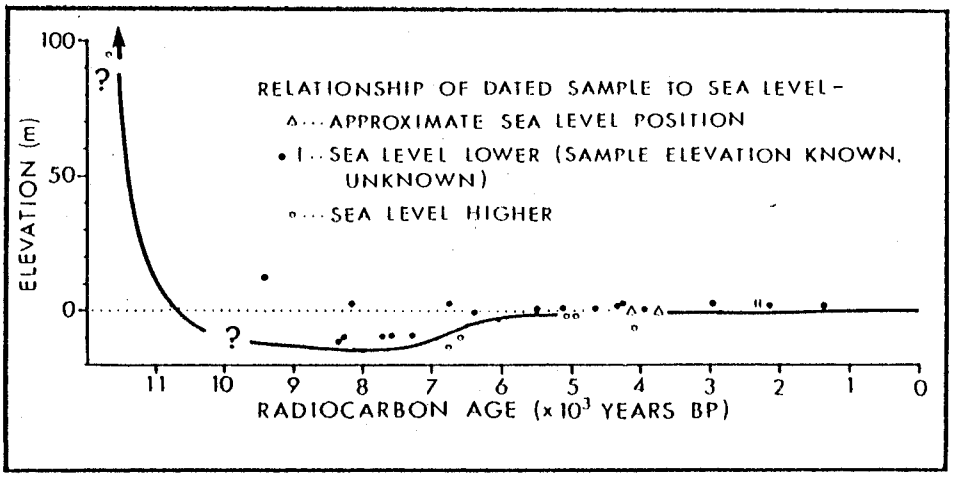

Figure 2.3 Fraser Lowland sea-level curve
(after Clague et al., 1982)

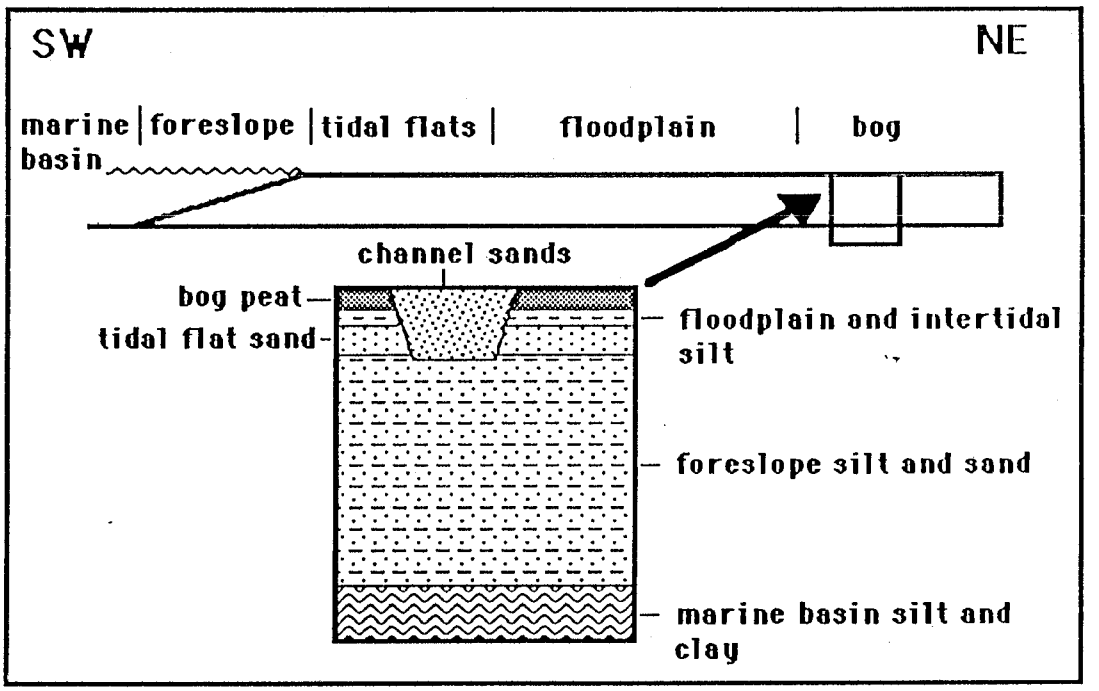

Figure 2.4 Generalized vertical section through the Fraser Delta
(after Clague et al., 1983)

Much of the information presently available consists of driller's logs from shallow bore-holes drilled for engineering studies. Many of these drill-holes are too shallow to reach the base of the delta, but they do indicate that the depth of deltaic deposits exceeds 100 m over a considerable area (Mathews and Shepard, 1962).

Mathews and Shepard (1962), classified the delta's deposits in terms of "topset" and "foreset" beds, in accordance with the classic delta model of Gilbert (1890) (Fig. 1.1). They point out, however, that the Fraser "foreset" beds are much less steeply inclined than their counterparts in the raised Pleistocene deltas described by Gilbert; and that there is no obvious distinction between "foreset" and "bottomset" beds on the present Fraser Delta front. In contrast to Gilbert's model, the Fraser "foreset" beds are seemingly indistinguishable from the clayey silt pro-delta deposits that mantle the uneven floor of the Strait.

In other respects, the classification of the Fraser Delta does resemble Gilbert's model, consisting of a very gently inclined (ca. 0.005^{o}) blanket of "topset" deposits (channel sands, floodplain silts, peat bog, intertidal and subaqueous platform sediments) overlying a wedge of gently inclined (ca. 1.5^{o}) "foreset" deposits (interbedded sand, sandy silt, silt and clayey silt), which mantle the pre-existing topography (Mathews and Shepard, 1962).

There is no evidence that subsidence has had a significant influence on the internal structure of the delta. Although

natural compaction of sediment upon incorporation into the delta foreslope is substantial, involving volume reductions of up to 46%, much of this compaction occurs soon after burial, almost entirely beneath the delta front or tidal flats (Mathews and Shepard, 1962). Thus, little additional settlement is anticipated within the deposits underlying the terrestrial part of the delta.

The lack of significant subsidence effects in the development of the delta is supported by evidence from Burns Bog on the southern part of the delta. The base of the bog, dated at about 5000 yr BP, generally lies within 2 m below mean sea level (Mathew et al., 1970; Hebda, 1977), indicating that subsidence of the land surface could not have exceeded 2 m in the 5000 years since the bog's formation.

Clague et al. (1983), produced a generalized vertical section through the delta based on bore-hole records (Fig. 2.4). Again, this model is characteristic of the Gilbert-type delta, in that the succession of sedimentary deposits from bottom to top of the section is the same as the lateral succession of present-day depositional environments on the Fraser River Delta.

2.4.2 AGE OF THE DELTA

Johnston (1921) estimated the average rate of advance of the western delta front to be 10 feet per year. This was based on a comparison of seven spot soundings made in 1859 and 1919 in the vicinity of the mouth of the Main Channel. Assuming the same rate of advance for the entire growth of the delta from its apex

at New Westminster, 80000 feet to the east, a figure of 8000 years was proposed for the age of the delta.

Johnston's estimated average rate of advance of 10 feet per year is based on a very limited data set, from a relatively small portion of the foreslope. The actual average rate of advance of the entire delta front could vary considerably from Johnston's estimate (Clague and Luternauer, 1983).

The assumption that the delta has advanced at a constant rate during its growth ignores possible variations in water depth, delta front length and sediment supply, as the delta built forward (Mathews and Shepard, 1962; Clague and Luternauer, 1983).

More recent estimates of the delta's age are based on radiocarbon dates and the reconstruction of sea level fluctuations in the Fraser Lowland region. Mathews and Shepard (1962) note that higher sea levels precluded development of the modern delta until at least 11000 yr BP. However, a radiocarbon date from peat deposits suggests that the Fraser River floodplain had advanced to within 8 km of the delta's apex (i.e. the vicinity of Port Mann - Fig. 2.1) prior to 7300 $\pm$ 120 yr BP (S-99). Thus, development of the modern delta has probably taken not less than about 7300 years and not more than 11000 years (Mathews and Shepard, 1962).

Clague et al. (1983), proposed that the Fraser River transported much larger amounts of sediment at the close of the Pleistocene than it does today. They suggested that the sediment supply was increased initially by the erosion of unvegetated

drift-covered slopes immediately following de-glaciation (Church and Ryder, 1972). Later, as the drift-covered slopes became stabilized by vegetation, high sediment loads were nevertheless maintained as rivers incised their earlier deposits, partly to attain grade with a falling sea level, and partly in response to a reduced sediment supply.

On the basis of these assumptions, it was proposed that the progradation of the Fraser River floodplain proceeded rapidly and that the modern Fraser River Delta began building out from New Westminster by about 10000 yr BP (Clague et al., 1983 - their Fig. 6).

A recently obtained radiocarbon date indicates a somewhat younger age for the delta. A date of 9490 $\pm$ 250 yr BP (GSC 3919) was obtained on a wood fragment from approximately 55 m below the surface of the delta in the vicinity of New Westminster. The wood was recovered from a drill core containing sandy to clayey silt with scattered shell fragments (R. Blunden, personal communication). This material probably represents pro-delta deposits laid down in front of the advancing Fraser River floodplain (W. H. Mathews, personal communication). This date suggests that the terrestrial surface of the delta did not emerge into the Strait of Georgia until about 9000 yr BP.

2.4.3 EVOLUTION OF THE DELTA

The Fraser River Delta started forming approximately 9000 years ago, when the prograding Fraser River floodplain reached the vicinity of New Westminster and the terrestrial surface of

the Fraser Delta first emerged into the Strait of Georgia (Fig. 2.1). At this time, sea level was lower than at present (Fig. 2.3) and may have been falling relative to the land (Mathews and Shepard, 1962; Mathews et al., 1970; Clague et al., 1982, 1983).

Sea level reached its lowest position of about -12 m prior to about 8000 years BP and remained stable long enough for peat deposits to accumulate on alluvial surfaces in the Fraser Lowland (section 2.3). Between about 9000 and 8000 BP, a fairly extensive "proto-delta", graded to the -12 m sea level, is thought to have developed to the southwest of New Westminster over a distance of at least 15 km (Clague and Luternauer, 1983; Clague et al., 1983). Evidence for the existence of an early "proto-delta" buried beneath more recent deltaic deposits, includes the following (Clague and Luternauer, 1983; Clague et al., 1983);

1) peat deposits 7300 $\pm$ 120 yr BP (S-99) to 8360 $\pm$ 170 yr BP (GSC-225), 10 to 11 m below the western Fraser River floodplain. It has been suggested that the peat represents organic accumulations on an alluvial surface, which is likely to have extended west of New Westminster onto the former terrestrial surface of the "proto-delta".

2) 6400 $\pm$ 197 yr BP (WAT-369) intertidal sediments at a shallow depth beneath Lulu Island, indicating that tidal flats were present more than 15 km southwest of New Westminster by about 6400 years ago and that a substantial subaerial "proto-delta" was in existence prior to this time.

3) the presence of ca. 6800 year old Mazama tephra (Bacon, 1983) at a shallow depth beneath eastern Lulu Island, again indicating that substantial deltaic deposits had formed prior to this time (Blunden, 1973, 1975).

After about 8000 yr BP, the sea rose until it was within 2 m of its present level by about 5000 yr BP (Fig. 2.3). During this period, aggradation is known to have occurred on the Fraser River floodplain (Clague et al., 1982). Beneath the floodplain at Pitt Meadows, peat at about -10 m elevation and dated 7710 ± 80 yr BP (GSC-3099), is overlain by 11.5 m of silt and sand interpreted as estuarine sediments deposited under aggradational conditions (Clague et al., 1982; 1983) (Fig. 2.5).

A tephra bed, assumed to be Mazama, occurs above the peat at an elevation of about -5 m (Fig. 2.5). This suggests that the sea probably rose about 5 m relative to the land between about 7700 and 6800 yr BP (Clague and Luternauer, 1983).

The occurrence of 4650 ± 80 yr BP (GSC-3045) to 5510 ± 80 yr BP (GSC-3066) terrestrial deposits at the base of the large peat bogs covering most of the eastern delta surface, indicates that aggradation also occurred on the Fraser "proto-delta" during the period of rising sea level.

Although there is some speculation that a marine transgression accompanied aggradation on the "proto-delta" (Clague and Luternauer, 1983; Clague et al., 1983), the manner by which aggradation commenced and details of the resulting facies sequence underlying the eastern delta region remain

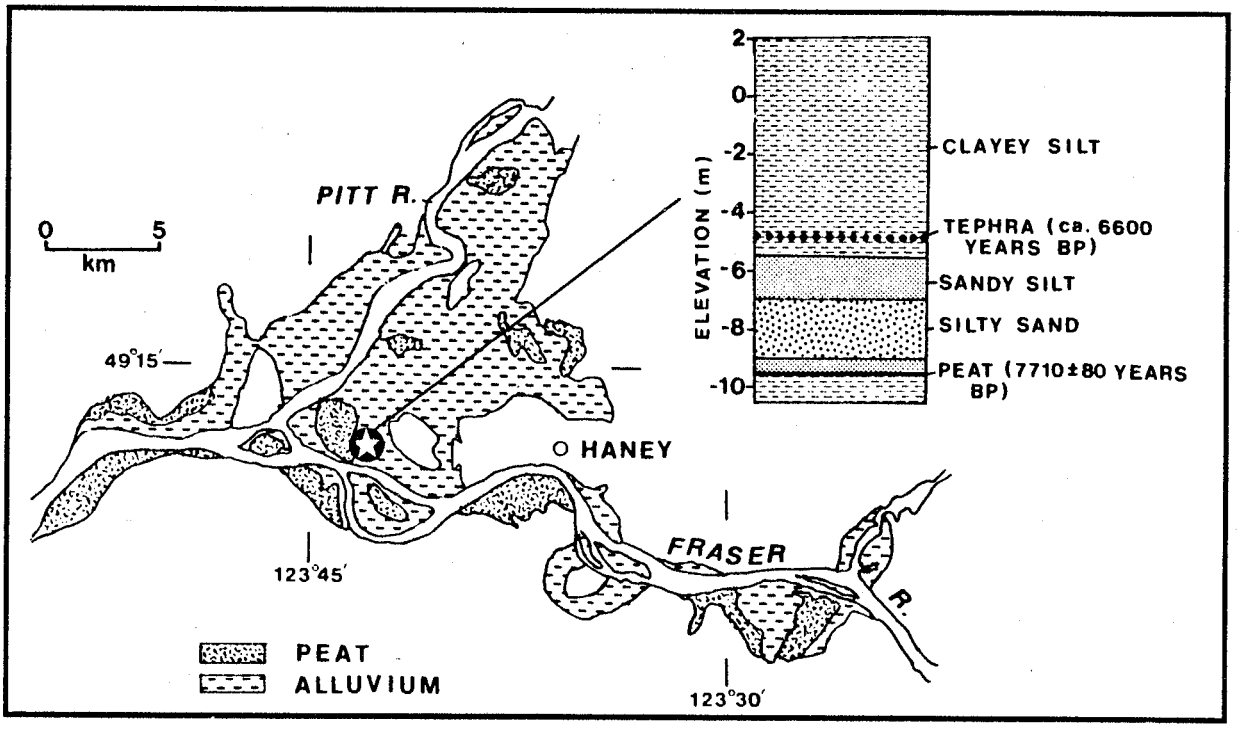

Figure 2.5 Stratigraphy of a core at Pitt Meadows (after Clague et al., 1983)

largely unknown.

The rise in sea level had slowed considerably by about 5000 yr BP (Fig. 2.3). At this time, the sea was within 2 m of its present level and peat was beginning to accumulate on the emergent eastern part of the delta. During about the last 5000 years the sea probably rose no more than 1 - 2 m to its present level (Clague and Luternauer, 1983). Progradation of the delta since about 5000 yr BP has proceeded under comparatively stable sea level conditions.

During this period, the eastern surface of Lulu Island has been built vertically to 1 to 2 m above present sea level by overbank sedimentation and to in excess of 3 m by peat accumulation. On the western part of Lulu Island, progradation of the delta front during a relatively stable sea level has resulted in a fairly uniform blanket of floodplain deposits overlying intertidal sediments.

SECTION TWO

CONSTRUCTION OF INTERPRETIVE FRAMEWORK AND SUBSURFACE DATA COLLECTION

CHAPTER THREE

LITHOLOGIC CHARACTERISTICS OF CONTEMPORARY DEPOSITIONAL ENVIRONMENTS

3.1 INTRODUCTION

This chapter deals with the lithologic characterisation of selected contemporary depositional environments on Lulu Island. Previous studies (section 2.2) indicate that the most pronounced lithologic contrasts are found within the intertidal zone. Floodplain sediments are lithologically similar to tidal marsh deposits and are more readily distinguished by palynological analyses (section 2.2.4). Subaqueous platform deposits are lithologically similar to lower tidal flat sands (section 2.2.2).

In order to construct an effective interpretive framework, environmental attributes selected for inclusion must be of sufficient contrast between different environments to enable the deposits of those environments to be readily distinguishable. Where two environments are very similar in terms of a particular attribute (e.g. lithology), some other attribute(s) (e.g. palynology) must be incorporated into the interpretative framework to differentiate the two environments.

Consequently, the subaqueous platform and floodplain were excluded from lithologic characterization, since deposits of these environments are lithologically similar to those of the lower tidal sands and upper tidal marsh, respectively, and can

not be distinguished from these deposits on the basis of lithologic criteria.

Only the lithologically-contrasting deposits of the environments forming the contemporary intertidal surface fringing Lulu Island (Fig. 2.2) were examined for their lithologic character. Previous studies (section 2.2.3) have indicated that three major depositional environments are present; the unvegetated lower tidal sands; the partially vegetated mid tidal silts and sands, and the vegetated upper tidal marsh.

3.2 FIELD PROCEDURES

Although grain size characteristics can often be assessed reasonably accurately by field observation alone (Miall, 1984b), it was decided to use field observation in conjunction with laboratory analysis of a limited number of samples, to provide a degree of quantitative support.

Data were collected by walking out onto the intertidal surface at low tide in order to observe the lithologic character of the intertidal environments and to carry out sampling of the surficial deposits.

Surface observations consisted of the visual assessment of grain size characteristics and the relative abundance of vegetation. Observations were made during the summer growing season when the intertidal vegetation cover was well developed. The locations of the seaward edge of continuous marsh vegetation and the landward edge of the lower tidal sands were also noted

whenever they were encountered.

Data were plotted onto a topographic map of the tidal flats produced for the National Harbours Board by Swan Wooster Engineering of Vancouver (Swan Wooster Engineering, Co., 1967).

Positioning on the tidal flats was determined on the basis of several compass bearings on fixed objects onshore, giving an estimated accuracy of 50 m.

Grab samples of surficial sediments were obtained from widely scattered locations over the intertidal surface (Fig. 3.1). Sampling of the most outlying part of the lower tidal environment was, however, limited to one excursion in the north of the intertidal zone due to a limited number of sufficiently low tides during the sampling period and the difficulty of access to this environment.

Sedimentary structures within the deposits were observed in the banks of tidal channels and in shallow trenches dug into the intertidal surface. In addition, five cores were obtained along a transect from the upper to the lower tidal zone (Fig. 3.1). The four most seaward cores were obtained by driving short (< 1.5 m) plastic tubes into the intertidal surface. Adjacent to the dyke, in the upper tidal marsh, a 4.5 m long core was obtained, using a vibracorer.

In addition to allowing the subsurface of the intertidal zone to be examined, the cores also enabled an assessment to be made of the degree to which the lithologic characteristics of contemporary intertidal environments are incorporated into subsurface facies.

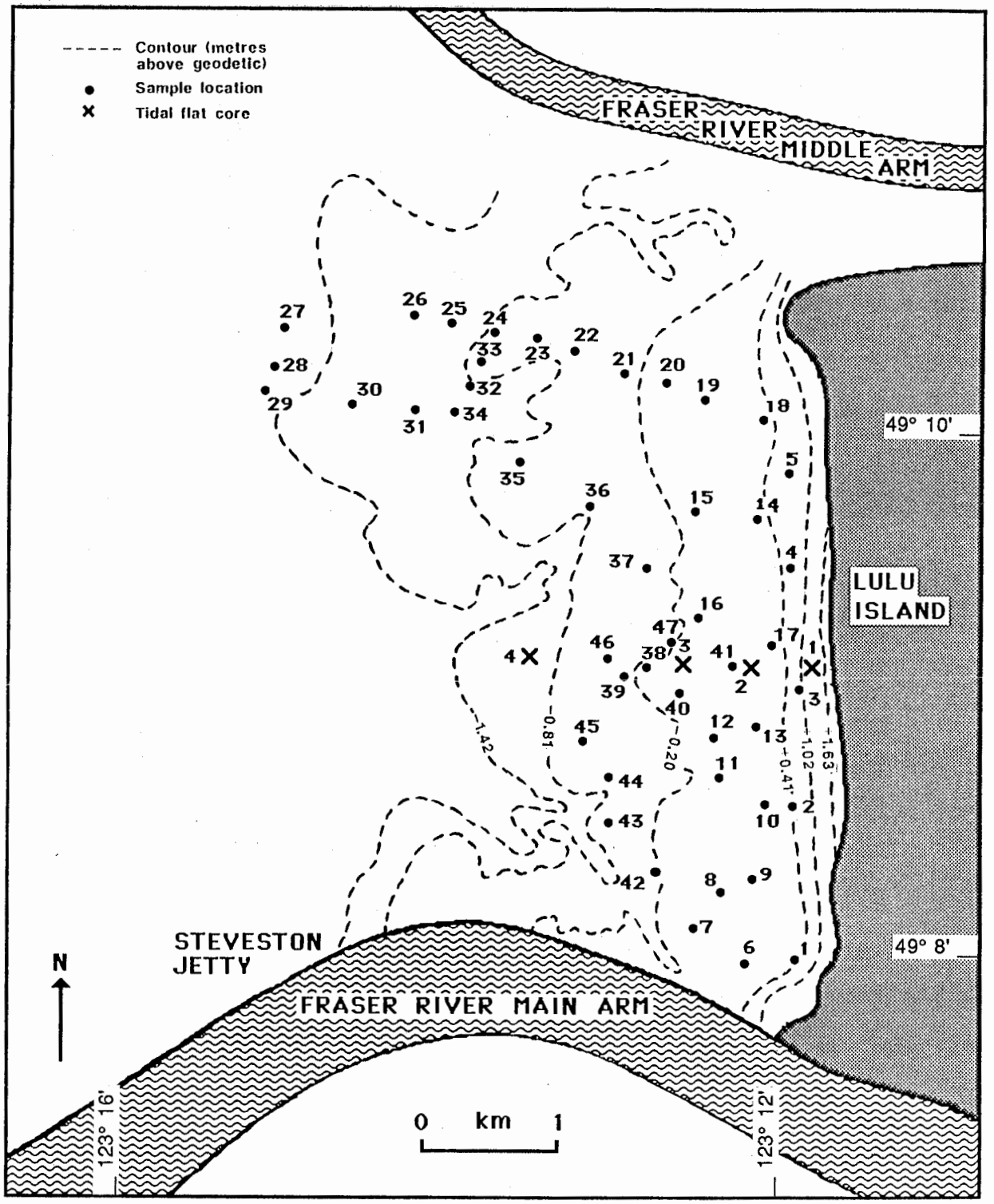

Figure 3.1 Lulu Island intertidal sample locations

3.3 LABORATORY ANALYSIS

The cores from the intertidal zone were split open and visually logged for mean grain size and sorting, sedimentary structures and organic matter content. Samples for grain size analyses were taken from the top of each core and from several depths within each core. Grain size distributions were determined for the 47 grab samples from the intertidal surface. Wet sieving at half phi intervals was used to analyse the sand size fractions. The silt and clay fractions were analysed on a Sedigraph 5000 particle size analyser. Folk and Ward's (1957) grain size parameters were computed for each grab sample and core sample (Appendix 1).

3.4 RESULTS

3.4.1 INTERTIDAL SURFACE SAMPLES

A plot of mean grain size against sorting indicates that the 47 grab samples from the intertidal surface fall into three distinct groupings on the basis of their grain size characteristics (Fig. 3.2). These data were used in conjunction with observations made on sedimentary structures and the relative abundance of incorporated organic material in the deposits to delimit three lithologically contrasting intertidal environments (Fig. 3.3).

The boundaries of these environments do not coincide with previously-documented divisions of the intertidal surface, which

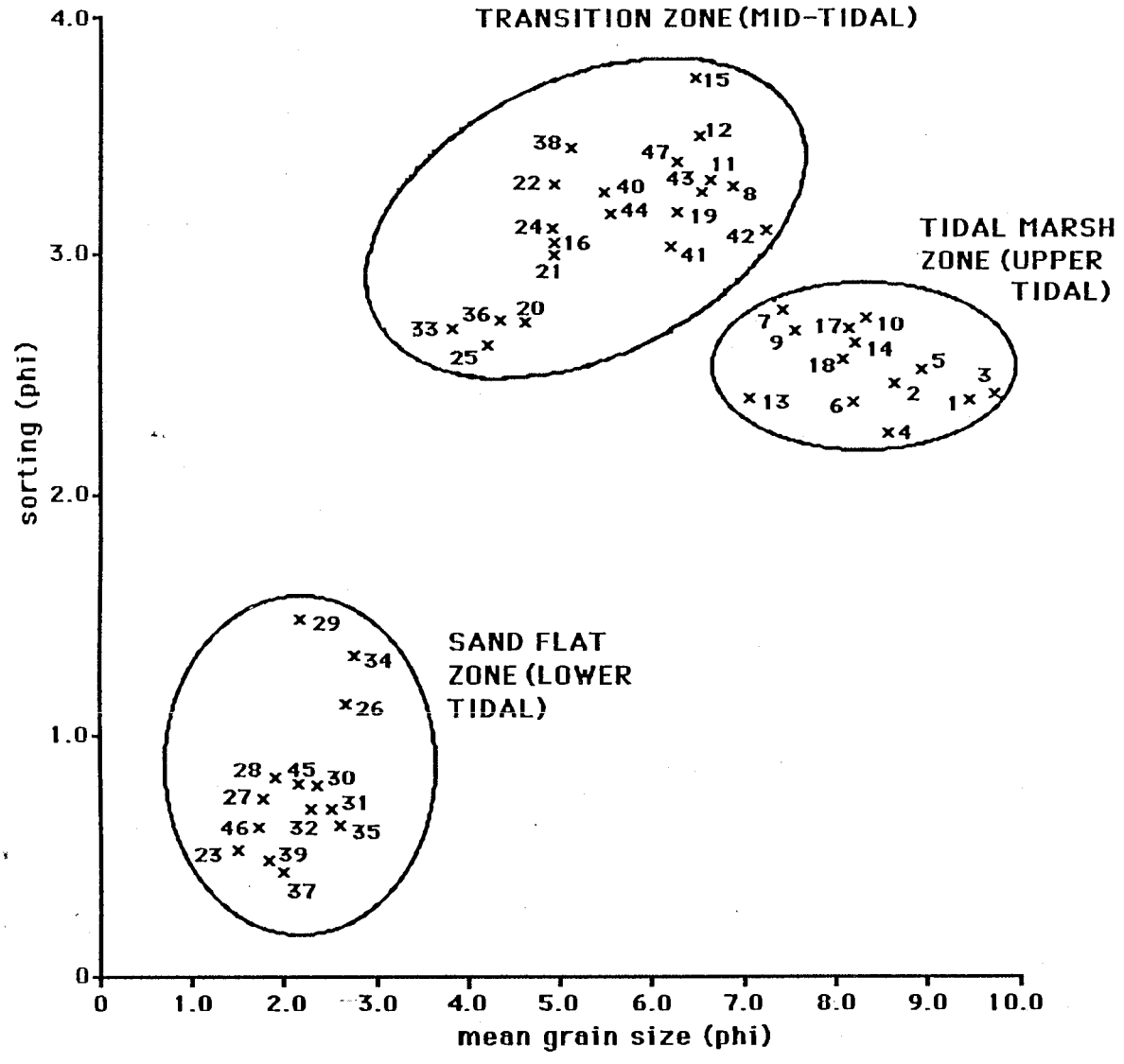

Figure 3.2 Mean grain size v sorting: intertidal surface samples

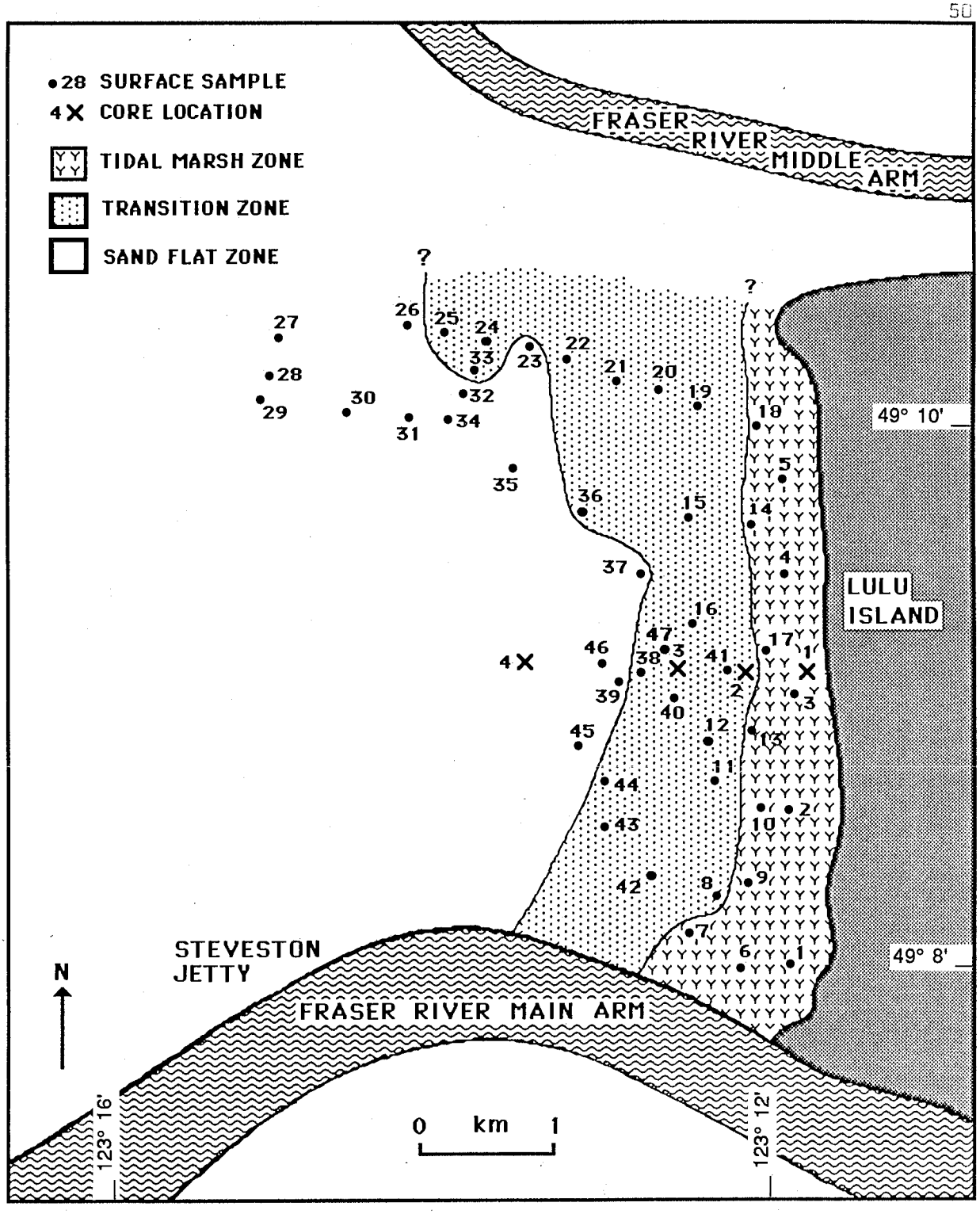

Figure 3.3 Lulu Island contemporary intertidal environments (based on lithologic characteristics)

are based mainly on vegetation cover rather than a combination of lithologic attributes (see section 2.2.3). Therefore, for the purposes of this study, these environments have been given the new designations:

Tidal marsh zone

Transition zone

Sand flat zone

The lithologic characteristics of each of these three intertidal zones are described in the following sections.

The tidal marsh zone, the most landward of these environments, consists of a large part of the continuously vegetated intertidal surface. The deposits in this zone are moderately sorted in comparison to the other intertidal environments (Fig. 3.2), and consist of very fine clayey silt. Sand content in the grab samples from this zone was in many cases zero and reached a maximum of only 7% (Appendix 1).

There is a dense vegetation cover throughout the tidal marsh zone (Fig. 3.4). Examination of channel banks and trenches indicates that abundant organic material is incorporated into the subsurface deposits. Although heavily bioturbated, the subsurface exposures also display clearly visible horizontal stratification (Fig. 3.5).

The most seaward environment, the sand flat zone, consists of unvegetated, relatively well sorted sandy sediments (Fig.

Figure 3.4 View of the tidal marsh zone

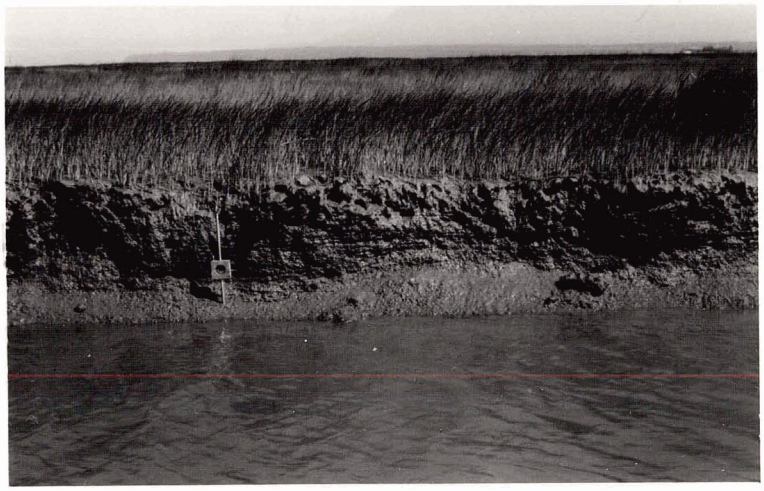

Figure 3.5 Exposed channel bank in the tidal marsh zone

3.2). Sand content in grab samples from this environment ranged from 92 to 99% (Appendix 1). Sedimentary structures, ranging from small-scale current ripples (Fig. 3.6), to large-scale low amplitude (< 0.5 m), long wavelength (50 - 100 m) sand swells, are common in this zone.

The subsurface of the sand flat zone was examined in a number of shallow trenches. Sedimentary structures, although common on the surface, were not visible in the subsurface. Organic material was very rarely observed. Generally, the subsurface of the sand flat zone consisted of clean, massive sands.

The transition zone, lying between the tidal marsh and sand flat zones (Fig. 3.3), contains the least well sorted sediments of all three intertidal environments (Fig. 3.2). Grab samples from this zone have sand contents ranging from 14 to 78% (Appendix 1).

This zone includes the leading edge of the continuously vegetated intertidal region, as well as isolated patches of vegetation. The vegetated areas often contain a thin veneer of silt overlying sandier sediments below (Fig. 3.7). Sediment textures in unvegetated parts of this zone vary from silty fine sand to fine sandy silt.

Examination of the subsurface of this zone in trenches and channel banks, revealed a similar variation in sediment texture as is present across the surface. Gradations from mostly fine sand to mostly silt are common. There are occasional sharp

Figure 3.6 View of the sand flat zone

Figure 3.7 Silt encroaching on rippled sand in the transition zone

contacts, overlain by coarser sediment, presumably marking the location of former tidal channels or storm wave deposits.

Bedding, as revealed by silt layers, is roughly horizontal and often disturbed by bioturbation. Occasional shallow angle (ca. 10^{0}) cross bedding, presumably formed by tidal channel point bar migration, was also observed. Organic material is common near the surface, but declines rapidly with depth. Alternations of finer and coarser sediments with depth are frequently observed in the subsurface, but overall a general coarsening of the deposits with depth is apparent.

3.4.2 SUBSURFACE FACIES OF THE INTERTIDAL ZONE

The intertidal core logs were used to construct a shallow lithostratigraphic cross-section across the intertidal deposits. The section reveals that there is a clear correspondence between the lithologic characteristics of the contemporary intertidal environments and the lithology of the subsurface facies (Fig. 3.8).

Environmental interpretations of core lithofacies suggests that only the relatively deep core (D41) from the upper tidal marsh zone penetrated underlying deposits corresponding to the other intertidal environments. This is confirmed by a plot of mean grain size and sorting values of the core samples onto a bivarate plot containing the enevelopes defined in Figure 3.2 (Figure 3.9).

Samples from the upper part of core D41, from 50, 100 and 150 cm depth, plot within the previously defined tidal marsh

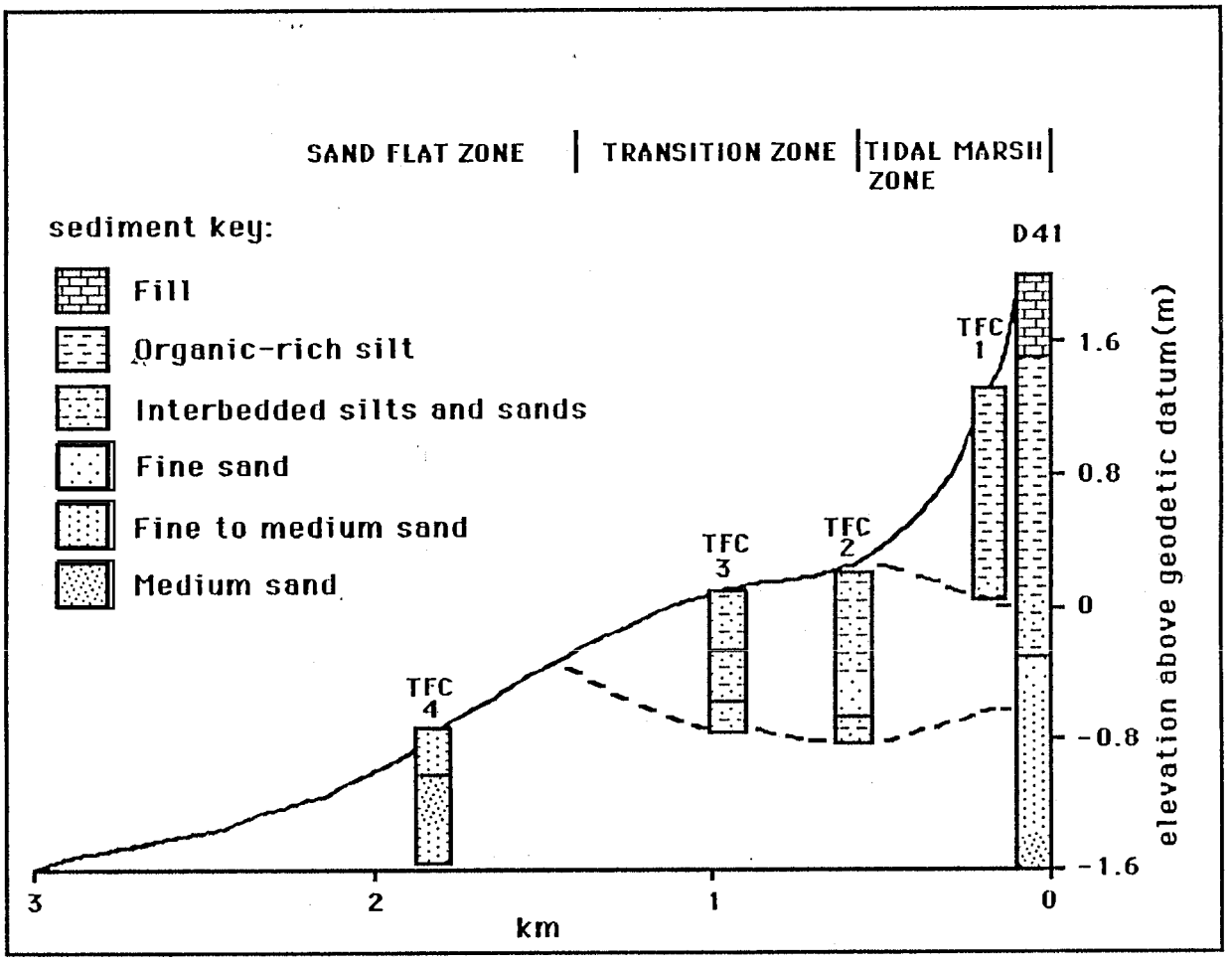

Figure 3.8 Tidal flats lithostratigraphic section (vertical exaggeration = 475x. Dashed lines represent lithostratigraphic boundaries between tidal marsh zone, transition zone and sand flat zone deposits)

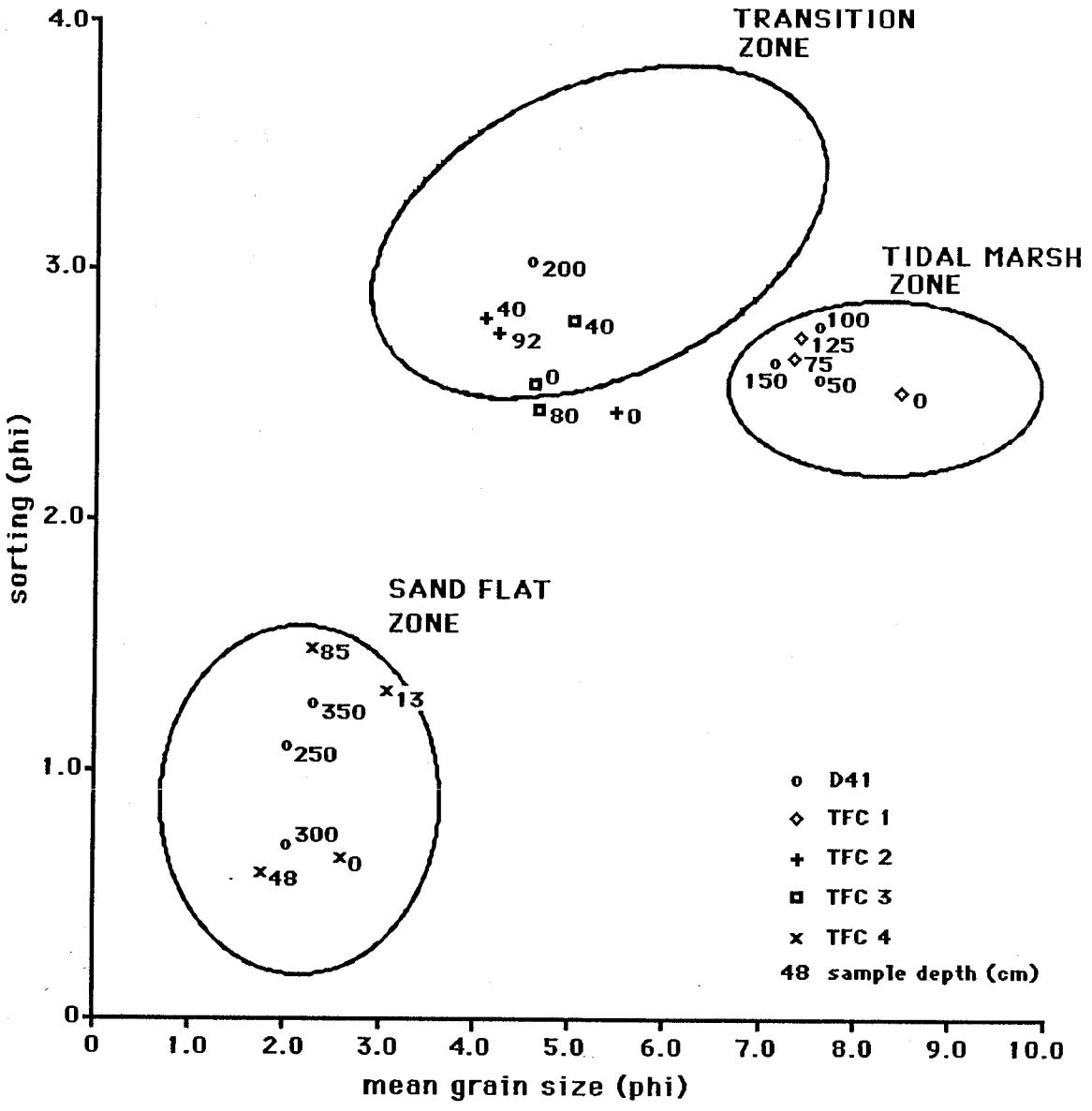

Figure 3.9 Mean grain size v sorting: intertidal core samples

envelop (section 3.4.1). The sample from a depth of 200 cm was apparently formed in the transition zone, having grain size characteristics corresponding to the transition zone envelop. The deeper samples from core D41, from 250, 300 and 350 cm, all plot within the sand flat zone envelop (Fig. 3.9).

Certain aspects of the variation of core litholgy with depth were particularly prominent when visually logging the cores and may provide useful interpretive criteria. The base of the tidal marsh facies corresponds to a marked decrease in the abundance of incorporated organic material. It was also at this depth that sand sized sediments first became apparent within the cores.

Deposits corresponding to the transition zone displayed a marked variation in sediment sizes, usually consisting of a downcore alternation of fine sand and silt. Organic material is scattered throughout these deposits and generally decreases in abundance with depth.

The beginning of the sand flat facies corresponds to the appearance of medium sand (0.25 - 0.5 mm) in the cores and the virtual absence of silt and organic material.

3.5 DISCUSSION AND SUMMARY

On the basis of both field observation and grain size analyses of surface samples, three lithologically contrasting intertidal environments have been defined - the sand flat zone, the transition zone and the tidal marsh zone.

The contrast in lithologic characteristics is most

pronounced between the tidal marsh and sand flat zones. In moving from the former to the latter environment, an increase in typical mean grain sizes approaching two orders of magnitude is observed and deposits rich in incorporated organic matter give way to deposits virtually free of organic material. Lying between these two extremes, the transition zone combines elements of both environments, resulting in its own distinctive lithologic character.

It is probable that the lithologic zonation of the tidal flats reflects wave and tidal energy thresholds on the intertidal surface. Relatively low energy conditions prevail in the tidal marsh zone due to wave attenuation on the lower and mid tidal flats, relatively shallow depths of inundation and the hydraulic resistance offered by the dense stands of tidal marsh vegetation (Hutchinson, 1982).

The seaward boundary of the tidal marsh zone presumably reflects the threshold above which wave and tidal energy is insufficient to transport significant quantities of sand sized sediment.

The transition zone is apparently subject to a wider variation in energy regimes. In places, sandy sediments dominate the surface deposits, suggesting relatively high energy conditions. Elsewhere, the hydraulic resistance offered by pioneering bulrush (Scirpus sp.) stands produces localized low energy environments and resultant silt accumulation (Fig. 3.7) (Hutchinson, 1982). Shoreline configuration and the sheltered landward sides of sand swell fields also appear to create

localized low energy environments in the mid tidal area (Luternauer, 1980).

The sand flat zone, on the lower tidal flats, is a relatively high energy environment. This part of the intertidal surface is exposed to the full force of waves and tidal currents. There is no protective vegetation cover to slow the movement of water or bind the surface sediments together. Inundation occurs frequently, for long periods and up to depths of several metres.

The landward boundary of the sand flat zone presumably corresponds to the threshold below which wave and tidal energy is sufficient to preclude the long-term deposition of silt and clay sized sediment.

Shallow coring of the intertidal zone indicates that the lateral succession of lithologic characteristics across the intertidal surface is incorporated into a vertical sequence of distinctive lithofacies in the subsurface.

A generalized facies model for the Lulu Island intertidal deposits can now be established (Fig. 3.10). The model consists of a generalized lithofacies assemblage, based on the internal characteristics of the intertidal lithofacies, their vertical order and typical extent.

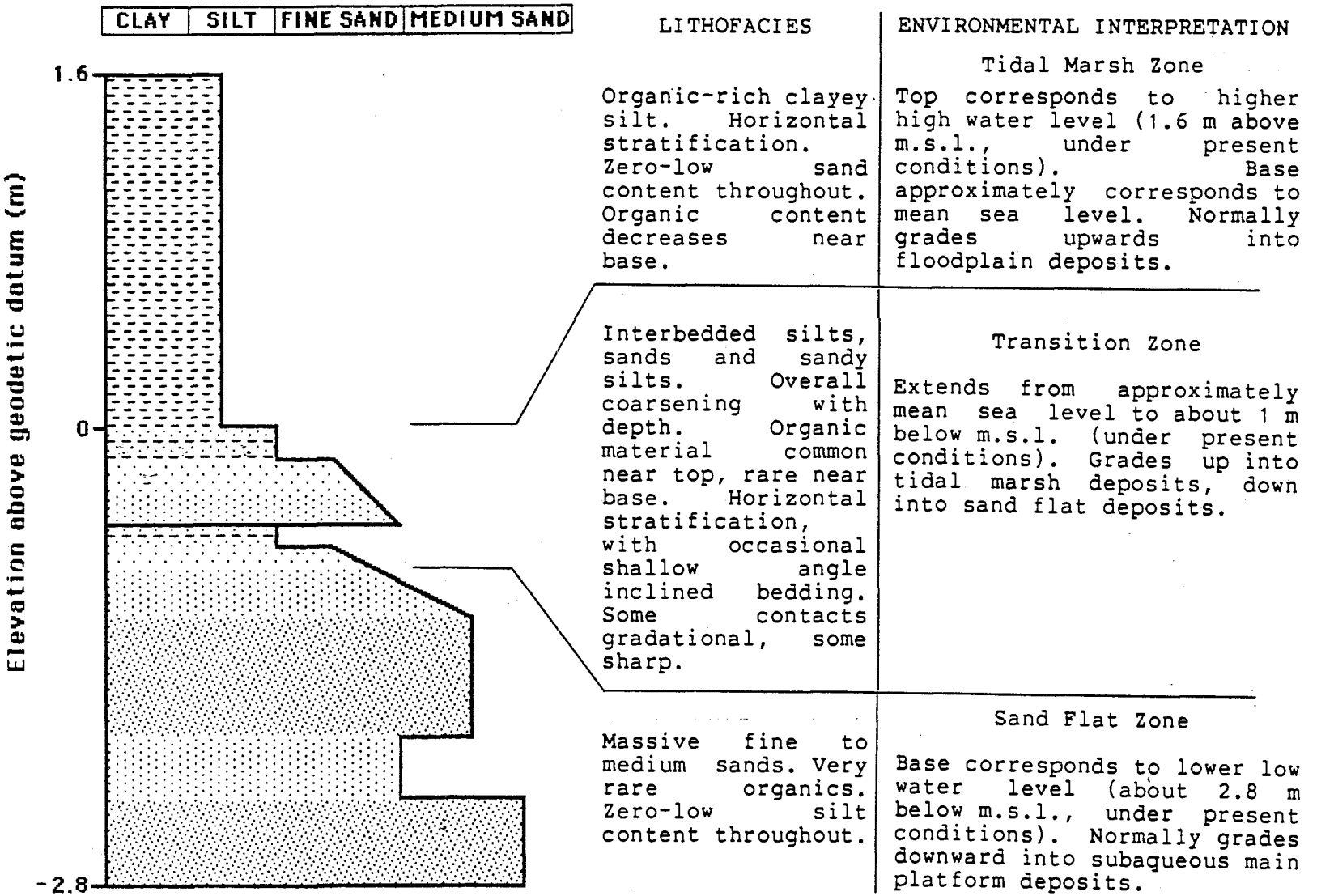

Figure 3.10 A generalized lithofacies model for the Lulu Island intertidal deposits

CHAPTER FOUR

PALYNOLOGICAL CHARACTERIZATION OF CONTEMPORARY DEPOSITIONAL ENVIRONMENTS

4.1 INTRODUCTION

The next two chapters detail characteristic microfossil assemblages for selected depositional environments on Lulu Island. This information will provide a basis for the paleoenvironmental interpretation of biofacies encountered in cores. In this chapter, palynological studies carried out on the delta will be reviewed, in order to establish characteristic pollen assemblages of selected depositional environments. Chapter 5 describes research carried out specifically for this study, to define elevational zonations of foraminifera on the Lulu Island intertidal surface.

4.2 CHARACTERISTIC POLLEN ASSEMBLAGES OF CONTEMPORARY DEPOSITIONAL ENVIRONMENTS ON THE FRASER DELTA

Characteristic pollen assemblages of surface samples from selected wetland environments on the Fraser Delta have already been established by Hebda (1977). That work will not be duplicated in this study; instead, the following sections contain a fairly detailed summary of Hebda's (1977) findings in order to present the basis of paleoenvironmental interpretations of pollen assemblages encountered in this study. In addition,

particular emphasis is given to the palynological distinction of floodplain and tidal marsh deposits. As noted previously (section 2.2.4), these deposits are not easily distinguished on the basis of the lithologic criteria used in this study.

Hebda (1977) characterized the vegetation cover and surface pollen spectra of six major vegetation zones on the Fraser Delta; peat bog (Burns Bog), Chenopodiaceae salt marsh (Boundary Bay), coastal grassland (Boundary Bay), river marsh (Ladner), river swamp (Ladner) and tidal marsh (Lulu Island) (see Fig. 2.1 for locations). The peat bog was further divided into five sub-environments, consisting of; wet heathland, dry heathland, pine woodland, birch woodland and Spiraea brushland. A summary of Hebda's findings is presented in the following sections.

4.2.1 PEAT BOG

4.2.1.1 Wet heathland

Vegetation in the wet heathland areas represents typical raised peat bog conditions, characterized by abundant Sphagnum sp. growth.

There is no significant tree overstorey, although occassional stunted Pinus contorta (shore pine), Tsuga heterophylla (western hemlock) and Betula occidentalis (western birch) do occur.

The shrub storey consists mainly of members of the Ericaceae (heaths) family. Ledum groenlandicum (common labrador tea) and Vaccinium uliginosum (bog blueberry) are the dominant species. Also present are Vaccinium myrtilloides (velvet-leaved

blueberry), Vaccinium oxycoccos (bog cranberry), Gaultheria shallons (salal), Kalmia microphylla subsp. occidentalis (western swamp kalmia), Andromeda polifolia (bog rosemary) and Empetrum nigrum (black crowberry).

The herb layer includes Rhynchospora alba (white topped beak rush), Eriophorum chamissonis (Chamisso's cotton grass), Dulichium arundinaceum (dulichium), Rubus chamaemorus (cloudberry), Drosera rotundiflora (round leaved sundew), Tofieldia glutinosa (sticky false asphodel) and Drosera anglica (great sundew). Nuphar lutea (yellow pond lily) occupy shallow, water-filled depressions on the bog surface.

The surface vegetation cover consists mainly of Sphagnum spp., with Sphagnum capillaceum the dominant species. Other mosses include Polytrichum juniperinum, Mylia anomala and Gymnocolea inflata. Two lichen species, Cladina mitis and Cladina rangiferina, often occupy the higher parts of Sphagnum hummocks.

Examination of pollen in shallow subsurface samples reveals that the preserved pollen spectrum is dominated by the influx of a regional pollen component, originating outside the local area (Fig. 4.1). Pinus, Alnus and Tsuga are all strongly represented. The Ericaceae, a major component of the local vegetation, are represented by only 4% of the preserved pollen; while Sphagnum spores comprise only 3%.

4.2.1.2 Dry heathland

In contrast to the wet heathland environment, little

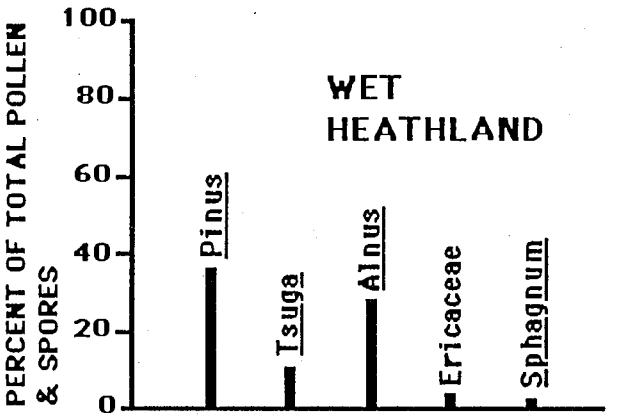

Figure 4.1 Major components of the surface pollen spectrum: wet heathland

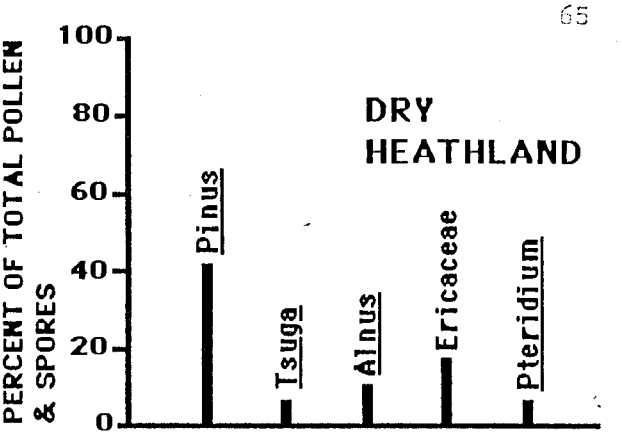

Figure 4.2 Major components of the surface pollen spectrum: dry heathland

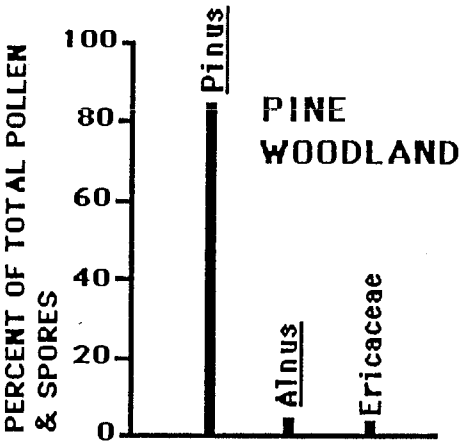

Figure 4.3 Major components of the surface pollen spectrum: pine woodland

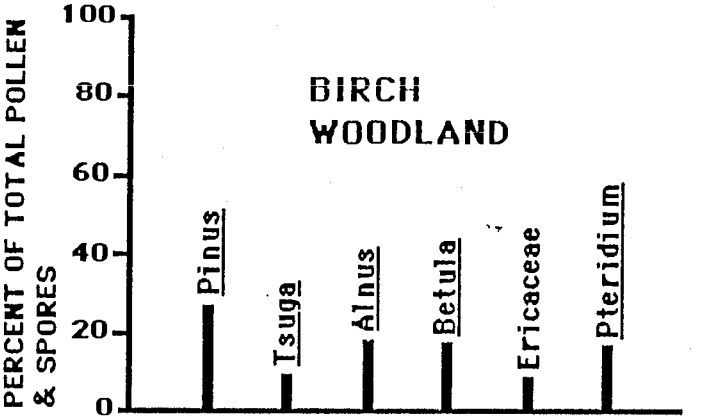

Figure 4.4 Major components of the surface pollen spectrum: birch woodland

(modified from Hebda, 1977)

Sphagnum ground cover is present. The dry heathland is characterized by Ledum groenlandicum (common labrador tea), which forms much of the shrub storey. Many of the shrubs found in wet heathland are also present, but are less abundant. Thickets of Spiraea douglasii (hardhack), Myrica gale (sweet gale) and Pteridium aquilinum (western bracken) occur on the margins of the heathland.

The herb cover is very poorly developed in the dry heathland. Mosses and lichens, however, are abundant and include, Polytrichum juniperinum, Aulocomnium androgynum, Dicranum scoparium, Stokesiella oregana, Hylocomium splendens, Pleurozium schreberi, Rhytidiadelphus loreus, Rhytidiadelphus triquetrus, Cladonia cenotea, Cladonia chlorophaea, Cladonia subsquamosa and Cladonia transcendens.

The surface pollen spectrum is again dominated by regional inputs of Pinus, Tsuga and Alnus (Fig. 4.2). Ericaceae species and Pteridium represent the local vegetation dominants.

4.2.1.3 Pine woodland

This environment is characterized by dense stands of Pinus contorta (shore pine), with an understorey of Ledum groenlandicum (common labrador tea) and Vaccinium uliginosum (bog blueberry).

The surface pollen spectrum is clearly dominated by the local influx of Pinus (Fig. 4.3). Alnus, representing the regional pollen rain, and Ericaceae, from local vgetation, are minor components.

4.2.1.4 Birch woodland

Local vegetation consists of stands of Betula occidentalis (western birch), with an understorey of Pteridium aquilinum (western bracken), Spiraea douglasii (hardhack) and Ledum groenlandicum (common labrador tea).

Surface samples contain approximately equal contributions of Pinus, Tsuga and Alnus representing regional pollen inputs, and Betula, Ericaceae and Pteridium from local vegetation (Fig. 4.4).

4.2.1.5 Spiraea brushland

Dense thickets of Spiraea douglasii (hardhack), with minor Ledum groenlandicum (common labrador tea), characterize this environment. The moss Polytrichum juniperinum forms a ground cover.

Alnus, from the regional pollen rain, dominates the surface pollen spectrum (Fig. 4.5), with Pinus, Tsuga, Betula and Spiraea forming the other major components.

4.2.2 CHENOPODIACEAE SALT MARSH

The salt marsh fringes the landward edge of Boundary Bay on the southern portion of the delta (Fig. 1.8). Major vegetation types are Salicornia virginica (american glasswort), Distichlis spicata (seashore salt grass), Puccinnellia grandis (large alkali grass) and Plantago maritima (sea plantain).

The surface pollen spectrum is dominated by local

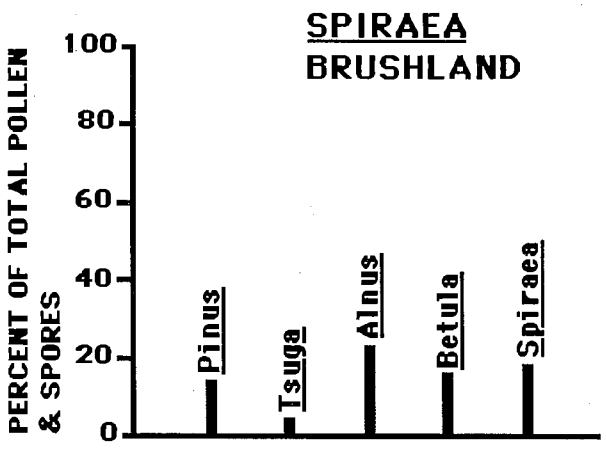

Figure 4.5 Major components of the surface pollen spectrum: Spiraea brushland

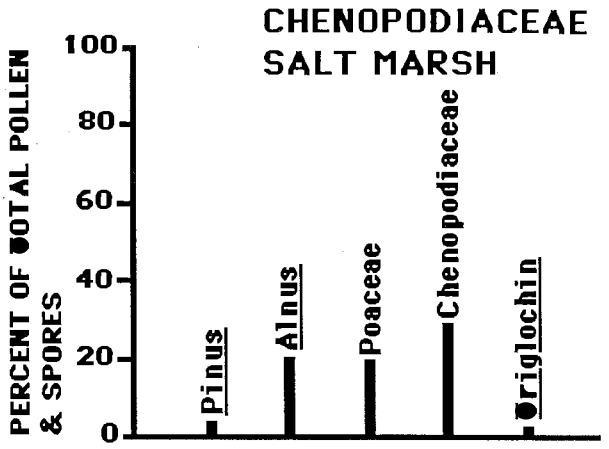

Figure 4.6 Major components of the surface pollen spectrum: Chenopodiaceae salt marsh

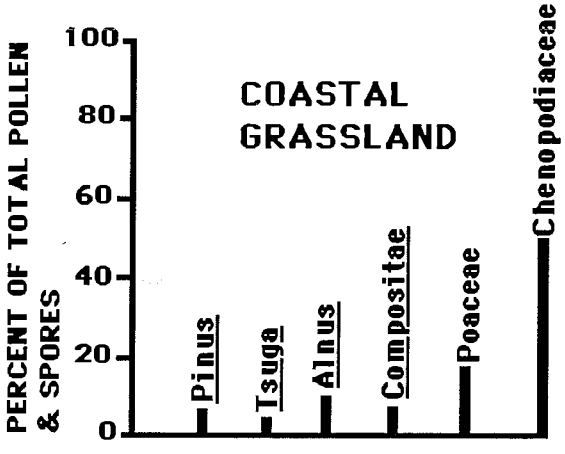

Figure 4.7 Major components of the surface pollen spectrum: Coastal grassland

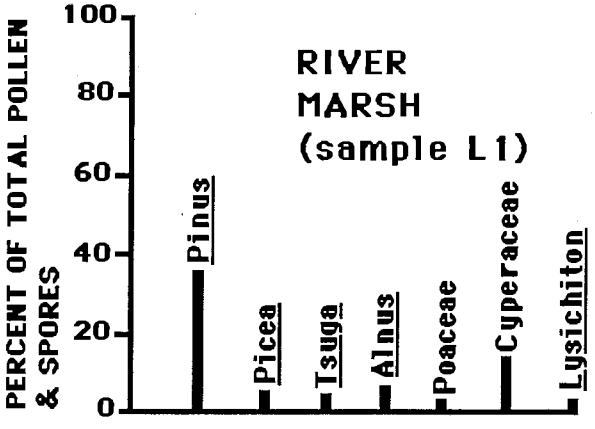

Figure 4.8 Major components of the surface pollen spectrum: River marsh

(modified from Hebda, 1977)

Chenopodiaceae. Pinus and Alnus represent a regional component from wooded areas of the delta and nearby uplands. Poaceae and Triglochin maritimum (sea-side arrow-grass) from surrounding coastal grasslands are also important contributors (Fig. 4.6).

4.2.3 COASTAL GRASSLAND

The Boundary Bay salt marsh grades landward into a coastal grassland environment. These coastal grasses occupy an area of beach deposits on the seaward side of the dyke and are not considered part of the delta's floodplain surface (Armstrong and Hicock, 1976). Aster subspicatus (Douglas' aster) and Achillea millefolium (common yarrow) are major components of this coastal grassland.

Analysis of pollen in shallow samples from this environment reveals a surprisingly low percentage of grasses (Poaceae) (Fig. 4.7). This is presumably due to poor preservation of grass pollen grains in the subsurface due to their relatively delicate nature (thin exine). Chenopods from the adjacent salt marsh dominate the pollen spectrum, with regional Pinus, Tsuga, Alnus and local Asteraceae forming the other main components.

4.2.4 RIVER MARSH (PROXIMAL FLOODPLAIN)

This marshy environment lies between the tree-covered river banks (Alnus rubra (red alder), Populus balsamifera subsp. trichocarpa (black cottonwood), Salix spp. (willows), Picea sitchensis (sitka spruce)) and the active distributary channels

of the delta. The vegetation is characterized by emergent freshwater aquatics. Lysichiton americanum (american skunk cabbage), Menyanthes trifoliata (buckbean), Carex spp. and Poaceae grow nearest the river banks. Scirpus sp., Equisetum sp., Alisma plantago-aquatica (water plantain), Sagittaria latifolia (broad-leaved arrowhead) and occasional Typha latifolia (common cattail) occupy sites nearer the water's edge.

Pollen spectra were determined for three samples from a shallow depth within this environment (Figs. 4.8 - 4.10). All three contain significant percentages of Pinus, Alnus, Tsuga and Picea pollen grains, many of which were considerably corroded. This indicates that river transport is probably responsible for the influx of at least part of the arboreal component.

Sedge (Cyperaceae) pollen forms a major component in all three samples. The remainder of the pollen spectra seemingly reflect local vegetation variations, with Poaceae, Lysichiton and Equisetum attaining prominence in at least one of the samples.

Menyanthes, Typha, Sagittaria and Alisma, although all fairly abundant in the vegetation cover, are poorly represented in the surface samples, indicating either low pollen production and or low rates of preservation in the subsurface.

4.2.5 RIVER SWAMP (DISTAL FLOODPLAIN)

This environment is represented by quiet backswamps, away from active distributaries and only infrequently inundated during periods of high water. The vegetation cover is similar to

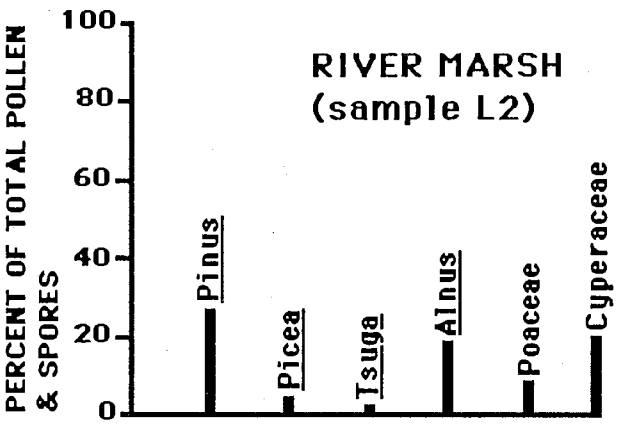

Figure 4.9 Major components of the surface pollen spectrum: River marsh (proximal floodplain) (sample L2)

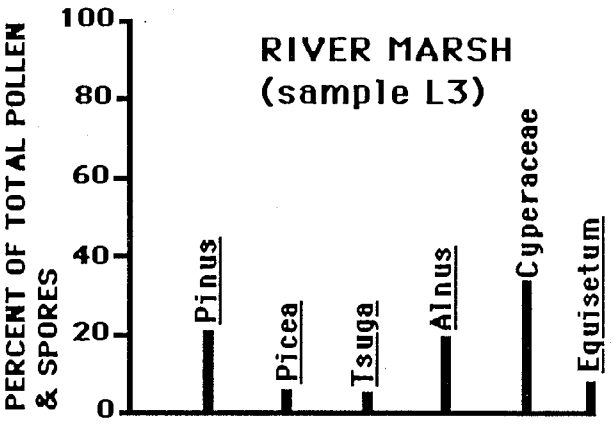

Figure 4.10 Major components of the surface pollen spectrum: River marsh (proximal floodplain) (sample L3)

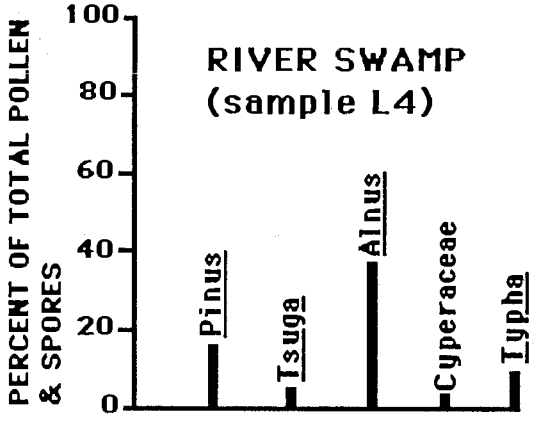

Figure 4.11 Major components of the surface pollen spectrum: River swamp (distal floodplain) sample L4

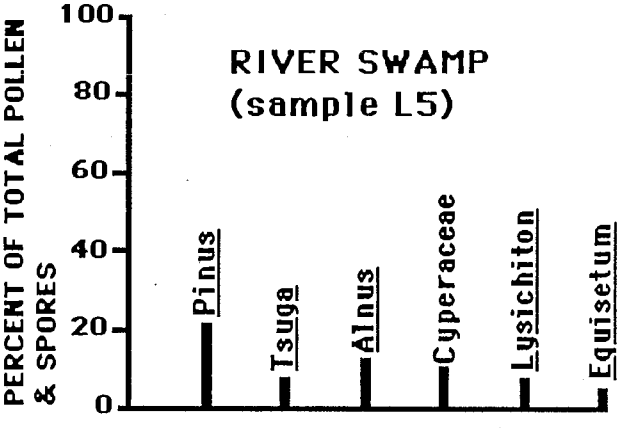

Figure 4.12 Major components of the surface pollen spectrum: River swamp (distal floodplain) sample L5

(modified from Hebda, 1977)

that of the river marsh, with Lysichiton americanum (american skunk cabbage), Typha latifolia (common cattail), Equisetum sp. and Scirpus sp. dominating.

Pinus, Alnus and Tsuga, probably in part floodwater derived, are again prominent in the surface pollen spectra (Figs. 4.11 - 4.12). The remainder of the spectra, in addition to reflecting local stands of Typha, Equisetum, Lysichiton and Cyperaceae, also indicate considerable percentages of Sphagnum spores. These spores are most likely derived from ditches draining the delta's peat bogs and do not represent local Sphagnum growth, which was not occurring in this environment.

4.2.6 TIDAL MARSH

Shallow surface samples were collected by Hebda (1977) from three distinct vegetation zones along a transect through the tidal marsh off north-west Lulu Island (Fig. 2.2). The most seaward zone consisted of pioneering Scirpus americanus (american bulrush) and Scirpus paludosus (alkali bulrush) stands. Further landward, a Typha latifolia (common cattail) dominated zone was sampled. The third zone, adjacent to the dyke, consisted of a Carex lyngbeyi (Lyngbye's sedge) - Potentilla pacifica (pacific silverweed) community.

The pollen assemblages of all three samples contain significant quantities of river-derived Pinus, Picea, Tsuga and Alnus pollen (Figs. 4.13 - 4.15). Grass pollen, also prominent in all three samples, is probably derived from nearby agricultural fields. Spores of monolete ferns, probably derived

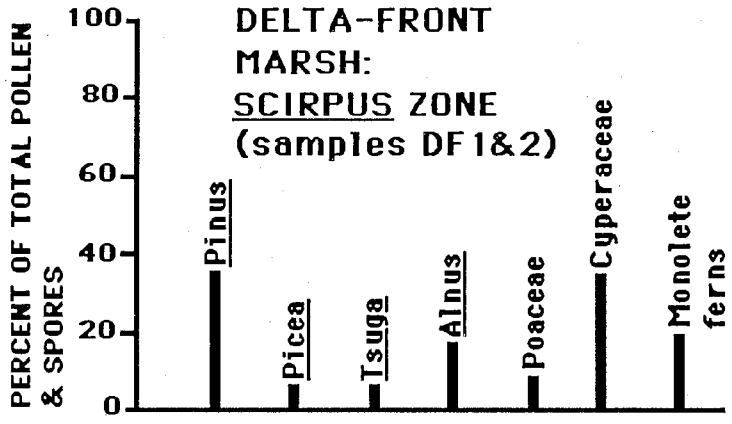

Figure 4.13
Major components of the surface pollen spectrum: Delta front marsh Scirpus zone

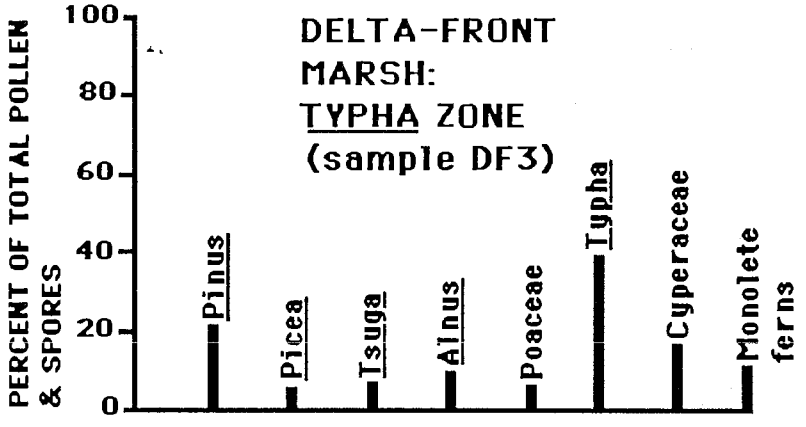

Figure 4.14
Major components of the surface pollen spectrum: Delta front marsh Typha zone

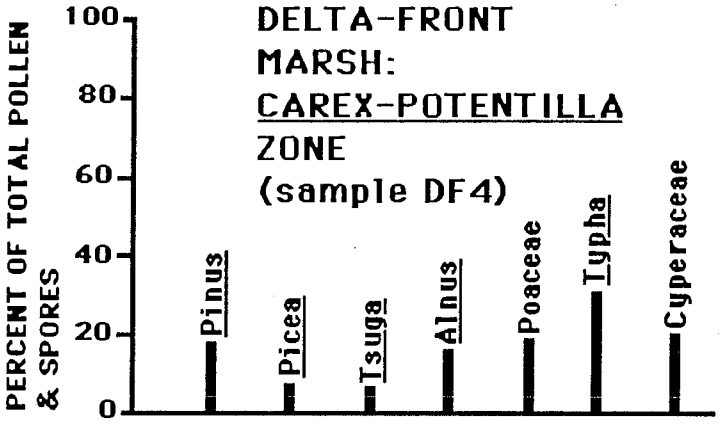

Figure 4.15
Major components of the surface pollen spectrum: Carex-Potentilla zone

(modified from Hebda, 1977)

from stands of Athyrium felix-femina (common lady fern) along river banks, reach relatively high percentages in the Scirpus and Typha zones.

The contrasts in vegetation between the three tidal marsh vegetation zones are reflected in the abundance of locally-produced pollen within the samples.

In the Scirpus zone, sedge pollen reaches 40 -50%, while Typha attains a value of only 2%. This contrast is reversed in the Typha dominated zone, which is characterized by high percentages (30%) of Typha pollen and a relatively low (20%) sedge component.

Both Typha and Cyperaceae are prominent members of the pollen assemblage in the Carex - Potentilla zone. However, this environment is distinguished from the other tidal marsh deposits by the absence of monolete fern spores and the presence of small quantities (2%) of Potentilla pollen.

4.3 POST-EUROPEAN SETTLEMENT VEGETATION CHANGES ON THE FRASER DELTA

Substantial changes in the vegetation of the Fraser Delta have resulted from widespread clearing, draining and burning, associated with the influx of European settlers during the last century (North et al., 1984). Hebda (1977) summarized these changes and attempted to reconstruct the original vegetation cover of the southern portion of the delta.

One of the major changes has resulted from attempts at land reclamation along the margins of the original peat bogs. In the

peripheral areas of the bog, pine woodland (section 4.2.1.3) and birch woodland (section 4.2.1.4) have replaced the original heathland environments. Records indicate that pine and birch woodland were not present on the delta prior to these disturbances (Hebda, 1977).

Much of the floodplain surface of the delta has been cleared, drained by extensive ditch networks and dyked to reduce flooding. Prior to its conversion to agricultural and urban uses, this area probably supported marshy grassland, sedges and mixed scrub (Rosaceae, Salix spp.) vegetation, similar to the present-day river marsh and swamp environments (sections 4.2.4, 4.2.5). River bank vegetation was apparently similar to that of the present-day, consisting of swamp forest and spruce forest (Picea (spruce), Alnus (alder), Thuja (cedar), Tsuga (hemlock), Salix (willow), Rosaceae) (Hebda, 1977; North et al., 1984)

4.4 THE PALYNOLOGICAL DISTINCTION OF FLOODPLAIN AND TIDAL MARSH DEPOSITS

The foregoing information on the characteristic palynological "fingerprints" of the floodplain and tidal marsh environments, provides a means of distinguishing deposits formed in these lithologically-similar settings.

A closer examination of the surface pollen spectra from these environments (Table 4.1), reveals many similarities in pollen content, but also a number of marked contrasts that will provide a basis for the interpretation of core samples from subsurface deposits.

Table 4.1 surface pollen spectra (%): floodplain (L) and tidal marsh (DF) environments

	FLOODPLAIN RIVER MARSH SITES			FLOODPLAIN RIVER SWAMP SITES		TIDAL MARSH SITES		
	L1	L2	L3	L4	L5	DF1&2	DF3	DF4
Pinus	35	28	22	18	25	35	21	19
Picea	5	5	7	2	3	5	6	8
Abies		0.5	1	1.5	1.5	0.5	1	
Tsuga	5	5	7	7	10	5	7	8
Pseudotsuga	0.5	1	1.5	3	1	0.5		2
cf. Thuja		2	0.5	2				1.5
Alnus	7	20	22	37	15	20	10	16
Betula	0.5	1	0.5		0.5	0.5	1	1
Salix		1	0.5			0.5	0.5	
Arceuthobium				0.5				
Myrica			0.5				0.5	
Ericaceae	1	0.5		2.5	3			
Poaceae	5	12		2	1.5	10	6	18
Asteraceae				0.5			0.5	0.5
Chenopodiaceae		2		0.5	0.5	0.5		0.5
Liliceae						1.5	1	
Lysichiton	5			1.5	12			
Cyperaceae	15	22	35	5	13	35	17	20
Typha	3	1.5	2	10	3	2	38	25
Sagittaria				1.5	0.5			
Alisma		0.5						
Apiaceae								0.5
Plantago						1.5		
Malvaceae					0.5			
Potentilla								2
Lamiaceae				1				
Equisetum	3.5	3.5	9	0.5	8			
Monolete ferns	3.5	4	3	1		22	15	
Sphagnum	2	3.5	1	8	13			

Based on Hebda (1977)
Figs. 23a,b; 24a,b; 26a,b,c.

Deposits formed in both environments often incorporate large quantities of river-transported arboreal pollen, especially Pinus and Alnus, which often dominate the pollen spectrum. Also, certain plant species, including Cyperaceae and Typha, are common to both environments and contribute pollen to the deposits of both (Table 4.1).

However, a clear contrast is apparent in the contribution of pollen and spores from the "emergent freshwater aquatics group", which characterize the floodplain environment. Equisetum (horsetail), Lysichiton (skunk cabbage) and to a lesser extent, Sagittaria (arrow-head) and Alisma (water plantain), are all represented in the floodplain samples, but do not appear at all in the tidal marsh deposits. (Sphagnum and Ericaceae in the floodplain deposits are probably derived from ditches draining nearby peat bogs and, as such, are not representative of natural conditions).

4.5 SUMMARY

The surface pollen spectra established by Hebda (1977) provide the basis for the interpretation of fossil pollen assemblages in core samples from the Fraser Delta.

Mature peat bog deposits contain an abundance of Pinus, Alnus, Ericaceae and, often, Sphagnum spores.

Salt marsh and coastal grassland environments, situated away from fluvial influences, are characterized by high concentrations of Chenopod and grass pollen.

Present-day floodplain sediments incorporate large amounts

of river-transported arboreal pollen, including Pinus, Picea, Tsuga and Alnus. Sedge pollen is also abundant. The floodplain deposits are distinguished by pollen and spores from emergent freshwater aquatics such as Lysichiton, Equisetum, Sagittaria and Alisma.

Tidal marsh deposits also contain large quantities of river-transported pollen and spores, especially Pinus, Picea, Tsuga, Alnus and monolete fern spores. Additional high concentrations in tidal marsh samples reflect locally dominant vegetation types. Cyperaceae levels are high in the Scirpus sp. and Carex-lyngbeyi - Potentilla-pacifica zones; while Typha reaches high values in sediments accumulating under Typha latifolia stands.

Changes in the original vegetation of the delta have resulted from the influx of European immigrants in the last century. Major changes included the reduction of the area of mature (Sphagnum) peat bog and the conversion of marginal bog heathland areas to pine and birch woodlands - environments not previously present on the delta. In addition, prior to these recent disturbances, the original floodplain of the delta probably consisted of a swampy grassland environment, characterized by grasses (Poaceae), sedges (Cyperaceae), emergent aquatics and mixed scrub (Rosaceae, Salix spp.).

Floodplain and tidal marsh deposits are lithologically similar, consisting of organic-rich, horizontally-bedded, clayey silt (section 3.3.1). However, the presence of pollen and spores from emergent freshwater aquatics (Equisetum, Lysichiton,

Sagittaria, Alisma) in the floodplain deposits, provides a means of distinguishing these two environments in core samples.

CHAPTER FIVE

FORAMINIFERAL ZONATIONS ON THE LULU ISLAND TIDAL FLATS

5.1 INTRODUCTION

Recent studies of foraminiferal distributions in tidal marshes have demonstrated how knowledge of present-day elevational zonations of marsh foraminifera can be used to interpret depositional environments and locate former sea levels within drill-cores (Scott, 1976, 1977; Scott and Medioli, 1978, 1980a; Scott, Williamson and Duffett, 1981).

The results of these studies indicate that distinct assemblages of foraminiferal species often occupy relatively narrow elevational zonations (with respect to sea level) on marsh surfaces. Once established, these zonations can be used on a comparative basis to locate former sea level positions within ancient marsh sequences.

Previous applications of this technique (Scott and Medioli, 1980b) suggest that biofacies analysis based on foraminiferal assemblages offers a high degree of elevational resolution, enabling, for example, lithologically identical upper, mid and lower tidal marsh deposits to be distinguished.

A potential accuracy of sea level relocation of $\pm$ 5 cm is proposed on the basis of results from Atlantic marshes (Scott and Medioli, 1978); whereas an accuracy of $\pm$ 20 cm is claimed for studies carried out in the Bay of Fundy (Smith et al., 1984).

This chapter describes the field and laboratory techniques used to define foraminiferal zonations on the Lulu Island tidal flats. It is anticipated that the establishment of intertidal foraminiferal distributions on Lulu Island will provide a means of identifying both the environment and the elevation of deposition of intertidal deposits encountered in drill cores.

5.2 PREVIOUS WORK

Phleger (1967) described the foraminifers present in five samples collected from Sea Island marsh and a further eight samples from marshes fringing Westham Island at the mouth of the main channel of the Fraser River (Fig. 1.8). The determination of foraminiferal zonations did not form part of that study and consequently precise sample locations were not obtained. Miliammina fusca was by far the most abundant species and dominated most of the assemblages. Trochammina macrescens was dominant in one sample from the Sea Island marsh. Other common species included Jadammina polystoma, Haplophragmoides subinvolutum, Ammobaculites sp., Ammotium cf. salsum and Pseudoclavulina sp.

The Sea Island specimens were wholly arenaceous in character, which was attributed to large inputs of sediment-laden fresh water from the Fraser River. The resulting low salinity, and possibly low pH, of the marsh water appears to deter the invasion of open-ocean species, most of which have calcareous tests (Phleger, 1967).

5.3 METHODS

5.3.1 SAMPLING

Samples were selected from the set of surface grab samples and core samples previously obtained from the tidal flats for grain size determinations (section 3.2). Sample locations were widely scattered over the tidal flats in order to determine lateral, as well as elevational, variations in foraminiferal distributions.

Positioning of the sampling points was determined on the basis of several compass bearings on fixed objects onshore, giving an estimated accuracy of $\pm$ 50 metres. Approximate elevations of the sampling locations were obtained by reference to a 1967 topographic map of the tidal flats, produced for the National Harbours board (Fig. 3.1). The presence or absence of vegetation was also noted at each sampling point. A total of 28 surface samples were selected - 24 grab samples and 4 samples from the tops of the short cores obtained from the tidal flats (section 3.2) (Fig. 5.1).

In addition to surface sampling, samples were also collected from several depths within each of the four short tidal flat cores (section 3.2). These samples were included for analysis in order to determine if distinct, identifiable foraminiferal assemblages are well-preserved in recently buried intertidal deposits.

5.3.2 SAMPLE ANALYSIS

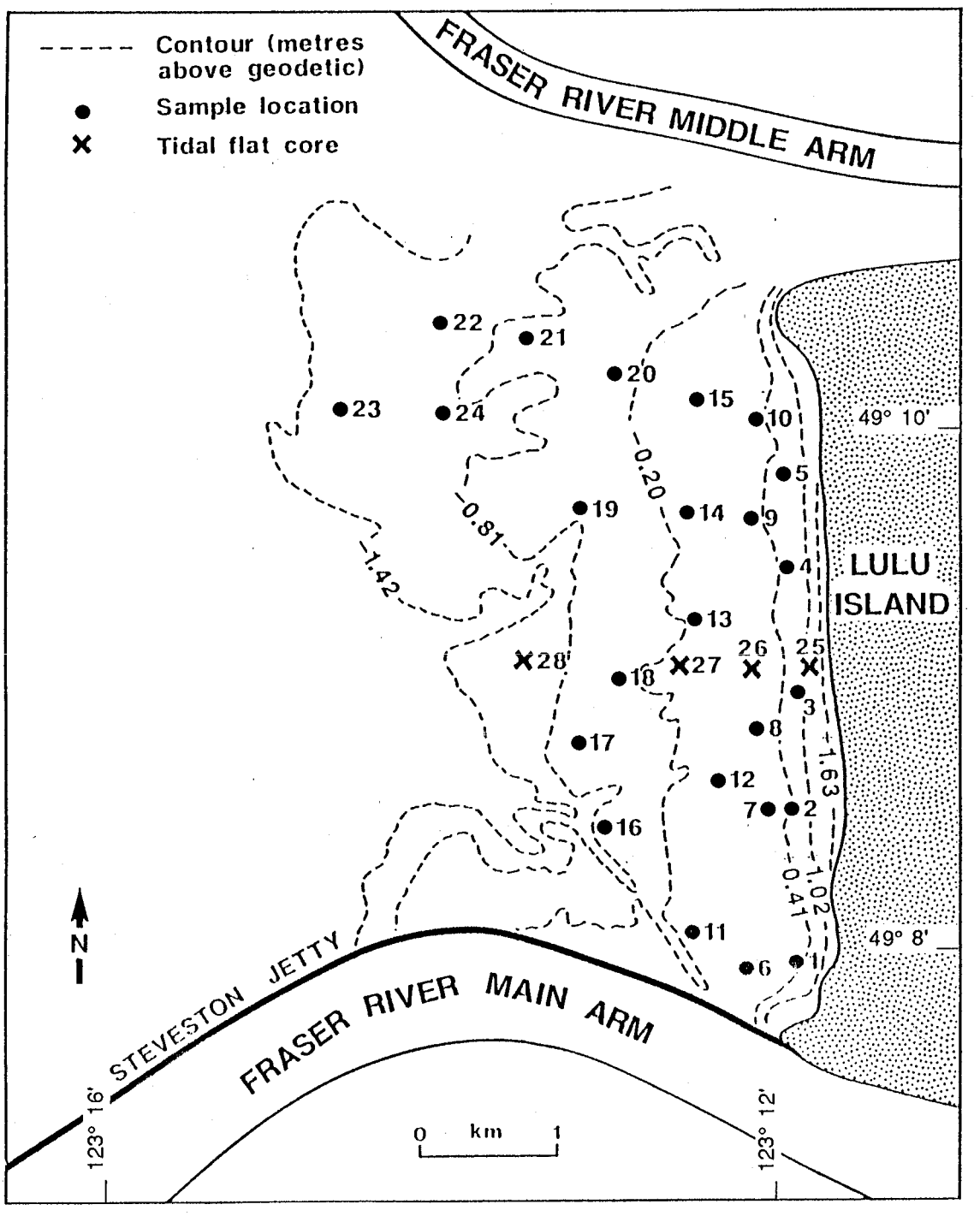

Figure 5.1 Sampling locations: foraminifera study

All samples were air-dried, weighed and wet sieved through 0.5 mm and 0.063 mm sieves. Coarse organics were retained in the 0.5 mm sieve; silt and clay were washed through the 0.063 mm sieve. Foraminifera were retained between the two sieves. Most of the fine organics were removed at this stage by decantation with water. Where the samples were sandy the foraminifera were separated by flotation in tetrachloroethylene.

Specimens were identified to the species or generic level. No attempt was made to distinguish living foraminifera from total populations (living + dead). Assemblages were established on a total population basis to ensure integration of all seasonal variations and to eliminate the risk of overemphasizing seasonal fluctuations in species abundance (Scott and Medioli, 1980b).

It should be noted that this technique does not necessarily reflect the distribution of living foraminifera, since some species may be more prone to redistribution after death than others (i.e. some species may be preferrentially washed into the upper marsh by incoming tides; some species may be more efficiently trapped by the filtering action of vegetation than others etc.).

However, since this study is concerned with the interpretation of subsurface deposits, it is only necessary to know the distribution of species upon incorporation into the intertidal sediments. Thus, this technique is still valid, regardless of how the foraminiferal distributions are derived, as long as the patterns of incorporation into the subsurface are

consistent through time - which is assumed to be the case in this study.

Where the number of foraminifera in a sample was low (<500), all the specimens present were counted. A number of samples contained several thousand specimens. In these cases a subsample was weighed, counted, and the resulting count multiplied by a proportionality factor (based on the weight of the original sample compared to the weight of the subsample), to provide an estimate of the total population.

Foraminiferal assemblages were devised on the basis of relative species abundances, measured as percentages of total counted populations. The sampling system used also yields a measure of foraminiferal density on a dry weight basis (number of specimens per 100 g of sample). Compared to the standard volume basis, this measure, when used as a comparative tool, is subject to some error due to variation in the bulk densities of samples. However, such error will not obscure overall patterns, since variations in foraminifera density are several orders of magnitude greater than estimated variation in sample bulk densities.

5.4 RESULTS

5.4.1 SURFACE SAMPLES

5.4.1.1 Introduction

Only five species were present in the twenty eight samples analysed; Polystomammina grisea, Haplophragmoides sp. cf. H.

canariensis, Ammonia beccarii, Miliammina fusca and Rosalina columbiensis (Table 5.1).

Foraminiferal densities varied greatly, ranging from 17913 to 4 specimens per 100 g. Three broadly defined density zones are apparent - a high density zone, with density values exceeding several thousand, in the upper reaches of the tidal marsh; an intermediate zone, with density values ranging from 50 to 3500, in the central part of the tidal flats, and a low density zone, with density values below 50, in the lower reaches of the tidal flats and adjacent to the Main Arm of the Fraser River (Fig. 5.2).

5.4.1.2 Elevational Zonations

A plot of sample elevation against relative species abundance suggests that apparently well-defined elevational zonations in foraminiferal assemblages are present across the tidal flat surface (Fig. 5.3). A high elevation zone, composed almost entirely of Polystomammina grisea and Haplophragmoides sp. cf. H. canariensis lies between higher high water (140 cm) and about 50 cm above geodetic datum. Ammonia beccarii is most abundant in a narrow elevational zone, from 50 cm to 30 cm. Miliammina fusca dominates a third zone, lying between 30 cm and geodetic datum. Elevations below geodetic datum constitute a fourth major zone, dominated by Miliammina fusca and Rosalina columbiensis.

Table 5.1 Absolute and relative species abundance, tidal flat samples

	SAMPLE NUMBER							
	1	2	3	4	5	6	7	8
Weight (g)	111.5	143.6	71.4	118.5	80.4	304.4	346.7	336.2
Elevation* (cm)	42	78	107	72	85	25	34	35
Mean grain size (um)	1.5	2.5	1.2	2.6	2.1	3.4	3.2	7.4
	No./%	No./%	No./%	No./%	No./%	No./%	No./%	No./%
Polystomammina grisea	113/93	164/53	48/31	71/65	60/65	78/89		
Haplophragmoides sp. cf.		148/47	108/69	38/35	31/33	2/2	1/4	
H. canariensis								
Ammonia beccarii							25/96	42/100
Miliammina fusca	9/7				2/2	8/9		
Rosalina columbiensis								

	9	10	11	12	13	14	15	16
Weight (g)	192.4	209.4	436.9	417.3	333.6	449.4	398.3	206.8
Elevation* (cm)	37	45	-7	11	-12	1	13	-60
Mean grain size (um)	3.4	3.7	5.6	8.7	28.4	9.2	13.2	9.0
	No./%	No./%	No./%	No./%	No./%	No./%	No./%	No./%
Polystomammina grisea		8/5	6/38		2/1	11/8	6/4	
Haplophragmoides sp. cf.		6/3	2/12			2/2	1/1	
H. canariensis								
Ammonia beccarii	187/100	152/89	8/50	6/2		7/5	2/1	
Miliammina fusca		5/3		334/98	134/99	116/85	135/94	8/6
Rosalina columbiensis								132/94

	17	18	19	20	21	22	23	24
Weight (g)	434.8	364.9	240.1	298.1	426.8	480.1	607.2	408.0
Elevation* (cm)	-55	-31	-70	-35	-64	-164	-114	-99
Mean grain size (um)	235.6	301.2	44.8	28.9	355.0	53.1	223.5	172.1
	No./%	No./%	No./%	No./%	No./%	No./%	No./%	No./%
Polystomammina grisea			3/3	2/1			2/8	
Haplophragmoides sp. cf.							1/4	
H. canariensis								
Ammonia beccarii								
Miliammina fusca	18/8	12/2	107/96	312/99	10/67	94/75	15/60	49/84
Rosalina columbiensis	208/92	646/98	2/1		5/33	31/25	7/28	9/16

* relative to geodetic

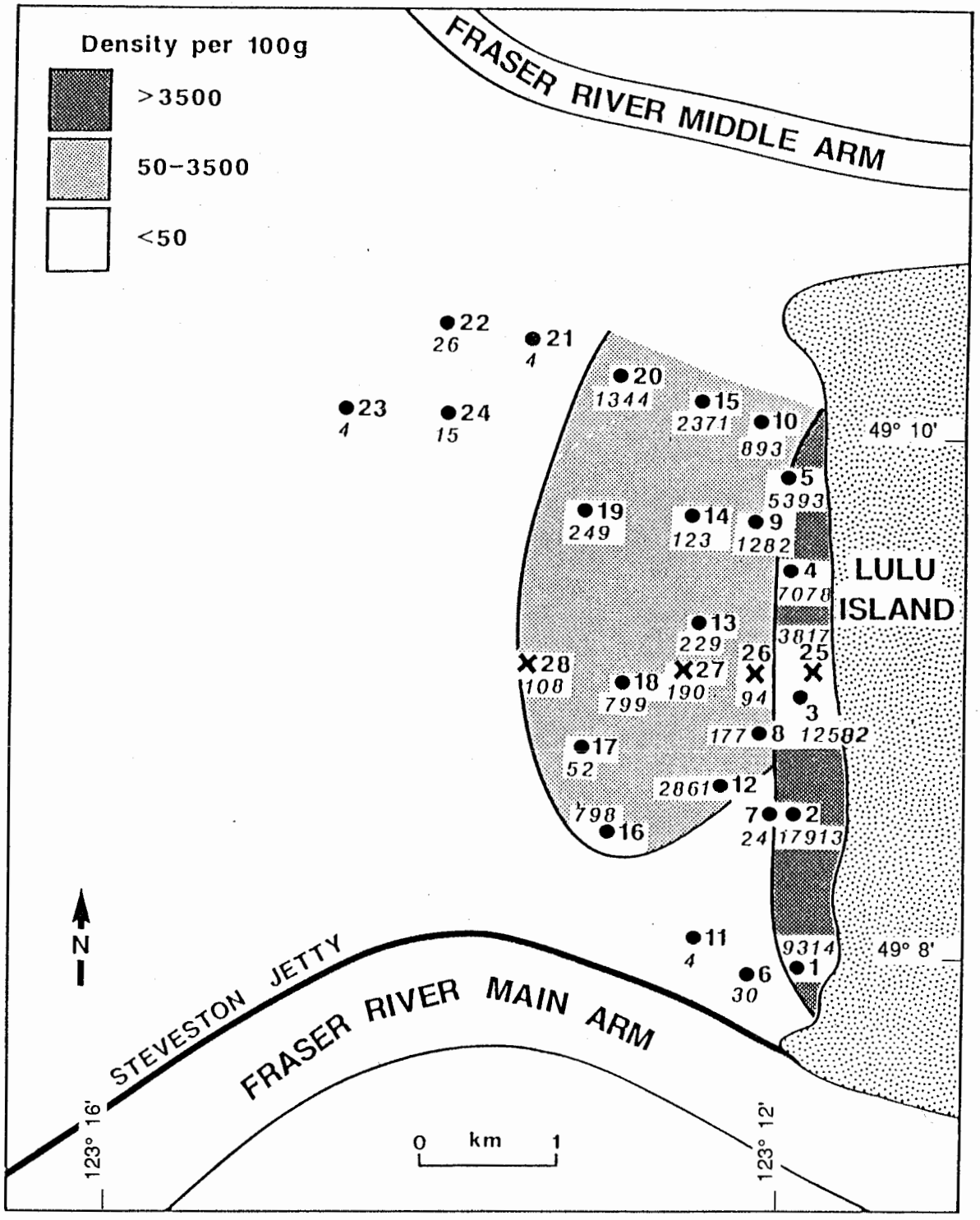

Figure 5.2 Foraminiferal densities: Lulu Island intertidal surface

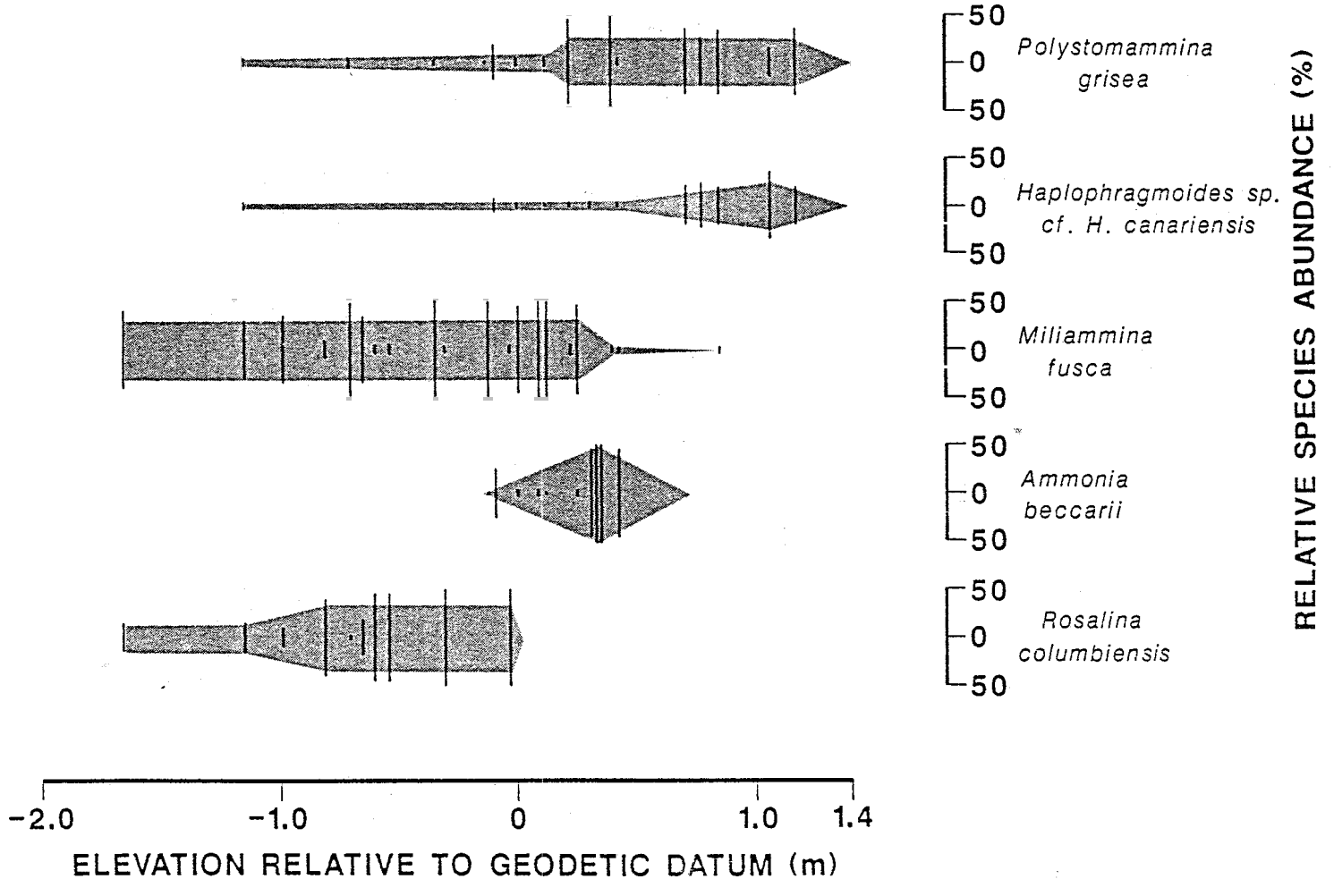

Figure 5.3 Foraminifera elevational zonations (Full width of the percentage scale (50 - 50) equals 100 % species abundance)

5.4.1.3 Lateral Variability

In order to gain an indication of the degree of lateral variability in the foraminiferal zonations, a cluster analysis was performed to group together samples on the basis of relative species abundance. Four clusters were generated (Fig. 5.4). The clusters consist of a Polystomammina grisea-Haplophragmoides sp. cf. H. canariensis grouping, these two species comprising at least 91% of the included assemblages; an Ammonia beccarii grouping, this species accounting for at least 50% of all specimens; a Miliammina fusca grouping, with all samples containing at least 60% of this species, and a Rosalina columbiensis grouping, in all cases containing at least 84% of this species.

The clusters were plotted on a map of the tidal flats to illustrate their spatial extent. The result (Fig. 5.5) indicates that the Miliammina fusca and Rosalina columbiensis distributions exhibit considerable lateral variability, unrelated to elevational changes. The Polystomammina grisea-Haplophragmoides sp. cf. H. canariensis and Ammonia beccarii distributions do appear to approximately correspond to elevational zonations.

To investigate further the apparent lateral variability of species distributions on the lower tidal flats, maps were constructed to show the distributions of species on a density basis (Number of species per 100 g of sample), rather than on a relative abundance (percentage) basis. This has the advantage of showing species distributions in absolute terms and eliminates

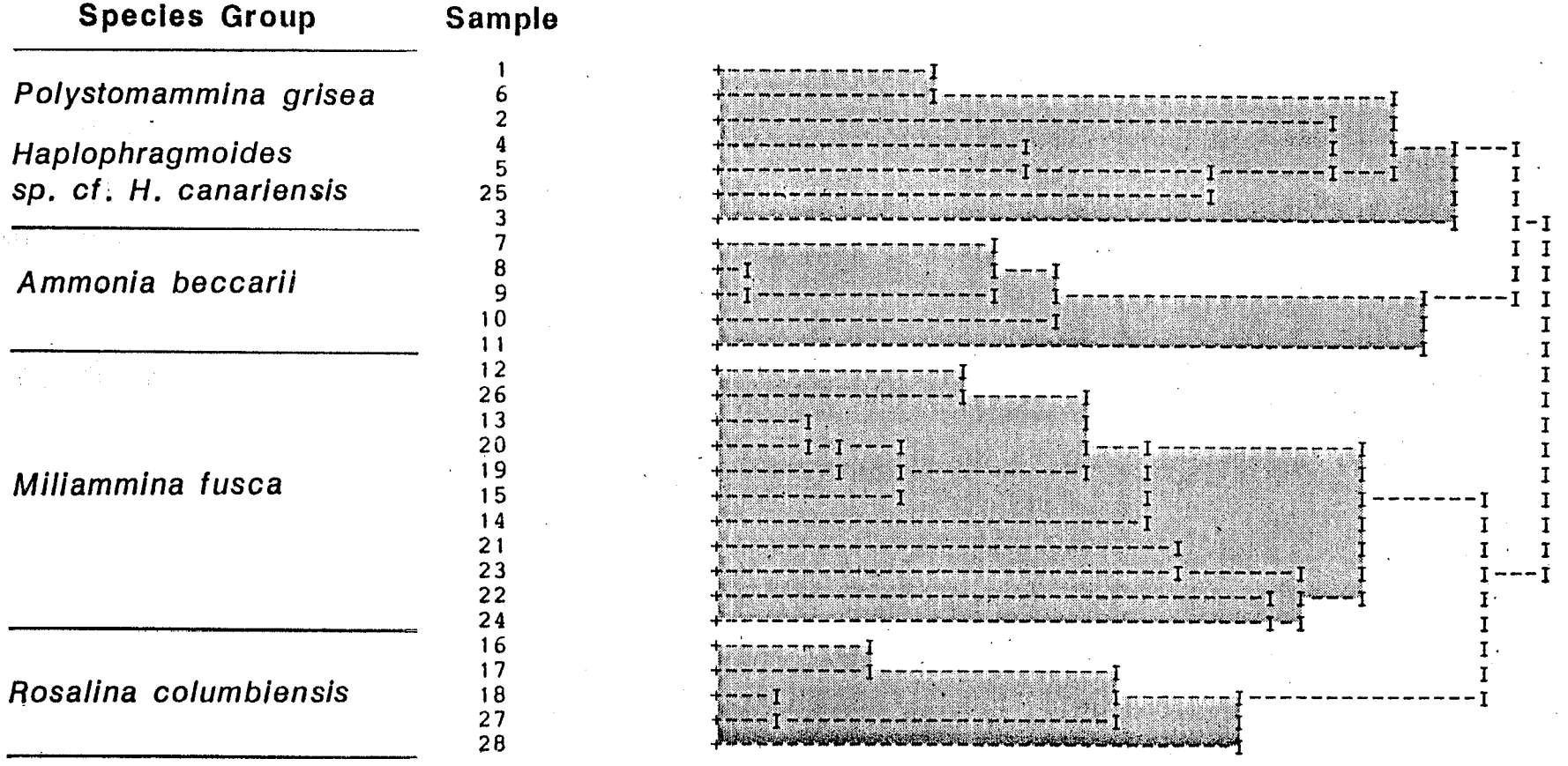

Figure 5.4 Results of cluster analysis

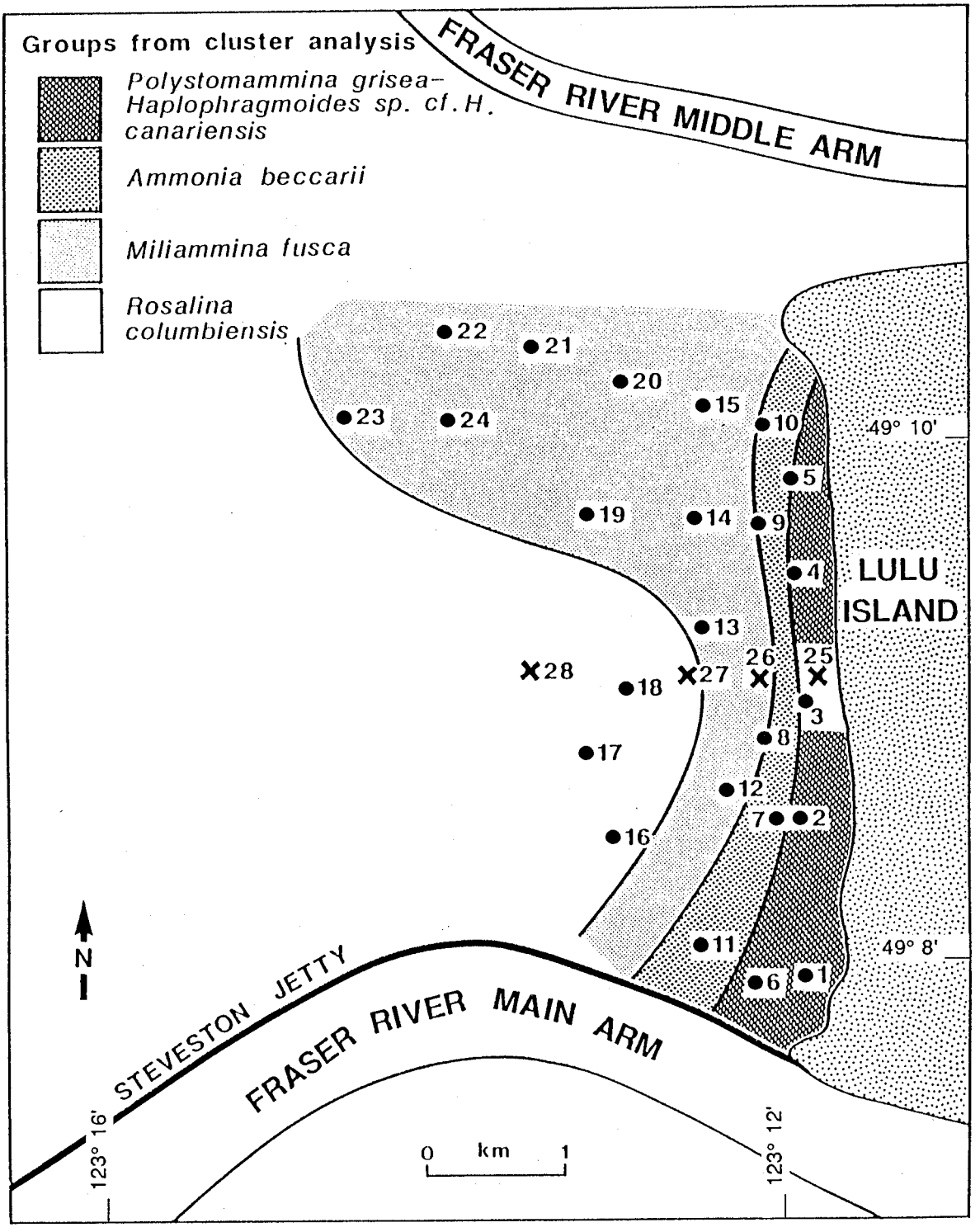

Figure 5.5 Map of species groupings from cluster analysis

apparent spatial variability in one species which may in fact result from variability in abundance of other species.

The results (Fig. 5.6a-f) suggest that the major concentrations of Polystomammina grisea, Haplophragmoides sp. cf. H. canariensis, Ammonia beccarii and Miliammina fusca all closely correspond to elevational zonations. Only the Rosalina columbiensis distribution displays a pronounced lateral variability, with considerably higher concentrations of this species occurring in the south of the lower tidal flats, than at corresponding elevations to the north. A composite map, consisting of the higher concentration zone for each species (Fig. 5.6f) clearly illustrates the concentration of Rosalina columbiensis in the southern part of the study area.

Environmental factors other than elevation which may influence foraminiferal distributions include sediment grain size and the presence or absence of vegetation (Murray, 1973). As data on these two factors were available for the intertidal surface, a scatter plot was constructed to illustrate the relationship between mean grain size, presence-absence of vegetation, elevation and the foraminiferal assemblage groupings derived from the cluster analysis (Fig. 5.7).

The Polystomammina grisea-Haplophragmoides sp. cf. H. canariensis and Ammonia beccarii clusters each occupy a distinct range of environmental conditions, occurring in vegetated sites, at higher elevations and with fine grained substrates. The Miliammina fusca and Rosalina columbiensis clusters clearly can not be distinguished on the basis of these factors. Both occur

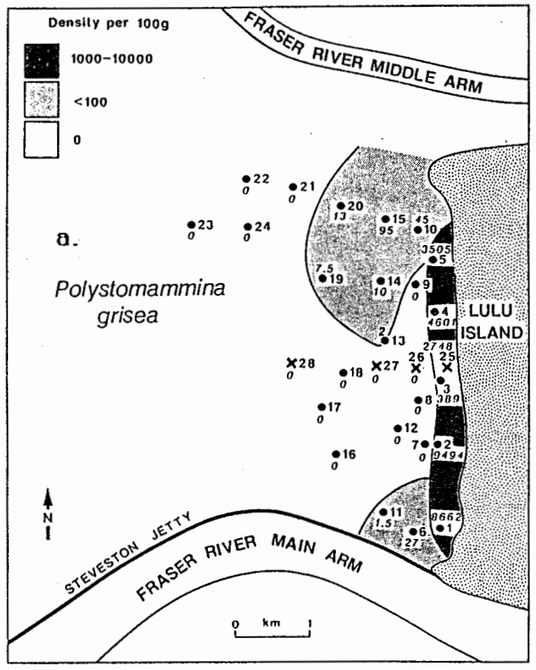

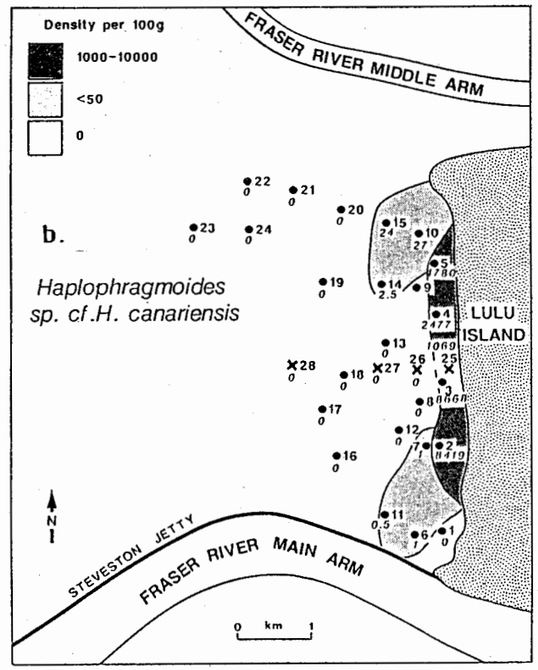

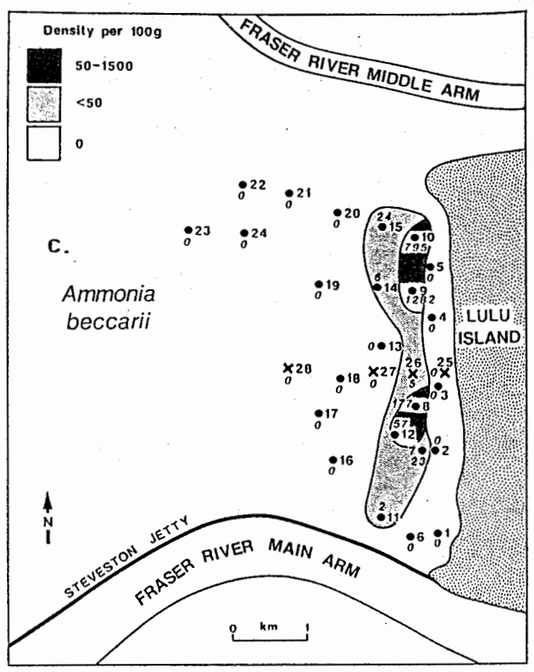

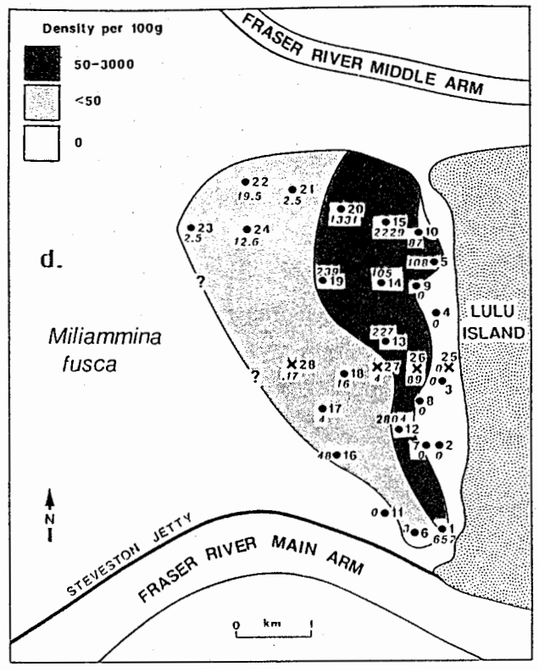

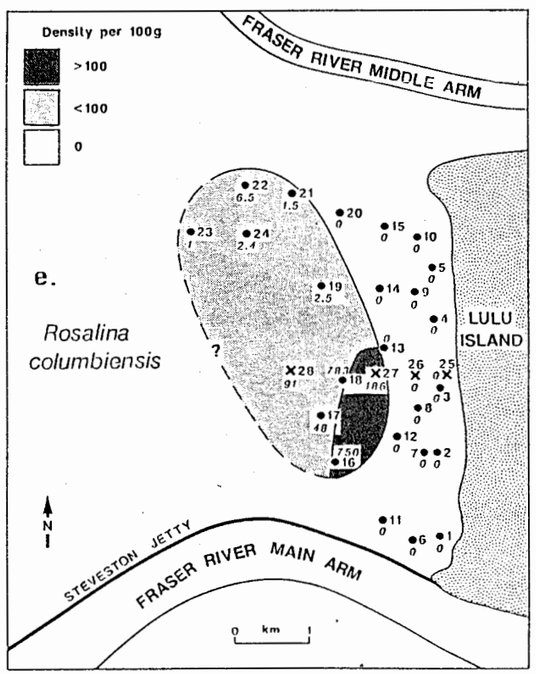

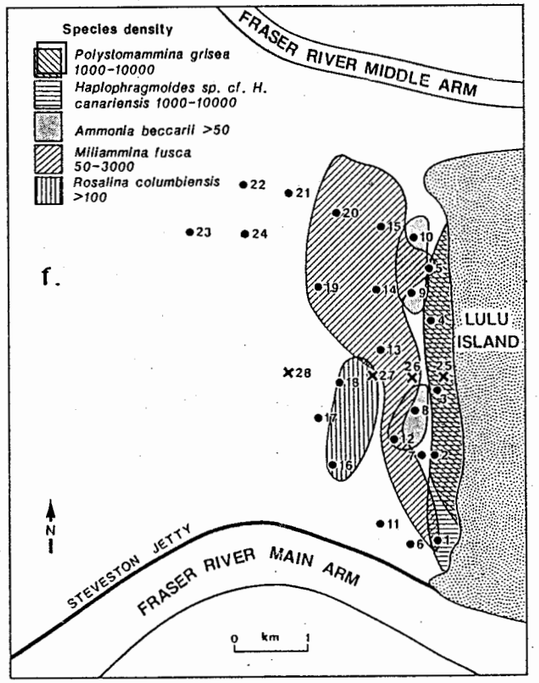

Figure 5.6 Foraminiferal densities by species:
a. Polystomammina grisea b. Haplophragmoides sp. cf. H. canariensis c. Ammonia beccarii d. Miliammina fusca e. Rosalina columbiensis f. Composite, showing highest density zone for each species

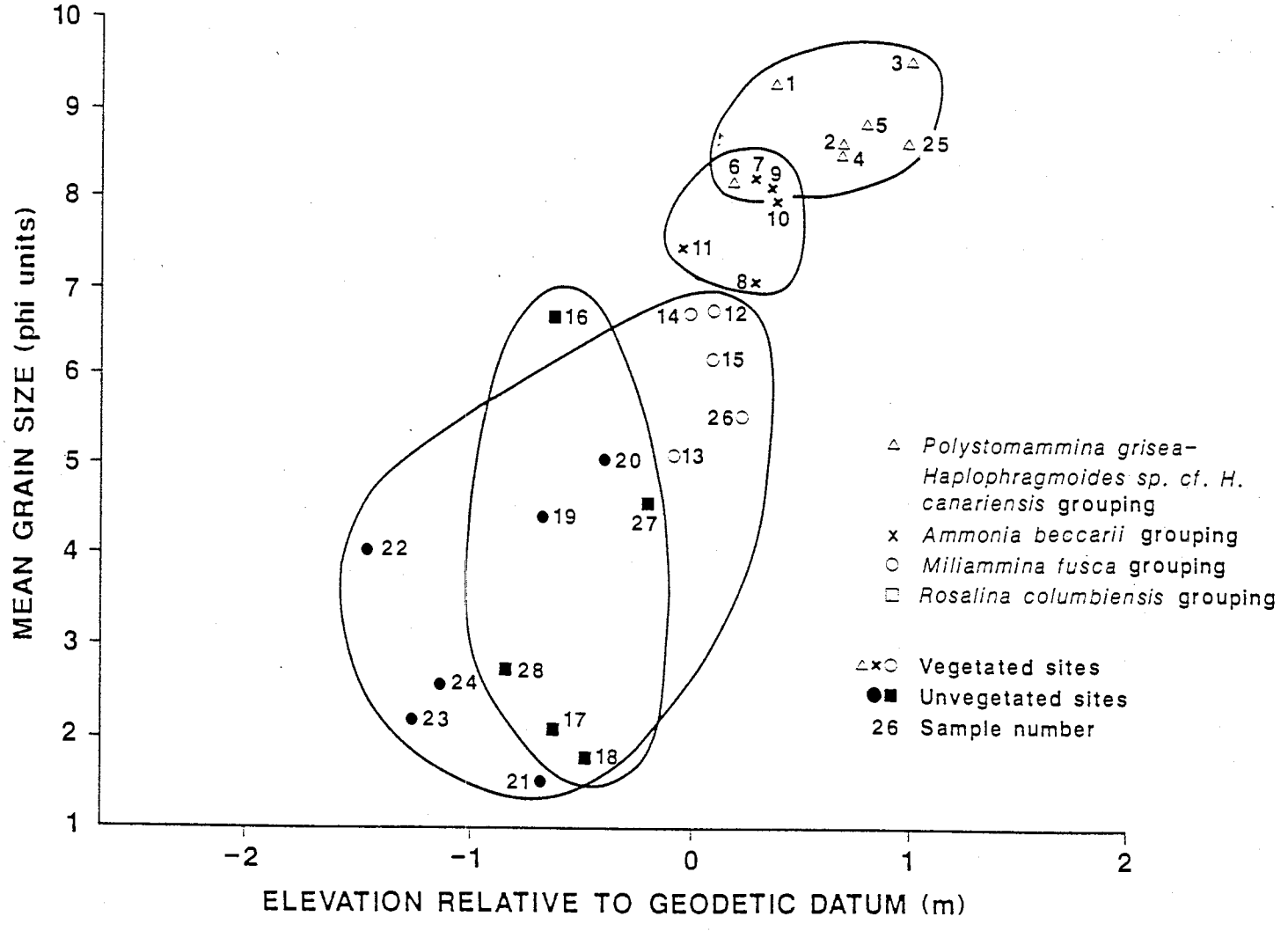

Figure 5.7 Scatter plot showing relationship between mean grain size, elevation, presence/absence of vegetation and the foraminiferal groupings from cluster analysis

at similar elevations, over a wide range of sediment sizes and in unvegetated locations. The results suggest that environmental factors other than those considered above are responsible for the concentration of Rosalina columbiensis in the southern part of the tidal flats (i.e. salinity, exposure, etc.).

5.4.2 CORE SAMPLES

The results of the analysis of the tidal flat core samples are shown in Table 5.2. Generally, these results indicate that there is a good correspondence between present-day foraminiferal zonations on the tidal flat surface and the foraminiferal assemblages incorporated into the subsurface (Fig. 5.8).

Only the sample from core TFC 1 at a depth of 125 cm does not conform to the expected pattern. This sample contained only 4 specimens (Table 5.2). The assignment of "dominance" to one particular species based on such low numbers is obviously tenuous and probably explains this anomaly.

The results also show that the numbers of foraminifers in the subsurface are surprisingly low. Foraminiferal densities decline rapidly with depth, falling to or near zero within 50 cm of the surface in three of the cores (Fig. 5.9). Only in the upper tidal marsh core (TFC 1) do foraminiferal densities remain reasonably high (33 specimens per 100 g) below 50 cm depth. The contrast between surface and subsurface foraminiferal densities suggests that the foraminiferal tests are not well preserved in the subsurface of the delta.

Table 5.2 Absolute and relative species abundance, tidal flat core samples

			Species abundance (number/density per 100 g)				
Sample No.	Depth (cm)	Weight (g)	*Polystomammina grisea*	*Haplophragmoides sp. cf. H. canariensis*	*Miliammina fusca*	*Ammonia beccarii*	*Rosalina columbiens.*
TFC 1	0	41.5	1140/2747	444/1070			
TFC 1	75	75.3	15/20	10/13			
TFC 1	125	404.1	2/0.5		1/0.25	1/0.25	
TFC 2	0	60.5			54/89	3/5	
TFC 2	40	87.7					
TFC 2	92	112.0		1/0.9			2/1.8
TFC 3	0	53.7				2/3.7	100/186
TFC 3	40	88.4	2/2.3		7/7.9		
TFC 3	80	89.5		2/2.2	2/2.2		18/20
TFC 4	0	47.2			8/17		43/91
TFC 4	13	75.2			2/2.7		
TFC 4	48	103.5					
TFC 4	85	90.6					

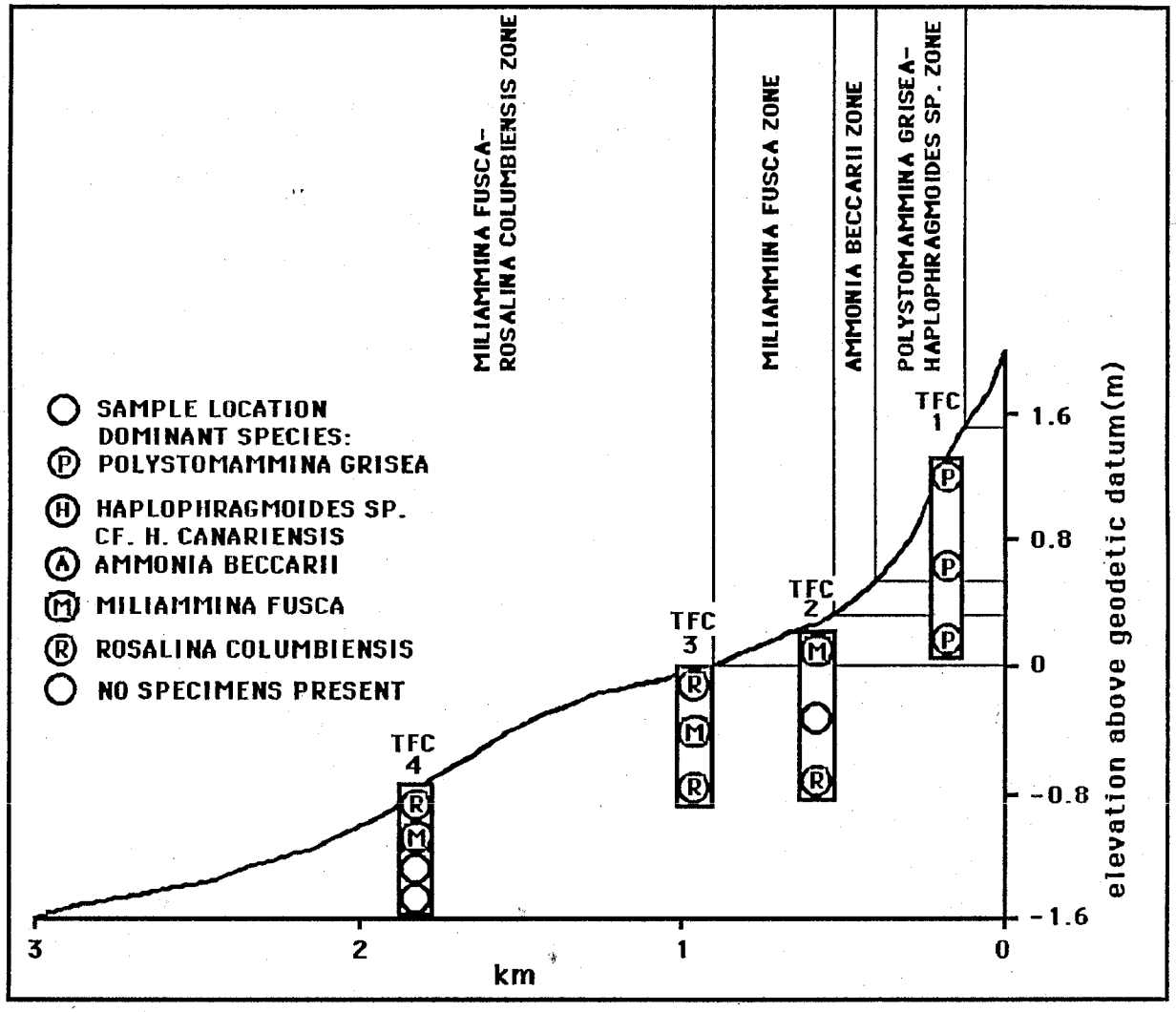

Figure 5.8 Intertidal surface foraminiferal zonations and subsurface biofacies

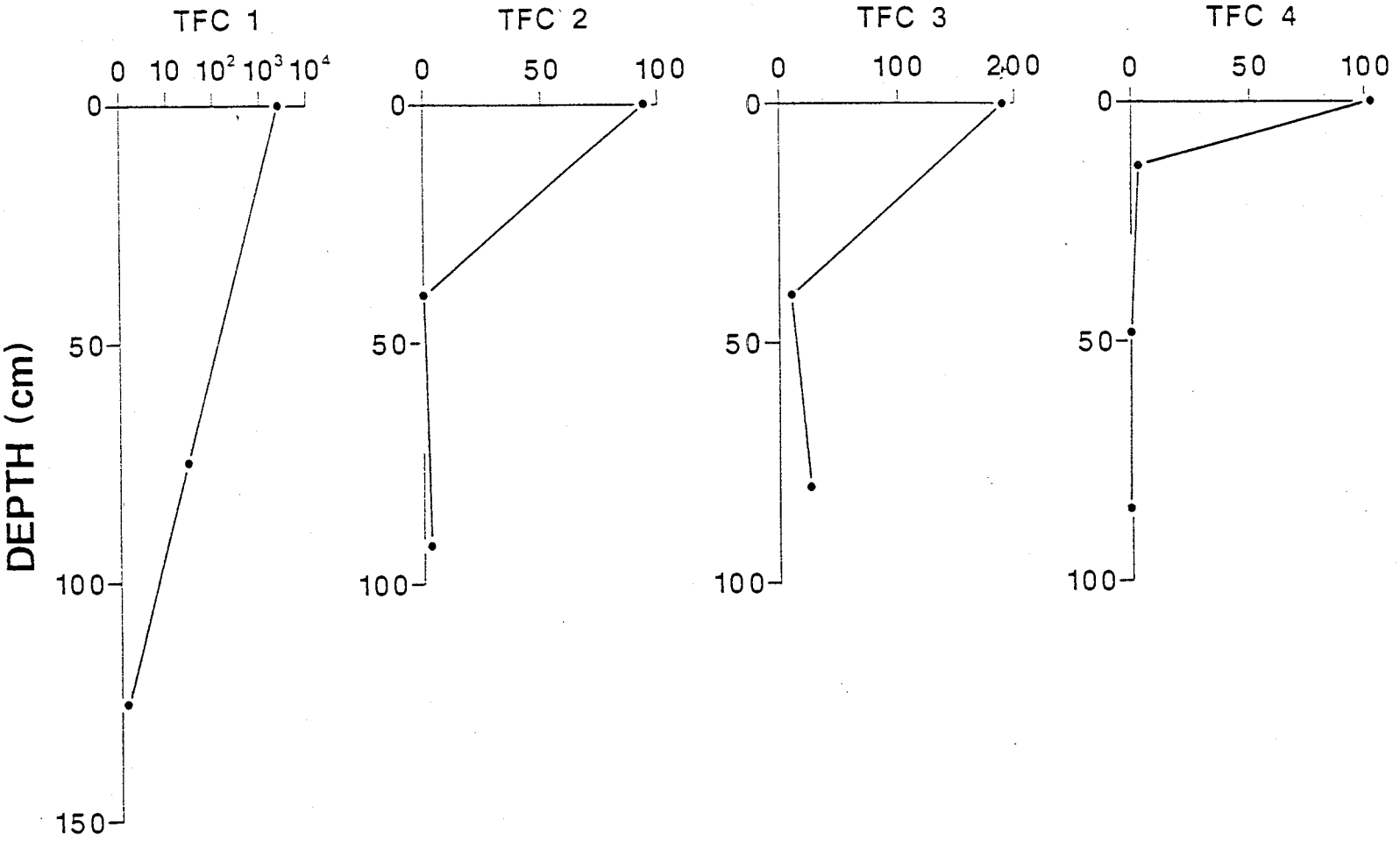

Figure 5.9 Foraminiferal density v depth: tidal flat core samples

5.5 DISCUSSION

The results demonstrate that well-defined foraminiferal zonations are present on the Lulu Island tidal flats. A Polystomammina grisea-Haplophragmoides sp. cf. H. canariensis dominated zone lies between 140 and 50 cm above geodetic datum; Ammonia beccarii is most abundant between 50 and 30 cm; Miliammina fusca dominates a zone between 30 cm and geodetic datum, and elevations below geodetic datum constitute a forth zone, dominated by Miliammina fusca and Rosalina columbiensis. For the most part these zones appear to coincide with elevational zonations, although one tidal flat species, Rosalina columbiensis, exhibits considerable lateral variability.

The lateral variability in the distribution of Rosalina columbiensis does not appear to be related to variations in sediment size or vegetation cover. Another possibility is suggested by the configuration of the intertidal surface (Fig. 5.1). A large dendritic drainage network occupies much of the southern part of the tidal flats (Luternauer, 1980). Drainage of ebb tides from the higher tidal marsh may thus be concentrated to the south. Such a tidal circulation pattern may act to maintain higher water levels over the southern tidal flats in contrast to the north. An obvious consequence of elevated water levels in this area would be to reduce exposure time, a condition favourable to Rosalina columbiensis which generally prefers normal marine conditions (Murray, 1973).

The low numbers of foraminifera found in the core samples indicates low rates of preservation of foraminiferal tests in

the subsurface of the Fraser Delta. The largest concentrations of foraminifera tests are apparently preserved within deposits corresponding to the contemporary high marsh environment. Here, surface foraminifera densities reach their highest values (Fig. 5.2). This environment corresponds to the Polystomammina grisea - Haplophragmoides sp. cf. H. canariensis dominated zone (Fig. 5.5). This assemblage, if found within a core sample, would suggest the deposit formed approximately 0.5 to 1.4 m above mean sea level, based on present-day conditions.

CHAPTER SIX

SUBSURFACE DATA COLLECTION

6.1 INTRODUCTION

Subsurface data were collected to meet two major objectives: firstly, to establish the regional lithostratigraphy of Lulu Island; and, secondly, to provide a basis for paleoenvironmental interpretation of subsurface deposits - which is dealt with in the next chapter.

In addition, a limited amount of subsurface investigation was carried out in the western Fraser River floodplain, in order to determine if the deposits related to the episode of aggradation on the delta could be traced laterally into the adjoining fluvial setting.

6.2 METHODS

6.2.1 DATA COLLECTION

Subsurface information was collected using a Concore C-68 drill rig and a vibracorer (Smith, 1984). Selected borehole logs and core samples (samples of the tephra layers in drill holes TH84-13 and TH85-14) were also provided by the B.C. Ministry of Transportation and Highways.

6.2.1.1 Concore C-68 drill rig

The Concore C-68 drill rig is a small, trailer-mounted research drill rig (Fig. 6.1), with the capability of auger, rotary and hammer drilling. Core samples are provided by 52 cm long, 4.75 cm diameter split-tube samplers. Cores are obtained by hydraulically pushing the split-tube into the ground, or, where deposits are more resistant, by hammering with a 145 lb weight.

6.2.1.2 Vibracorer

The vibracorer consists of a motor-driven eccentric-rotor vibrator attached to a clamp (Fig. 6.2). The clamp is fastened to a 9.15 m (30') length of 7.5 cm (3") diameter aluminum irrigation tubing. In wet, fine grained deposits (medium sand or finer), the vibrations cause liquefaction of the sediment immediately in contact with the tube, enabling it to be pushed down into the ground.

The tube is then extracted by a continuous chain hoist attached to a quadrapod (Fig. 6.2). A core-catcher at the bottom of the tube retains the core within. The tube is then suspended at an angle of about 30 , the core-catcher is removed and the core is vibrated out onto a length of plastic guttering. In this way, a 9.15 m long, 7.5 cm diameter continuous core can be obtained in about two hours.

In comparison to the drill rig, the vibracorer has the advantage of being portable (it could be carried into sites

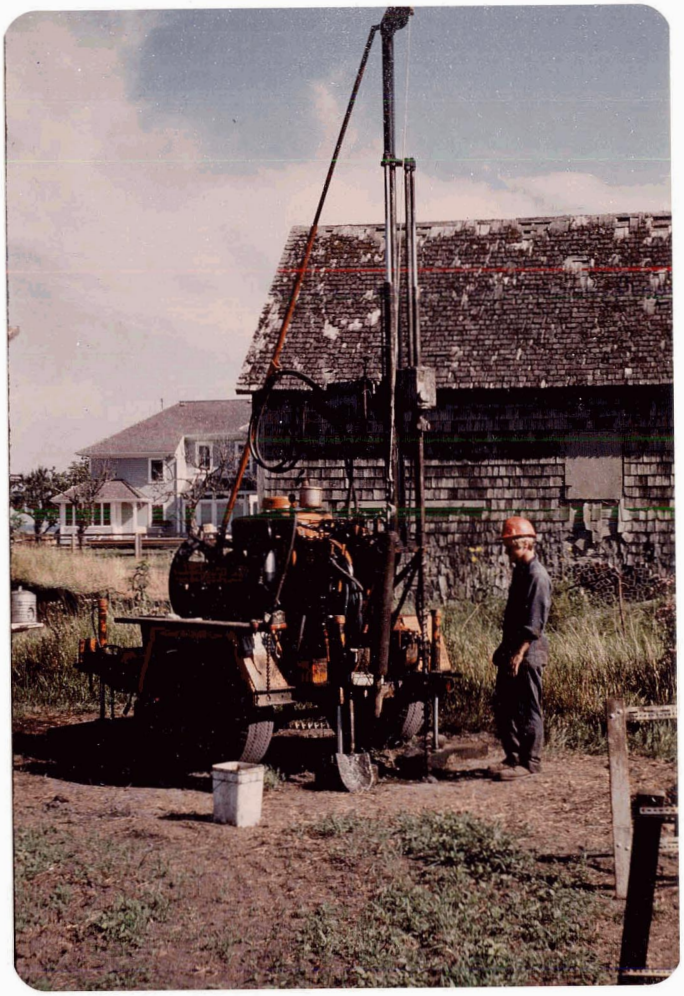

Figure 6.1 Concore C-68 drill rig

Figure 6.2 Vibracorer

inaccessible to vehicles) and considerably faster. The drawback of the vibracorer is that 9 to 10 meters is the maximum practical depth of operation.

6.2.1.3 B.C. Dept. of Highways borehole logs

The B.C. Department of Highways provided borehole logs and a number of core samples from drill sites on Lulu Island and the adjoining Fraser River floodplain. The logs provide a generalized description of grain size, sorting and organic matter content. Sedimentary structures are not recorded.

While the logs are fairly accurate indicators of major lithology changes (silt to sand, for example), smaller details (such as tephra layers) are often ignored. Certain lithologic classifications are also prone to some error; organic-rich silt, for example, may be recorded as "peat".

6.2.1.4 Field logging of cores

Cores from both the drill rig and vibracorer were logged in the field. Logging consisted of the visual assessment of grain size sorting, organic matter content and sedimentary structures (including the nature of contact between successive sedimentary units i.e. gradational - sharp). Selected core samples were retained for laboratory analyses of particle size characteristics and microfossil content.

Large amounts of organic material, when encountered in cores, were retained for possible radiocarbon dating. Some cores

contained tephra layers, these were collected for laboratory identification.

6.2.2 DRILL SITE LAYOUT (SAMPLING DESIGN)

Drill site locations were arranged about the central axis of Lulu Island, in order to sample the full chronological range of deposits, from the oldest in the vicinity of New Westminster, to the newest on the western edge of the island. Drill sites were also placed sufficiently far north and south of the central axis to allow a three-dimensional, regional lithostratigraphy of Lulu Island to be developed. A number of drill sites were also located on the floodplain of the Fraser River between New Westminster and Pitt Meadows (Fig. 1.8).

The precise location of drill sites depended on access and, as such, could only be finally determined in the field. Modifications were made to the drill site layout as field work proceeded. Greater coverage was provided in areas where subsurface variation appeared most pronounced and lesser coverage where subsurface deposits seemed to be fairly uniform from site to site.

The abandoned channel cutting across eastern Lulu Island (Fig. 2.2) is underlain by relatively recent fluvial deposits, probably formed within the last 5000 years (section 2.2.6). As the primary purpose of this study is to determine the nature and extent of aggradational deposits formed on Lulu Island in the early Holocene (ca. 8000 - 5000 years BP), no drill sites were located in the abandoned channel area.

Drill site elevations were determined where possible by levelling to nearby benchmarks. Some sites were too remote from benchmarks for practical levelling. In these cases, site elevation was estimated from knowledge of the local surface (i.e. relationship of site to general level of surrounding surface) and reference to topographic maps. Due to the low relief of the natural delta surface, the error associated with the estimated elevations is likely to be small - probably of the order of 50 cm.

Data were collected from a total of 51 sites - 35 drill rig or vibracore drill sites and 16 B.C. Dept. of Highways drill sites. Site locations are shown in Figure 6.3 (Precise site locations and elevations are presented in Appendix II).

6.3 RESULTS

6.3.1 DRILL HOLE LOGS

The field logs and B.C. Dept. of Highways borehole logs are protrayed graphically in Figures 6.4 - 6.6.

6.3.2 LITHOFACIES DESCRIPTIONS

Based on visual logging of core lithology, six major lithofacies are proposed:

peat

organic-rich silt

interbedded silts, sands and sandy silts

massive sands

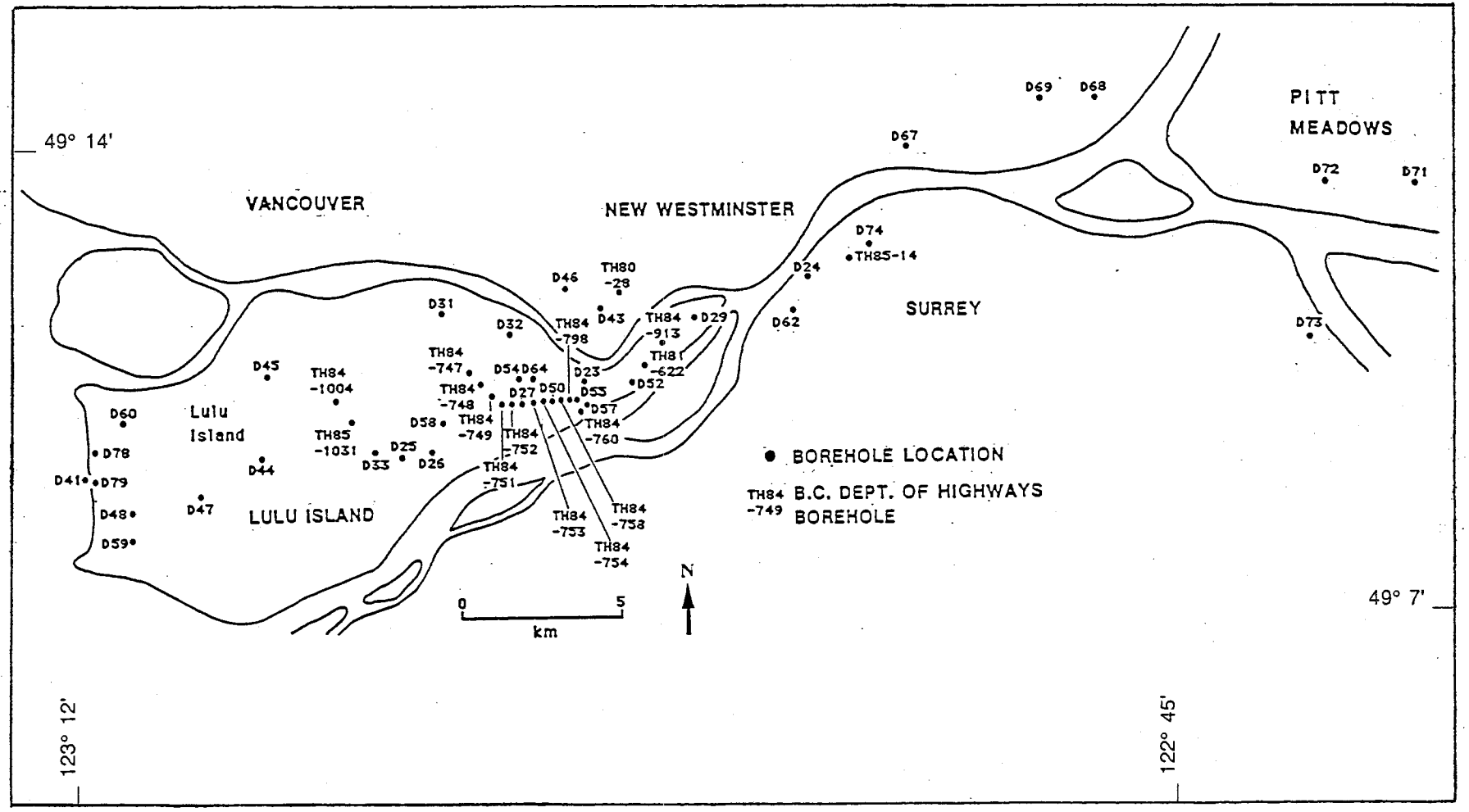

Figure 6.3 Drill site locations

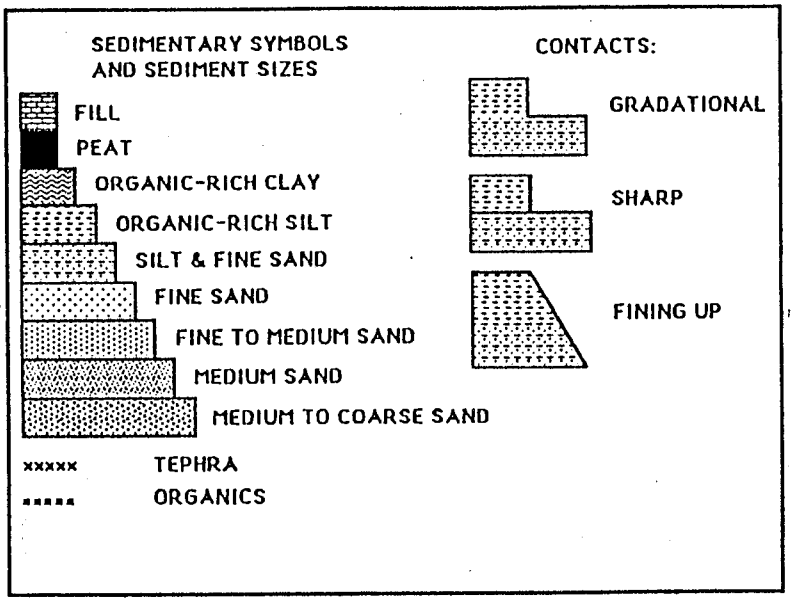

Key to core logs
(Figures 6.4 - 6.6)

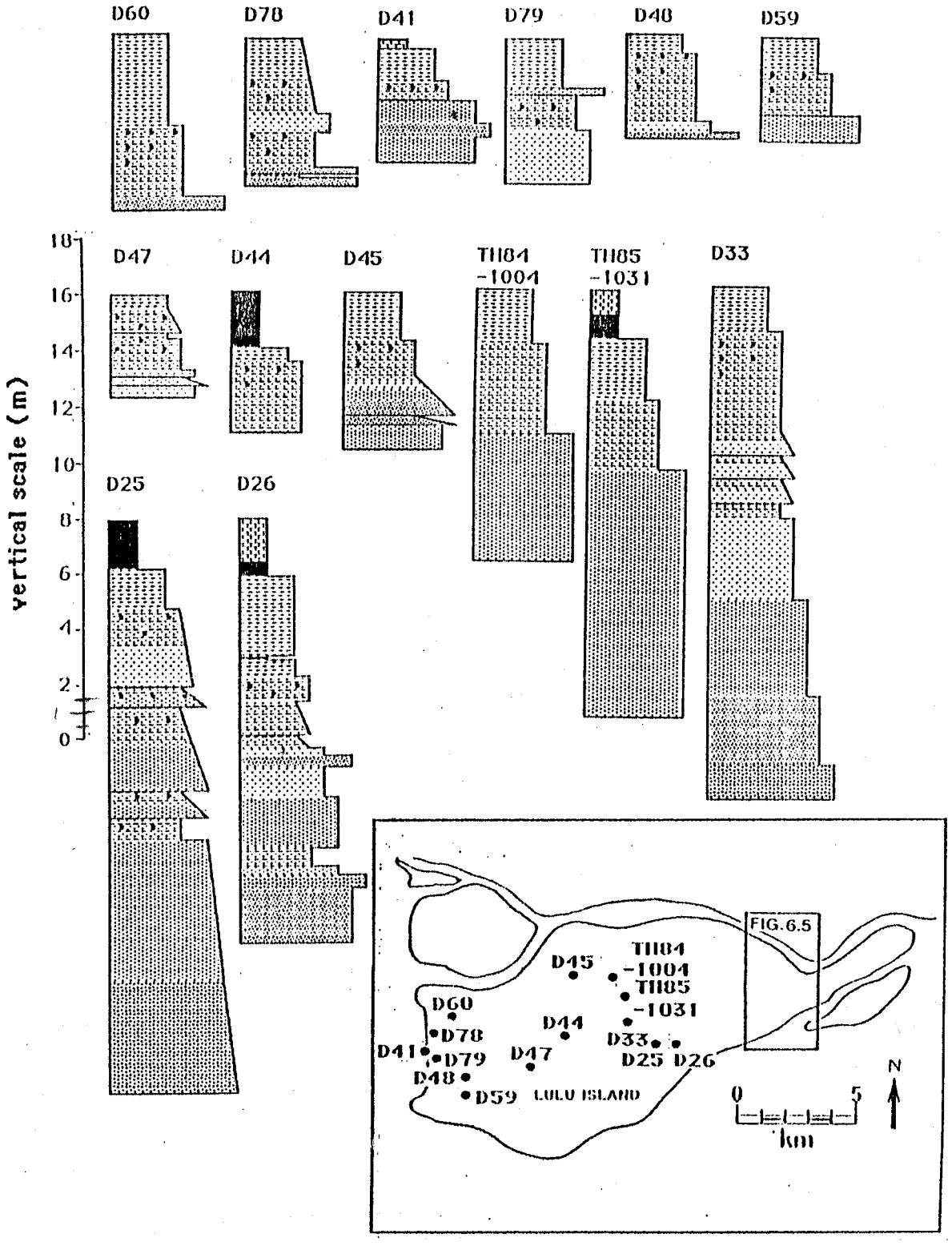

Figure 6.4 Core logs - western Lulu Island

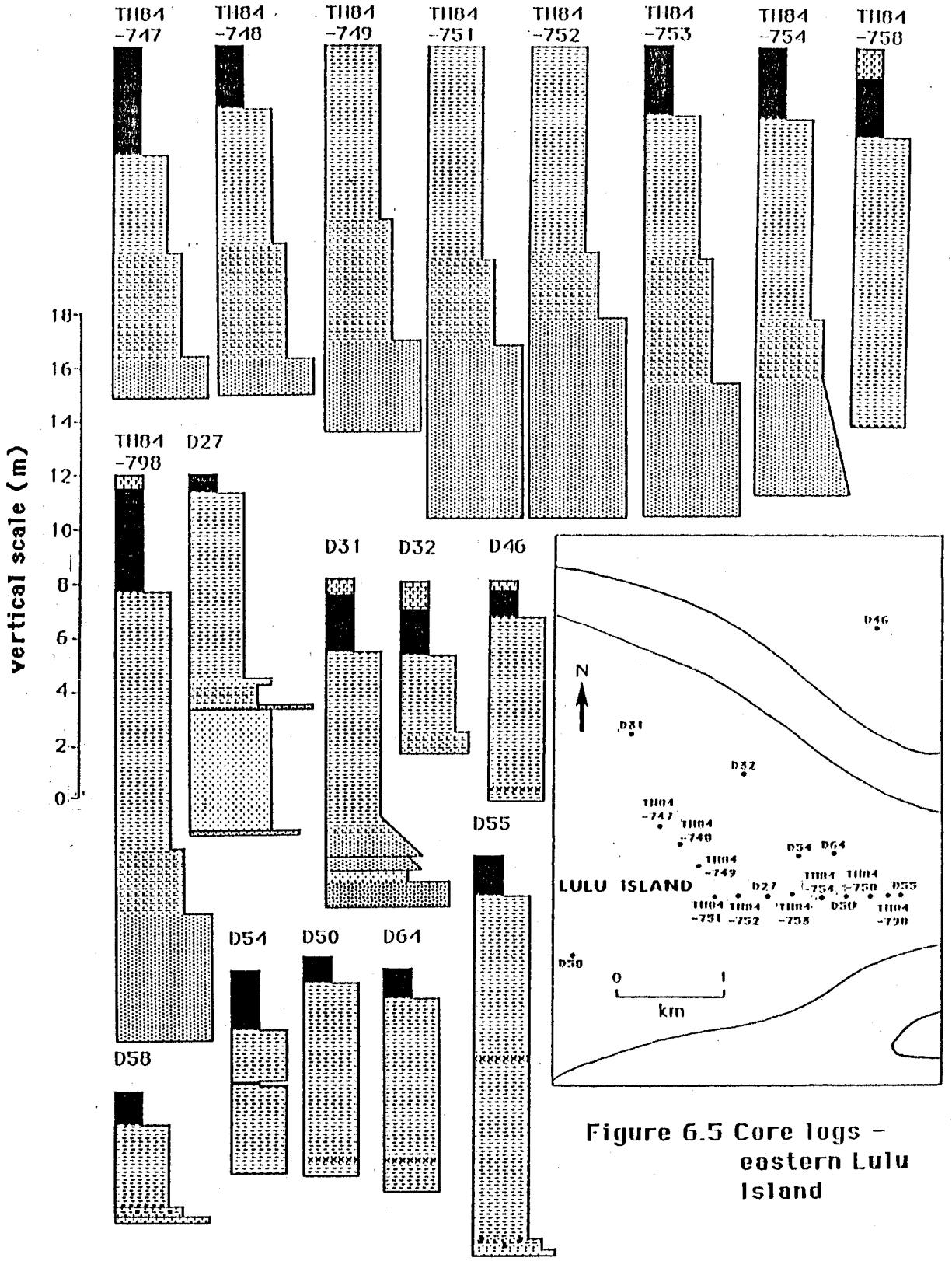

Figure 6.5 Core logs – eastern Lulu Island

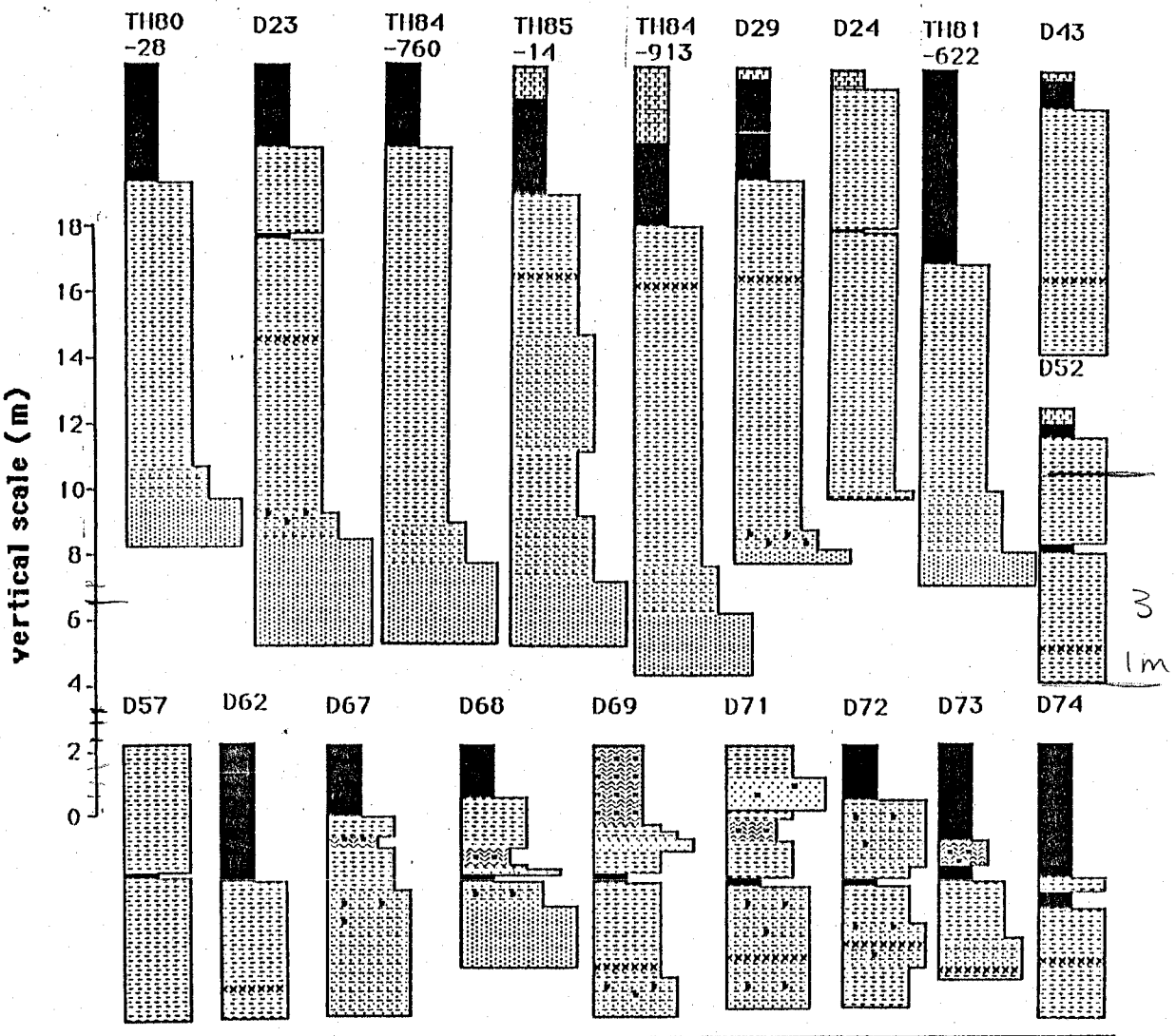

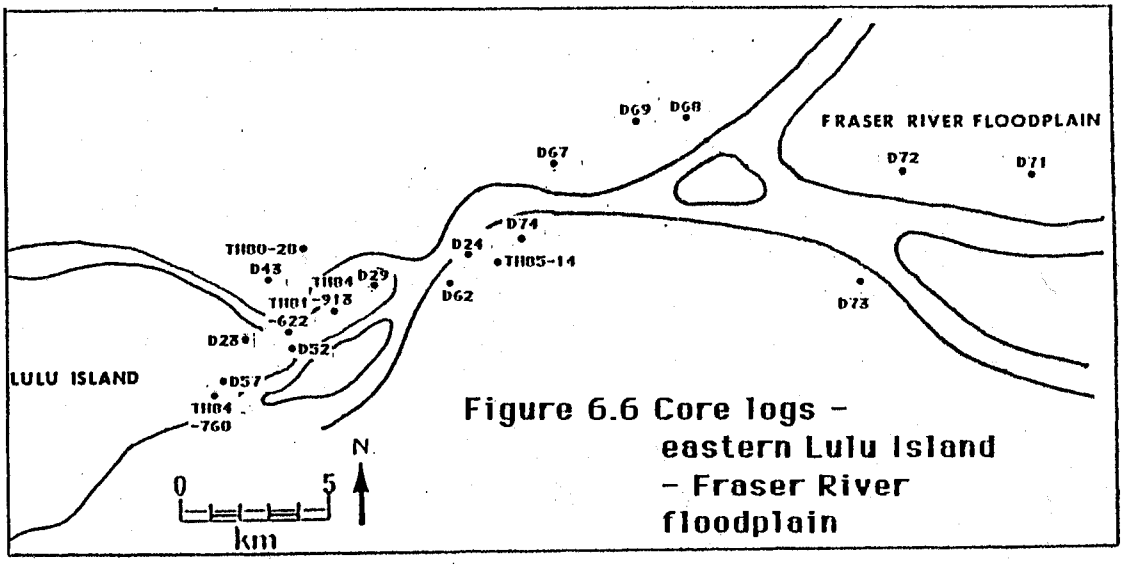

Figure 6.6 Core logs – eastern Lulu Island – Fraser River floodplain

organic-rich clay

tephra

Each lithofacies is defined on the basis of a consistent and distinctive internal lithology (grain size characteristics, organic matter content and sedimentary structures) and contrasts sufficiently with the other lithofacies to be distinguishable in the field. Descriptions of these lithofacies are presented in the following sections.

6.3.2.1 Peat

The peat lithofacies consists of partially decomposed organic matter, containing no visible mineral material. Horizontal bedding is commonly observed and large wood fragments (2-3 cm) are occasionally present.

Peat was found extensively at the surface of eastern Lulu Island and the Fraser River floodplain (Figs. 6.5, 6.6). The base of the peat is generally 1 to 2 m below mean sea level. The peat is typically from 1 to 3 m in thickness. The unusually thick peat indicated on one of the B.C. Dept. of Highways borehole logs (Fig. 6.5 - TH81-622), extending to more than 5 m below mean sea level, is presumably organic-rich silt in its lower part (see section 6.2.1.3). In all cases, the base of the surface peat layer was marked by a gradational contact with the underlying deposit (Fig. 6.7).

In addition to the surface peat accumulations, buried peat layers were found in 12 of the drill holes drilled in the eastern part of the study area (Fig. 6.4-6.6). The buried peat beds varied from about 10 to 50 cm in thickness and were found

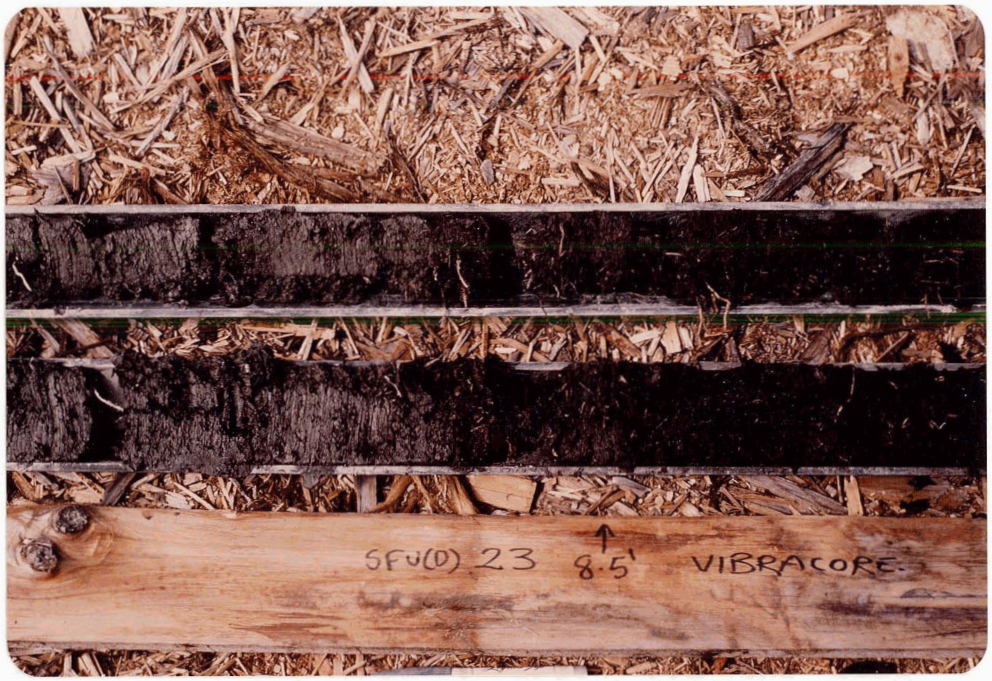

Figure 6.7 Peat (on the right) grading down into organic-rich silt, core D23 (depth = 2.6 m below surface)

Figure 6.8 Organic-rich silt, core D23 (depth = 3.9 m below surface)

at depths of 2.2 to 3.8 m below mean sea level. In almost all cases, the buried peat layer had gradational contacts with the enclosing material, which most commonly was organic-rich silt. The one exception was at site D68 (Fig. 6.6), where the top of the buried peat unit was marked by a sharp contact overlain by a 10 cm thick bed of fine sand.

6.3.2.2 Organic-rich silt

The organic-rich silt lithofacies consists of predominately silt-sized particles and contains abundant organic material, which often clearly forms horizontal laminations (Fig. 6.8). This unit is usually found at the surface on western Lulu Island (Fig. 6.4), or in gradational contact with the base of the surface peat deposits in the eastern part of the study area (Figs. 6.5-6.7).

The organic-rich silts grade downward into interbedded silts, sands and sandy silts (Figs. 6.4 - 6.6). This transition is marked by the first appearance of sand-sized particles in core samples and a progressive decrease in the abundance of organic material (Fig. 6.9).

The thickness of this unit is about 1 - 2 m on western Lulu Island (Fig. 6.4). Thicknesses generally undergo a progressive increase across central Lulu Island (Fig. 6.5). East of site D55, the thickness of the organic-rich silts stabilizes at about 11 - 12 m (Fig. 6.6).

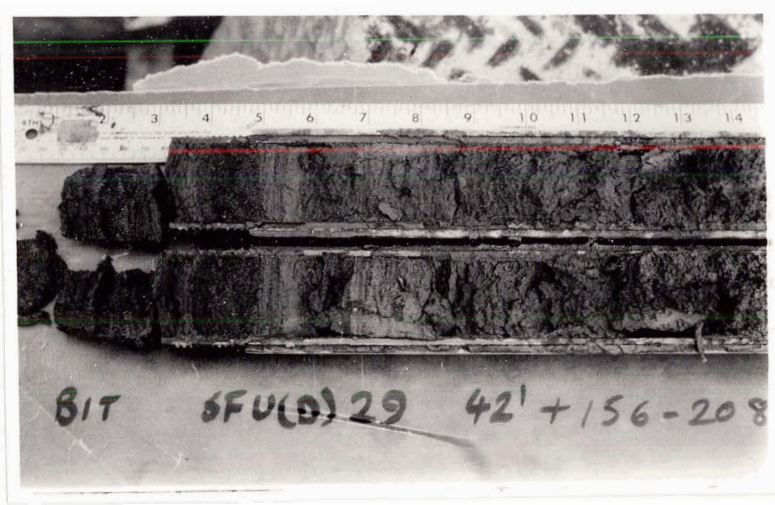

Figure 6.9 Organic-rich silt (on the right) grading down into interbedded silts and sands, core D29 (bit is 14.89 m below surface)

Figure 6.10 Interbedded silts and sands (top of core is to the right), core D25 (depth approx. 8 m)

6.3.2.3 Interbedded silts, sands and sandy silts

This lithofacies is generally found below, and in gradational contact with the organic-rich silt lithofacies. It consists of interbeds of silt, sand and poorly-sorted mixtures of silt and sand (Fig. 6.10). Organic material is scattered throughout and large wood fragments (2-3 cm) are occasionally present.

Some contacts between beds within this unit are sharp, others are gradational. Sharp contacts are usually overlain by sand, which often grades upward into silty sand or silt. Bedding, for the most part, is roughly horizontal, although occasional gently inclined (ca. 10^{0}) beds are present.

The base of this unit is marked by a gradational or sharp transition to underlying sandy deposits. The interbedded silts, sands and sandy silts attain a maximum thickness of about 8 m beneath central Lulu Island (Fig. 6.4, e.g. site D25). Beneath both the western and eastern parts of Lulu Island and the Fraser River floodplain, this unit has a typical thickness of 1 - 2 m (Fig. 6.4 - 6.6).

6.3.2.4 Massive sands

Sandy deposits underlie the interbedded silts, sands and sandy silts and are distinguished from them by the virtual lack of silt and organic material in core samples. The sands for the most part appear structureless, although occasional faint indications of horizontal bedding and gradations from finer to coarser sand, are observed. Wood fragments were found in some

core samples from this unit, but overall they are rarely encountered.

Based on the available drill hole data, this sandy unit extends to a depth of at least 21 m below mean sea level under the east side of Lulu Island (Fig. 6.5, e.g. site TH84-798), and to at least 19 m below mean sea level beneath central Lulu Island (Fig. 6.4, e.g. site D25). In general, this unit appears to become progressively coarser with depth (Fig. 6.4 - 6.6).

6.3.2.5 Organic-rich clay

Clayey sediments were present in some of the cores obtained from the Fraser River floodplain (Fig. 6.6). In the field, these deposits were distinguished by their stickiness, a lack of particles visible under a hand lens and a distinctive blue-grey colouration. The clays contained common to abundant organic material and displayed horizontal bedding.

The clay deposits were not found below 4 m depth and in all cases graded into the enclosing material, which was either organic-rich silt or peat (Fig. 6.6).

6.3.2.6 Tephra

Tephra beds, 1-2 cm thick, were found in 15 locations, at depths ranging from about 4 to 6.5 m below mean sea level (Fig. 6.5, 6.6). Although not volumetrically significant, the tephra was nevertheless defined as a major lithofacies because of its geochronological importance.

All occurrences of the tephra bed were located east of

drill site D46 (Fig. 6.5). The tephra beds were enclosed by organic-rich silt deposits and were bounded by sharp contacts, both above and below (Fig. 6.11 - 6.14).

6.3.3 LITHOSTRATIGRAPHIC SECTIONS

The drill logs were used to construct a number of lithostratigraphic sections across Lulu Island and along the Fraser River floodplain between Lulu Island and Pitt Meadows. All elevations were adjusted to geodetic datum (approximates mean sea level). Spacing of the drill logs along the sections is based on the straight-line distance between drill sites.

For the sake of clarity, not all drill logs along a section line were included in the diagrams. A number of logs which did not contribute any further detail to the sections were excluded.

The most detailed section (Fig. 6.15) approximates the central axis of Lulu Island and is assumed to roughly parallel the direction of progradation of this part of the Fraser Delta.

The other Lulu Island sections (Figs. 6.16 - 6.20) are strike sections, running approximately at right angles (north-south) across the main east-west (dip) section. These sections are included in order to assess the degree of lateral continuity of the general lithostratigraphic framework established by the main east-west section (Fig. 6.15).

A section between site D23 on Lulu Island and site D71 on the Fraser River floodplain, is also presented (Fig. 6.21). This section is included in order to determine if the aggradational deposits on the delta can be traced laterally into the adjoining

Figure 6.11 Tephra layer, core D23, depth = 8.7 m below surface

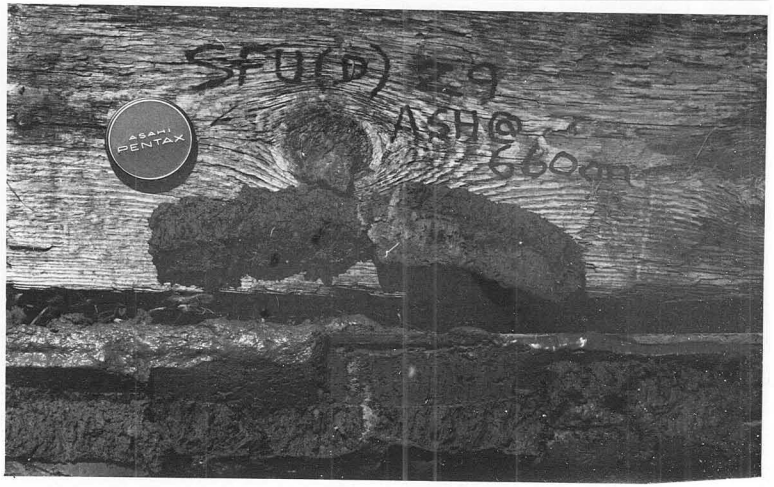

Figure 6.12 Tephra layer, core D29, depth = 6.6 m below surface

Figure 6.13 Tephra layer, core D52, depth = 7.4 m below surface

Figure 6.14 Tephra layer, core D55, depth = 7.95 m below surface

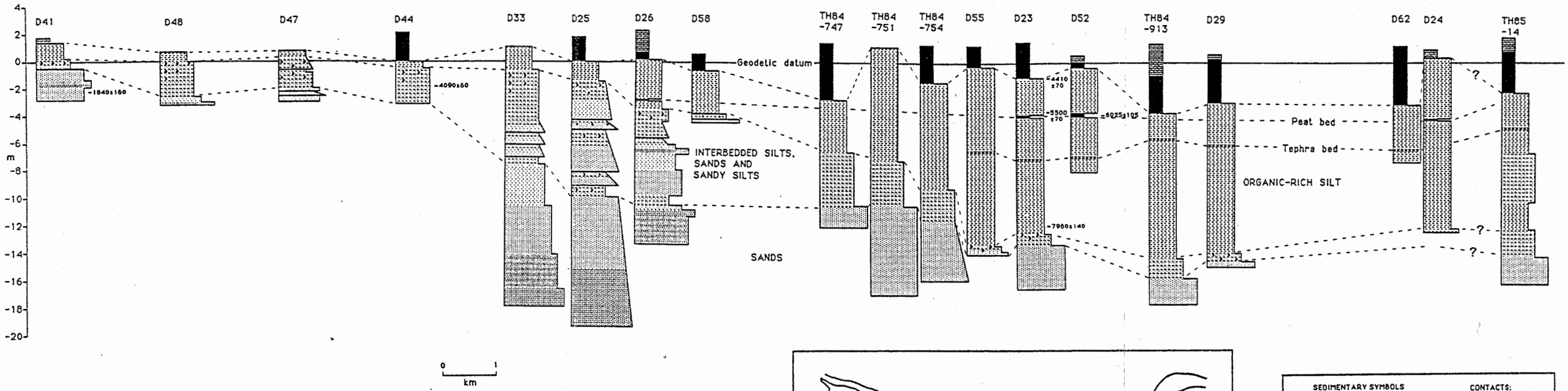

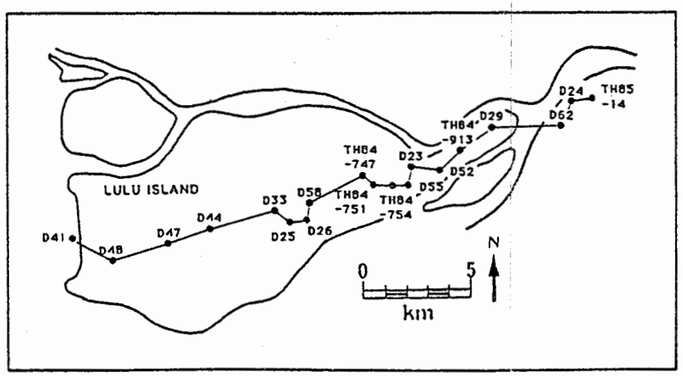

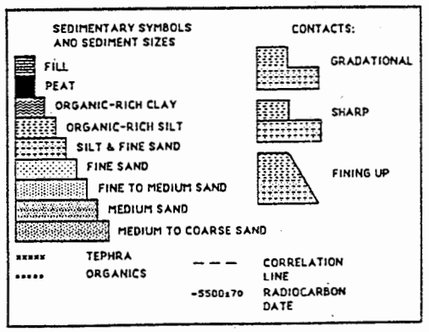

Figure 6.15 East-west lithostratigraphic section: Lulu Island

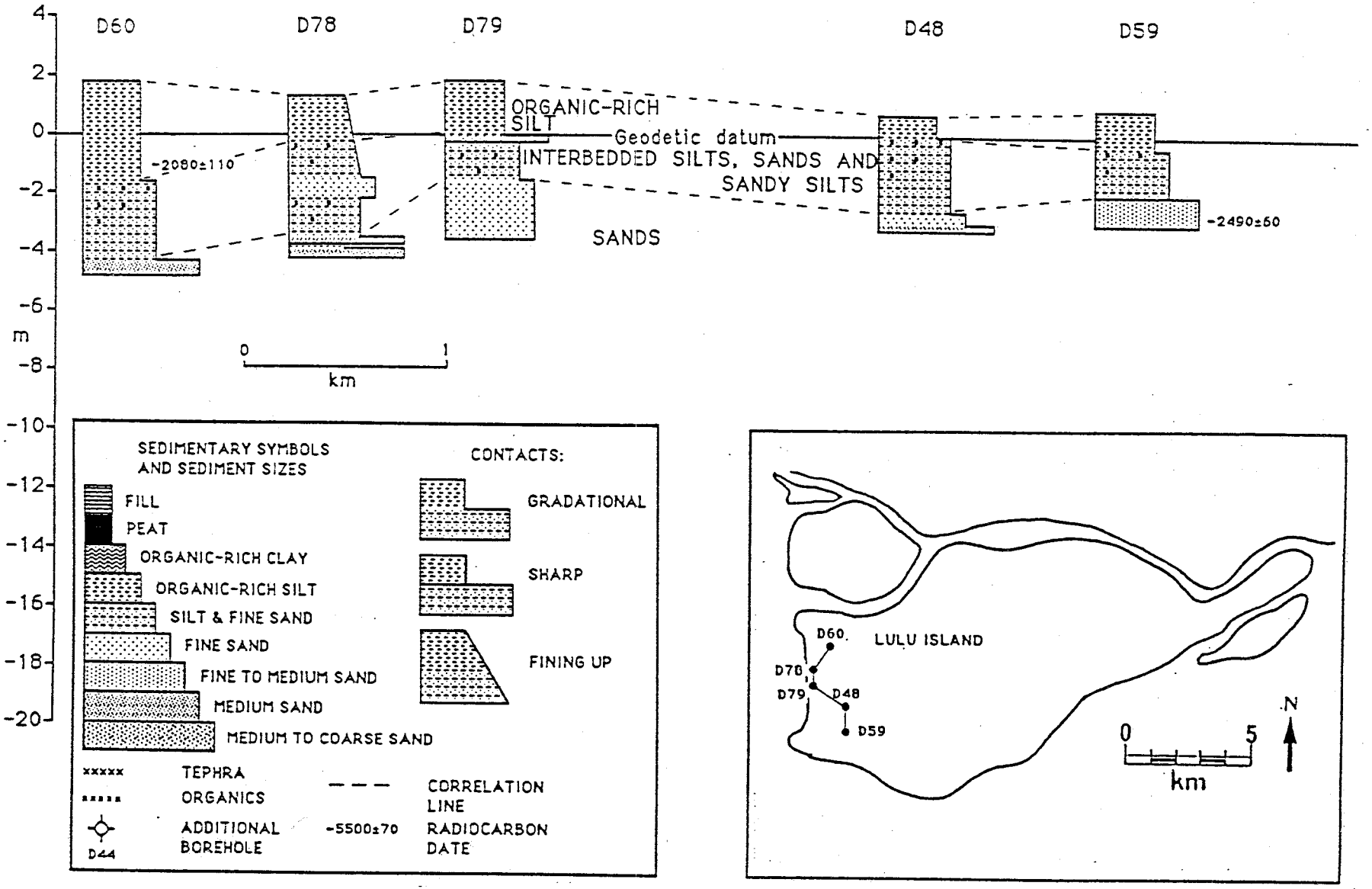

Figure 6.16 North-south lithostratigraphic section: western Lulu Island

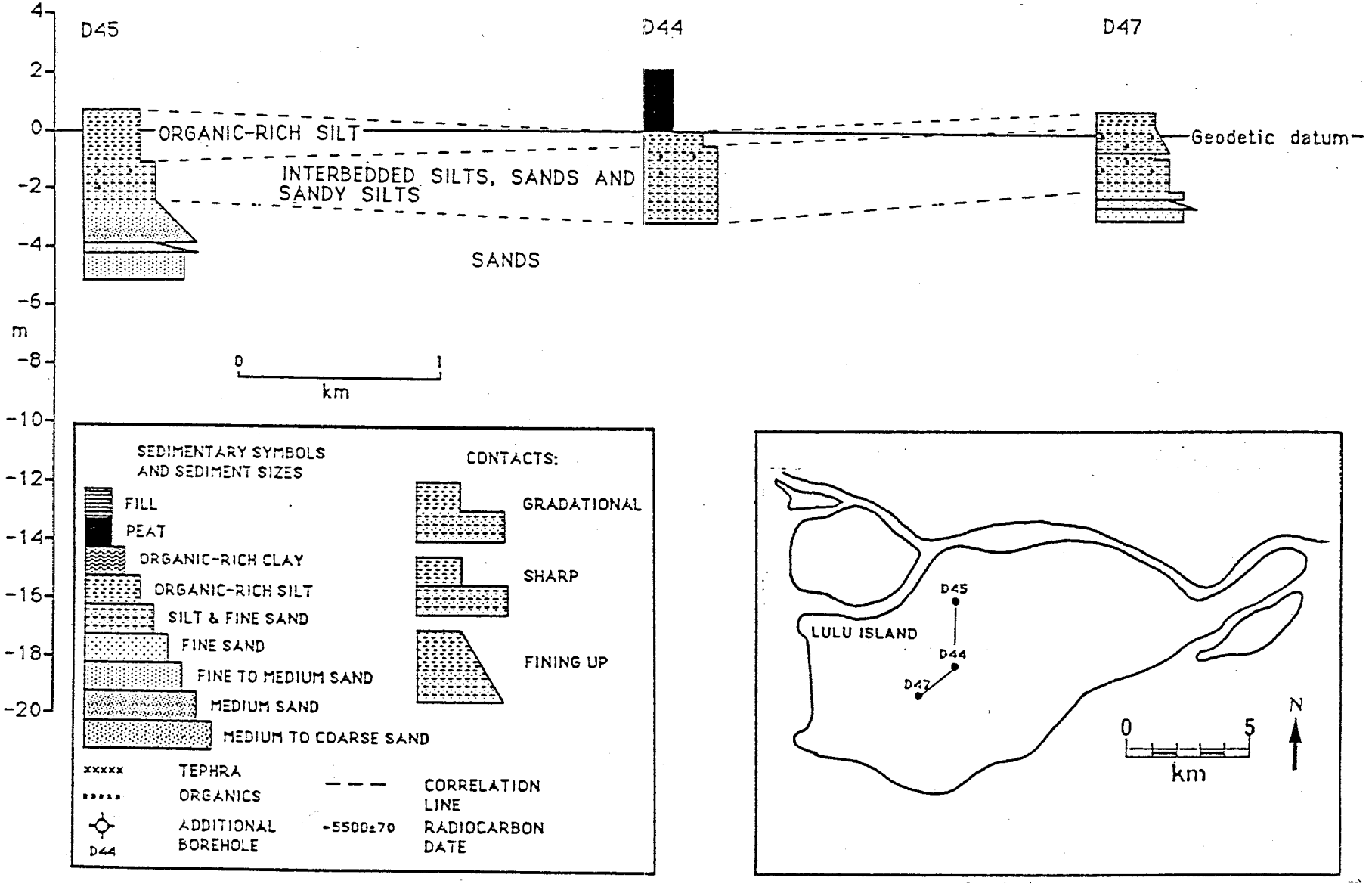

Figure 6.17 North-south lithostratigraphic section: west-central Lulu Island

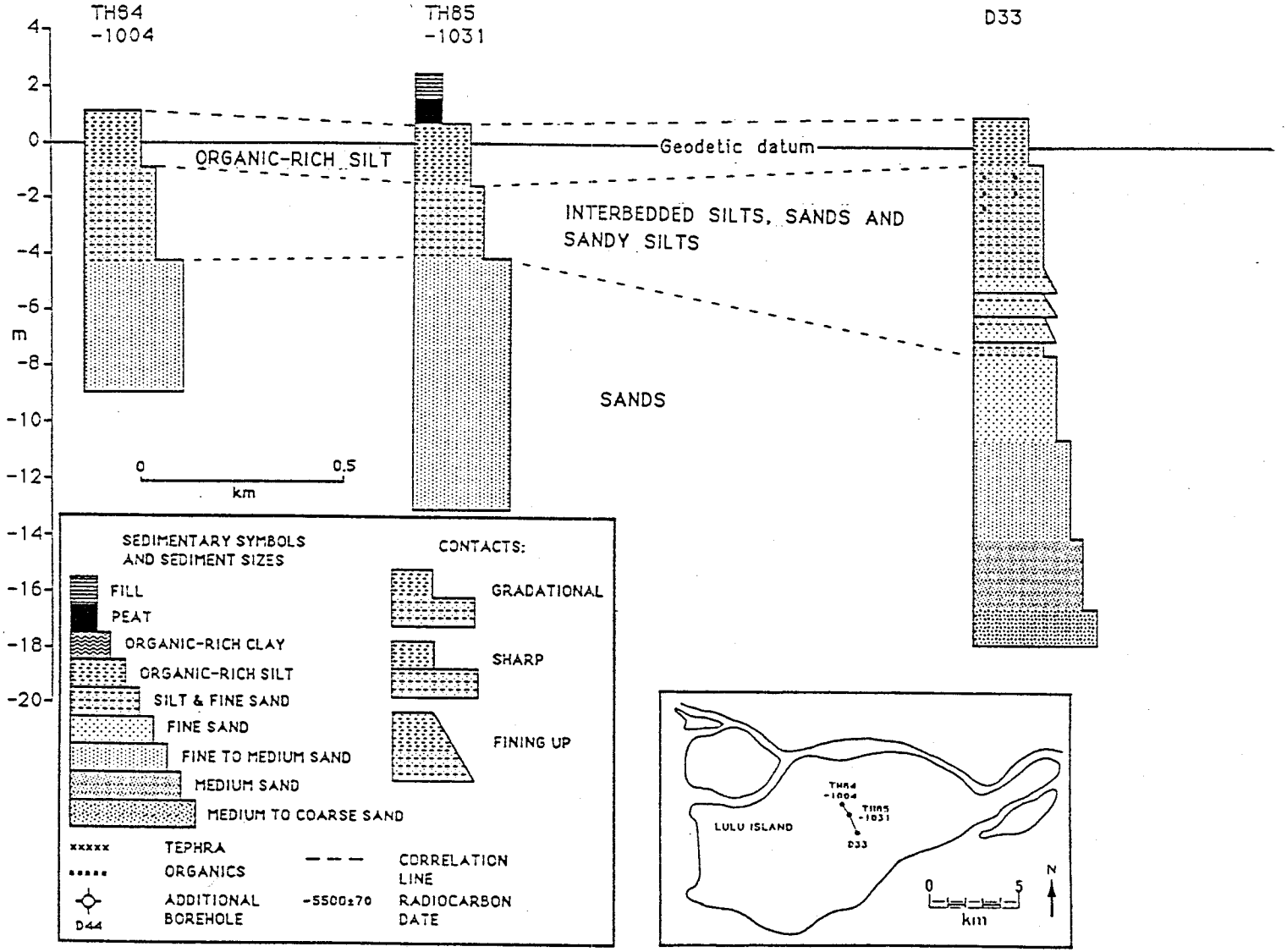

Figure 6.18 North-south lithostratigraphic section: central Lulu Island

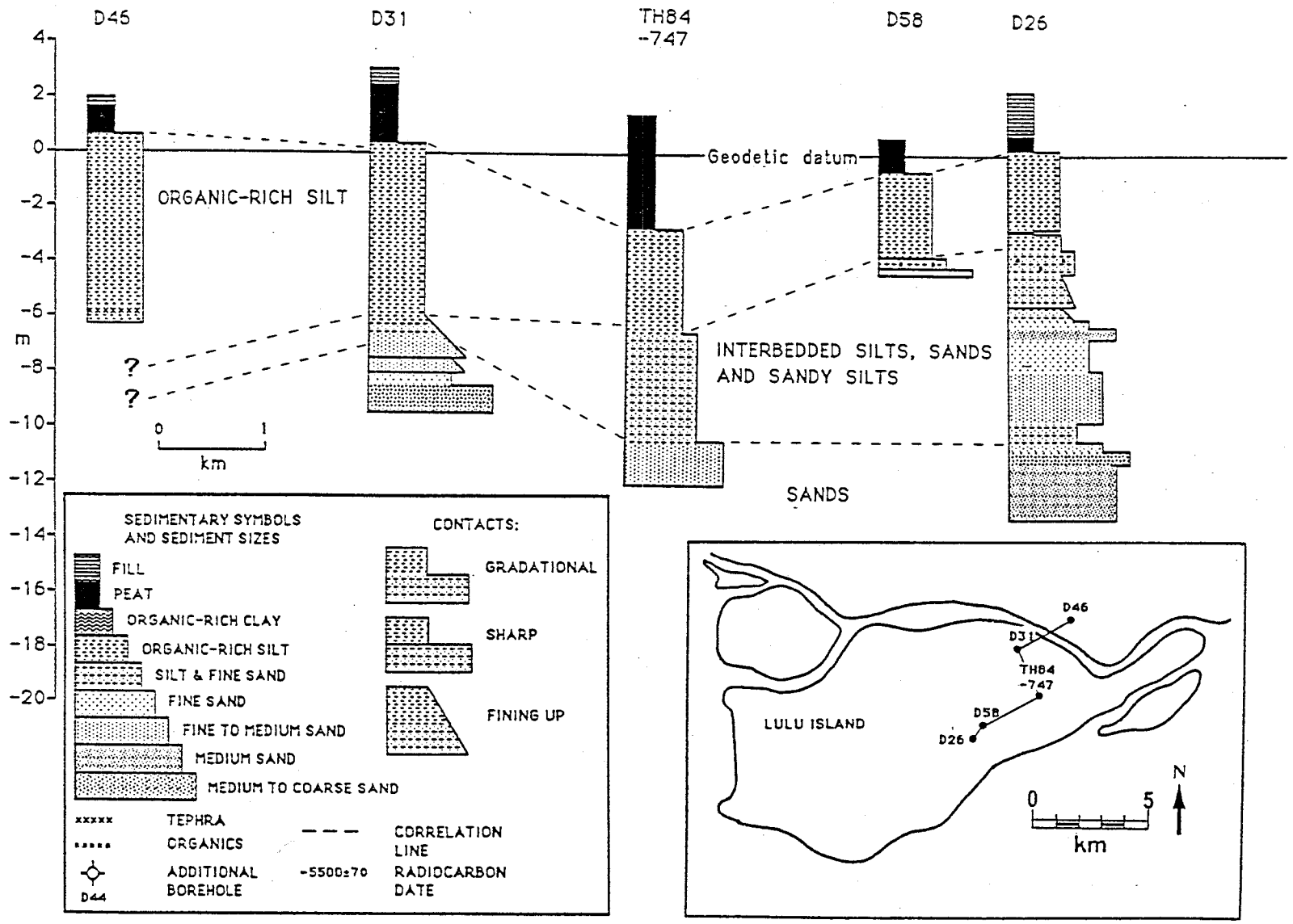

Figure 6.19 North-south lithostratigraphic section: east-central Lulu Island

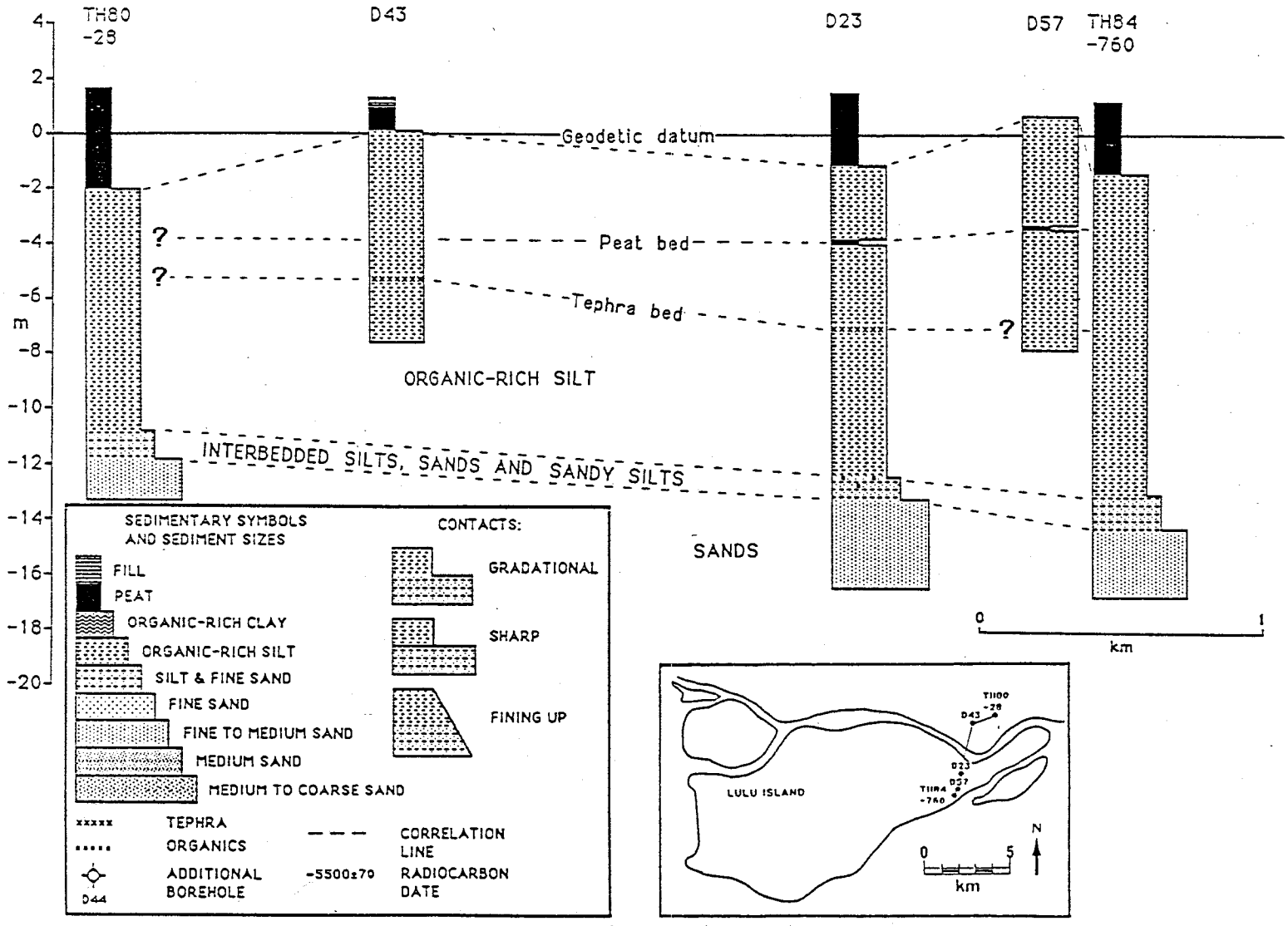

Figure 6.20 North-south lithostratigraphic section: eastern Lulu Island

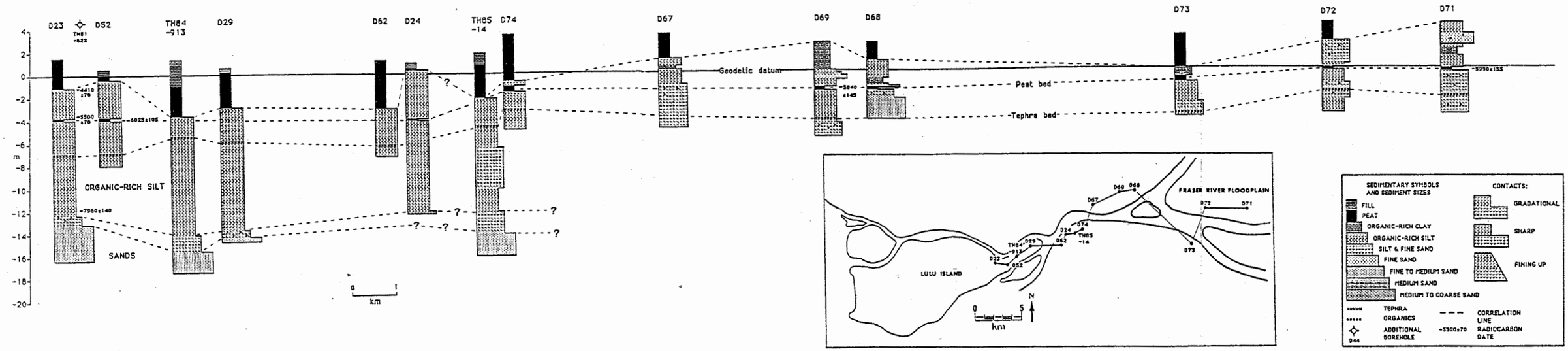

Figure 6.21 East-west lithostratigraphic section: eastern Lulu Island -western Fraser River floodplain

floodplain sediments.

Correlation lines have been added to the sections in order to delimit the vertical extent of the major lithofacies defined previously (section 6.3.2). For the sake of brevity, radiocarbon dates obtained for this study have also been added to the sections. These will be discussed in a following chapter. At this stage no attempt has been made to apply environmental interpretations to the subsurface lithofacies. This will also be covered in a following chapter.

6.4 DISCUSSION

6.4.1 LULU ISLAND LITHOSTRATIGRAPHY

The major features of Lulu Island's lithostratigraphy are apparent on the east-west section (Fig. 6.15). The organic-rich silt unit attains a fairly uniform thickness of 11 to 12 m under the eastern part of the island. This thick silt extends from the apex of the delta in the vicinity of site D24, approximately 8 km to the southwest to the vicinity of site D55 on Lulu Island.

The base of the silt in this region lies at a depth of about 13 m below mean sea level. The top of the silt unit grades into the overlying surface peat deposits at an elevation of about 1 to 2 m below mean sea level (excluding what are probably erroneously deep peats on the Department of Highways profiles - see sections 6.2.1.3, 6.3.2.1).

To the west of site D55, the organic-rich silt unit becomes

progressively thinner, except for between sites D26 and D58, where the base of the silt unit levels off, remaining at about 3.5 m below mean sea level (Fig. 6.15).

The thickness of the silt unit becomes fairly uniform, at about 1 to 2 m, west of site D47, with its base lying approximately at the elevation of mean sea level. A tephra bed occurs within the organic-rich silt unit underlying eastern Lulu Island (Fig. 6.15). The tephra bed occurs at a depth of 6 to 7 m below mean sea level and appears to extend from the apex of the delta to at least as far as site D55.

A buried peat layer occurs at an elevation of approximately 3.5 m below mean sea level within the silt unit. The peat bed appears to extend from the apex of the delta to the vicinity of site D26 (Fig. 6.15).

The interbedded silts, sands and sandy silts underlying the organic-rich silt unit, are about 1 to 2 m thick in both the eastern and western parts of the section (Fig. 6.15). Under the central part of Lulu Island, however, the thickness of this unit increases considerably, attaining a thickness of about 8 m beneath site D25.

Massive sands underlie the interbedded silts, sands and sandy silts, occurring at a depth of about 15 m below mean sea level under eastern Lulu Island, but at only 1 to 2 m below mean sea level beneath the island's western margins.

The strike sections (Fig. 6.16 - 6.20) attest to the lateral continuity of the general lithostratigraphic framework established by the main east-west section (Fig. 6.15). The

section running across the eastern part of Lulu Island (Fig. 6.20), shows that the thick organic-rich silt unit continues to be present, both north and south of the central axis of the island. The section shows that the tephra bed occurs near the northern edge of the deltaic deposits in this area (Fig. 6.20 - site D43) and that the peat bed also occurs further to the south (Fig. 6.20 - site D57).

The section across the western edge of the island (Fig. 6.16) confirms that both the organic-rich silt unit and the interbedded silts, sands and sandy silts remain relatively thin (<3 m each) both north and south of the central region.

The central north-south section (Fig. 6.18) indicates that the increase in thickness of the interbedded silts, sands and sandy silts unit continues to be found to the north of the central axis of the island.

Similarly, the two remaining north-south sections (Fig. 6.17, 6.19) confirm the lateral continuation of deposits shown on the main east-west section, in respect of their vertical order and extent. In addition, the east-central section (Fig. 6.19) contains another occurrence of the tephra bed (site D46) at approximately the same elevation as it occurs on the central east-west section (Fig. 6.15).

These findings enable a generalized model of Lulu Island's lithostratigraphic framework along proximal-distal trends to be developed (Fig. 6.22).

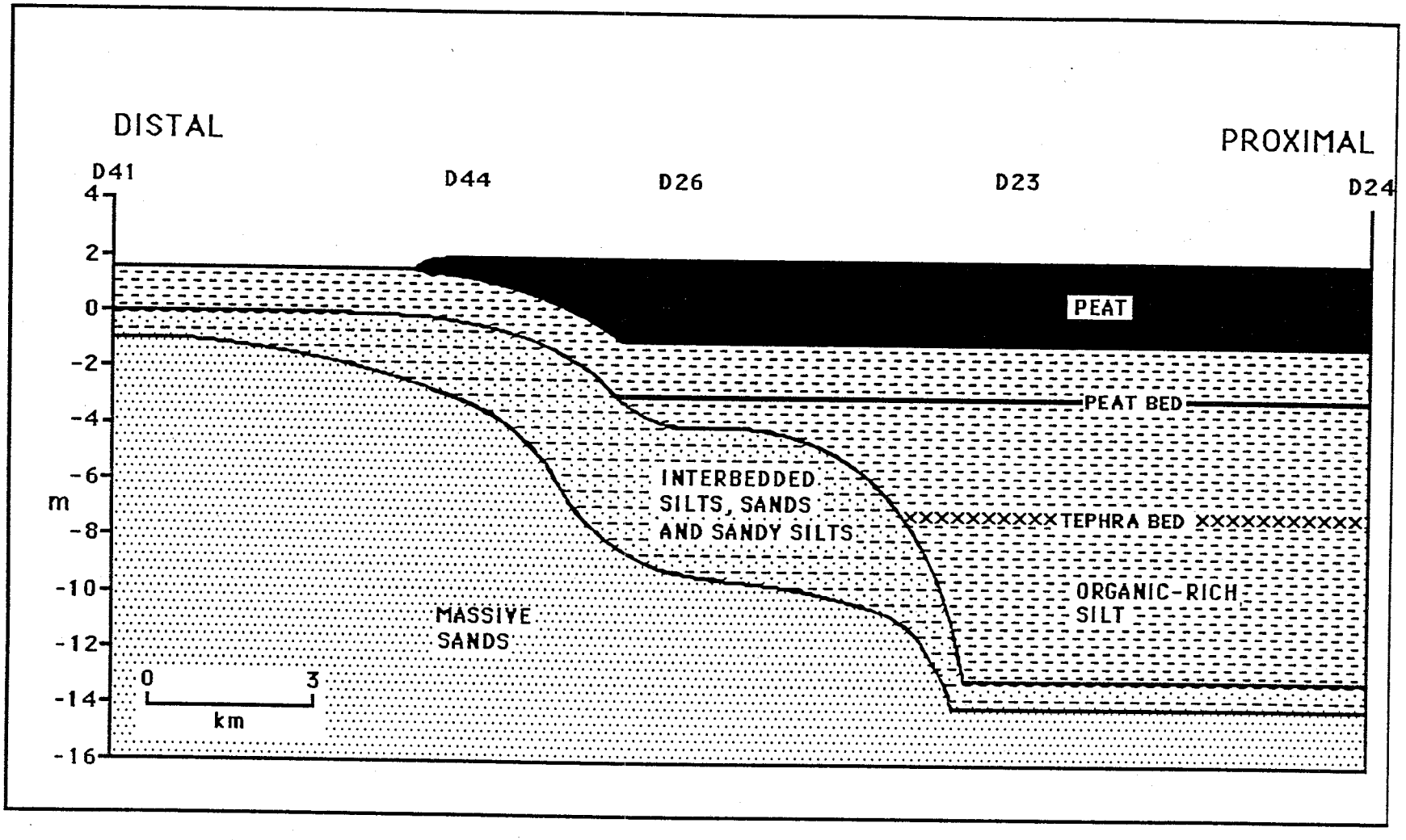

Figure 6.22 Generalized lithostratigraphy of Lulu Island

6.4.2 LULU ISLAND-FRASER RIVER FLOODPLAIN LITHOSTRATIGRAPHY

The east-west lithostratigraphic section (Fig. 6.21) shows that the subsurface peat and tephra layers are clearly traceable from the deltaic deposits into the adjoining floodplain sediments.

On the basis of this clear correlation between the two areas, the organic-rich silts, clays, sandy silts and fine sands that enclose the peat and tephra beds in the floodplain deposits, are tentatively correlated with the organic-rich silt unit that encloses the two marker beds on Lulu Island (Fig. 6.21).

Similarly, the interbedded silts, sands and sandy silts unit and the massive sands underlying eastern Lulu Island are tentatively correlated with deposits that are present at a similar depth beneath the Fraser River floodplain (Fig. 6.21 - site TH85-14).

The similarity in depth to the two marker beds (peat and tephra) on the delta and on the floodplain (Fig. 6.21), further supports the contention that subsidence has not been a significant factor in the evolution of the delta (section 2.4.1). Had significant subsidence occurred on the delta, these two marker beds would presumably be encountered at a greater depth than on the adjoining floodplain.

6.5 SUMMARY

On the basis of the lithostratigraphic sections, the major features of the regional lithostratigraphy of Lulu Island and

the adjoining Fraser River floodplain, to a depth of about 20 m, have been established (Fig. 6.22).

The deposits underlying these areas consist of six major lithofacies: peat; organic-rich silt; interbedded silts, sands and sandy silts; massive sands; organic-rich clay, and tephra.

Surface peat accumulations blanket much of the Fraser River floodplain, eastern and central Lulu Island, extending to within about 5.5 km of the western delta front.

Underlying the peat on eastern Lulu Island is an 11 to 12 m thick organic-rich silt layer which merges laterally with apparently coeval floodplain sediments, consisting of 11 to 12 m of clays, silts, sandy silts and sands.

The organic-rich silts become progressively thinner across central Lulu Island, attaining a uniform thickness of 1 to 2 m within 4 km of the western delta front.

Relatively thin (1 to 2 m) interbedded silts, sands and sandy silts underlie the organic-rich silts in both the western and eastern parts of Lulu Island. These deposits become considerably thicker (up to 8 m) beneath central Lulu Island. In the east of the island, this unit is encountered at 13 to 15 m depth and is tentatively correlated to a silty sand layer present at a similar depth beneath the adjoining floodplain sediments (Fig. 6.21, site TH85-14).

Massive sands underlie all other deposits on Lulu Island, being encountered at a depth of about 15 m below mean sea level in the east, but at only 1 to 2 m in the west. Borehole evidence from the adjoining Fraser River floodplain suggests that the

massive sands underlying eastern Lulu Island also extend eastward beneath the floodplain deposits (Fig. 6.21, site TH85-14).

Two marker horizons - a peat bed and a tephra layer - closely parallel the present-day surface, at depths of about 5 m and 8 m respectively (Fig. 6.21). These marker horizons are clearly traceable from the floodplain sediments down into the adjoining deltaic deposits.

SECTION THREE

ANALYSIS

CHAPTER SEVEN

FACIES INTERPRETATIONS

7.1 INTRODUCTION

This chapter concerns the establishment of depositional environments for the facies present in the subsurface of Lulu Island. This will be based on a comparison of the lithologic, structural and organic characteristics of the subsurface facies to those of contemporary depositional environments, using the interpretive framework developed in chapters 3, 4 and 5.

7.2 LITHOFACIES INTERPRETATIONS

7.2.1 INTERPRETATIONS BASED ON FIELD LOGGING OF CORE LITHOLOGY

On the basis of field logging alone, there would appear to be a clear correspondence between the organic-rich silt, interbedded silts, sands and sandy silts, and massive sands lithofacies (Fig. 6.22) and deposits of the contemporary tidal marsh/floodplain zone[1], transition zone and sand flat zone, respectively (Fig. 3.10).

Visually, the organic-rich silt lithofacies is identical to contemporary tidal marsh/floodplain zone deposits. Both consist of predominantly silt-sized particles, contain abundant organic

---

[1] Tidal marsh and floodplain deposits are lithologically similar - see sections 2.2.4, 3.1.

material, show signs of horizontal bedding and, for the most part, contain little or no sand (e.g. compare Figures 3.5 and 6.8).

Similarly, the interbedded silts, sands and sandy silts lithofacies has the lithologic character of transition zone deposits (section 3.4.1). Both contain a relatively wide variation in sediment sizes, incorporate scattered organic material and contain fining-upward sequences overlying erosional bases, presumably formed by shifting tidal channels.

The massive sands lithofacies has a sediment character that is similar to that of the contemporary sand flat zone (section 3.4.1). These deposits are relatively coarse, well-sorted, contain little or no organic material and appear mostly structureless.

The only obvious contrast between the subsurface lithofacies and the contemporary intertidal deposits is the greater thicknesses attained by the organic-rich silt and interbedded silts, sands and sandy silts underlying Lulu Island, in comparison to the vertical extent of their contemporary counterparts (Fig. 3.10).

In addition to the lithologic similarity, the lithostratigraphy of Lulu Island (Fig. 6.15), strongly suggests that the contemporary tidal marsh/floodplain zone, transition zone and sand flat zone do, indeed, have a direct correlation with the organic-rich silt, interbedded silts, sands and sandy silts, and massive sands underlying Lulu Island.

In particular, the base of the organic-rich silt

lithofacies, marked by a pronounced lithologic transition, forms a prominent lithostratigraphic marker which is readily traceable from the subsurface deposits to the base of the contemporary tidal marsh zone environment (approximates mean sea level on Fig. 6.15).

7.2.2 INTERPRETATIONS BASED ON GRAIN SIZE ANALYSIS

In order to add a degree of quantitative support to the interpretations based on field logging, mean grain size and sorting values were determined for a series of samples from core D25 (central Lulu Island) and core D23 (eastern Lulu Island) (Fig. 6.15). These values were plotted onto a bivariate plot containing the previously defined envelopes corresponding to the grain size characteristics of the three intertidal environments (section 3.1 - Fig. 3.2).

The result (Fig. 7.1) shows that samples from the organic-rich silt lithofacies from both cores plot within or adjacent to the tidal marsh/floodplain zone envelope[1]. This includes samples from 200 to 1450 cm depth in core D23, but from only 200 and 310 cm depth in core D25, where the organic-rich silt unit is relatively thin (Fig. 6.15).

Samples from the interbedded silts, sands and sandy silts unit within both cores fall within or adjacent to the transition

---

[1] Since floodplain sediments are known to be sedimentologically similar to tidal marsh deposits (section 2.3.4), for the purposes of interpretation the envelope defined by tidal marsh grain size characteristics has been renamed 'tidal marsh/floodplain'.

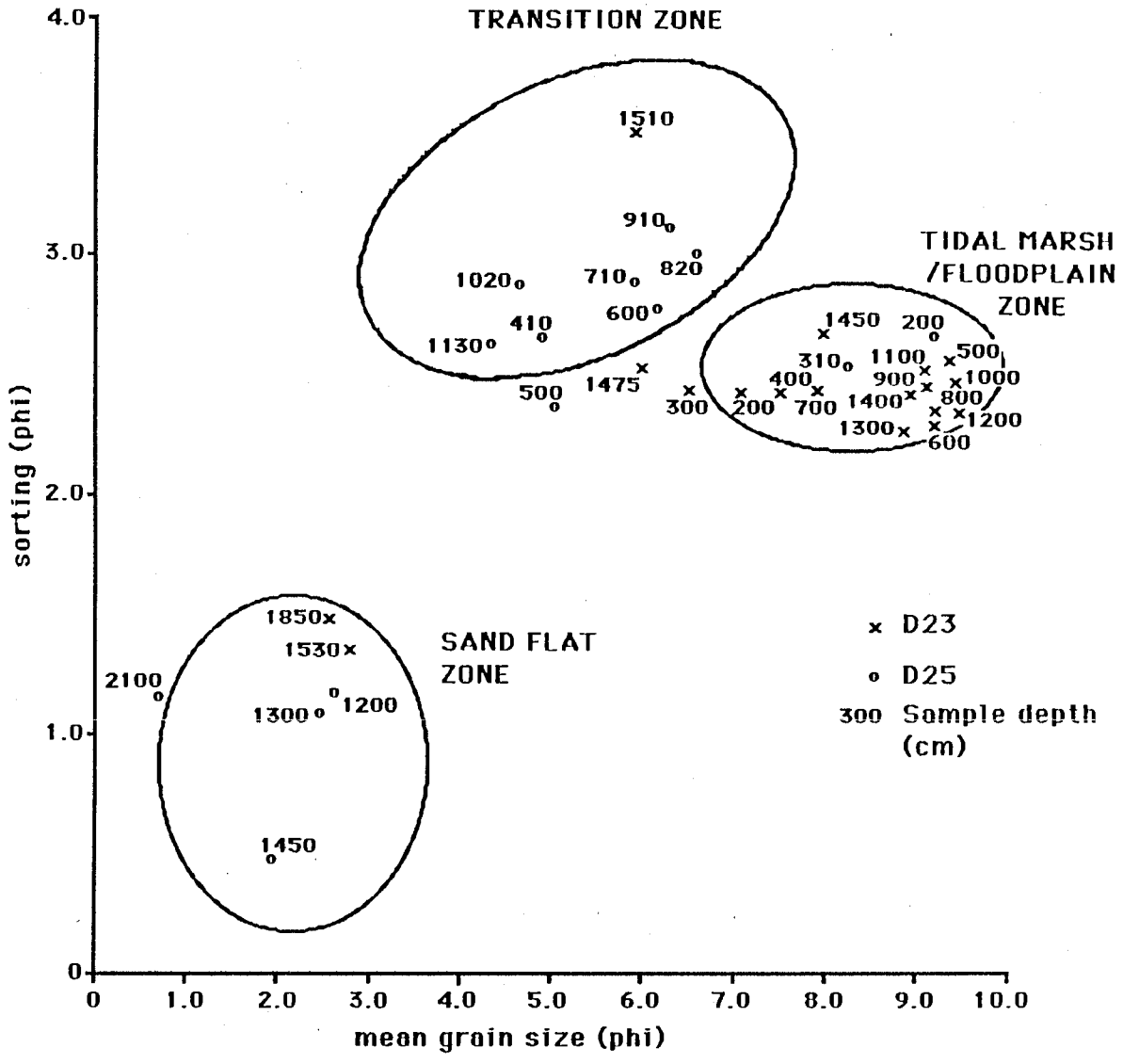

Figure 7.1 Mean grain size v sorting: cores D23 and D25

zone (mid-tidal) envelope. This includes the majority of samples (410 - 1130 cm depth) from core D25, where this unit attains its greatest thickness, but only two samples (1475 and 1510 cm depth) from core D23, where the unit is much thinner.

Samples from the massive sands unit from the basal parts of both core D25 and core D23, plot within or adjacent to the sand flat zone envelope (Fig. 7.1).

7.2.3 SUMMARY OF LITHOFACIES INTERPRETATIONS

An examination of the lithology of Lulu Island's subsurface deposits based on drill cores, suggests that there is a close lithologic similarity between the subsurface organic-rich silt, interbedded silts, sands and sandy silts and massive sands, and deposits of the contemporary tidal marsh/floodplain zone, transition zone and sand flat zone, respectively.

An analysis of particle size distributions of samples collected from the three subsurface lithofacies confirms this similarity. Grain size characteristics of the subsurface deposits do closely match those of their apparent contemporary counterparts.

Further support is provided by consideration of Lulu Island's lithostratigraphy. Apparent correlations between the drill cores indicate that the subsurface deposits are contiguous landward extensions of the aforementioned contemporary depositional environments.

On the basis of these findings, the organic-rich silt lithofacies is tentatively interpreted as being of tidal marsh

zone and or floodplain origin; the interbedded silts, sands and sandy silts lithofacies is tentatively interpreted as a mid-tidal transition zone deposit, and the massive sands lithofacies is tentatively interpreted as a lower tidal sand flat zone deposit.

7.3 BIOFACIES INTERPRETATIONS

7.3.1 PALYNOLOGICAL ANALYSIS

7.3.1.1 Introduction

The primary purpose of the palynological component of this study was to provide a means of distinguishing between lithologically-similar tidal marsh and floodplain deposits; a secondary purpose was to provide some independent confirmation of the environmental interpretations based on lithlogic criteria (section 7.2)[1].

For these reasons, and because palynological techniques can be time-consuming, samples were selected from only one core - D23, located on eastern Lulu Island where the thick organic-rich silt unit is known to be present (Fig. 6.15).

Twenty-nine samples were collected from depths ranging from 145 cm (within the surface peat layer) to 1510 cm (within the

---

[1] Raw pollen counts were provided by R. Hebda, Provincial Museum, Victoria, B.C. All other aspects of the pollen analysis were carried out by the author.

interbedded silts, sands and sandy silts, tentatively identified as mid-tidal deposits). The samples were analysed for their pollen and spore contents using standard palynological techniques. The resulting raw pollen counts were then plotted using the MICHAGAMA (Futyma, 1986) plotting program, enabling the variations in pollen and spore assemblages to be examined and pollen zones to be determined.

7.3.1.2 Results

The resulting pollen diagram (Fig. 7.2) contains six apparent zonations of contrasting pollen and spore assemblages:

ZONE D23-1: 1510-1420 cm. Pinus zone

This zone is distinguished by a very high arboreal non-arboreal pollen ratio (95-96%), reflecting high Pinus values (60-67%), in two of its samples and relatively high values of Cyperaceae (sedge) pollen (0.7-33.7%) and monolete fern spores (2.8-9.4%). Contributions from Poaceae (grasses), Lysichiton americanum (skunk cabbage) and Equisetum (horsetail) also reach relatively high values in some samples within this zone, but attain zero or very low percentages in other samples. The contribution from shrub vegetation is for the most part zero or very low (0-1.7%).

The occurrence of very high percentages of Pinus pollen within this zone strongly suggests an intertidal environment. This is supported by the relatively large contributions from Cyperaceae (sedges), which are known to be abundant in the

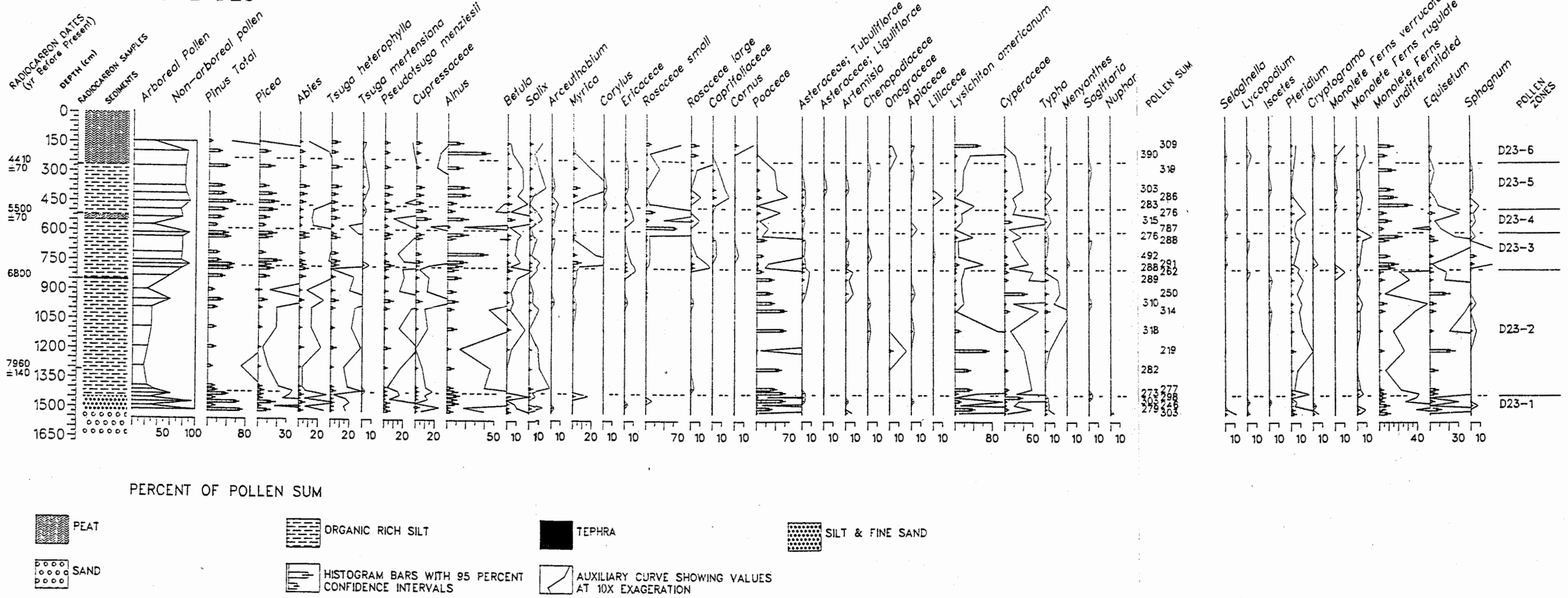

Figure 7.2 pollen diagram for site D23 (see table 8.1 for listing of ^{14}C dates)

contemporary intertidal setting (Hebda, 1977). However, the occurrence of a Lysichiton and Equisetum component is somewhat contradictory, since these are known to usually be absent in intertidal deposits (section 4.4, Table 4.1).

These findings suggest that the deposits of this zone originated in a brackish-water intertidal environment with a considerable fluvial influence, probably due to the close proximity of a fluvial source. It may be that in the delta's natural state (prior to river training, dyke construction etc.) the boundaries between the intertidal and supratidal environments were less clear-cut, allowing the intrusion of characteristic floodplain vegetation into the upper intertidal zone at the delta front. Consequently, the pollen spectrum is dominated by large fluvial inputs of arboreal pollen (especially Pinus) and reflects local stands of marshy delta front vegetation (Cyperaceae, Lysichiton, Equisetum).

ZONE D23-2: 1420-780 cm. Poaceae - Lysichiton - Equisetum zone

This zone is characterized by consistently high values of the emergent freshwater aquatics Lysichiton americanum (skunk cabbage) (0.3-51.3%) and Equisetum (horsetail) (1.7-22.7%). Cyperaceae (sedges) (1.2-35.3%) and Poaceae (grasses) (0.7-55.3%) are also abundant. The relative contribution from arboreal sources declines sharply (to about 30%). The shrub component is low to non-existent throughout (0.1-1.0%).

This assemblage indicates that these deposits formed in a marshy supratidal environment, somewhat more distal from the

delta front than the preceeding zone and similar to the present-day river marsh setting (section 4.2.4). Regular frequent flooding of this environment would favour the development of a wetland plant community, while excluding the establishment of a shrub storey. The lower proportion of fluvially derived arboreal pollen in these deposits probably reflects dilution of the fluvial component by local inputs; the wetland plants being capable of abundant pollen and spore production (Hebda, pers. comm.).

ZONE D23-3: 780-590 cm. Arboreal-shrub zone

This zone is distinguished by the appearance of a substantial shrub component (Myrica (sweet gale) (0-5.7%), Ericaceae (0-1%), Rosaceae (0.3-2.0%), Caprifoliaceae (0-0.4%), Cornus (dogwood) (0-0.4%)); a pronounced increase in the ratio of arboreal to non-arboreal pollen (to about 80%) and a marked decline in Poaceae (grasses) (1-14.6%), Cyperaceae (sedges) (1-5%) and the emergent aquatics, Lysichiton americanum (skunk cabbage) (0.6-6%) and Equisetum (horsetail) (0.3-6.2%).

The establishment of shrub vegetation suggests a slight increase in the relative elevation of the site, probably to just about high tide level, and/or a more distal setting for the site relative to fluvial sources (distributary channels and delta front).

A more distal setting would tend to reduce the amount of fluvially-derived nutrients reaching the site, rendering it less eutrophic than the preceeding river marsh site (zone D23-2).

This condition is favourable to shrub development (Hebda, pers. comm.).

ZONE D23-4: 580-470 cm. Rosaceae zone

This zone is dominated by shrubs of the Rosaceae family (1-62.5%) and contains a sharp drop in the arboreal pollen component (to about 30%). The herbaceous contribution remains at reduced values (0-4.7%), as in the preceeding zone.

These findings suggest that the site became sufficiently elevated, and or distal to fluvial sources, to increase the dominance of shrub vegetation (probably in the form of Spiraea douglasii (hardhack) - Hebda, pers. comm.) and reduce the input of flood-derived arboreal pollen.

The pollen assemblages of this zone and the preceeding zone D23-3, together resemble the natural successional sequence that accompanies the progressive elevation of the delta surface above sea level and which may culminate in raised peat bog conditions (Hebda, 1977 - the lower part of his Fig. 50).

ZONE D23-5: 470-232 cm. Arboreal-shrub zone

This zone resembles zone D23-3. Shrubs dominate the local vegetation (0.3-4.1%), while grasses and marsh plants (Lysichiton, Equisetum) remain comparatively subdued (0-6.3%). The return of the arboreal component to relatively high levels (to about 80%) suggests an increasing fluvial influence at the site and hence more regular and frequent flooding and or a site more proximal to fluvial sources.

ZONE D23-6: 232-145 cm. Rosaceae- Lysichiton zone

The contribution from Rosaceae undergoes a distinct increase in this zone (0.7-7.1%), while there is a pronounced drop in the ratio of arboreal to non-arboreal pollen (89 to 33%, from 190 to 145 cm). Lysichiton americanum (skunk cabbage) attains a high value at 145 cm (48.3%), although other emergent aquatics (Poaceae, Cyperaceae, Equisetum) remain comparatively low (0-2.2%).

These findings suggest the site was characterized by shrubby thickets containing marshy openings occupied by Lysichiton americanum (skunk cabbage). The decrease in the arboreal component suggests a reduced fluvial influence, indicating that the relative elevation of the site had increased and or the site had become more distal to fluvial sources.

As for zones D23-3 and D23-4, the pollen assemblages of zones D23-5 and D23-6 together resemble the natural vegetational successional sequence associated with the early stages of raised peat bog development (Hebda, 1977).

7.3.1.3 Summary of palynological interpretations

A major result of the palynological analysis is the resolution of the thick organic-rich silt unit into its 'tidal marsh' and 'floodplain' components.

The findings indicate that the bulk of the organic-rich silt unit formed in a 'floodplain-like' setting, dominated by fluvially-derived floodwater deposition in the supratidal zone. This part of the unit is characterized by pollen and spores of

Poaceae (grasses) and the emergent aquatics Lysichiton and Equisetum. The arboreal component is comparatively small.

Tidal marsh deposits are apparently restricted to a relatively thin layer (up to about 1420 cm depth) in contact with the underlying interbedded silts, sands and sandy silts unit. High percentages of arboreal pollen (especially Pinus) occur within this zone, as well as a relatively high proportion of pollen and spores from Cyperaceae (sedges), monolete ferns and emergent aquatics. The shrub contribution is low. This assemblage most likely represents an intertidal, delta front location, but with a significant fluvial influence.

In general, the results of the palynological study confirm the findings based on lithology: the interbedded silts, sands and sandy silts unit has a pollen and spore assemblage characteristic of the intertidal zone; the organic-rich silt unit consists of a thin basal layer of tidal marsh deposits, overlain by a much thicker accumulation of floodplain sediments.

Within the floodplain deposits there are two zones containing the successional sequence corresponding to peat bog development: one at a depth of about 780 to 470 cm, associated with the buried peat layer at 525-550 cm depth; and another at about 470 to 145 cm depth, associated with the surface peat horizon.

7.3.2 MICROPALEONTOLOGICAL ANALYSIS

7.3.2.1 Introduction

Distinct elevational zonations of foraminifera species have been established for the contemporary intertidal surface (chapter 5). These findings offer the potential for the environmental interpretation of core samples based on their incorporated foraminiferal assemblages. Such interpretations may provide further independent support for the environmental interpretations based on lithology and palynology.

Whereas the palynological study was primarily designed to enhance interpretive resolution within the organic-rich silt lithofacies (by intensive sampling of one core), the foraminifera study was aimed at providing a more general confirmation of the environmental interpretations based on core lithology.

Consequently, a total of 41 samples were collected from 15 widespread core locations. In each case, a few samples were obtained from the section of the core tentatively interpreted as being of intertidal origin, based on lithologic criteria.

The samples were examined for their foraminiferal contents using the procedures outlined in section 5.3.2.

7.3.2.2 Results

The results of the analysis of the core samples are shown in Table 7.1. Surprisingly low numbers of foraminifera were found in the samples. Only nine samples, from four of the cores

Table 7.1 Absolute and relative species abundance: core samples

Sample No	Depth cm	Weight g	Species Abundance (No/density per 100 g) Polystomammina grisea	Haplophragmoides sp. cf. H. canariensis	Miliammina fusca
D79	200	251.50	18/7.2		1/0.4
D79	250	628.10	5/0.8		
D79	300	502.70			
D79	350	464.20			
D79	400	555.70	1/0.18		
D79	450	416.80			
D79	500	487.00			
D79	530	419.60			
D78	200	331.40			
D78	250	410.00	12/3		
D78	300	440.40			
D78	350	424.30	7/1.6		
D78	400	615.60			
D78	450	493.00	1/0.2		
D78	500	517.70			
D78	550	248.00			
D60	370	475.80			
D60	460	443.20			
D60	590	267.50			
D60	630	320.10			
D59	310	491.90			
D59	350	563.90	2/0.35	1/0.18	
D59	450	664.20		2/0.3	
D59	550	511.10			
D48	250	343.00			
D48	380	458.00			
D47	340	285.60			
D58	390	450.30			
D58	430	292.70	40/14		
D58	475	301.20			
D25	310	46.40			
D27	460	44.40			
D27	560	43.40			
D27	660	54.50			
D26	570	39.80			
D26	670	68.40			
D33	380	57.70			
D54	740	144.40			
D45	260	240.80			
D44	265	226.70			
D55	900	335.10			

studied, were found to contain any foraminifera.

Within these nine samples, only three of the five known contemporary intertidal species were present - Polystomammina grisea, Haplophragmoides sp. cf. H. canariensis and Miliammina fusca. In most cases, specimen density was very low - five of the nine samples had densities of less than one specimen per 100 g of sample (Table 7.1).

7.3.2.3 Discussion

The finding that so few samples contain foraminifera, and in such low numbers, appears to support the suggestion made in section 5.5, that foraminiferal tests are not well preserved in the subsurface of the delta. The lack of foraminifera in itself does not imply a non-marine origin. It has already been established that samples of known intertidal deposits may have a zero foraminifera content (Table 5.2, samples TFC2: 40; TFC4: 48, and TFC4: 85).

Consequently, environmental interpretations may only be suggested for the nine samples that do contain foraminifera specimens. Of these samples, only one contained a sufficient number of specimens to support an environmental interpretation in terms of the elevational zonations established in chapter 5. The sample from core D58 at a depth of 430 cm contained 40 specimens of Polystomammina grisea (a density of 14 per 100 g).

The presence of a relatively large concentration of this species indicates an upper intertidal origin for this sample, probably between 50 and 140 cm above mean sea level (sections

5.4.1.2, 5.5) (B. Cameron, Pacific Geoscience Centre, pers. comm.).

The presence of intertidal foraminiferal species in the other eight samples, although in insufficient numbers to indicate the elevation of deposition, does at least indicate that these deposits probably accumulated within the intertidal zone.

7.3.2.4 Summary of micropaleontological interpretations

Interpretations of depositional environment could be applied to deposits of only four cores used in the foraminifera study, due to apparently poor preservation of foraminifera tests in the subsurface.

Samples from a depth of 200, 250 and 400 cm in core D79; 250, 350 and 450 cm in core D78, and 350 and 450 cm in core D59, are all given the general interpretation of "intertidal deposits".

The sample containing the greatest density of foraminifera specimens, at 430 cm depth in core D58, can be given a more specific environmental interpretation. This sample probably formed in the upper intertidal zone, between 50 and 140 cm above mean sea level. Given the present elevation of this sample (-3.67 m), this finding suggests that mean sea level at the time of deposition was some 4.17 to 5.07 m lower than at present.

7.4 SUMMARY AND SYNTHESIS OF LITHOFACIES AND BIOFACIES INTERPRETATIONS

The paleoenvironmental interpretations based on lithology, palynology and foraminiferal analysis, are summarized in diagram form in Figure 7.3. Table 7.2 summarizes the contribution from each aspect of the study towards the overall facies interpretations.

The overall lithostratigraphic framework and preliminary facies interpretations are provided by logging of core lithology. These interpretations are supported and improved upon by the palynological analysis, which provide a means of distinguishing between the lithologically-similar floodplain and tidal marsh deposits. The results of the foraminifera study, although very limited, nevertheless provide further independent confirmation of the facies interpretations based on lithology and palynology, and additional evidence of a lower sea level during Lulu Island's development.

On the assumption that the results of the palynological analysis of core D23 can be extended to the rest of the organic-rich silt unit (i.e. the relative proportions of tidal marsh and floodplain deposits remain about the same throughout the unit), generalized facies interpretations can now be established for the subsurface deposits of Lulu Island (Fig. 7.4).

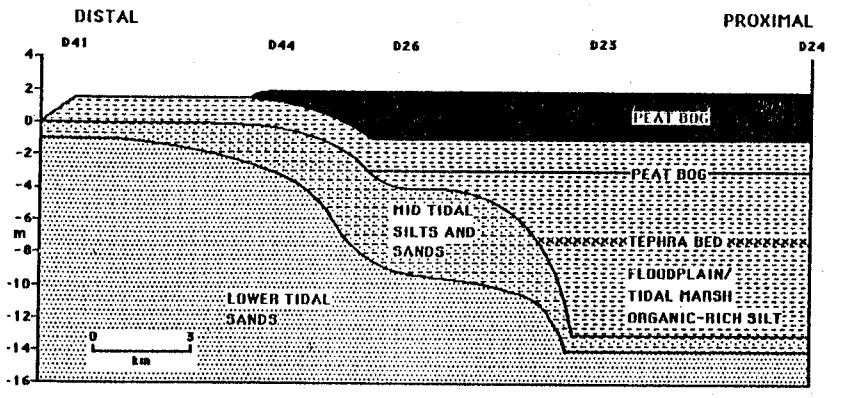

(a) Lithology

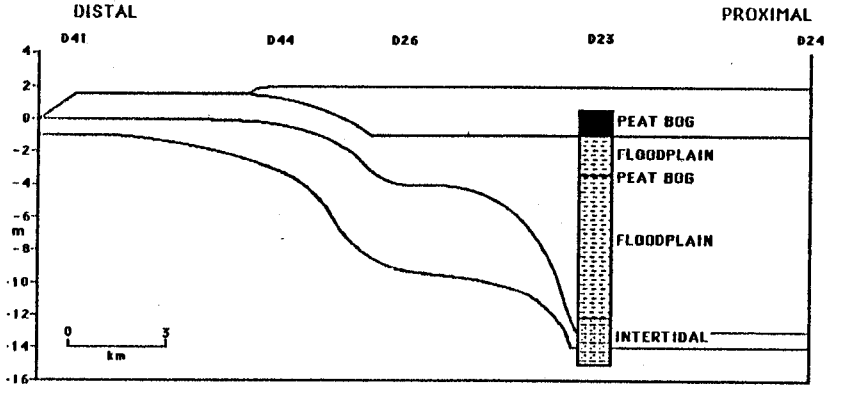

(b) Palynology

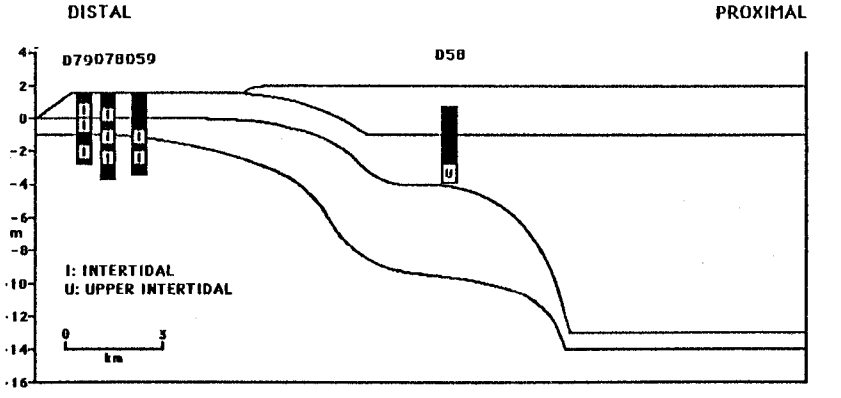

(c) Micropaleontology

Figure 7.3 paleoenvironmental interpretations
(a) interpretations based on generalized lithostratigraphy
(b) interpretations of the deposits in core D23, based on palynological analysis
(c) interpretations based on foraminiferal assemblages

Table 7.2 Facies characteristics and paleoenvironmental interpretations

LITHOLOGIC CHARACTERISTICS	DISTINCTIVE PALYNOLOGICAL COMPONENTS	FORAMINIFERAL CONTENT	PALEOENVIRONMENTAL INTERPRETATION
Peat. Horizontally bedded.	Rosaceae. Reduced arboreal component.	None.	Peat bog.
Organic-rich silt, horizontally bedded. bioturbated.	Substantial shrub component (Myrica, Ericaceae, Rosaceae, Caprifoliaceae, Cornus). Increased arboreal component. Decreased grasses, sedges and emergent aquatics.	None.	Distal floodplain (less eutrophic, increased elevation and/or more distal to fluvial sources).
Organic-rich silt, horizontally bedded. bioturbated.	Emergent aquatics. Lysichiton, Equisetum, poaceae, Cyperaceae. Reduced arboreal and shrub components.	None.	Proximal floodplain (marshy, frequent flooding, proximal to fluvial sources).
Organic-rich silt, horizontally bedded. bioturbated.	High arboreal/non arboreal pollen ratio. relatively high Cyperaceae, and monolete fern spores. Variable grasses/ emergent aquatics component. Zero to low shrub component.	Polystomammina * grisea, Haplophragmoides sp. cf. H. canariensis.	Tidal marsh (upper tidal)
Interbedded silts and sands. scattered organics. Horizontal bedding. Some gradations in grain size, some shallow angle cross bedding, some aburpt contacts. Bioturbated.	Very high arboreal/non arboreal pollen ratio. Relatively high monolete fern spore component.	May include * Polystomammina grisea, Haplophragmoides sp. cf. H. canariensis, Ammonia beccarii, Miliammina fusca, Rosalina columbiensis.	Transition zone (mid tidal)
Well sorted fine to medium sand. Very little silt or organics. Some gradations in grain size, otherwise appears structureless.	Very high arboreal/non arboreal pollen ratio. Relatively high monolete fern spore component.	May include * Polystomammina grisea, Haplophragmoides sp. cf. H. canariensis, Ammonia beccarii, Miliammina fusca, Rosalina columbiensis.	Sand flat zone (lower tidal)

* Foraminifera tests are apparently poorly preserved in the subsurface of the delta and few, if any, may be present in the intertidal samples.

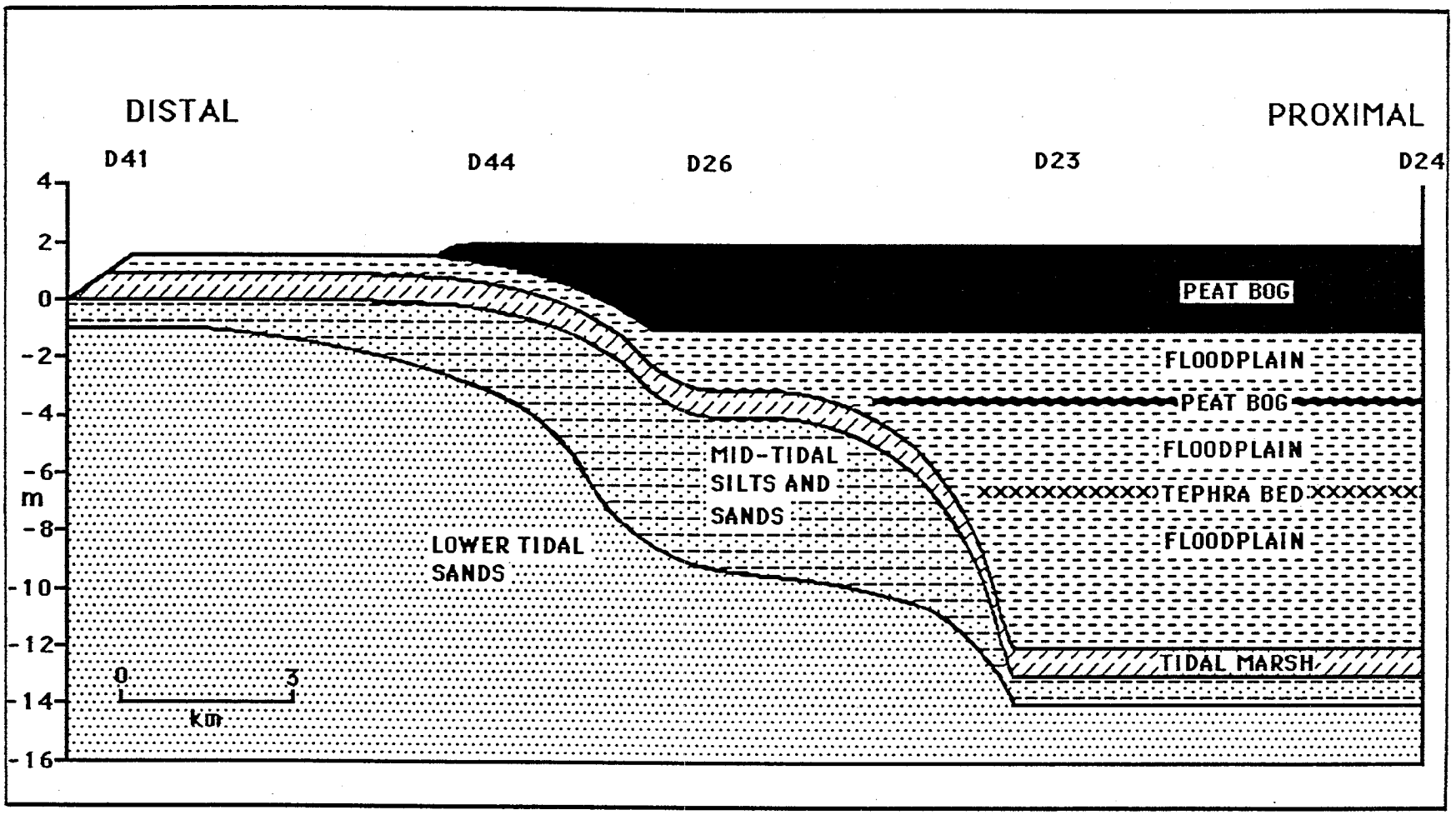

Figure 7.4 Lulu Island facies interpretations

CHAPTER EIGHT

CHRONOLOGY

8.1 INTRODUCTION

This chapter outlines a chronology of Lulu Island's growth. Chronological control was obtained from two sources - ^{14}C dates, obtained specifically for this study and from previous research, and identification of the source of the tephra bed underlying eastern Lulu Island and the adjoining Fraser River floodplain.

8.2 ^{14}C DATES

8.2.1 INTRODUCTION

Cores obtained from the eastern part of the study area contained an abundant amount of organic material suitable for ^{14}C dating. Samples were obtained from the surface and buried peat layers, as well as from throughout the organic-rich silt unit.

On the western side of Lulu Island, sampling opportunities were more limited. Here, there was no surface peat layer and the organic-rich silt unit was much thinner than in the east. Large (ca. 5 cm) wood fragments were, however, found in some of the cores from western Lulu Island and these were retained for possible ^{14}C dating.

Most of the samples submitted for dating consisted of peat or organic-rich silt. In all cases, these samples were obtained from the central part of a core (away from possible contamination near the edges) and were collected from deposits that were clearly in situ, as indicated by the presence of intact sedimentary structures within, or enclosing, the sample (e.g. horizontal laminations within the organic-rich silt unit - see Fig. 6.8).

8.2.2 SAMPLE SELECTION

The selection of samples for ^{14}C dating was designed to meet three major objectives:

(i) in order to calculate vertical sedimentation rates pertaining to the thick floodplain deposits underlying the eastern delta, three samples were collected from the top, central and basal parts of the organic-rich silt unit of core D23 (Fig. 6.1).

(ii) in order to provide a proximal to distal series of dates (including the dates from the eastern delta in (i) above), to facilitate calculations of the delta's lateral progradation rates during the Holocene, a number of samples were obtained from cores in the central and western parts of Lulu Island (D60, D41, D59, D44, D32 - Fig. 6.1).

(iii) in order to date the buried peat bed and to confirm that the peat bed does, in fact, represent a contiguous, coeval paleosurface, samples of the buried peat bed were obtained from three widely spaced locations (D52, D69, D71 - Fig. 6.1).

8.2.3 RESULTS

A total of eleven samples were submitted for dating; the results, along with details of other dates referred to in this study (see chapter 2), are presented in Table 8.1.

8.2.4 DISCUSSION

The series of three dates from core D23 (Fig. 6.15) show that the thick floodplain deposits underlying eastern Lulu Island began forming about 7960 yr BP (GSC-4255). The accumulation of floodplain sediments ended at about 4410 yr BP (GSC-4194) and the overlying peat deposits began to form. The date of 5500 ± 70 yr BP (GSC-4238) from the central part of core D23, suggests that the rate of deposition of the floodplain unit was greater between ca. 7960-5500 yr BP than between ca. 5500-4410 yr BP[1].

The dates from the central and western parts of Lulu Island, ranging from 4090 ± 60 to 1840 ± 160 yr BP (TO-407 and GSC-4275, respectively), reflect the more recent growth of this part of the delta. The most recent date - 1840 ± 160 yr BP (GSC-4275) - was, as would be expected, obtained from the most westerly sampling location (D41 - Fig. 6.3).

The three dates obtained on the samples from the buried peat layer are in remarkably close agreement. Dates of 6025 ± 105, 5840 ± 145 and 5990 ± 155 (S-2872, S-2866 and S-2867, respectively) were yielded by these samples, the most westerly

---

[1] Calculation and discussion of sedimentation rates will appear in chapter 9.

Table 8.1 Listing of ^{14}C dates used in this study

(i) dates obtained for this study:

LABORATORY DATING No.	DATE (yr BP)	CORE No.	LOCALITY	LOCATION Lat.	LOCATION Long.	MATERIAL	DEPOSITIONAL ENVIRONMENT	ELEVATION (m) (b.m.s.l.)
GSC-4275	1840±160	D41	LULU ISLAND TIDAL MARSH	49° 8.8'	123° 11.6'	WOOD	LOWER TIDAL	2.30
TO-409	2080±110	D60	WESTERN LULU ISLAND	49° 10.0'	123° 11.8'	WOOD	MID TIDAL	1.22
TO-408	2490±60	D59	WESTERN LULU ISLAND	49° 8.0'	123° 10.1'	WOOD	LOWER TIDAL	3.15
S-2865	3755±240	D32	CENTRAL LULU ISLAND	49° 11.3'	123° 0.6'	DETRITUS	FLOODPLAIN	0.90
TO-407	4090±60	D44	CENTRAL LULU ISLAND	49° 9.4'	123° 6.7'	WOOD	MID TIDAL	1.82
GSC-4194	4410±70	D23	EASTERN LULU ISLAND	49° 10.5'	122° 58.3'	DETRITUS	FLOODPLAIN	1.19
GSC-4238	5500±70	D23	EASTERN LULU ISLAND	49° 10.5'	122° 58.3'	DETRITUS	FLOODPLAIN	3.55
S-2866	5840±145	D69	COQUITLAM	49° 14.3'	122° 48.6'	PEAT	PEAT BOG	1.80
S-2867	5990±155	D71	PITT MEADOWS	49° 12.7'	122° 41.3'	PEAT	PEAT BOG	0.30
S-2872	6025±105	D52	EASTERN LULU ISLAND	49° 10.5'	122° 57.7'	PEAT	PEAT BOG	3.77
GSC-4255	7960±140	D23	EASTERN LULU ISLAND	49° 10.5'	122° 58.3'	DETRITUS	FLOODPLAIN	11.71

(ii) Significant dates from other studies:

LABORATORY DATING No.	DATE (yr BP)	LOCALITY	LOCATION Lat.	LOCATION Long.	MATERIAL	SIGNIFICANCE	ELEVATION (m) (b.m.s.l.)
GX-0781	4350±100	BOUNDARY BAY	49° 4.5'	122° 55.0'	PEAT	SEA LEVEL AT LEAST 1.8 m LOWER	0.8
GSC-3045	4650±80	EASTERN LULU ISLAND	49° 11.9'	122° 59.0'	PEAT	BASE OF PEAT BOG	0.0
GSC-3066	5510+80	EASTERN LULU ISLAND	49° 10.6'	122° 58.6'	PEAT	BASE OF PEAT BOG	0.0
WAT-369	6400+197	CENTRAL LULU ISLAND	49° 9.0'	123° 1.0'	SILT	SEA LEVEL LOWER	>0.0
S-99	7300±120	PORT MANN	49° 13.0'	122° 48.0'	PEAT	SEA LEVEL AT LEAST 10 m LOWER	10.0
GSC-3099	7710±80	PITT MEADOWS	49° 13.3'	122° 42.9'	PEAT	SEA LEVEL AT LEAST 10 m LOWER	9.5
GSC-225	8360±170	SUMAS	49 2.0'	122° 16.0'	WOOD	SEA LEVEL AT LEAST 11 m LOWER	11.0
GSC-3919	9490±250	NEW WESTMINSTER	49° 12.5'	122° 53.7'	WOOD	MAXIMUM AGE FOR FRASER DELTA	55.0

and easterly of which (from cores D52 and D71, respectively) were separated by over 20 km (Fig. 6.21).

These results strongly support the contention that the buried peat layer represents organic accumulations on a contiguous, coeval paleosurface, underlying eastern Lulu Island and the adjoining Fraser River floodplain. Based on the radiocarbon dates, the peat marker horizon is assigned an age of ca. 6000 yr BP.

This evidence suggests that a hitherto unknown stillstand of sea level occurred at ca. 6000 yr BP. The stillstand was of sufficient duration (presumably several hundred years) to allow extensive peat deposits to develop on the (former) terrestrial surface of the delta.

The approximate duration of the stillstand can be estimated from the thickness of the resulting peat deposits. Hebda (1977) calculated an average rate of peat accumulation in Burns Bog on the southern Fraser Delta, of 6.67 cm per 100 years. A figure of 7 cm per 100 years was determined for Jesmond Bog in southern B.C. (Nasmith et al., 1967). In addition, the base of the surface peat deposits on Lulu Island, which average about 3 m in thickness, has been dated in this study at 4410 $\pm$ 70 yr BP (GSC-4194 - Table 8.1), giving an average accumulation rate of 6.8 cm per 100 years.

On the basis of these accumulation rates, the buried peat layer, which averages about 25 - 30 cm in thickness, probably formed in approximately 400 years. Therefore, it will be assumed that the stillstand occurred from about 6200 to 5800 yr BP.

The estimated timing of the stillstand appears reasonable in terms of the dates which bracket the buried peat layer in core D23. A date of 5500 ± 70 yr BP (GSC-4238) occurs 22 cm above the peat, and tephra, presumably 6800 yr BP Mazama (section 2.4.3), occurs 3 m below the peat bed (Fig. 6.6).

8.3 TEPHRA IDENTIFICATION

8.3.1 INTRODUCTION

The tephra beds found throughout the eastern part of the study area may represent a potentially valuable time-stratigraphic marker horizon. In order to determine if this is the case, the source of the tephra must be identified and it must be shown that all occurences of the tephra bed are part of a single tephra deposit, originating from the same source.

Tephra from three major Holocene eruptions are known to be widely distributed throughout southern British Columbia. These are, Mazama (6800 yr BP), Mt. St. Helens Yn (3400 yr BP) and Bridge River (2350 yr BP) (Nasmith et al., 1967; Westgate and Dreimanis, 1967; Westgate et al., 1970; Mathewes and Westgate, 1980).

The presently-known distributions of these three tephra units in British Columbia suggest that only Mazama tephra occurs in the vicinity of the Fraser River delta (Fig. 8.1). The possibility does remain, however, that the actual distributions of the Mt. St. Helens Yn and Bridge River tephras are considerably larger than shown, but have yet to be positively

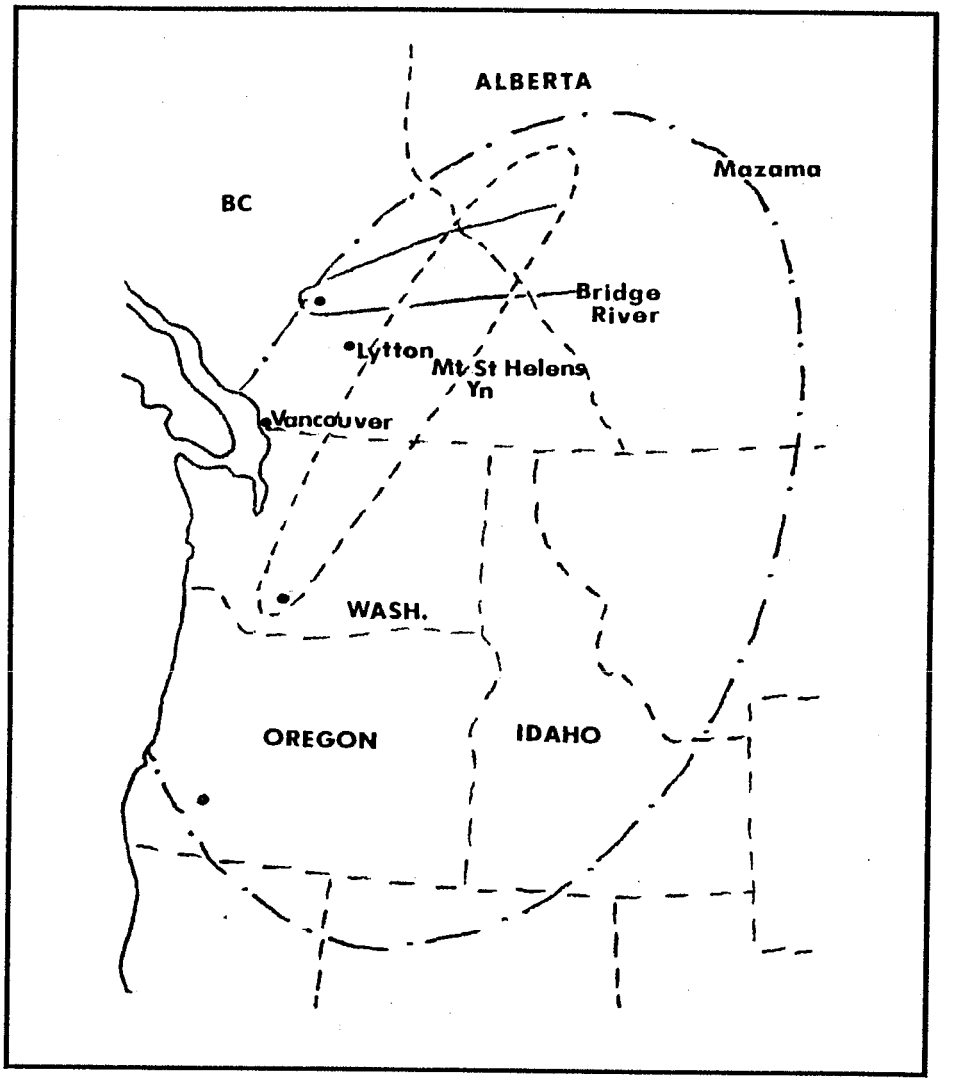

Figure 8.1 Distribution of Mazama, Mt. St. Helens Yn and Bridge River tephras in the Pacific Northwest (modified from Westgate et al., 1970)

identified beyond the boundaries indicated. Tephra related to the Bridge River eruption, for example, has been tentatively identified in lake sediments near Lytton in southern British Columbia, a considerable distance south of the previously documented fallout zone (Mathewes and Westgate, 1980) (Fig. 8.1).

Nevertheless, the distributions shown in Figure 8.1 and the stratigraphic position of tephra layers in relation to nearby radiocarbon dates, have been used as a basis for (tentative?) identification of tephra as "Mazama" in previous studies in the Lower Mainland (Blunden, 1973, 1975; Clague et al., 1983).

The radiocarbon dates obtained for this study also provide good evidence that many of the tephra beds encountered in this study are of Mt. Mazama origin. The tephra bed in core D23, for example, is bracketed by dates of 7960 $\pm$ 140 yr BP (GSC-4255) and 5500 $\pm$ 70 yr BP (GSC-4238). Six of the other fifteen occurences of tephra in this study (in cores D52, D69, D71, D72, D73 and D74) are found stratigraphically below the buried peat marker horizon dated at ca. 6000 yr BP (section 8.2.4), precluding a Mt. St. Helens Yn or Bridge River origin for these tephra layers.

However, the peat marker horizon was not encountered in cores containing the remaining nine tephra layers (in cores D29, D43, D46, D50, D55, D64, D62, TH84-913 and TH85-14). The identification of these tephra beds as Mazama can only be inferred from their stratigraphic positions.

Since the tephra beds have the potential of providing very

valuable geochronological control for this study (and for future studies in the same area), it was decided to examine the chemical composition of the tephra, in an attempt to show that; firstly, all the tephra beds have similar chemical characteristics and thus are likely part of the same widespread tephra layer, originating from the same source; and secondly, that the "chemical fingerprints" of these tephra layers match those of known Mazama tephras and are distinct from those of Mt. St. Helens Yn and Bridge River.

The technique of energy dispersive X-ray fluorescence (XES) analysis was used to examine the chemical composition of the tephra deposits.

8.3.2 XES ANALYSIS

8.3.2.1 Introduction

Energy dispersive X-ray fluorescence (XES) analysis provides a means of simultaneously analysing a wide range of elements, including the major elements K to Fe and the trace elements Rb to Nb, in analysis times as short as 5 minutes per sample (Cormie et al., 1981).

The more widely applied technique of microprobe analysis can provide very accurate results, because it is a grain-discrete method (Smith and Westgate, 1969). However, the microprobe has the disadvantage of requiring several tedious and time-consuming sample preparation procedures and is capable of analysing only the major elements, even though the most

prominent dissimilarities in tephra composition occur in the trace element range (Bird et al., 1978).

Cormie (1981) developed an XES technique that met with a high level of success in distinguishing Mazama tephra samples from those of Bridge River and Mt. St. Helens Yn, on the basis of relatively high Zr concentrations in Mazama tephra. The only pretreatment used was sieving to produce samples in the < 62 um size range. Using this technique, Cormie was able to identify 34 out of 39 samples of Mazama tephra - a success rate of about 87% (Cormie, 1981 - p. 110).

8.3.2.2 Methods

Details of the principles of X-ray fluorescence analysis can be found in a number of texts (e.g. Bertin, 1970; Woldseth, 1973). Only a brief summary of the technique is presented below to aid in understanding the methods used in this study.

XES analysis utilizes a monochromatic beam of primary X-rays to induce fluorescence in a sample target. Absorption of the X-ray beam produces the photoelectric effect, leaving vacancies in the innermost (K) electron shells of the elements that make up the sample. During the resulting electron transitions, characteristic X-rays are emitted, the energies of which equal the binding energy between the innermost (K) and outermost electrons of the elements. Most electron transitions produce K-alpha (Ka) secondary X-rays, although it is possible (but less likely) that K-beta (Kb), L-alpha (La), L-beta (Lb) or L-gamma (Lγ) X-rays will be produced.

The energies and intensities of the secondary X-rays are measured on a multi-energy detector, enabling an energy spectrum to be obtained in an analysis time typically of 5 or 10 minutes. Each element within the sample will be reflected by a peak in the spectrum, the area (or height) of which will be proportional to the concentration of the element (Fig. 8.2).

The spectrum also contains Compton (inelastic) and Rayleigh (elastic) scatter peaks, produced by backscatter of the primary X-ray beam. Both scatter peaks increase with an increase in the energy of the overall sample matrix. Additional backscatter of secondary X-rays produces a background continuum within the spectrum (Fig. 8.2). This is subtracted from the area of peaks in order to calculate net peak areas.

The method developed for this study was based on the following criteria:

(i) there was already evidence from ^{14}C dating that the tephra beds under investigation are of Mazama origin. Consequently, the XES analysis was designed simply to distinguish Mazama from Mt. St. Helens Yn and Bridge River tephras. The XES analysis was, therefore, directed at providing support and confirmation of the findings based on ^{14}C dating.

(ii) Cormie (1981) has shown that chemical pretreatments to remove contaminants are unnecessary for the identification of Mazama tephra, since Zr (as well as other trace elements) is not affected as much by contamination as the major elements such as Ca, Ti and Fe (Cormie, 1981 - her Table 4.1). In this study, it

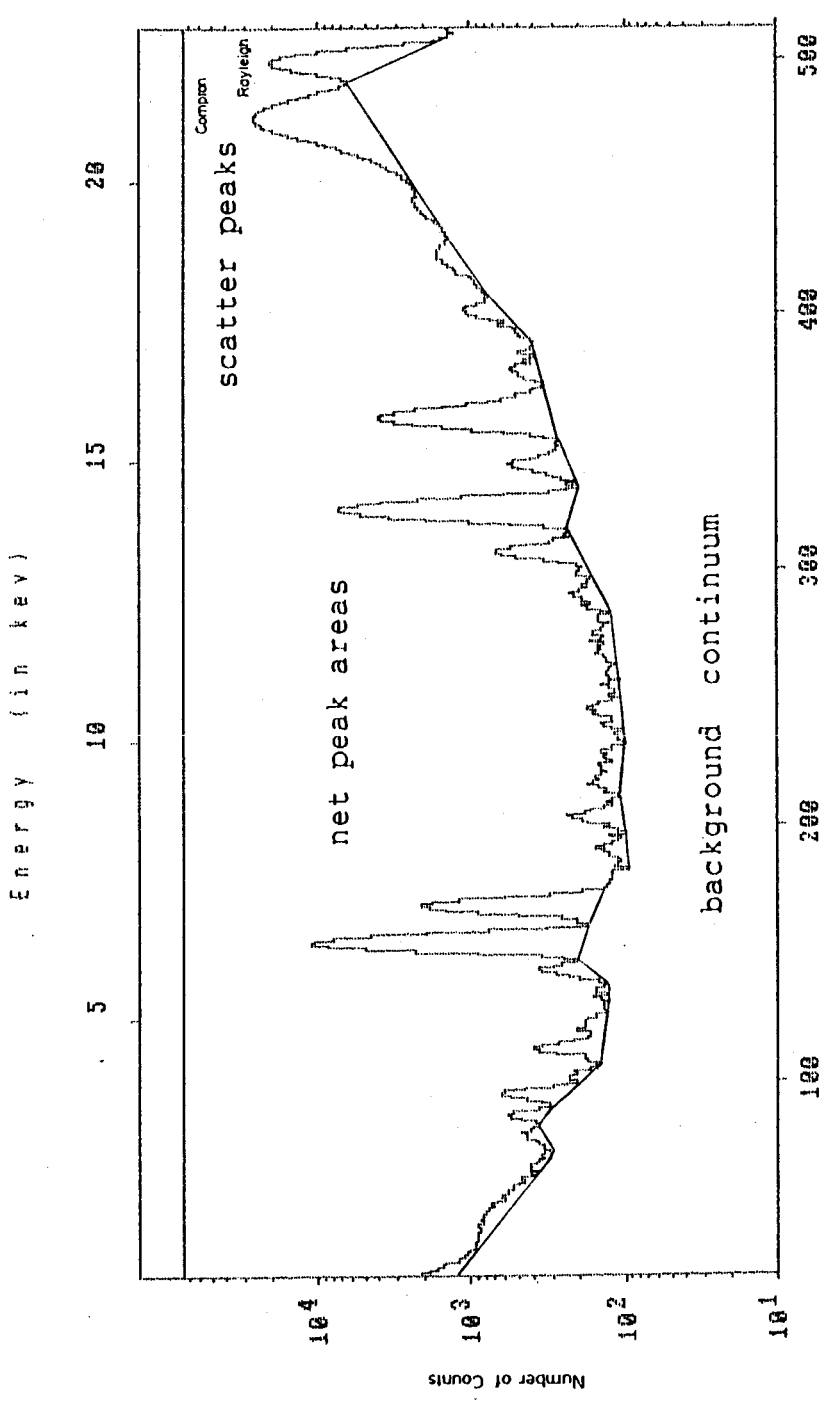

Figure 8.2 Components of a typical tephra spectrum produced by XES

was decided to minimize sample pretreatment and, additionally, to avoid any procedure which might alter the composition of the tephra samples. Thus, sample pretreatment consisted simply of oven-drying the tephra for 24 hours, removal of visible contaminants (e.g. plant remains) by hand, accurately weighing 200 mg subsamples, and pelletization of the subsamples to standardize sample presentation to the X-ray beam.

(iii) Cormie's (1981) method of identifying Mazama was based on normalizing the Zr net peak area to the Compton peak height. However, the drawback of this method is that contamination in the sample (e.g. organic detritus) is likely to change the Compton peak height (by altering the overall composition of the sample matrix), but may have little or no effect on the Zr net peak area. An alternative approach, which was used in this study, is to characterize the tephras on the basis of the relative concentrations of two trace elements within the samples. This approach has a number of advantages: tephras are distinguished on the basis of two elements, rather than only one; trace elements appear to be less prone to contamination effects than the major elements; the greatest dissimilarities between tephra groups occur in the trace element range; and, all forms of operational, instrumentational and preparational errors which can affect the absolute size of peaks within the spectrum, can be assumed to operate equally over the entire spectrum and thus the relative size of two peaks within a spectrum should not be affected (J. D'Auria, Department of Chemistry, SFU, pers. comm.).

In order to investigate variations in trace element composition between the three tephra groups, known samples from each of the tephras had to be examined. A total of 8 Mazama, 8 Mt. St. Helens Yn and 8 Bridge River tephra samples were obtained.

One of the Mazama samples and one of the Mt. St. Helens Yn samples were collected from known exposures in Washington State by Dr. S. Porter (University of Washington). The remaining seven samples in each of these two sample sets were collected from known exposures in the vicinity of Kamloops, B.C., by Dr. M. C. Roberts (SFU).

The samples from the Kamloops area were obtained from exposures containing both the Mazama and Mt. St. Helens Yn tephra beds, with the Mazama clearly occurring stratigraphically below the Mt. St. Helens Yn, leaving no possibility of misidentification.

The 8 Bridge River samples were all collected by Dr. M. C. Roberts (SFU) from thick tephra deposits close to the source vent, in the vicinity of Lillooet, B.C.

These samples were prepared and analysed using the techniques outlined above. The primary X-ray beam was produced by a silver secondary target to preferrentially excite the trace elements Rb to Nb (Fig. 8.2).

Examination of the resulting spectra revealed that four peaks were particularly prominent in the trace element range - RbKa, SrKa, YKa+RbKb and ZrKa+SrKb (Fig. 8.3).

To compare the relative size of peaks both within and

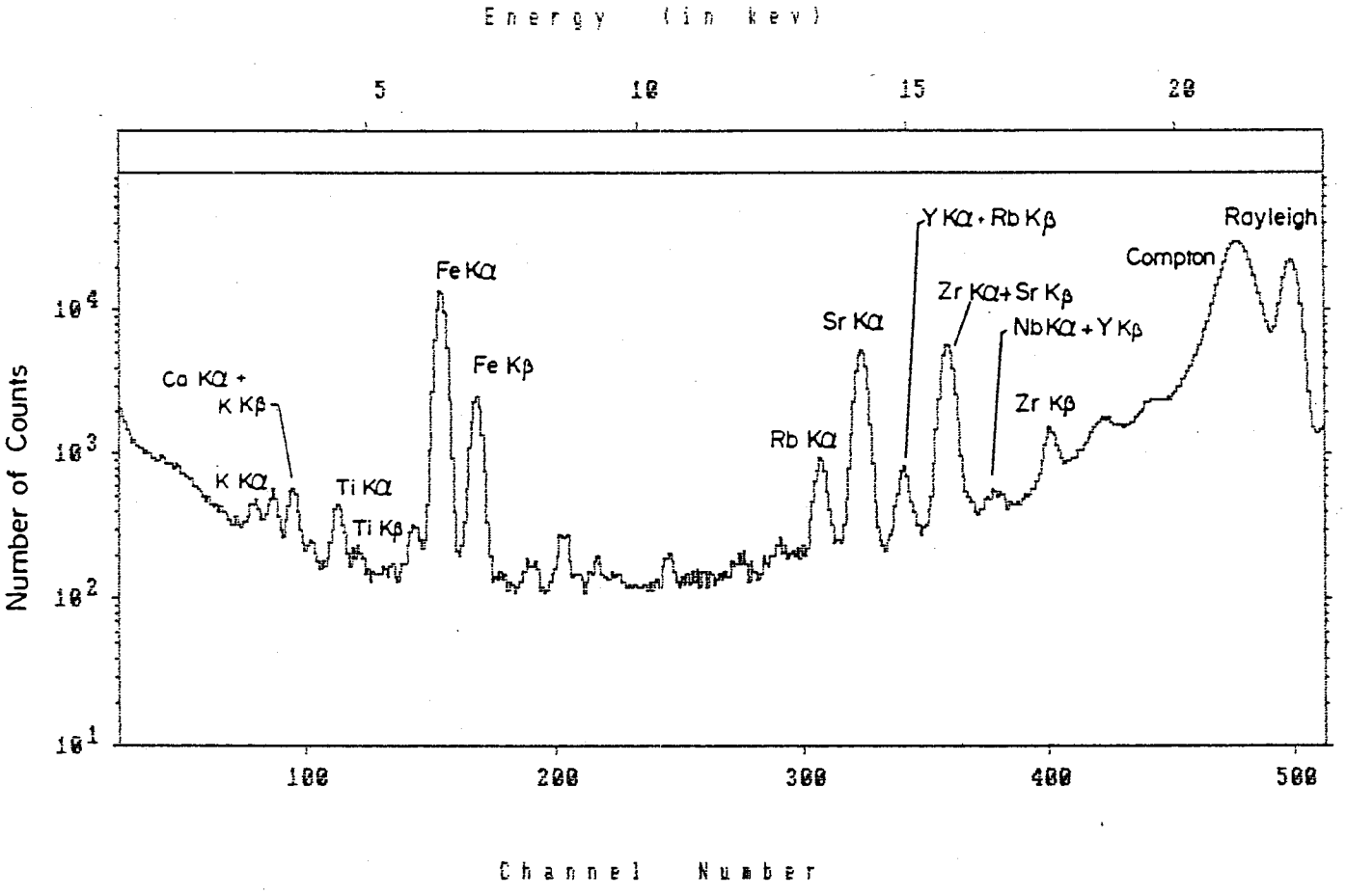

Figure 8.3 Typical tephra spectrum analysed with a silver secondary target

between samples, the net peak areas were calculated and normalized by dividing by the Compton peak area (top ten channels of Compton peak). The magnitudes of the RbKb and SrKb components were determined by analysing 5 samples each of Rb and Sr laboratory standards. In both cases, the Kb net peak area was found to average 20% of the Ka net peak area. Therefore, for each spectrum, 20% of the RbKa peak was subtracted from the YKa+RbKb peak and 20% of the SrKa peak was subtracted from the ZrKa+SrKb peak. The resulting relative concentrations of the elements Rb, Sr, Y and Zr, along with their mean and standard deviation values, are shown in Table 8.2.

Examination of the figures in Table 8.2 reveals that there is a clear contrast in the relative size of Sr to Zr peaks within the Mazama samples, in comparison to the relative sizes of the same peaks within the Mt. St. Helens Yn and Bridge River samples. The relative Sr and Zr net peak areas of the Mazama samples are much closer in magnitude (averaging 127.775 to 110.030), than the Mt. St. Helens Yn (averaging 163.365 to 61.271) or Bridge River samples (averaging 183.391 to 70.304).

In order to provide a more direct comparison between samples, the ratio Sr:Zr was calculated for each tephra sample. The resulting ratios, mean ratio values and standard deviations, are shown in Table 8.3.

These results show that the ratio Sr:Zr, averages 1.16 for Mazama; 2.70 for Mt. St. Helens Yn, and 2.62 for Bridge River. These findings suggest that there may be sufficient contrast in the ratio Sr:Zr to enable Mazama tephra samples to be

Table 8.2 Net peak areas of RbKa, SrKa, YKa and ZrKa normalized to compton peak areas

SAMPLE No.	RbKa	SrKa	YKa	ZrKa
M1	13.446	139.040	8.210	108.892
M2	14.717	124.151	7.878	112.746
M3	14.836	122.625	9.000	108.505
M4	15.694	123.766	8.919	114.840
M5	15.484	123.070	9.275	113.457
M6	15.100	127.814	8.351	108.395
M7	14.330	125.551	7.680	110.061
M8	14.953	136.182	8.099	103.350
X	14.820	127.775	8.430	110.030
S	0.655	5.920	0.535	3.415
Yn1	7.855	193.203	4.274	55.244
Yn2	13.374	156.460	6.423	63.678
Yn3	12.295	169.219	4.402	60.149
Yn4	12.128	171.057	3.436	58.756
Yn5	12.669	147.549	6.061	69.437
Yn6	12.480	153.651	4.948	59.269
Yn7	12.090	180.986	3.556	57.186
Yn8	11.806	134.792	6.889	66.450
X	11.837	163.365	4.999	61.271
S	1.569	17.688	1.232	4.526
BR1	10.175	180.000	5.069	69.338
BR2	10.980	146.582	4.732	68.748
BR3	12.875	168.614	7.544	75.747
BR4	10.877	209.029	12.969	72.690
BR5	13.650	181.332	6.880	74.812
BR6	11.626	211.603	10.332	66.922
BR7	10.194	205.450	5.470	63.440
BR8	11.723	164.515	6.600	70.734
X	11.513	183.391	7.450	70.304
S	1.156	22.037	2.665	3.836

M: MAZAMA
Yn: Mt. St. HELENS Yn
BR: BRIDGE RIVER
X: MEAN
S: STANDARD DEVIATION

Table 8.3 Sr:Zr ratios of known tephra samples

Tephra Sample	Sr:Zr Ratio
M1	1.27
M2	1.10
M3	1.13
M4	1.08
M5	1.08
M6	1.18
M7	1.14
M8	1.32
X	1.16
S	0.09
Yn1	3.50
Yn2	2.46
Yn3	2.82
Yn4	2.91
Yn5	2.13
Yn6	2.60
Yn7	3.17
Yn8	2.03
X	2.70
S	0.50
BR1	2.60
BR2	2.13
BR3	2.23
BR4	2.88
BR5	2.42
BR6	3.17
BR7	3.24
BR8	2.32
X	2.62
S	0.43

M: Mazama
Yn: Mt. St. Helens Yn
BR: Bridge River
X: Mean
S: Standard deviation

Table 8.4 Sr:Zr ratios of unknown tephra samples

Tephra Sample	Sr:Zr Ratio
1	0.95
2	1.10
3	1.21
4	1.05
5	0.97
6	1.01
7	0.95
8	1.23
9	1.35
10	1.30
11	1.07
12	1.34
13	1.54
14	0.89
15	0.87

distinguished from those of Mt. St. Helens Yn and Bridge River.

Of the 16 tephra beds encountered in this study, one, from core D43, was too small to provide a sufficient sample size and was excluded from the XES analysis. The remaining 15 tephra samples were oven-dried for 24 hours and then examined under a petrographic microscope to confirm the presence of volcanic glass fragments (based on: the presence of abundant clear glass shards; extinction in cross-polarized light; and, the Becke Test measurement of refractive index to confirm that the RI of the glass fragments corresponded to the RI of glass - i.e. 1.50-1.52). The 15 samples were then analysed using the XES technique outlined previously and the ratio Sr:Zr was determined for each (Table 8.4).

It has already been established by Cormie (1981) that element concentrations within the tephras are normally (or Gaussian) distributed. Therefore, the technique of discriminant analysis (SPSS Inc., 1986) was used to attempt to classify the 15 'unknown' samples from the study area, in terms of the 3 'known' tephra groups. The ratio Sr:Zr was used as the single discriminating variable.

Discriminant analysis attempts to classify unknown samples in terms of known sample groups by calculating the probability that a sample belongs to a particular group. This probability is based on a value of a variable(s) within the sample, compared to the mean and variance of the same variable(s) within the known groups. The actual comparison is carried out on the basis of

discriminant scores (based on the value of a variable(s) within the samples).

The probability that a sample belongs to a particular group depends on how close its discriminant score is to the mean discriminant score of the group (group centroid) and how far its discriminant score is from the mean discriminant scores of the other groups.

The technique used also provides the opportunity to test the effectiveness of the discriminating variable(s) by first calculating the discriminating functions, and then by classifying the known samples to determine if they fall within the 'correct' groups.

8.3.2.3 Results

The output from the discriminant analysis program is shown in Table 8.5. A graphical representation of the discriminant scores of both 'known' and 'unknown' samples is shown in Figure 8.4.

Table 8.5 lists the probability (P(G/D)) that a sample belongs to an indicated group (HIGHEST GROUP). The results show that all 8 samples in group 1 (Mazama) were correctly identified as belonging to that group (all with greater than 99% probability). The results for group 2 (Mt. St. Helens Yn) and group 3 (Bridge River) show a number of misclassifications (**), caused by the similarity in Sr:Zr ratios between these two tephra groups.

These findings confirm that, on the basis of the available

Table 8.5 Results of discriminant analysis

Sample No. and depth	ACTUAL GROUP		HIGHEST PROBABILITY GROUP	P(D/G)	P(G/D)	2ND HIGHEST GROUP	P(G/D)	DISCRIMINANT SCORES...
M1	1		1	0.7794	0.9970	3	0.0021	-2.3265
M2	1		1	0.8706	0.9995	3	0.0004	-2.7694
M3	1		1	0.9325	0.9993	3	0.0005	-2.6912
M4	1		1	0.8298	0.9996	3	0.0003	-2.8215
M5	1		1	0.8298	0.9996	3	0.0003	-2.8215
M6	1		1	0.9636	0.9988	3	0.0008	-2.5610
M7	1		1	0.9533	0.9992	3	0.0006	-2.6652
M8	1		1	0.6815	0.9950	3	0.0034	-2.1962
Yn1	2		2	0.0377	0.6100	3	0.3900	3.4837
Yn2	2	**	3	0.6696	0.5261	2	0.4720	0.7740
Yn3	2		2	0.7595	0.5209	3	0.4790	1.7120
Yn4	2		2	0.5888	0.5329	3	0.4670	1.9465
Yn5	2	**	3	0.1983	0.5413	2	0.4071	-0.0858
Yn6	2	**	3	0.9507	0.5082	2	0.4913	1.1388
Yn7	2		2	0.2232	0.5673	3	0.4327	2.6239
Yn8	2	**	3	0.1219	0.5076	2	0.3618	-0.3463
BR1	3		3	0.9507	0.5082	2	0.4913	1.1388
BR2	3		3	0.1983	0.5413	2	0.4071	-0.0858
BR3	3		3	0.3049	0.5468	2	0.4338	0.1748
BR4	3	**	2	0.6437	0.5289	3	0.4710	1.8683
BR5	3		3	0.5955	0.5309	2	0.4662	0.6698
BR6	3	**	2	0.2232	0.5673	3	0.4327	2.6239
BR7	3	**	2	0.1614	0.5765	3	0.4235	2.8063
BR8	3		3	0.4287	0.5414	2	0.4507	0.4093
D23-8.7 m	UNGRPD		1	0.5798	0.9999	3	0.0001	-3.1602
D29-6.6 m	UNGRPD		1	0.8706	0.9995	3	0.0004	-2.7694
D46-8.1 m	UNGRPD		1	0.9015	0.9983	3	0.0011	-2.4828
D50-7.8 m	UNGRPD		1	0.7694	0.9997	3	0.0002	-2.8997
D52-7.4 m	UNGRPD		1	0.6160	0.9999	3	0.0001	-3.1081
D55-7.9 m	UNGRPD		1	0.6911	0.9998	3	0.0002	-3.0039
D62-7.5 m	UNGRPD		1	0.5798	0.9999	3	0.0001	-3.1602
D64-7.1 m	UNGRPD		1	0.8604	0.9980	3	0.0014	-2.4307
D69-6.8 m	UNGRPD		1	0.6252	0.9932	3	0.0045	-2.1180
D71-6.7 m	UNGRPD		1	0.7202	0.9959	3	0.0028	-2.2483
D72-6.2 m	UNGRPD		1	0.8096	0.9996	3	0.0003	-2.8476
D73-7.1 m	UNGRPD		1	0.6437	0.9939	3	0.0041	-2.1441
D74-6.8 m	UNGRPD		1	0.3253	0.9554	3	0.0288	-1.6230
TH84-13-7.0 m	UNGRPD		1	0.4777	0.9999	3	0.0000	-3.3165
TH85-14-6.6 m	UNGRPD		1	0.4460	0.9999	3	0.0000	-3.3687

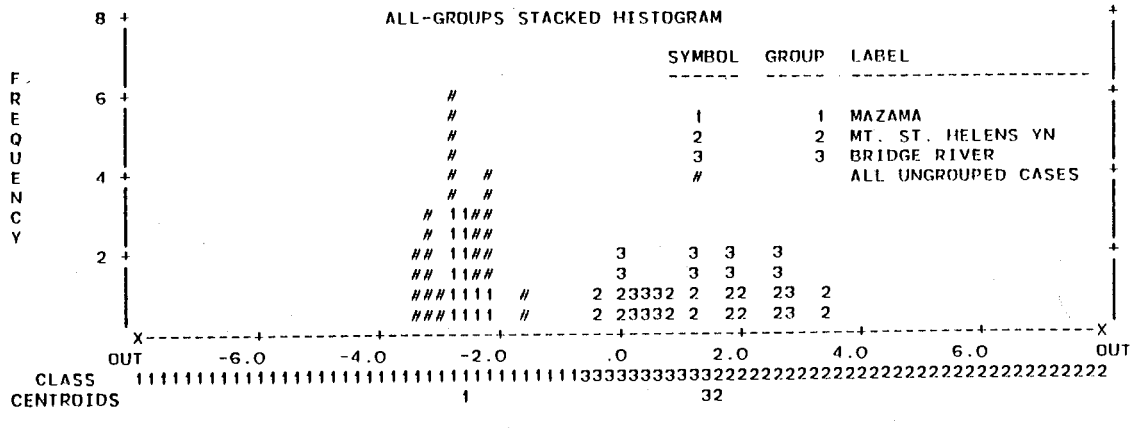

Figure 8.4 Frequency histogram of discriminant scores

data, the contrasts in Sr:Zr ratios is sufficient to distinguish Mazama tephra samples from those of Mt. St. Helens Yn and Bridge River.

The 15 samples from the study area are all identified as belonging to group 1 (Mazama). The probabilities that these samples belong to the Mazama group, rather than one of the other two groups, are in 14 cases greater than 99% and in the remaining case, greater than 95%.

These results are supported by the distribution of discriminant scores (Fig. 8.4), which clearly shows the clustering of the unknown samples (#) about the centroid for group 1 (Mazama).

Although the findings of the XES analysis are based on a fairly limited data set, when combined with the evidence from radiocarbon dating and stratigraphic position, the XES results further improve the degree of confidence with which the tephra beds can be identified as Mazama. As such, it is proposed that all 16 tephra beds encountered in this study are Mazama tephra and represent part of a contiguous marker horizon, with an age of about 6800 yr BP.

8.4 A CHRONOLOGICAL FRAMEWORK FOR THE DELTA

The chronological control provided by the ^{14}C dates and peat and tephra marker horizons can be combined with Lulu Island's generalized lithostratigraphy (Fig. 6.22) to develop a chronological framework for the northern part of the delta (Fig. 8.5).

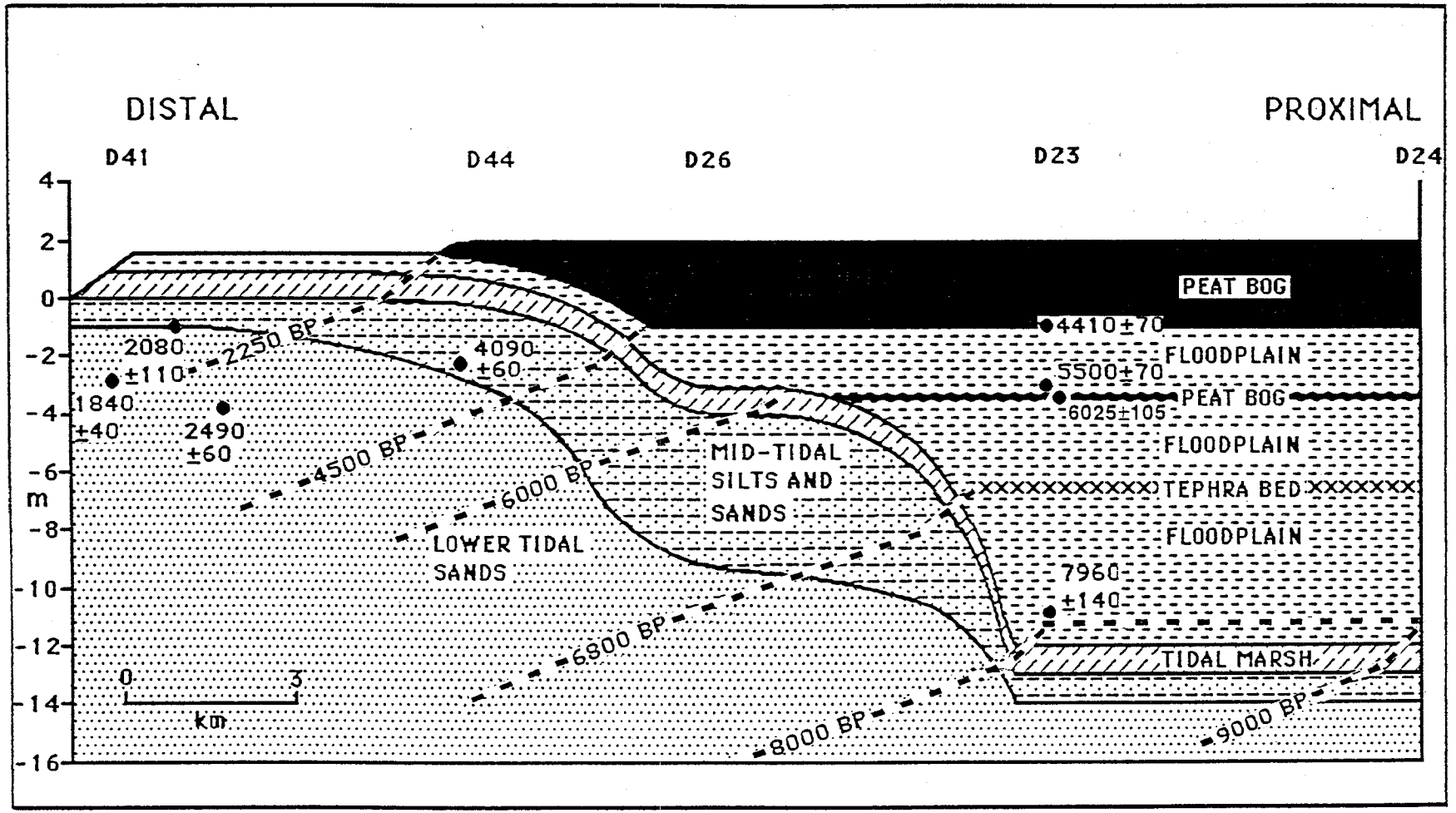

Figure 8.5 Depositional evolution of Lulu Island

To construct this framework, it has been necessary to assume that the longitudinal profile of the delta has remained constant throughout it's growth: hence the paleosurfaces incorporated into the section have the same generalized morphology as the contemporary delta surface along proximal to distal trends.

It has also been assumed that the terrestrial surface of the delta first emerged into the Strait of Georgia in the vicinity of New Westminster at 9000 yr BP (see section 2.4.1).

The ^{14}C dates have been positioned along the proximal-distal section on the basis of their location relative to either the western delta front (distal end of section) or the delta apex (proximal end of section).

SECTION FOUR

DISCUSSION AND CONCLUSIONS

CHAPTER NINE

DISCUSSION AND CONCLUSIONS

9.1 INTRODUCTION

In this chapter, the depositional response of the northern Fraser Delta to the mid-Holocene rise in sea-level will be discussed in the context of the hypothetical framework established in chapter 1.

The establishment of the depositional chronology of Lulu Island (Fig. 8.5) will provide the basis for construction of a revised sea-level curve for the Fraser Lowland region and for calculations of Lulu Island's vertical accretion and lateral progradation rates during the Holocene. The interrelationships between rising sea level, vertical accretion and lateral progradation will be examined.

In addition, the study findings will be used to provide estimates of the Fraser River's sediment discharge rates throughout the Holocene period.

The implications of the study findings for future research in the same area, and in other similar settings, will be briefly discussed.

The major findings of the study will be summarized at the end of the chapter.

9.2 DEPOSITIONAL RESPONSE TO THE RISE IN SEA LEVEL

Upon examination of the depositional chronology shown in Fig. 8.5, it is apparent that aggradation of Lulu Island, in response to the mid-Holocene sea level rise, took the form of a depositional regression (Fig. 1.7c).

This finding is based on the lack of a reversal or cyclic repetition of the facies sequence within the deposits (associated with a marine transgression) and the sequence of paleosurfaces, which show that the island grew progressively seaward, even during the period of sea-level rise.

Hence, growth of the island during the rise in sea level was accomplished by simultaneous vertical accretion and lateral progradation. The depositional architecture shown in Fig. 8.5 has essentially resulted from the upward and seaward shift of the delta's lateral succession of depositional environments, between about 8000 and 2250 yr BP.

It would appear that the delta's rising base level triggered aggradation of the deltaic plain, such that the rate of sediment accumulation kept pace with the rate of sea level rise. This vertical growth is exemplified by the thick silty floodplain deposits underlying eastern Lulu Island (Fig. 8.5).

These deposits attest to the propensity for flooding and overbank sedimentation to continue throughout early to mid-Holocene time and to keep pace with the rise in sea level. The resulting floodplain deposits have attained a considerably greater thickness than their modern analogues on western Lulu Island, formed under stable sea level conditions.

Examination of the internal character of the deposits formed during rising sea level, reveals that they represent a "stalled successional phase" in the evolution of the delta. In other words, the normal succession of depositional environments, which occurs as the delta progrades, was halted or at least slowed considerably, during the periods of rising sea level. In the parts of the delta subject to vertical accretion, a balance appears to have been achieved between the rate of sediment deposition and the rate of sea level rise. Thus, the elevation of any point on the delta surface, relative to mean sea level, was held constant for long periods and depositional conditions (sediment input, frequency of flooding, flora and fauna...) were perpetuated.

The effect of the perpetuation of depositional conditions within the vertical accretion deposits is particularly well demonstrated by the palynological analysis of the floodplain deposits formed between ca. 8000 and 6800 yr BP (section 7.3.1.2, zone D23-2). The pollen analysis showed that the "normal" course of vegetation succession on the floodplain was "arrested" for the ca. 1200 year period of rising sea level. The emergent "swamp vegetation" phase was "stalled" during this period, as deposition on the floodplain surface maintained its elevation relative to the rising sea level and "river swamp" conditions were perpetuated.

It was only later, during the decline and eventual pause in the rate of sea level rise associated with the stillstand at ca. 6000 yr BP, that "normal" vegetation succession was able to

continue. This resulted in the shrub phase (section 7.3.1.2, zone D23-3) and then the onset of peat bog conditions (section 7.3.1.2, zone D23-4), culminating in the formation of the buried peat layer (Fig. 8.5).

In other respects as well as palynology, the internal character of the facies underlying Lulu Island attest to the perpetuation of depositional conditions during rising sea level (e.g. the floodplain deposits underlying eastern Lulu Island consist of about 11 m of horizontally bedded organic-rich silt, instead of the "usual" ca. 1 m of horizontally bedded organic-rich silt formed under stable sea level conditions.). The result is the development of facies with the same internal character and vertical order as their modern counterparts, but of considerably greater vertical extent.

9.3 REVISED SEA LEVEL CURVE FOR THE FRASER LOWLAND REGION

Observation of contemporary depositional environments (section 3.5) and palynological analysis of core D23 (section 7.3.1.2), have indicated that mean sea level approximately corresponds to the base of the tidal marsh environment.

This finding has led to the recognition that former sea level positions can be identified in core by the lithologic transition from the organic-rich silts of tidal marsh origin, to the silts and sands of transition zone origin. This method of identifying former sea level positions enables a more precise and detailed Holocene sea level curve to be developed for the Fraser Lowland region.

The lithologic transition corresponds to the base of the tidal marsh facies in Fig. 8.5. Thus, the intersections of the tidal marsh base with the paleosurfaces in Fig. 8.5 provide a chronological record of sea level change throughout the Holocene period.

The resulting curve (Fig. 9.1) indicates that sea level was relatively stable in the early Holocene (9000 - 8000 yr BP) at about -13 m elevation. During this period, the sediments forming the level base of the organic-rich silts underlying eastern Lulu Island were deposited as the delta prograded seaward (Fig. 8.5).

A relatively rapid rise in sea level occurred between about 8000 and 6200 yr BP, bringing the sea to an elevation of about -4.4 m. This was followed by the previously unknown stillstand with an estimated duration of about 400 years (section 8.2.4), during which the buried peat layer accumulated.

Sea level rise recommenced at about 5800 yr BP, slowed considerably by ca. 4500 yr BP and continued until about 2250 yr BP, when the sea reached its present level. The sea appears to have remained comparatively stable for about the last 2250 years.

9.4 VERTICAL ACCRETION, LATERAL PROGRADATION AND RISING SEA LEVEL

The Holocene evolution of the northern Fraser Delta (Lulu Island) can be divided into six distinct stages of vertical and lateral growth (Fig. 8.5):

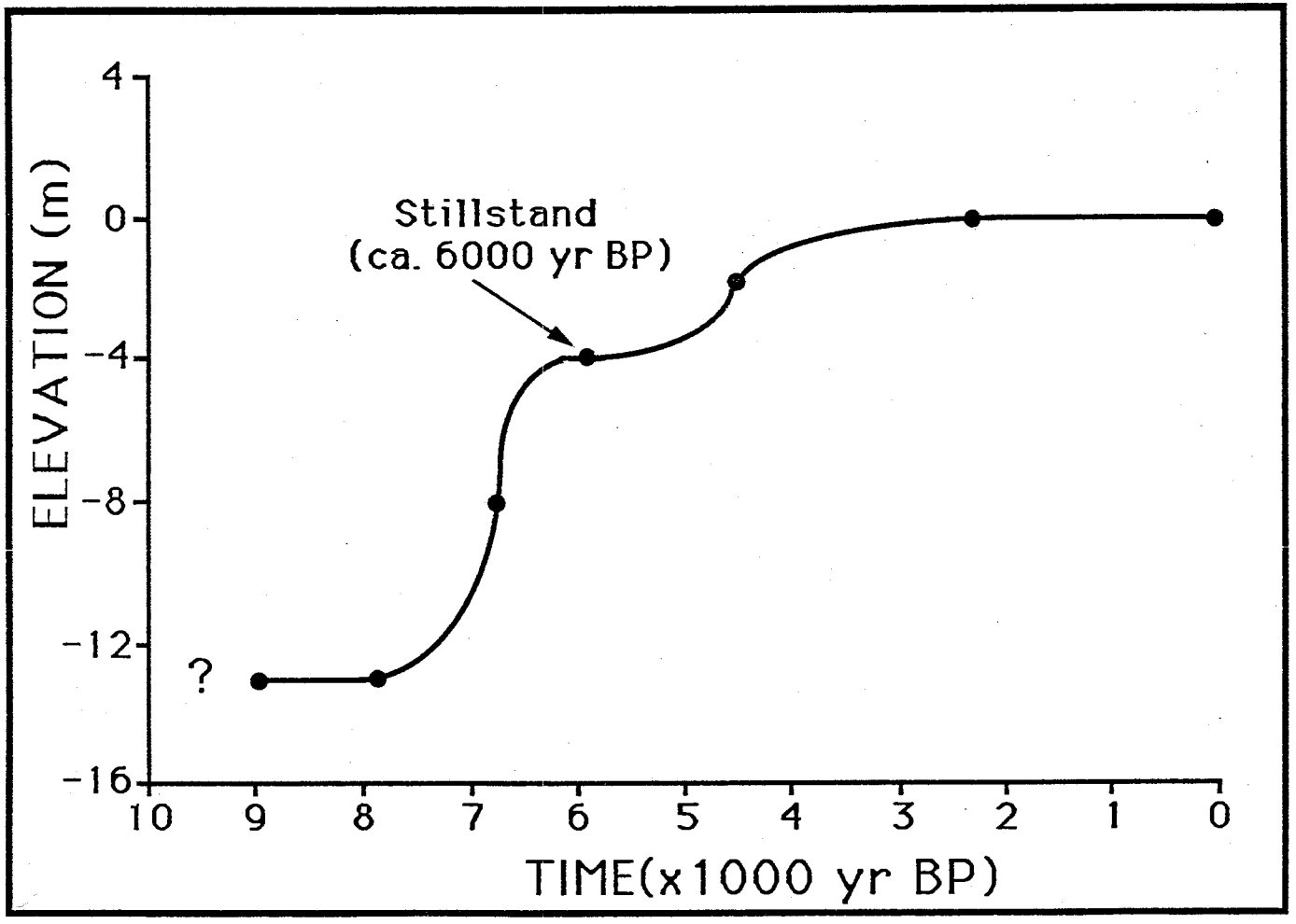

Figure 9.1 Revised sea-level curve for the Fraser Lowland region

I. 9000 - 8000 yr BP. It was at the commencement of this stage that the delta, graded to a sea level 13 m lower than at present, first begun its growth into the Strait of Georgia from its apex near New Westminster (Fig. 1.8). During this stage, the delta's subaerial surface extended some 6.5 km into the Strait. Sea level was apparently stable during this time.

II. 8000 - 6200 yr BP. Rising sea level induced some 8.6 m of vertical accretion, while at the same time the delta front grew a further 3.7 km into the Strait of Georgia. It was in this period that the Mazama tephra (6800 yr BP) was incorporated into the vertically accreting floodplain sediments. About 5.4 m of the vertical accretion and 1.2 km of the lateral growth, occurred prior to deposition of the tephra.

III. 6200 - 5800 yr BP. A stillstand of sea level occurred during this period, allowing widespread peat formation over the delta surface. Progradation of the delta continued, moving the delta front about 1.5 km further seaward.

IV. 5800 - 4500 yr BP. Sea level rise recommenced, inducing a further 2.2 m of vertical accretion. Lateral progradation also continued, extending the delta front a further 1.65 km into the Strait. The rate of sea level rise at the close of this period appears to have slowed considerably, allowing peat bogs to develop on the eastern delta surface.

V. 4500 - 2250 yr BP. The sea slowly rose a further 2 m during this period, bringing it to its present level. Lateral progradation of the delta front was 4 km.

VI. 2250 - Present. The delta continued to prograde under stable sea level conditions, extending the delta front another 5.4 km, to its present position.

On the basis of the information above, Holocene vertical accretion rates and lateral progradation rates for the northern Fraser Delta were calculated. The results are shown in Table 9.1.

The figures in Table 9.1 indicate that progradation proceeded relatively rapidly in the first 1000 years of the delta's growth, averaging 6.5 m/yr. This was presumably due to: early growth being confined to a laterally restricted embayment of the Strait (Fig. 1.8); shallower water depths adjacent to the uplands surrounding the apex of the delta; a relatively short delta front in the early stages of growth; and, the possibility that sediment supply rates were enhanced by "paraglacial" conditions prevailing in the Fraser River basin during early post-glacial time (Church and Ryder, 1972).

The progradation rate of 2.4 m/yr for the most recent period (2250 yr BP to Present) is in close agreement with estimates of contemporary progradation rates based on bathymetric surveys. Johnson (1921) compared surveys of the delta front made in 1859 and 1919 and arrived at a figure of

Table 9.1 The Fraser Delta's lateral progradation and vertical accretion rates during the Holocene

PERIOD (yr BP)	TIMESPAN (yr)	PERIOD MIDPOINT (yr)	LATERAL PROGRADATION (km)	VERTICAL ACCRETION (m)	MEAN LATERAL PROGRADATION RATE (m/yr)	MEAN VERTICAL ACCRETION RATE (mm/yr)
9000-8000	1000	8500	6.50	0.00	6.50	0.00
8000-6800	1200	7400	1.20	5.40	1.00	4.50
6800-6200	600	6500	2.50	3.20	4.20	5.30
6200-5800	400	6000	1.50	0.00	3.80	0.00
5800-4500	1300	5150	1.65	2.20	1.30	1.70
4500-2250	2250	3375	4.00	2.00	1.80	0.90
2250-PRESENT	2250	1125	5.40	0.00	2.40	0.00

3.05 m/yr for the whole delta front. Mathews and Shepard (1962) calculated a rate of 2.29 m/yr for the advance of the upper foreslope between 1929 and 1959.

Vertical accretion rates reflect the rate of sea level rise. Relatively rapid vertical accretion, averaging between 4.5 and 5.3 mm/yr, occurred between 8000 and 6200 yr BP, when sea level rose sharply (Fig. 9.1). Lower vertical accretion rates, averaging between 1.7 and 0.9 mm/yr, occurred during the second, more subdued, sea level rise between 5800 and 2250 yr BP.

The mean lateral and vertical sedimentation rates in Table 9.1 can be used to examine the relationship between Lulu Island's lateral progradation and vertical accretion throughout the Holocene period (Fig. 9.2).

The variation in estimated progradation and vertical accretion rates in Fig. 9.2, suggests that there is an inverse relationship between lateral progradation and vertical accretion. This finding suggests that the diversion of sediment into vertical accretion deposits on the delta surface and on the Fraser River floodplain to the east, was responsible for a reduced supply of sediment to the delta front and a consequent reduction in the progradation rate.

Superimposed onto this relationship is the progressive reduction in Lulu Island's progradation rate through the Holocene period. This presumably resulted from increasing water depth and lengthening delta front as the delta grew seaward. The reduction is indicated by the mean progradation rates during periods of stable sea level. These rates declined from 6.5 m/yr

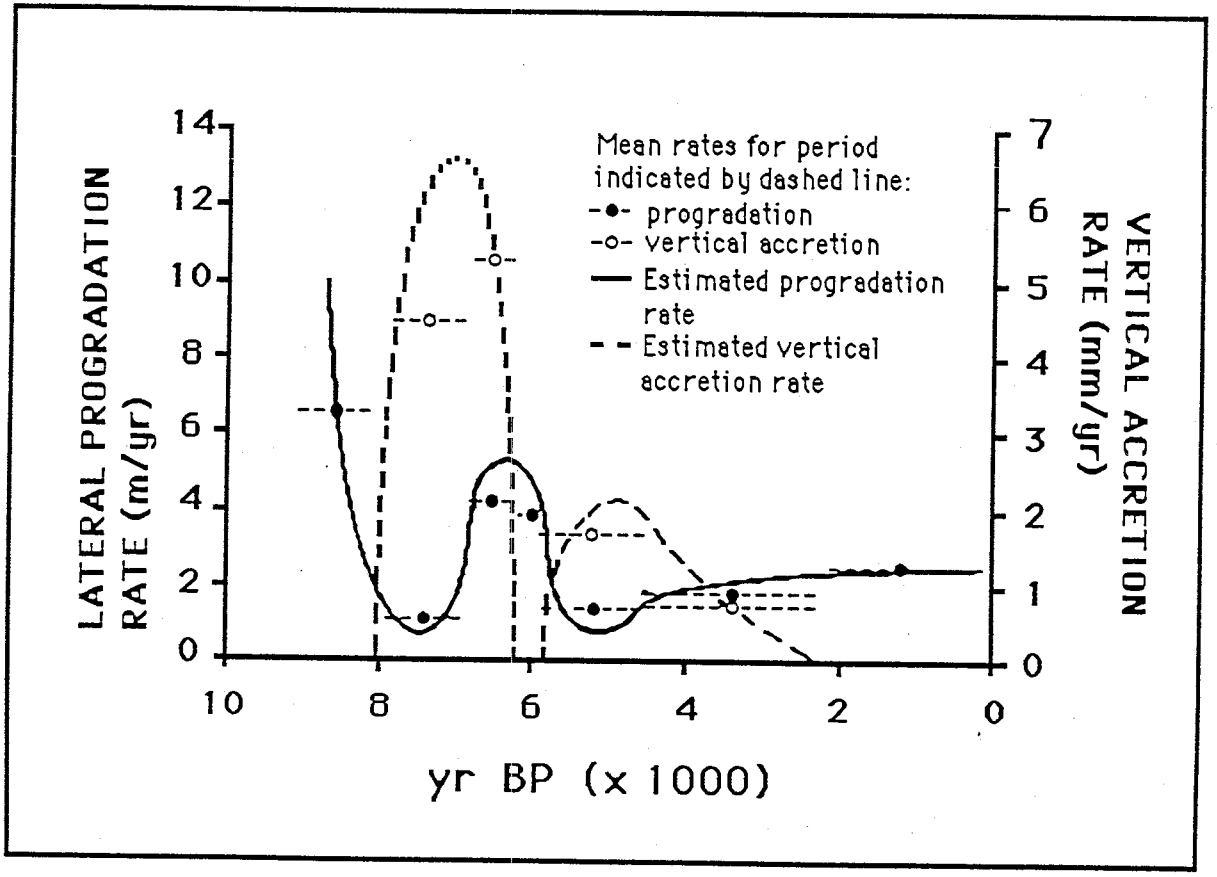

Figure 9.2 Lulu Island's estimated lateral progradation and vertical accretion rates throughout the Holocene

(9000-8000 yr BP), to 3.8 m/yr (6200-5800 yr BP) and finally to 2.4 m/yr (2250 yr BP to Present).

It should be noted that these apparently simple relationships are complicated by other factors which have probably influenced the delta's progradation rate, but which are difficult to quantify. The bottom topography of the part of the Strait of Georgia now covered by the delta remains unknown. The configuration of the Strait bottom may have caused unpredictable variations in water depth as the delta prograded seaward, with a corresponding effect on the progradation rate.

There is also evidence of a period of higher summer temperatures and lower precipitation in southern British Columbia during mid-Holocene time (Heusser et al., 1985). This climatic thermal maximum may have resulted in reduced river flows and sediment discharges and the consequent reduction of the delta's progradation rate.

Finally, the joining of the southern part of the delta to the former island of Point Roberts presumably caused a considerable shortening of the active delta front. This may have resulted in increased sediment supply and higher progradation rates along the western delta front.

9.5 ESTIMATES OF THE FRASER RIVER'S SEDIMENT DISCHARGE RATES DURING THE HOLOCENE

9.5.1 INTRODUCTION

The estimation of the Fraser River's sediment discharge rates during the Holocene is a potentially valuable exercise, since it may provide useful insights into the overall level of geomorphic activity within the Fraser River basin throughout the post-glacial period.

Major changes in sediment discharge regimes may have resulted from the effects of paraglaciation (Church and Ryder, 1972) and climatic fluctuations (Heusser et al., 1985). These changes may be recorded within the Fraser Delta in the form of variations in the sediment accumulation rate pertaining to successive periods of the delta's growth.

Although the findings of the present study provide a basis for estimating the sediment discharge rates, it is acknowledged that this section of the study remains spectulative in nature. There is only limited data available on several important aspects of the delta's evolution - particularly the depth of deltaic deposits, the changing shape of the delta during its development and the growth of the southern part of the delta - consequently, a number of simplifying assumptions are required in order to perform the sediment discharge calculations.

9.5.2 METHODS

9.5.2.1 The Fraser Delta

The rates of sediment accumulation within the delta were calculated on a volumetric basis (area multiplied by mean depth). This approach has been adopted from previous studies, where it has been employed to estimate the volume of the entire delta (Mathews and Shepard, 1962; Clague and Luternauer, 1983).

The major contribution from the present study is that it establishes the approximate areal extent of the delta at given times within the Holocene period. Hence, a number of successive volumetric increments to the delta, occurring over the last 9000 years, may now be calculated.

The method used is dependent upon a number of assumptions which are stated below:

(i) It is assumed that the delta grew out radially from its apex and that the growth of the southern part of the delta proceeded in the same manner and at the same rate as the growth of the northern part of the delta (Lulu Island). There is some evidence to support this assumption. Burns Bog, on the southern delta, has approximately the same areal extent (covering roughly the eastern half of the delta) and the same age (ca. 5000 yr BP - Hebda, 1977) as the Lulu Island peat bog. The exception to this assumption is in the period 4500 - 2250 yr BP, when it is assumed that the southern delta became joined to Pt. Roberts. It is also assumed that further growth of the Boundary Bay tidal flats and foreslope after 2250 yr BP was negligible.

(ii) The depth of deltaic deposits remains unknown over a large area. However, three depths are known: the depth of the Strait of Georgia at the base of the contemporary foreslope is 300 m; a drill hole at Steveston, on the western edge of Lulu Island, passed through 214 m of deltaic silts and sands before encountering bouldery material, presumably of glacial origin (Johnson, 1921); and another drill hole, on Annacis Island, adjacent to eastern Lulu Island, indicates that deltaic deposits extend to more than 90 m depth (Clague and Luternauer, 1983). Therefore, it is assumed that the base of the delta forms a flat surface, passing through 300 m and 214 m depth in the west and below 90 m depth in the east (Fig. 9.3). Although there is some evidence from seismic surveys that the base of the delta is in fact quite irregular in places (Luternauer et al., 1986), this assumption will at least provide a "first approximation" based on the limited data available.

(iii) It is assumed that the longitudinal profile of the delta has remained constant during its growth. Thus, it is assumed that the tidal flats and subaqueous platform have always formed a 7 km wide zone fringing the terrestrial surface of the delta and that the foreslope has always been inclined at 1.5^{o}.

(iv) There is evidence that some of the Fraser River's sediment load is deposited beyond the delta foreslope on the floor of the Strait of Georgia (Luternauer et al., 1983). It is assumed that this portion of the river's sediment load is negligible in comparison to the total sediment discharge.

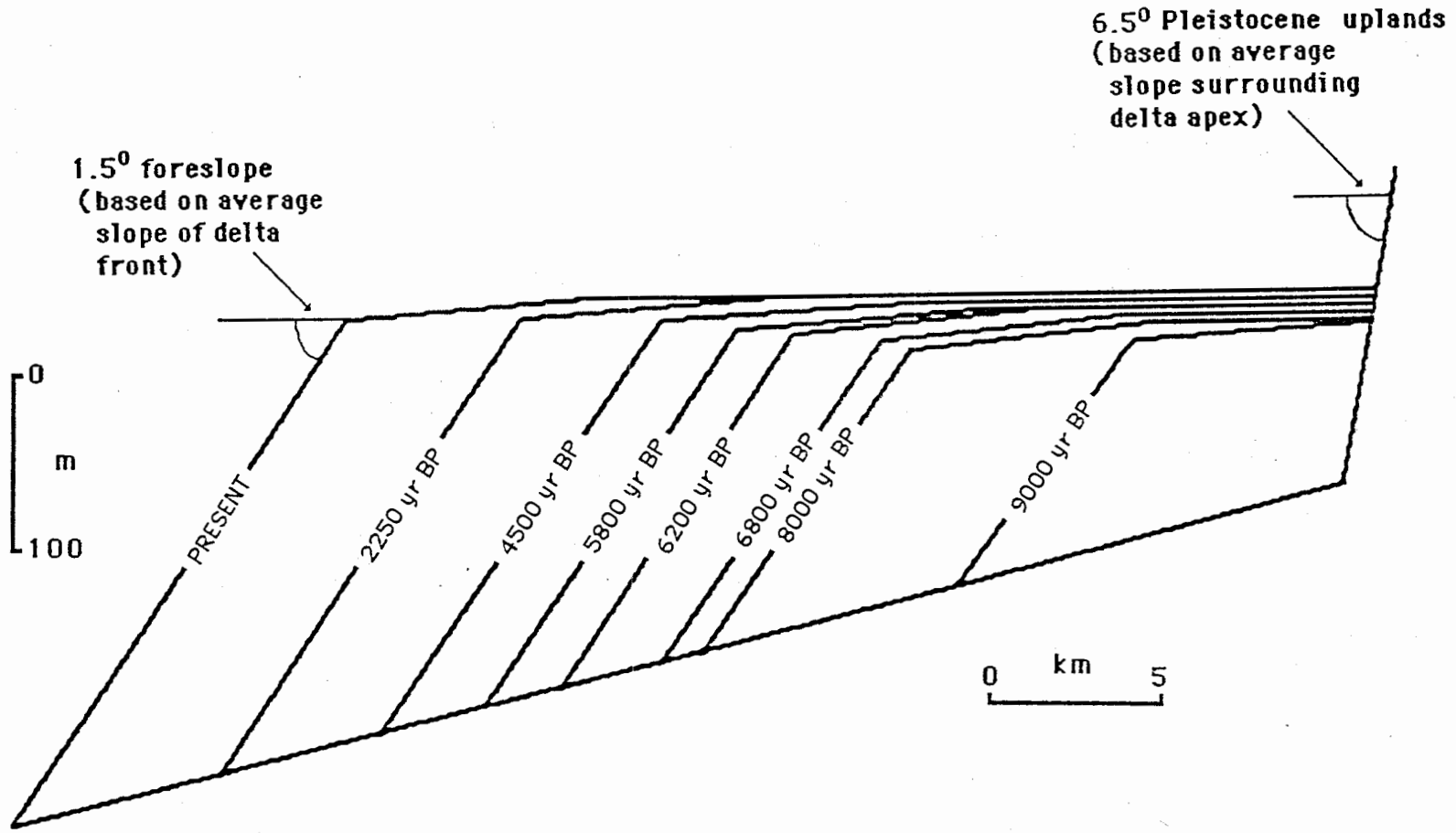

FIGURE 9.3 ESTIMATED LONGITUDINAL PROFILE OF THE FRASER DELTA AT SUCCESSIVE STAGES OF GROWTH

On the basis of the assumptions above and the progradation figures in Table 9.1, the areal extent of the delta, at successive stages of its growth, was approximated (Fig. 9.4 - Note: no attempt was made to estimate the configuration of the delta's surface at successive stages of growth).

The terrestrial surface of the Holocene Fraser Delta probably first reached the vicinity of the present delta apex at about 9000 yr BP. At this time the gently sloping tidal flats and subaqueous platform already extended 7 km into the Strait of Georgia. The foreslope formed a ca. 4.5 km wide fringe beyond the subaqueous platform.

The delta grew rapidly in the early Holocene, so that by 8000 yr BP the terrestrial surface had advanced some 6.5 km into the Strait. The edge of the subaqueous main platform was about 13.5 km southwest of New Westminster and the base of the foreslope, at a water depth of about 184 m, was approximately 19 km from the delta apex.

By 6800 yr BP, the time of Mazama tephra deposition, the terrestrial surface of the delta extended some 7.7 km beyond New Westminster and the base of the foreslope was lying just off the island of Point Roberts, at a water depth of about 190 m.

Over the next 2300 years, to 4500 yr BP, the delta probably continued to grow out to the south and west from New Westminster. At the end of this period, the delta's tidal flats were probably within a few km of the island of Point Roberts. At about this time sea-level rise slowed considerably and peat bogs began to develop over the terrestrial surface of the delta.

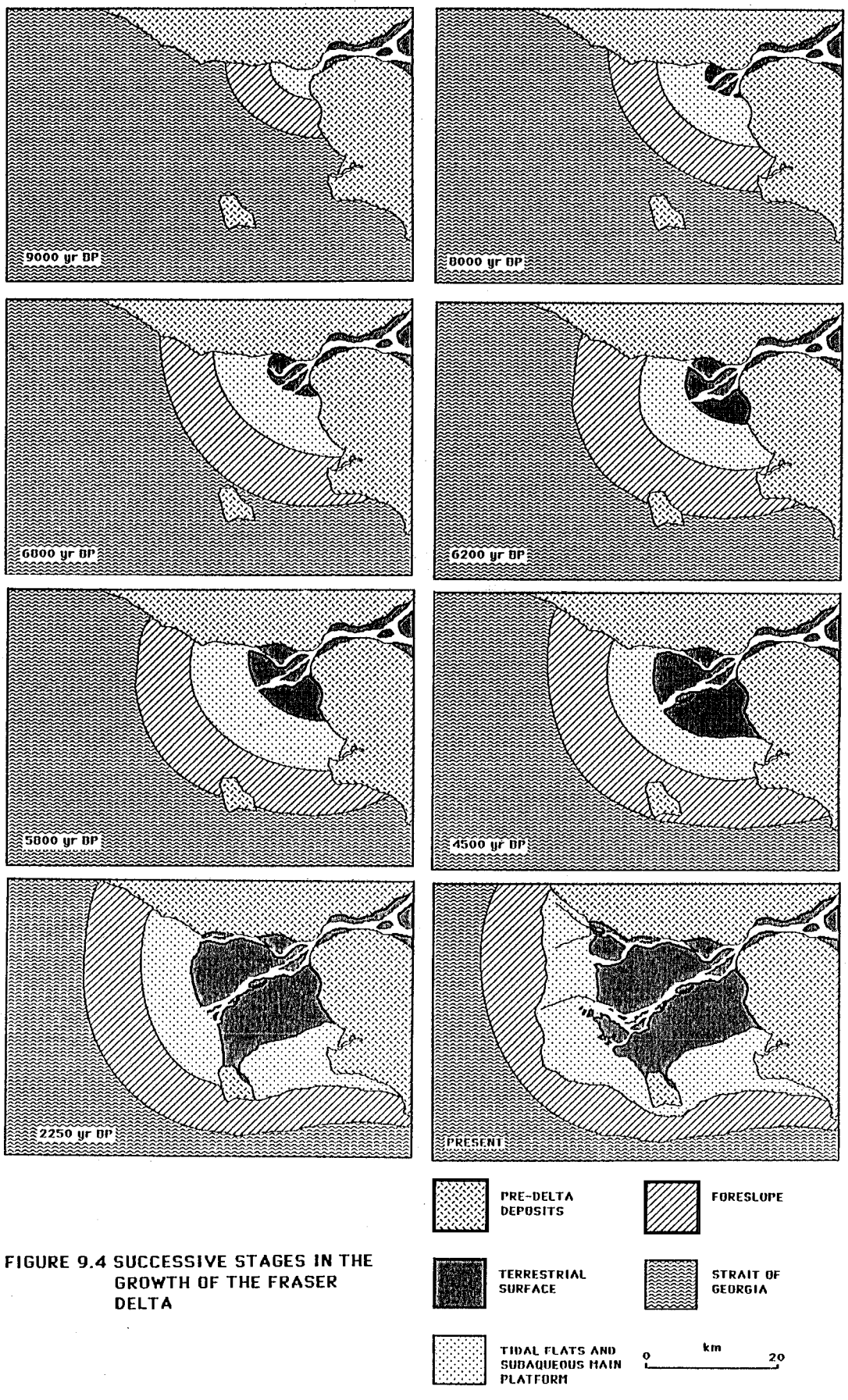

FIGURE 9.4 SUCCESSIVE STAGES IN THE GROWTH OF THE FRASER DELTA

The former island of Point Roberts probably became joined to the terrestrial surface of the delta sometime after 4500 yr BP, but before 2250 yr BP. On the basis of the estimated progradation rates for the southern delta front, this probably occurred around 3000 yr BP. Little further growth of the delta occurred in the Boundary Bay area after this period.

During the last 2250 years, the western edge of the delta has continued to prograde into the Strait. The terrestrial surface now reaches some 22 km beyond New Westminster and the base of the foreslope lies approximately 17 km seaward of the terrestrial delta in 300 m depth of water.

The areas shown in Figure 9.4 were combined with estimates of the delta's depth from Figure 9.3, to calculate the volume of sediment added to the delta during each stage of its growth. Details of these calculations can be found in Appendix III.

9.5.2.2 The Fraser River floodplain

There is considerable evidence that aggradation of the Fraser River floodplain occurred in response to the rise in sea level (Fig. 6.21, section 6.4.2) (Clague et al., 1983). The aggradation probably took the form of a depositional wedge of sediment extending some distance upvalley (Knighton, 1984, p.159-161). The volume of these aggradational deposits must be added to the volume of deltaic deposits, in order to calculate the total Fraser River sediment discharge for each stage of the delta's growth (Fig. 9.4).

There is evidence that the depth of aggradation on the

floodplain equals the depth of aggradation on the delta. Figure 6.21, for example, shows that the separation of the Mazama tephra bed and the buried peat layer remains about the same from the delta to the western part of the floodplain.

In order to determine the area of the floodplain over which aggradation occurred, two approaches were taken:

(i) the upvalley limit of the aggradational deposits should be marked by a break in slope between the aggradational wedge and the older, unaggraded, floodplain surface (Knighton, 1984). Therefore, the longitudinal profile of the floodplain surface was constructed on the basis of benchmarks found on 1:50000 topographic maps of the Fraser Valley (it was assumed that the benchmarks approximated the general level of the surrounding floodplain surface).

(ii) Knighton (1984) suggests that the aggradational deposits may be marked by changes in channel planform or cross-sectional morphology due to adjustments of the channel to the reduced gradient of the depositional wedge.

The resulting longitudinal profile of the floodplain surface (Fig. 9.5) shows a distinct break in slope at about 47 km east of New Westminster, in the vicinity of Hatzic Lake. This location also coincides with a change in planform of the Fraser River, from a wandering gravel bed section to the east, to a

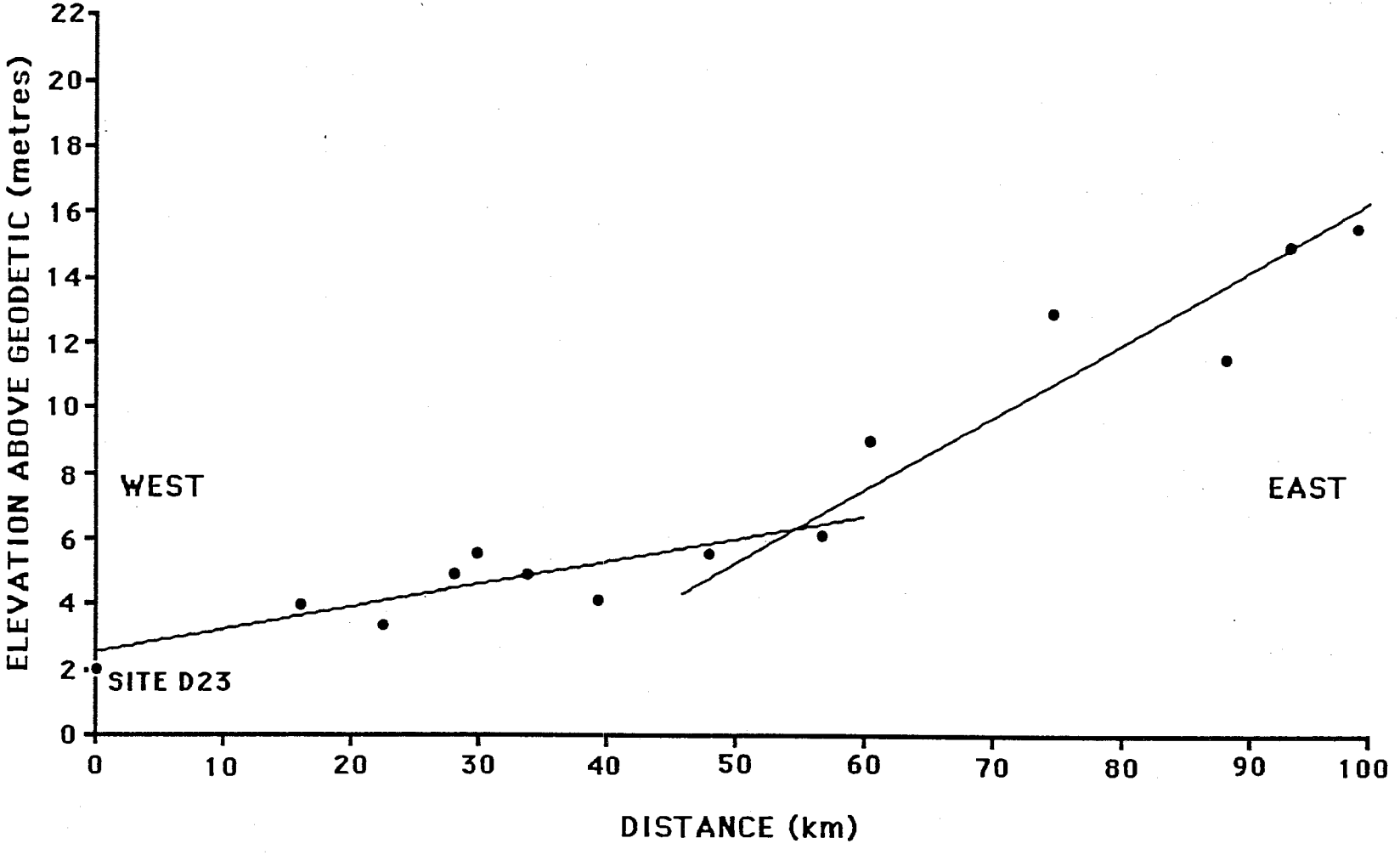

Figure 9.5 Longitudinal profile of the Fraser River floodplain

meandering reach to the west (Appendix III).

On the basis of this evidence, it was assumed that the aggradational deposits extended to 47 km east of New Westminster. It was further assumed that the area of the floodplain that was aggraded during each stage of the delta's growth (Fig. 9.4), depended on the amount of sea level rise that occurred. Details of the calculations of the volumes of aggradational deposits on the floodplain can be found in Appendix III.

9.5.3 RESULTS

Table 9.2 shows the volumetric increments to the delta and the floodplain at a number of stages over the last 9000 years. The total volume added to the delta and floodplain during each stage, has been used to calculate the mean annual sediment discharge of the Fraser River on a volume basis (m^3/yr)[1].

Mathews and Shepard (1962) calculated a mean porosity of 46.5%, and a mean grain density of 2.71 g/cm^3, for sediment within the delta (their Table 1). These values were used to convert the mean annual volume discharges in Table 9.2, to mean annual sediment discharges on a mass basis (tonnes/yr - Table 9.2). The figures in Table 9.2 were used to estimate the sediment discharge, in tonnes/yr, of the Fraser River for the Holocene period (Fig. 9.6).

---

[1] Volumes are given on a compacted sediment basis, with a mean porosity of 46.5% (Mathews and Shepard, 1962).

Table 9.2 The Fraser River's estimated sediment discharge rates during the Holocene

PERIOD (yr BP)	VOLUME ADDED TO: DELTA ($x10^{10}$ m^3)	FLOODPLAIN ($x10^8$ m^3)	TOTAL VOLUME ($x10^{10}$ m^3)	FRASER RIVER SEDIMENT DISCHARGE ($x10^7$ m^3/yr)	($x10^7$ tonnes/yr)
9000-8000	2.01		2.01	2.01	2.91
8000-6800	1.91	4.94	1.96	1.64	2.37
6800-6200	1.53	6.32	1.59	2.65	3.84
6200-5800	1.30		1.30	3.24	4.70
5800-4500	1.81	5.06	1.87	1.43	2.08
4500-2250	3.69	5.60	3.74	1.66	2.41
2250-PRESENT	3.39		3.39	1.51	2.18

TOTAL VOLUME OF DELTA=$1.63x10^{11}$ m^3
(VOLUME PRIOR TO 9000 yr BP=$6.75x10^9$ m^3)
TOTAL MASS OF DELTA=$2.36x10^{11}$ TONNES
(density=2.71 g/cm^3, porosity=46.5%)

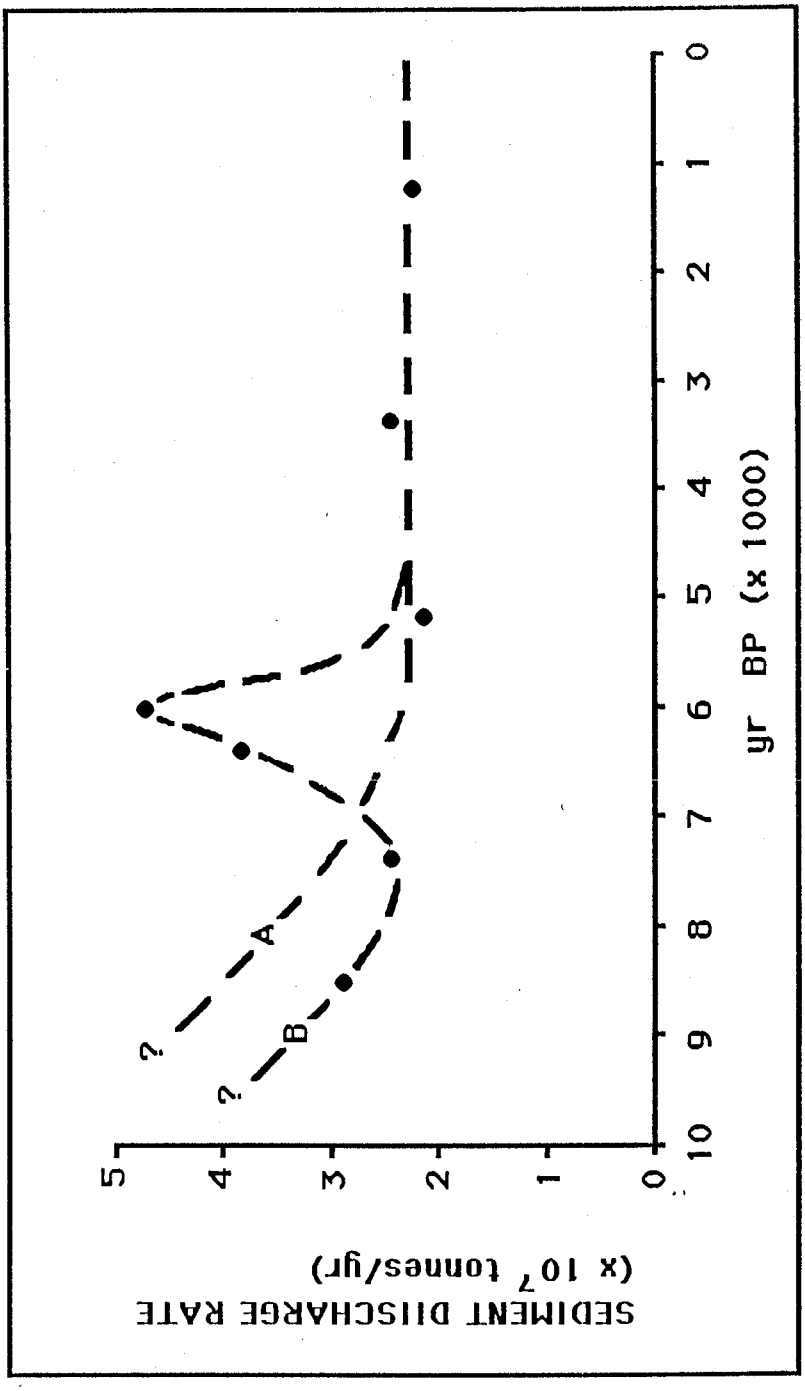

Figure 9.6 The Fraser River's estimated sediment discharge during the Holocene – scenario A and B

9.5.4 DISCUSSION

The calculated magnitude of the Fraser River's annual sediment discharge for the last 2250 years, of 2.18×10^7 tonnes/yr or 1.506×10^7 m^3/yr, is comparable to estimates of contemporary sediment discharge rates made in other studies.

Mathews and Shepard (1962), calculated a rate of about 1.85×10^7 tonnes/yr or 1.27×10^7 m^3/yr, on the basis of bathymetric surveys of the delta front made in 1929 and 1959. These figures take into account natural compaction of sediment upon burial and losses due to dredging in the Fraser estuary. These values may, however, be underestimates, since they do not include sediment added to the delta by the North and Middle Arms of the Fraser River.

Kidd (1953) measured the suspended sediment load of the Fraser River at Hope, 140 km from the delta apex, for the three year period 1950-1952. A mean rate of 1.68×10^7 tonnes/yr or 1.16×10^7 m^3/yr was calculated. Milliman (1980) calculated the suspended sediment discharge of the Fraser River for the six year period 1967-1972. A mean rate of 1.84×10^7 tonnes/yr or 1.27×10^7 m^3/yr was found at Hope. At Port Mann, 5 km east of the delta apex, a rate of 1.68×10^7 tonnes/yr or 1.16×10^7 m^3/yr was calculated.

The downstream decrease in suspended sediment discharge (between Hope and Port Mann) indicates deposition and infers increased importance of bed load transport in the lower part of the river (Milliman, 1980).

The sediment discharge rates calculated by Kidd and

Milliman may also underestimate the actual values, since the bed load component of the sediment load is not included in their measurements. Although bed load may only represent about 5% of the total load at Hope (Milliman, 1980), the bed load component may reach as high as 20% in the lower estuary, where substantial sediment transport occurs in the form of migrating sand waves (Milliman, 1980; Kostachuk et al., 1986).

There is considerable scatter in the data points in Figure 9.6, which may result from errors in the volume estimates. Nevertheless, two generalized scenarios can be developed on the basis of this data and are approximated by the dashed lines A and B (Fig. 9.6).

scenario A:

This scenario assumes that much of the scatter in the data points is due to errors in the volume estimates and sediment discharge can be approximated by a simple curve, falling between the data points (line A). Two general trends are apparent in this scenario:

(i) the sediment discharge rate appears to have been fairly stable, at about 2.2×10^7 tonnes/yr, for about the last 6000 years. The beginning of this period coincides with the end of paraglacial conditions, proposed by Church and Ryder (1972).

(ii) sediment discharge rates appear to have been substantially higher during the period 9000-6000 yr BP. Considering the estimated total mass of the delta of about 2.36×10^{11} tonnes (Table 9.2) and assuming a constant rate of 2.2×10^7 tonnes/yr

for the last 6000 years, sediment discharge would have averaged about 3.47×10^7 tonnes/yr between 9000 and 6000 yr BP. At the beginning of this period, sediment discharge may have been as high as 4.5×10^7 tonnes/yr (Fig. 9.6), approximately double the contemporary rate.

Church and Ryder (1972) suggest that sediment yields from small watersheds in south-central B.C. were about an order of magnitude larger at the peak of the paraglacial period, compared to the present-day (their Fig. 9 and Table 3.B). The discrepency between their findings and those of this scenario, may be due to the tendency for an increasing proportion of mobilized sediment to be redeposited and stored (in the form of alluvial fans, valley fills, lacustrine sediments, etc.) as basin size increases (Brune, 1948; Schumm, 1963).

It is also likely that the deposits stored within the delta represent only the later "waning" stages of the paraglacial period. The highest Fraser River sediment discharges, associated with the peak of paraglaciation during and immediately following deglaciation (ca. 11300 - 9000 yr BP), probably were responsible for filling in a former arm of the sea between New Westminster and Chilliwack, along the course presently occupied by the Fraser River floodplain (Armstrong, 1983).

Scenario B:

This scenario assumes greater accuracy in the data points, enabling three general trends to be recognized, which are approximated by the dashed line B (Fig. 9.6).

(i) as in scenario A, sediment discharge has been relatively stable over the last 6000 years, at about 2.2×10^7 tonnes/year.
(ii) a peak in sediment discharge, reaching about 5×10^7 tonnes/yr occurred at about 6000 yr BP.
(iii) sediment discharge rates were higher in the early Holocene than at present. Discharges may have been as high as about 3.5×10^7 tonnes/yr around 9000 yr BP and declined to about 2.4×10^7 tonnes/yr by 7400 yr BP.

The timing of the mid-Holocene peak in sediment discharge in this scenario coincides with a period of climatic amelioration in the Pacific Northwest (Heusser et al., 1984). Little is known about the effect of this climatic thermal maxima on sediment discharge rates in southern British Columbia.

A possible explanation is that warmer summer temperatures shortened the snowmelt period, increasing peak run-offs and causing a "flushing" effect on sediment stored within fluvial systems. Such conditions are known to have been responsible for higher-than-normal river discharges in historical time (e.g. the 1948 flood in southern B.C. - B. Sagar, pers. comm.).

The other two trends in this scenario - the stable sediment discharge over the last 6000 years and the increased sediment discharges in the early Holocene - correspond to the same trends outlined in scenario A and may, therefore, also be explained in terms of the effects of "paraglaciation".

9.6 IMPLICATIONS OF THE STUDY FINDINGS

9.6.1 THE DEPOSITIONAL REGRESSION AS A MODEL OF COASTAL DEVELOPMENT

The finding that the response of the Fraser Delta to the mid-Holocene sea-level rise took the form of a depositional regression, provides a model of coastal development which may be applicable to many coastal depositional settings.

In formerly glaciated coastal areas, such as the Pacific Northwest, post-glacial conditions may have been particularly favourable for this form of depositional response. The combination of eustatically rising sea-levels coupled with paraglacially-enhanced sediment supplies, would presumably have increased the likelyhood of this form of coastal development occurring.

The southwestern coast of mainland British Columbia, the eastern and southern coasts of Vancouver Island and the coastal areas surrounding Puget Sound, all experienced a sea-level rise in the post-glacial period (Clague et al., 1982; Mathews et al., 1970).

These same coastal belts are also flanked by mountainous terrain, which contained extensive drift deposits in immediate post-glacial time (Armstrong et al., 1965). Thus, local rivers presumably supplied enhanced "paraglacially-primed" sediment loads to many deltas, estuaries and low-lying floodplains, during the post-glacial rise in sea-level.

The response of any one particular site would, of course,

depend on local conditions. The local rate of sediment deposition would be determined not only by the rate of sediment supply, but also by the characteristics of the receiving basin. The depth of water, degree of lateral confinement and the rate of sediment removal by coastal processes, would all play a role in determining the nature of the depositional response.

The fjord-head deltas of the British Columbia coast, for example, may have been likely sites for depositional regression, due to the lateral confinement on delta growth. This restriction of the delta's area presumably tends to increase local rates of deposition (in terms of mass $area^{-1}$ $time^{-1}$).

Although formerly glaciated areas may have been particularly favourable for the development of depositional regressions, it also follows that coastal deposits in non-glaciated areas may produce the same response if local conditions are suitable. A delta building into a shallow, laterally-restricted embayment, for example, might sustain a rate of deposition which is sufficient to keep pace with a local rise in sea-level.

The findings from the Fraser Delta serve to act as a model of the depositional regression style of coastal aggradation. The model has a number of implications for research concerned with coastal evolution both in the Pacific Northwest and elsewhere:
(i) the facies sequences within the Fraser Delta can be used on a comparative basis to aid in identifying similar styles of coastal aggradation. There are two aspects of the comparison: firstly, the presence of facies in the "correct" vertical order,

but of unusually large vertical extent (compared to facies formed under stable sea level conditions), may indicate that base-level induced vertical accretion has occurred; and, secondly, in a prograding deposit, such as a delta, the vertically accreted facies should undergo a progressive thinning in the direction of progradation.

(ii) the internal architecture of the Fraser Delta has resulted from the upward and seaward shift of depositional environments in response to a rise in sea level. Consequently, a shift in the positioning of a given facies within similarly-formed deposits, coupled with some form of dating control on the timing of the facies shift, can be used to determine both the magnitude and duration of the sea-level rise. Figure 8.5, for example, shows that the base of the tidal marsh facies underwent a vertical shift of about 13 m between ca. 8000 and 2250 yr BP, in response to rising sea level.

(iii) the sequence of paleosurfaces within the Fraser Delta may serve to act as a guide in establishing the chronological framework of other deposits formed by depositional regression. Comparison of Figures 1.7a, b and c indicates that the aggradational style can have a substantial effect on the chronological framework of a deposit. In the case of the Fraser Delta, for example, shallow deposits (ca. 2 m below mean sea level) underlying the entire eastern half of the delta are virtually isochronous (ca. 5000 yr BP). This includes shallow deposits adjacent to the delta apex, despite the fact that the delta started forming at about 9000 yr BP. This is in sharp

contrast to a delta formed under stable sea-level conditions (or by renewed progradation following a marine transgression - Figure 1.7a), where a progressive decrease in the age of deposits occurs along proximal - distal trends. The establishment of an accurate depositional chronology will be of obvious benefit in areas such as the calculation of progradation rates, sedimentation rates, sediment supply rates, paleoenvironmental reconstruction and so on.

(iv) the study findings indicate that aggradation, of up to about 13 m depth, occurred over a considerable area of the lower Fraser River floodplain in response to the rise in sea-level. The preservation of the peat and tephra marker beds, in the western portion of the floodplain at least (Figure 6.21), suggests that fluvial reworking has not occurred and that vertically-accreted, overbank sedimentation may represent a substantial component of the floodplain deposits. Consequently, vertical accretion (as opposed to lateral accretion due to meander migration) may have played a major role in floodplain construction in the lower reaches of the Fraser and other rivers in the Pacific Northwest. Evidence from the study further suggests that the planform change of the Fraser River in the lower ca. 47 km of its course, may be related to the presence of the aggradational sediment wedge. Similar relationships may, therefore, be present in the lower reaches of other rivers in the region, where coastal aggradation has occurred in response to sea-level rise.

(v) in the Fraser Delta, the fluvial-marine interface is a zone

of pronounced lithologic contrasts, apparently related to the dissipation of wave and tidal-current energy over the broad, gently-inclined intertidal platform. Former sea-level positions could be identified in core by the lithologic transition from organic-rich silts of tidal marsh origin, to the silts and sands of mid-tidal origin. This technique has the potential for application in other coastal settings where lithologically contrasting environments bracket sea-level position. The sandy deltas on the east coast of Vancouver Island may be well suited for this technique.

9.6.2 REVISED SEA-LEVEL CURVE

The revised sea-level curve for the Fraser Lowland region (Fig. 9.1), contains a previously unknown stillstand of approximately 400 years duration, occurring between ca. 6200 and 5800 yr BP. Evidence of this stillstand may be preserved in other coastal deposits in this region, in the form of peat or other terrestrial deposits, now lying at some depth below sea-level.

In addition to providing a valuable time-stratigraphic marker horizon, the ca. 6000 yr BP paleosurface may also have some utility in studies of relative sea-level changes in the Strait of Georgia region. The depth of the former terrestrial surface below present sea-level may provide an indication of the relative vertical displacement that has occurred over the last ca. 6000 years.

The evidence from the Fraser Delta also suggests that the

sea did not stabilize at its present level until about 2250 yr BP. This represents a considerable modification of the sea-level curve for this area. Previously, it was known only that the sea attained its present level some time after ca. 5000 yr BP. This finding is of relevance to studies concerned with the evolution of coastal deposits in this region and may also have significant implications for archaeological studies of middens located in low-lying coastal sites.

9.6.3 FRASER RIVER SEDIMENT DISCHARGE DURING THE HOLOCENE

Although somewhat spectulative, the Fraser River sediment discharge curves for the last 9000 years (Fig. 9.6), do at least appear to indicate two general trends: firstly, sediment discharge seems to have been fairly stable for about the last 6000 years; and, secondly, sediment discharges were higher in the early Holocene.

These findings suggest that the effects of "paraglaciation" in the Fraser River basin were transmitted, at least in part, throughout the entire Fraser River system, to be recorded in the form of increased sediment accumulation rates in the Fraser Delta.

The stabilization of sediment discharge rates at present levels, by about 6000 yr BP, suggests that sources of readily available sediment were exhausted at this time. This may have been due to the depletion of unstable drift deposits on valley slopes and/or the completion of fluvial reworking of deposits

stored earlier within the river system.

The implications of these findings for Holocene sediment discharges of other rivers in the Pacific Northwest are unclear at this time. It is probable that drainage basin size is an important factor, since storage effects presumably increase in significance with increasing basin area. Consequently, paraglacial sediment discharges may have been more pronounced, but also more short-lived in smaller basins (i.e. larger basins probably have a "dampening" effect on paraglacial sediment discharges, but may also prolong the duration of the paraglacial effect due to reworking of stored deposits).

Since elevated sediment discharges apparently occurred in the Fraser River, and it is the largest river reaching the west coast of Canada, it seems likely that most other river systems in the region also experienced increased sediment discharges in the "paraglacial period." It is also probable that 6000 yr BP is a reasonable minimum age for the end of "paraglacially-enhanced" sediment discharges.

9.7 CONCLUSIONS

The findings of this study support the following conclusions:

1. the response of the northern part of the Fraser Delta (Lulu Island) to a mid-Holocene sea-level rise took the form of a depositional regression. This resulted in a distinctive depositional framework incorporating elements of both lateral

progradation and vertical accretion.

2. depositional environments underwent vertical accretion during the periods of rising sea-level. The resulting vertical facies sequences are characterised by facies of the same internal character and vertical order as their modern analogues, but of considerably greater vertical extent.

3. the vertical shift in the positioning of facies sequences within the body of the deltaic deposit that occurs during a depositional regression, can be used as both an indicator and measure of sea-level rise.

4. the study illustrates how an interpretative framework based on a combination of depositional characteristics, both lithologic and biologic in nature, ensures greater resolution of, and improved confidence in, interpretation of subsurface facies.

5. the findings from this study, concerning the nature, spatial arrangement and chronology of facies within the delta, serve as a model of the depositional regression style of coastal aggradation.

APPENDIX 1

FOLK AND WARD (1957) GRAIN SIZE PARAMETERS

Key

phi	size class in phi units
cumpercent	cumulative percentage retained in size class
mean	mean grain size in phi units
meanmm	mean grain size in mm
stddev	sorting index
skewness	skewness index
kurtosis	kurtosis index
nkurtosis	normalized kurtosis
%5 - %95	percentile values in phi units

For further details refer to Folk and Ward (1957)

INTERTIDAL SURFACE SAMPLES

Sample No.																		
1	phi	1.00	1.50	2.00	2.50	3.00	3.50	4.00	4.50	5.00	5.50	6.00	6.50	7.00	7.50	8.00	8.50	9.00	14.00
	cumpercent	0	0	0	0	0	0	0	0	0	0	2	6	13	25	36	47	55	100
	mean= 9.345 meanmm= 0.0015 stddev= 2.345 skewness= 0.366 kurtosis= 0.778 nkurtosis= 0.438																		
	%tile5= 6.375 %tile16= 7.125 %tile25= 7.500 %tile50= 8.687 %tile75= 11.222 %tile84= 12.222 %tile95= 13.444																		
2	phi	1.00	1.50	2.00	2.50	3.00	3.50	4.00	4.50	5.00	5.50	6.00	6.50	7.00	7.50	8.00	8.50	9.00	14.00
	cumpercent	0	0	0	0	0	0	0	0	0	2	9	19	31	43	52	60	66	100
	mean= 8.629 meanmm= 0.0025 stddev= 2.468 skewness= 0.421 kurtosis= 0.866 nkurtosis= 0.464																		
	%tile5= 5.714 %tile16= 6.350 %tile25= 6.750 %tile50= 7.889 %tile75= 10.324 %tile84= 11.647 %tile95= 13.265																		
3	phi	1.00	1.50	2.00	2.50	3.00	3.50	4.00	4.50	5.00	5.50	6.00	6.50	7.00	7.50	8.00	8.50	9.00	14.00
	cumpercent	0	0	0	0	0	0	0	0	0	0	1	6	12	21	32	40	47	100
	mean= 9.665 meanmm= 0.0012 stddev= 2.397 skewness= 0.204 kurtosis= 0.738 nkurtosis= 0.425																		
	%tile5= 6.400 %tile16= 7.222 %tile25= 7.682 %tile50= 9.283 %tile75= 11.642 %tile84= 12.491 %tile95= 13.528																		
4	phi	1.00	1.50	2.00	2.50	3.00	3.50	4.00	4.50	5.00	5.50	6.00	6.50	7.00	7.50	8.00	8.50	9.00	14.00
	cumpercent	0	0	0	0	0	0	0	0	0	0	2	13	27	42	54	65	70	100
	mean= 8.591 meanmm= 0.0026 stddev= 2.247 skewness= 0.499 kurtosis= 0.992 nkurtosis= 0.498																		
	%tile5= 6.136 %tile16= 6.607 %tile25= 6.929 %tile50= 7.833 %tile75= 9.833 %tile84= 11.333 %tile95= 13.167																		
5	phi	1.00	1.50	2.00	2.50	3.00	3.50	4.00	4.50	5.00	5.50	6.00	6.50	7.00	7.50	8.00	8.50	9.00	14.00
	cumpercent	0	0	0	0	0	0	0	0	0	1	6	14	25	36	46	55	61	100
	mean= 8.921 meanmm= 0.0021 stddev= 2.470 skewness= 0.384 kurtosis= 0.806 nkurtosis= 0.446																		
	%tile5= 5.900 %tile16= 6.591 %tile25= 7.000 %tile50= 8.222 %tile75= 10.795 %tile84= 11.949 %tile95= 13.359																		
6	phi	1.00	1.50	2.00	2.50	3.00	3.50	4.00	4.50	5.00	5.50	6.00	6.50	7.00	7.50	8.00	8.50	9.00	14.00
	cumpercent	0	0	0	0	0	0	0	0	2	5	14	26	39	48	59	70	74	100
	mean= 8.199 meanmm= 0.0034 stddev= 2.352 skewness= 0.411 kurtosis= 1.130 nkurtosis= 0.531																		
	%tile5= 5.500 %tile16= 6.083 %tile25= 6.458 %tile50= 7.591 %tile75= 9.192 %tile84= 10.923 %tile95= 13.038																		
7	phi	1.00	1.50	2.00	2.50	3.00	3.50	4.00	4.50	5.00	5.50	6.00	6.50	7.00	7.50	8.00	8.50	9.00	14.00
	cumpercent	0	0	0	0	1	4	7	8	11	22	36	47	55	63	68	73	77	100
	mean= 7.479 meanmm= 0.0056 stddev= 2.725 skewness= 0.397 kurtosis= 1.206 nkurtosis= 0.547																		
	%tile5= 3.667 %tile16= 5.227 %tile25= 5.607 %tile50= 6.687 %tile75= 8.750 %tile84= 10.522 %tile95= 12.913																		
8	phi	1.00	1.50	2.00	2.50	3.00	3.50	4.00	4.50	5.00	5.50	6.00	6.50	7.00	7.50	8.00	8.50	9.00	14.00
	cumpercent	0	0	1	2	7	11	18	19	24	33	40	49	57	64	68	72	75	100
	mean= 7.073 meanmm= 0.0074 stddev= 3.281 skewness= 0.241 kurtosis= 1.060 nkurtosis= 0.515																		
	%tile5= 2.800 %tile16= 3.857 %tile25= 5.056 %tile50= 6.562 %tile75= 9.000 %tile84= 10.800 %tile95= 13.000																		
9	phi	1.00	1.50	2.00	2.50	3.00	3.50	4.00	4.50	5.00	5.50	6.00	6.50	7.00	7.50	8.00	8.50	9.00	14.00
	cumpercent	0	0	0	0	0	1	3	4	11	22	35	49	57	64	69	73	75	100
	mean= 7.530 meanmm= 0.0054 stddev= 2.670 skewness= 0.524 kurtosis= 1.021 nkurtosis= 0.505																		
	%tile5= 4.571 %tile16= 5.227 %tile25= 5.615 %tile50= 6.562 %tile75= 9.000 %tile84= 10.800 %tile95= 13.000																		
10	phi	1.00	1.50	2.00	2.50	3.00	3.50	4.00	4.50	5.00	5.50	6.00	6.50	7.00	7.50	8.00	8.50	9.00	14.00
	cumpercent	0	0	0	0	0	0	0	1	2	8	19	32	42	52	58	62	66	100
	mean= 8.304 meanmm= 0.0032 stddev= 2.660 skewness= 0.466 kurtosis= 0.803 nkurtosis= 0.445																		
	%tile5= 5.250 %tile16= 5.864 %tile25= 6.231 %tile50= 7.400 %tile75= 10.324 %tile84= 11.647 %tile95= 13.265																		

	phi	1.00	1.50	2.00	2.50	3.00	3.50	4.00	4.50	5.00	5.50	6.00	6.50	7.00	7.50	8.00	8.50	9.00	14.00
	cumpercent	0	0	0	1	7	14	21	23	28	38	47	54	60	65	69	73	76	100
11	mean= 6.841 meanmm= 0.0087 stddev= 3.290 skewness= 0.300 kurtosis= 1.004 nkurtosis= 0.501																		
	%tile5= 2.833 %tile16= 3.643 %tile25= 4.700 %tile50= 6.214 %tile75= 8.833 %tile84= 10.667 %tile95= 12.958																		
	phi	1.00	1.50	2.00	2.50	3.00	3.50	4.00	4.50	5.00	5.50	6.00	6.50	7.00	7.50	8.00	8.50	9.00	14.00
	cumpercent	0	0	1	5	13	21	26	27	31	39	47	53	59	65	69	73	76	100
12	mean= 6.701 meanmm= 0.0096 stddev= 3.454 skewness= 0.232 kurtosis= 0.869 nkurtosis= 0.465																		
	%tile5= 2.500 %tile16= 3.187 %tile25= 3.900 %tile50= 6.250 %tile75= 8.833 %tile84= 10.667 %tile95= 12.958																		
	phi	1.00	1.50	2.00	2.50	3.00	3.50	4.00	4.50	5.00	5.50	6.00	6.50	7.00	7.50	8.00	8.50	9.00	14.00
	cumpercent	0	0	0	0	0	1	4	5	10	25	43	56	65	71	75	78	81	100
13	mean= 7.086 meanmm= 0.0074 stddev= 2.387 skewness= 0.551 kurtosis= 1.342 nkurtosis= 0.573																		
	%tile5= 4.500 %tile16= 5.200 %tile25= 5.500 %tile50= 6.269 %tile75= 8.000 %tile84= 9.789 %tile95= 12.684																		
	phi	1.00	1.50	2.00	2.50	3.00	3.50	4.00	4.50	5.00	5.50	6.00	6.50	7.00	7.50	8.00	8.50	9.00	14.00
	cumpercent	0	0	0	0	1	2	3	4	5	10	20	30	41	51	59	65	70	100
14	mean= 8.194 meanmm= 0.0034 stddev= 2.621 skewness= 0.402 kurtosis= 0.934 nkurtosis= 0.483																		
	%tile5= 5.000 %tile16= 5.800 %tile25= 6.250 %tile50= 7.450 %tile75= 9.833 %tile84= 11.333 %tile95= 13.167																		
	phi	1.00	1.50	2.00	2.50	3.00	3.50	4.00	4.50	5.00	5.50	6.00	6.50	7.00	7.50	8.00	8.50	9.00	14.00
	cumpercent	0	0	8	12	21	27	31	32	34	37	42	48	54	60	66	71	74	100
15	mean= 6.771 meanmm= 0.0092 stddev= 3.751 skewness= 0.087 kurtosis= 0.785 nkurtosis= 0.440																		
	%tile5= 1.812 %tile16= 2.722 %tile25= 3.333 %tile50= 6.667 %tile75= 9.192 %tile84= 10.923 %tile95= 13.038																		
	phi	1.00	1.50	2.00	2.50	3.00	3.50	4.00	4.50	5.00	5.50	6.00	6.50	7.00	7.50	8.00	8.50	9.00	14.00
	cumpercent	0	0	5	9	25	41	51	51	55	61	66	70	73	77	80	83	85	100
16	mean= 5.140 meanmm= 0.0284 stddev= 3.073 skewness= 0.607 kurtosis= 0.996 nkurtosis= 0.499																		
	%tile5= 2.000 %tile16= 2.719 %tile25= 3.000 %tile50= 3.950 %tile75= 7.250 %tile84= 8.750 %tile95= 12.333																		
	phi	1.00	1.50	2.00	2.50	3.00	3.50	4.00	4.50	5.00	5.50	6.00	6.50	7.00	7.50	8.00	8.50	9.00	14.00
	cumpercent	0	0	0	0	0	0	1	1	2	10	24	35	45	54	60	65	68	100
17	mean= 8.164 meanmm= 0.0035 stddev= 2.663 skewness= 0.469 kurtosis= 0.813 nkurtosis= 0.448																		
	%tile5= 5.187 %tile16= 5.714 %tile25= 6.045 %tile50= 7.278 %tile75= 10.094 %tile84= 11.500 %tile95= 13.219																		
	phi	1.00	1.50	2.00	2.50	3.00	3.50	4.00	4.50	5.00	5.50	6.00	6.50	7.00	7.50	8.00	8.50	9.00	14.00
	cumpercent	0	0	0	0	1	2	3	3	3	9	20	34	46	55	61	67	72	100
18	mean= 8.061 meanmm= 0.0037 stddev= 2.534 skewness= 0.477 kurtosis= 0.969 nkurtosis= 0.492																		
	%tile5= 5.167 %tile16= 5.818 %tile25= 6.179 %tile50= 7.222 %tile75= 9.536 %tile84= 11.143 %tile95= 13.107																		
	phi	1.00	1.50	2.00	2.50	3.00	3.50	4.00	4.50	5.00	5.50	6.00	6.50	7.00	7.50	8.00	8.50	9.00	14.00
	cumpercent	0	1	2	6	13	22	31	32	35	42	50	58	65	72	76	79	82	100
19	mean= 6.241 meanmm= 0.0132 stddev= 3.148 skewness= 0.202 kurtosis= 0.997 nkurtosis= 0.499																		
	%tile5= 2.375 %tile16= 3.167 %tile25= 3.667 %tile50= 6.000 %tile75= 7.875 %tile84= 9.556 %tile95= 12.611																		

	phi	1.00	1.50	2.00	2.50	3.00	3.50	4.00	4.50	5.00	5.50	6.00	6.50	7.00	7.50	8.00	8.50	9.00	14.00
	cumpercent	0	1	2	4	27	44	55	56	59	64	69	73	77	81	84	86	88	100
20	mean= 4.845 meanmm= 0.0348 stddev= 2.733 skewness= 0.674 kurtosis= 1.015 nkurtosis= 0.504																		
	%tile5= 2.522 %tile16= 2.761 %tile25= 2.957 %tile50= 3.773 %tile75= 6.750 %tile84= 8.000 %tile95= 11.917																		
	phi	1.00	1.50	2.00	2.50	3.00	3.50	4.00	4.50	5.00	5.50	6.00	6.50	7.00	7.50	8.00	8.50	9.00	14.00
	cumpercent	0	1	3	6	28	45	54	54	55	57	61	65	70	74	78	82	85	100
21	mean= 5.113 meanmm= 0.0289 stddev= 3.042 skewness= 0.684 kurtosis= 0.873 nkurtosis= 0.466																		
	%tile5= 2.333 %tile16= 2.727 %tile25= 2.932 %tile50= 3.778 %tile75= 7.625 %tile84= 8.833 %tile95= 12.333																		
	phi	1.00	1.50	2.00	2.50	3.00	3.50	4.00	4.50	5.00	5.50	6.00	6.50	7.00	7.50	8.00	8.50	9.00	14.00
	cumpercent	0	3	12	17	33	46	52	52	53	56	61	66	71	76	79	82	84	100
22	mean= 5.078 meanmm= 0.0296 stddev= 3.290 skewness= 0.578 kurtosis= 0.954 nkurtosis= 0.488																		
	%tile5= 1.611 %tile16= 2.400 %tile25= 2.750 %tile50= 3.833 %tile75= 7.400 %tile84= 9.000 %tile95= 12.437																		
	phi	1.00	1.50	2.00	2.50	3.00	3.50	4.00	4.50	5.00	5.50	6.00	6.50	7.00	7.50	8.00	8.50	9.00	14.00
	cumpercent	4	55	90	94	95	96	97	97	97	97	98	98	98	98	98	98	98	100
23	mean= 1.494 meanmm= 0.3550 stddev= 0.501 skewness= 0.360 kurtosis= 1.407 nkurtosis= 0.584																		
	%tile5= 1.010 %tile16= 1.118 %tile25= 1.206 %tile50= 1.451 %tile75= 1.786 %tile84= 1.914 %tile95= 3.000																		
	phi	1.00	1.50	2.00	2.50	3.00	3.50	4.00	4.50	5.00	5.50	6.00	6.50	7.00	7.50	8.00	8.50	9.00	14.00
	cumpercent	0	0	1	4	35	50	58	58	59	62	65	68	72	76	79	82	84	100
24	mean= 5.065 meanmm= 0.0299 stddev= 3.080 skewness= 0.773 kurtosis= 0.896 nkurtosis= 0.473																		
	%tile5= 2.516 %tile16= 2.694 %tile25= 2.839 %tile50= 3.500 %tile75= 7.375 %tile84= 9.000 %tile95= 12.437																		
	phi	1.00	1.50	2.00	2.50	3.00	3.50	4.00	4.50	5.00	5.50	6.00	6.50	7.00	7.50	8.00	8.50	9.00	14.00
	cumpercent	0	2	6	16	53	67	73	74	75	77	79	81	83	85	87	89	90	100
25	mean= 4.236 meanmm= 0.0531 stddev= 2.646 skewness= 0.791 kurtosis= 1.659 nkurtosis= 0.624																		
	%tile5= 1.875 %tile16= 2.500 %tile25= 2.622 %tile50= 2.959 %tile75= 5.000 %tile84= 7.250 %tile95= 11.500																		
	phi	1.00	1.50	2.00	2.50	3.00	3.50	4.00	4.50	5.00	5.50	6.00	6.50	7.00	7.50	8.00	8.50	9.00	14.00
	cumpercent	1	7	21	51	81	90	92	92	92	93	94	95	95	95	95	95	96	100
26	mean= 2.490 meanmm= 0.1779 stddev= 1.119 skewness= 0.285 kurtosis= 2.541 nkurtosis= 0.718																		
	%tile5= 1.333 %tile16= 1.821 %tile25= 2.067 %tile50= 2.483 %tile75= 2.900 %tile84= 3.167 %tile95= 6.500																		
	phi	1.00	1.50	2.00	2.50	3.00	3.50	4.00	4.50	5.00	5.50	6.00	6.50	7.00	7.50	8.00	8.50	9.00	14.00
	cumpercent	5	44	71	82	93	96	97	97	97	97	97	97	97	97	97	97	98	100
27	mean= 1.781 meanmm= 0.2910 stddev= 0.716 skewness= 0.414 kurtosis= 1.033 nkurtosis= 0.508																		
	%tile5= 1.000 %tile16= 1.141 %tile25= 1.256 %tile50= 1.611 %tile75= 2.182 %tile84= 2.591 %tile95= 3.333																		
	phi	1.00	1.50	2.00	2.50	3.00	3.50	4.00	4.50	5.00	5.50	6.00	6.50	7.00	7.50	8.00	8.50	9.00	14.00
	cumpercent	9	30	63	77	93	96	97	97	97	97	97	97	97	97	97	97	97	100
28	mean= 1.896 meanmm= 0.2687 stddev= 0.809 skewness= 0.141 kurtosis= 1.087 nkurtosis= 0.521																		
	%tile5= 0.556 %tile16= 1.167 %tile25= 1.381 %tile50= 1.803 %tile75= 2.429 %tile84= 2.719 %tile95= 3.333																		
	phi	1.00	1.50	2.00	2.50	3.00	3.50	4.00	4.50	5.00	5.50	6.00	6.50	7.00	7.50	8.00	8.50	9.00	14.00
	cumpercent	2	15	53	69	89	93	94	94	94	94	94	94	94	94	94	95	96	100
29	mean= 2.116 meanmm= 0.2306 stddev= 1.459 skewness= 0.557 kurtosis= 2.972 nkurtosis= 0.748																		
	%tile5= 1.115 %tile16= 1.513 %tile25= 1.632 %tile50= 1.961 %tile75= 2.650 %tile84= 2.875 %tile95= 8.500																		

30	phi	1.00	1.50	2.00	2.50	3.00	3.50	4.00	4.50	5.00	5.50	6.00	6.50	7.00	7.50	8.00	8.50	9.00	14.00
	cumpercent	2	11	51	64	87	93	95	95	95	95	95	95	95	95	95	95	95	100

mean= 2.162 meanmm= 0.2235 stddev= 0.772 skewness= 0.401 kurtosis= 1.091 nkurtosis= 0.522
%tile5= 1.167 %tile16= 1.562 %tile25= 1.675 %tile50= 1.988 %tile75= 2.739 %tile84= 2.935 %tile95= 4.000

31	phi	1.00	1.50	2.00	2.50	3.00	3.50	4.00	4.50	5.00	5.50	6.00	6.50	7.00	7.50	8.00	8.50	9.00	14.00
	cumpercent	0	6	35	59	89	94	96	96	96	96	96	96	96	96	96	96	96	100

mean= 2.301 meanmm= 0.2030 stddev= 0.665 skewness= 0.102 kurtosis= 1.018 nkurtosis= 0.505
%tile5= 1.417 %tile16= 1.672 %tile25= 1.828 %tile50= 2.312 %tile75= 2.767 %tile84= 2.917 %tile95= 3.750

32	phi	1.00	1.50	2.00	2.50	3.00	3.50	4.00	4.50	5.00	5.50	6.00	6.50	7.00	7.50	8.00	8.50	9.00	14.00
	cumpercent	0	10	51	61	91	96	97	97	97	97	97	97	97	97	97	97	97	100

mean= 2.148 meanmm= 0.2256 stddev= 0.653 skewness= 0.340 kurtosis= 0.839 nkurtosis= 0.456
%tile5= 1.250 %tile16= 1.573 %tile25= 1.683 %tile50= 1.988 %tile75= 2.733 %tile84= 2.883 %tile95= 3.400

33	phi	1.00	1.50	2.00	2.50	3.00	3.50	4.00	4.50	5.00	5.50	6.00	6.50	7.00	7.50	8.00	8.50	9.00	14.00
	cumpercent	0	2	9	37	60	72	78	78	78	79	80	82	84	86	88	90	91	100

mean= 3.969 meanmm= 0.0638 stddev= 2.659 skewness= 0.753 kurtosis= 2.661 nkurtosis= 0.727
%tile5= 1.714 %tile16= 2.125 %tile25= 2.286 %tile50= 2.783 %tile75= 3.750 %tile84= 7.000 %tile95= 11.222

34	phi	1.00	1.50	2.00	2.50	3.00	3.50	4.00	4.50	5.00	5.50	6.00	6.50	7.00	7.50	8.00	8.50	9.00	14.00
	cumpercent	0	2	23	44	80	90	94	94	94	94	94	94	94	95	95	95	95	100

mean= 2.539 meanmm= 0.1721 stddev= 1.316 skewness= 0.294 kurtosis= 2.984 nkurtosis= 0.749
%tile5= 1.571 %tile16= 1.833 %tile25= 2.048 %tile50= 2.583 %tile75= 2.931 %tile84= 3.200 %tile95= 8.000

35	phi	1.00	1.50	2.00	2.50	3.00	3.50	4.00	4.50	5.00	5.50	6.00	6.50	7.00	7.50	8.00	8.50	9.00	14.00
	cumpercent	1	7	21	43	90	95	97	97	97	97	97	97	97	97	98	99	99	100

mean= 2.444 meanmm= 0.1838 stddev= 0.607 skewness= -0.248 kurtosis= 1.185 nkurtosis= 0.542
%tile5= 1.333 %tile16= 1.821 %tile25= 2.091 %tile50= 2.574 %tile75= 2.840 %tile84= 2.936 %tile95= 3.500

36	phi	1.00	1.50	2.00	2.50	3.00	3.50	4.00	4.50	5.00	5.50	6.00	6.50	7.00	7.50	8.00	8.50	9.00	14.00
	cumpercent	0	0	1	5	48	63	71	72	73	75	77	78	80	83	85	87	88	100

mean= 4.482 meanmm= 0.0448 stddev= 2.707 skewness= 0.854 kurtosis= 1.395 nkurtosis= 0.582
%tile5= 2.500 %tile16= 2.628 %tile25= 2.733 %tile50= 3.067 %tile75= 5.500 %tile84= 7.750 %tile95= 11.917

37	phi	1.00	1.50	2.00	2.50	3.00	3.50	4.00	4.50	5.00	5.50	6.00	6.50	7.00	7.50	8.00	8.50	9.00	14.00
	cumpercent	0	4	60	90	96	97	97	97	97	97	97	97	97	97	97	97	97	100

mean= 1.973 meanmm= 0.2548 stddev= 0.412 skewness= 0.332 kurtosis= 1.026 nkurtosis= 0.506
%tile5= 1.509 %tile16= 1.607 %tile25= 1.687 %tile50= 1.911 %tile75= 2.250 %tile84= 2.400 %tile95= 2.917

38	phi	1.00	1.50	2.00	2.50	3.00	3.50	4.00	4.50	5.00	5.50	6.00	6.50	7.00	7.50	8.00	8.50	9.00	14.00
	cumpercent	0	0	5	13	35	55	65	65	66	67	69	71	73	75	77	79	81	100

mean= 5.244 meanmm= 0.0264 stddev= 3.424 skewness= 0.760 kurtosis= 0.926 nkurtosis= 0.481
%tile5= 2.000 %tile16= 2.568 %tile25= 2.773 %tile50= 3.375 %tile75= 7.500 %tile84= 9.789 %tile95= 12.684

	phi	1.00	1.50	2.00	2.50	3.00	3.50	4.00	4.50	5.00	5.50	6.00	6.50	7.00	7.50	8.00	8.50	9.00	14.00
	cumpercent	1	17	81	90	95	97	98	98	98	98	98	98	98	98	98	98	98	100

39 mean= 1.798 meanmm= 0.2876 stddev= 0.459 skewness= 0.248 kurtosis= 1.967 nkurtosis= 0.663
%tile5= 1.125 %tile16= 1.469 %tile25= 1.562 %tile50= 1.758 %tile75= 1.953 %tile84= 2.167 %tile95= 3.000

phi	1.00	1.50	2.00	2.50	3.00	3.50	4.00	4.50	5.00	5.50	6.00	6.50	7.00	7.50	8.00	8.50	9.00	14.00
cumpercent	0	0	1	6	19	40	51	52	55	59	63	67	70	74	77	80	81	100

40 mean= 5.543 meanmm= 0.0215 stddev= 3.284 skewness= 0.694 kurtosis= 0.932 nkurtosis= 0.482
%tile5= 2.400 %tile16= 2.885 %tile25= 3.143 %tile50= 3.955 %tile75= 7.667 %tile84= 9.789 %tile95= 12.684

phi	1.00	1.50	2.00	2.50	3.00	3.50	4.00	4.50	5.00	5.50	6.00	6.50	7.00	7.50	8.00	8.50	9.00	14.00
cumpercent	0	0	0	0	5	18	29	31	39	50	57	63	68	72	76	79	81	100

41 mean= 6.238 meanmm= 0.0133 stddev= 3.059 skewness= 0.416 kurtosis= 0.978 nkurtosis= 0.495
%tile5= 3.000 %tile16= 3.423 %tile25= 3.818 %tile50= 5.500 %tile75= 7.875 %tile84= 9.789 %tile95= 12.684

phi	1.00	1.50	2.00	2.50	3.00	3.50	4.00	4.50	5.00	5.50	6.00	6.50	7.00	7.50	8.00	8.50	9.00	14.00
cumpercent	0	0	0	1	3	9	14	15	18	27	37	46	53	61	66	71	74	100

42 mean= 7.458 meanmm= 0.0057 stddev= 3.060 skewness= 0.295 kurtosis= 1.064 nkurtosis= 0.515
%tile5= 3.167 %tile16= 4.667 %tile25= 5.389 %tile50= 6.786 %tile75= 9.192 %tile84= 10.923 %tile95= 13.038

phi	1.00	1.50	2.00	2.50	3.00	3.50	4.00	4.50	5.00	5.50	6.00	6.50	7.00	7.50	8.00	8.50	9.00	14.00
cumpercent	0	0	0	0	8	16	24	25	28	36	45	52	59	65	70	74	77	100

43 mean= 6.793 meanmm= 0.0090 stddev= 3.286 skewness= 0.242 kurtosis= 0.993 nkurtosis= 0.498
%tile5= 2.812 %tile16= 3.500 %tile25= 4.500 %tile50= 6.357 %tile75= 8.667 %tile84= 10.522 %tile95= 12.913

phi	1.00	1.50	2.00	2.50	3.00	3.50	4.00	4.50	5.00	5.50	6.00	6.50	7.00	7.50	8.00	8.50	9.00	14.00
cumpercent	0	0	0	1	17	38	50	50	53	57	61	65	69	73	76	79	82	100

44 mean= 5.508 meanmm= 0.0220 stddev= 3.160 skewness= 0.706 kurtosis= 0.881 nkurtosis= 0.469
%tile5= 2.625 %tile16= 2.969 %tile25= 3.190 %tile50= 4.000 %tile75= 7.833 %tile84= 9.556 %tile95= 12.611

phi	1.00	1.50	2.00	2.50	3.00	3.50	4.00	4.50	5.00	5.50	6.00	6.50	7.00	7.50	8.00	8.50	9.00	14.00
cumpercent	1	19	56	68	87	96	99	99	99	99	99	99	99	99	99	99	99	100

45 mean= 2.086 meanmm= 0.2356 stddev= 0.730 skewness= 0.320 kurtosis= 0.867 nkurtosis= 0.464
%tile5= 1.111 %tile16= 1.417 %tile25= 1.581 %tile50= 1.919 %tile75= 2.684 %tile84= 2.921 %tile95= 3.444

phi	1.00	1.50	2.00	2.50	3.00	3.50	4.00	4.50	5.00	5.50	6.00	6.50	7.00	7.50	8.00	8.50	9.00	14.00
cumpercent	5	29	78	90	95	97	98	98	98	98	98	98	98	98	98	98	98	100

46 mean= 1.731 meanmm= 0.3012 stddev= 0.558 skewness= 0.168 kurtosis= 1.483 nkurtosis= 0.597
%tile5= 1.000 %tile16= 1.229 %tile25= 1.417 %tile50= 1.714 %tile75= 1.969 %tile84= 2.250 %tile95= 3.000

phi	1.00	1.50	2.00	2.50	3.00	3.50	4.00	4.50	5.00	5.50	6.00	6.50	7.00	7.50	8.00	8.50	9.00	14.00
cumpercent	0	0	0	1	10	30	40	41	43	47	52	57	62	67	72	76	79	100

47 mean= 6.380 meanmm= 0.0120 stddev= 3.288 skewness= 0.318 kurtosis= 0.827 nkurtosis= 0.453
%tile5= 2.722 %tile16= 3.150 %tile25= 3.375 %tile50= 5.800 %tile75= 8.375 %tile84= 10.190 %tile95= 12.810

INTERTIDAL CORE SAMPLES

Core number and sample depth (cm)																		
TFC1-0	phi	1.00	1.50	2.00	2.50	3.00	3.50	4.00	4.50	5.00	5.50	6.00	6.50	7.00	7.50	8.00	8.50	9.00	14.00
	cumpercent	0	0	0	0	0	0	0	0	0	2	8	18	29	42	51	60	67	100
	mean= 8.640 meanmm= 0.0025 stddev= 2.429 skewness= 0.409 kurtosis= 0.905 nkurtosis= 0.475																		
	%tile5= 5.750 %tile16= 6.400 %tile25= 6.818 %tile50= 7.944 %tile75= 10.212 %tile84= 11.576 %tile95= 13.242																		
TFC1-75	phi	1.00	1.50	2.00	2.50	3.00	3.50	4.00	4.50	5.00	5.50	6.00	6.50	7.00	7.50	8.00	8.50	9.00	14.00
	cumpercent	0	0	0	0	1	5	8	9	15	25	34	42	51	62	70	76	80	100
	mean= 7.331 meanmm= 0.0062 stddev= 2.639 skewness= 0.245 kurtosis= 1.300 nkurtosis= 0.565																		
	%tile5= 3.500 %tile16= 5.050 %tile25= 5.500 %tile50= 6.944 %tile75= 8.417 %tile84= 10.000 %tile95= 12.750																		
TFC1-125	phi	1.00	1.50	2.00	2.50	3.00	3.50	4.00	4.50	5.00	5.50	6.00	6.50	7.00	7.50	8.00	8.50	9.00	14.00
	cumpercent	0	0	1	3	6	10	13	13	15	20	28	38	48	60	69	76	80	100
	mean= 7.394 meanmm= 0.0059 stddev= 2.728 skewness= 0.167 kurtosis= 1.554 nkurtosis= 0.608																		
	%tile5= 2.833 %tile16= 5.100 %tile25= 5.812 %tile50= 7.083 %tile75= 8.429 %tile84= 10.000 %tile95= 12.750																		
TFC2-0	phi	1.00	1.50	2.00	2.50	3.00	3.50	4.00	4.50	5.00	5.50	6.00	6.50	7.00	7.50	8.00	8.50	9.00	14.00
	cumpercent	0	0	0	1	7	16	26	27	35	51	64	72	78	82	85	87	88	100
	mean= 5.601 meanmm= 0.0206 stddev= 2.460 skewness= 0.256 kurtosis= 1.330 nkurtosis= 0.571																		
	%tile5= 2.833 %tile16= 3.500 %tile25= 3.950 %tile50= 5.469 %tile75= 6.750 %tile84= 7.833 %tile95= 11.917																		
TFC2-40	phi	1.00	1.50	2.00	2.50	3.00	3.50	4.00	4.50	5.00	5.50	6.00	6.50	7.00	7.50	8.00	8.50	9.00	14.00
	cumpercent	1	4	33	43	47	54	62	63	64	67	72	77	82	86	89	91	92	100
	mean= 4.057 meanmm= 0.0601 stddev= 2.804 skewness= 0.547 kurtosis= 0.864 nkurtosis= 0.464																		
	%tile5= 1.517 %tile16= 1.707 %tile25= 1.862 %tile50= 3.214 %tile75= 6.300 %tile84= 7.250 %tile95= 10.875																		
TFC2-92	phi	1.00	1.50	2.00	2.50	3.00	3.50	4.00	4.50	5.00	5.50	6.00	6.50	7.00	7.50	8.00	8.50	9.00	14.00
	cumpercent	0	3	13	24	41	59	67	68	71	74	77	80	83	86	88	89	90	100
	mean= 4.184 meanmm= 0.0550 stddev= 2.758 skewness= 0.612 kurtosis= 1.293 nkurtosis= 0.564																		
	%tile5= 1.600 %tile16= 2.136 %tile25= 2.529 %tile50= 3.250 %tile75= 5.667 %tile84= 7.167 %tile95= 11.500																		
TFC3-0	phi	1.00	1.50	2.00	2.50	3.00	3.50	4.00	4.50	5.00	5.50	6.00	6.50	7.00	7.50	8.00	8.50	9.00	14.00
	cumpercent	0	0	1	2	17	47	64	66	70	74	77	80	82	84	86	87	88	100
	mean= 4.685 meanmm= 0.0389 stddev= 2.545 skewness= 0.757 kurtosis= 1.507 nkurtosis= 0.601																		
	%tile5= 2.600 %tile16= 2.967 %tile25= 3.133 %tile50= 3.588 %tile75= 5.667 %tile84= 7.500 %tile95= 11.917																		
TFC3-40	phi	1.00	1.50	2.00	2.50	3.00	3.50	4.00	4.50	5.00	5.50	6.00	6.50	7.00	7.50	8.00	8.50	9.00	14.00
	cumpercent	0	0	1	3	21	43	61	62	65	68	70	72	75	78	81	84	86	100
	mean= 5.019 meanmm= 0.0309 stddev= 2.873 skewness= 0.734 kurtosis= 1.013 nkurtosis= 0.503																		
	%tile5= 2.556 %tile16= 2.861 %tile25= 3.091 %tile50= 3.694 %tile75= 7.000 %tile84= 8.500 %tile95= 12.214																		
TFC3-80	phi	1.00	1.50	2.00	2.50	3.00	3.50	4.00	4.50	5.00	5.50	6.00	6.50	7.00	7.50	8.00	8.50	9.00	14.00
	cumpercent	0	0	2	6	18	51	62	63	66	69	72	76	80	84	88	90	92	100
	mean= 4.634 meanmm= 0.0403 stddev= 2.434 skewness= 0.745 kurtosis= 1.066 nkurtosis= 0.516																		
	%tile5= 2.375 %tile16= 2.917 %tile25= 3.109 %tile50= 3.485 %tile75= 6.375 %tile84= 7.500 %tile95= 10.875																		

TFC4-0

phi	1.00	1.50	2.00	2.50	3.00	3.50	4.00	4.50	5.00	5.50	6.00	6.50	7.00	7.50	8.00	8.50	9.00	14.00
cumpercent	0	3	14	25	65	89	96	96	96	96	96	96	96	96	96	96	96	100

mean= 2.766 meanmm= 0.1470 stddev= 0.680 skewness= -0.076 kurtosis= 1.353 nkurtosis= 0.575
%tile5= 1.591 %tile16= 2.091 %tile25= 2.500 %tile50= 2.812 %tile75= 3.208 %tile84= 3.396 %tile95= 3.929

TFC4-13

phi	1.00	1.50	2.00	2.50	3.00	3.50	4.00	4.50	5.00	5.50	6.00	6.50	7.00	7.50	8.00	8.50	9.00	14.00
cumpercent	0	1	5	11	60	79	87	87	88	89	90	91	92	93	94	95	96	100

mean= 3.087 meanmm= 0.1177 stddev= 1.300 skewness= 0.587 kurtosis= 3.543 nkurtosis= 0.780
%tile5= 2.000 %tile16= 2.551 %tile25= 2.643 %tile50= 2.898 %tile75= 3.395 %tile84= 3.812 %tile95= 8.500

TFC4-48

phi	1.00	1.50	2.00	2.50	3.00	3.50	4.00	4.50	5.00	5.50	6.00	6.50	7.00	7.50	8.00	8.50	9.00	14.00
cumpercent	1	19	70	88	94	95	95	95	95	95	95	95	95	95	95	96	97	100

mean= 1.870 meanmm= 0.2736 stddev= 0.605 skewness= 0.312 kurtosis= 1.688 nkurtosis= 0.628
%tile5= 1.111 %tile16= 1.417 %tile25= 1.559 %tile50= 1.804 %tile75= 2.139 %tile84= 2.389 %tile95= 3.500

TFC4-85

phi	1.00	1.50	2.00	2.50	3.00	3.50	4.00	4.50	5.00	5.50	6.00	6.50	7.00	7.50	8.00	8.50	9.00	14.00
cumpercent	0	1	22	60	84	91	93	93	93	94	94	94	94	94	94	94	94	100

mean= 2.409 meanmm= 0.1883 stddev= 1.534 skewness= 0.459 kurtosis= 4.368 nkurtosis= 0.814
%tile5= 1.595 %tile16= 1.857 %tile25= 2.039 %tile50= 2.368 %tile75= 2.812 %tile84= 3.000 %tile95= 9.833

Core number and sample depth (cm)

CORE SAMPLES (D23, D25, D41)

D23-200

phi	1.00	1.50	2.00	2.50	3.00	3.50	4.00	4.50	5.00	5.50	6.00	6.50	7.00	7.50	8.00	8.50	9.00	14.00
cumpercent	0	0	0	0	1	3	8	9	11	22	36	48	59	67	73	78	82	100

mean= 7.125 meanmm= 0.0072 stddev= 2.432 skewness= 0.361 kurtosis= 1.409 nkurtosis= 0.585
%tile5= 3.700 %tile16= 5.227 %tile25= 5.607 %tile50= 6.591 %tile75= 8.200 %tile84= 9.556 %tile95= 12.611

D23-300

phi	1.00	1.50	2.00	2.50	3.00	3.50	4.00	4.50	5.00	5.50	6.00	6.50	7.00	7.50	8.00	8.50	9.00	14.00
cumpercent	0	0	0	0	1	5	14	15	19	27	40	50	60	69	76	81	85	100

mean= 6.667 meanmm= 0.0098 stddev= 2.401 skewness= 0.219 kurtosis= 1.418 nkurtosis= 0.586
%tile5= 3.500 %tile16= 4.625 %tile25= 5.375 %tile50= 6.500 %tile75= 7.929 %tile84= 8.875 %tile95= 12.333

D23-400

phi	1.00	1.50	2.00	2.50	3.00	3.50	4.00	4.50	5.00	5.50	6.00	6.50	7.00	7.50	8.00	8.50	9.00	14.00
cumpercent	0	0	0	0	0	1	2	3	8	17	30	41	52	62	69	75	79	100

mean= 7.515 meanmm= 0.0055 stddev= 2.415 skewness= 0.419 kurtosis= 1.234 nkurtosis= 0.552
%tile5= 4.700 %tile16= 5.444 %tile25= 5.808 %tile50= 6.909 %tile75= 8.500 %tile84= 10.190 %tile95= 12.810

D23-500

phi	1.00	1.50	2.00	2.50	3.00	3.50	4.00	4.50	5.00	5.50	6.00	6.50	7.00	7.50	8.00	8.50	9.00	14.00
cumpercent	0	0	0	0	0	0	0	0	0	0	0	0	2	9	21	33	42	100

mean= 10.034 meanmm= 0.0010 stddev= 2.170 skewness= 0.217 kurtosis= 0.708 nkurtosis= 0.415
%tile5= 7.214 %tile16= 7.792 %tile25= 8.167 %tile50= 9.690 %tile75= 11.845 %tile84= 12.621 %tile95= 13.569

D23-600

phi	1.00	1.50	2.00	2.50	3.00	3.50	4.00	4.50	5.00	5.50	6.00	6.50	7.00	7.50	8.00	8.50	9.00	14.00
cumpercent	0	0	0	0	0	0	0	0	0	0	2	8	16	26	36	44	50	100

mean= 9.467 meanmm= 0.0014 stddev= 2.448 skewness= 0.250 kurtosis= 0.734 nkurtosis= 0.423
%tile5= 6.250 %tile16= 7.000 %tile25= 7.450 %tile50= 9.000 %tile75= 11.500 %tile84= 12.400 %tile95= 13.500

D23-700

phi	1.00	1.50	2.00	2.50	3.00	3.50	4.00	4.50	5.00	5.50	6.00	6.50	7.00	7.50	8.00	8.50	9.00	14.00
cumpercent	0	0	0	0	0	1	3	4	5	10	20	32	43	56	64	71	76	100

mean= 7.912 meanmm= 0.0042 stddev= 2.422 skewness= 0.413 kurtosis= 1.212 nkurtosis= 0.548
%tile5= 5.000 %tile16= 5.800 %tile25= 6.208 %tile50= 7.269 %tile75= 8.900 %tile84= 10.667 %tile95= 12.958

D23-800

phi	1.00	1.50	2.00	2.50	3.00	3.50	4.00	4.50	5.00	5.50	6.00	6.50	7.00	7.50	8.00	8.50	9.00	14.00
cumpercent	0	0	0	0	0	0	0	0	0	0	2	5	12	25	38	49	58	100

mean= 9.268 meanmm= 0.0016 stddev= 2.282 skewness= 0.419 kurtosis= 0.803 nkurtosis= 0.445
%tile5= 6.500 %tile16= 7.154 %tile25= 7.500 %tile50= 8.556 %tile75= 11.024 %tile84= 12.095 %tile95= 13.405

D23-900

phi	1.00	1.50	2.00	2.50	3.00	3.50	4.00	4.50	5.00	5.50	6.00	6.50	7.00	7.50	8.00	8.50	9.00	14.00
cumpercent	0	0	0	0	0	0	0	0	0	1	4	9	19	31	42	52	60	100

mean= 9.083 meanmm= 0.0018 stddev= 2.390 skewness= 0.383 kurtosis= 0.822 nkurtosis= 0.451
%tile5= 6.100 %tile16= 6.850 %tile25= 7.250 %tile50= 8.400 %tile75= 10.875 %tile84= 12.000 %tile95= 13.375

D23-1000

phi	1.00	1.50	2.00	2.50	3.00	3.50	4.00	4.50	5.00	5.50	6.00	6.50	7.00	7.50	8.00	8.50	9.00	14.00
cumpercent	0	0	0	0	0	0	0	0	0	1	3	5	11	24	36	47	55	100

mean= 9.367 meanmm= 0.0015 stddev= 2.310 skewness= 0.388 kurtosis= 0.773 nkurtosis= 0.436
%tile5= 6.500 %tile16= 7.192 %tile25= 7.542 %tile50= 8.687 %tile75= 11.222 %tile84= 12.222 %tile95= 13.444

D23-1100	phi	1.00	1.50	2.00	2.50	3.00	3.50	4.00	4.50	5.00	5.50	6.00	6.50	7.00	7.50	8.00	8.50	9.00	14.00
	cumpercent	0	0	0	0	0	0	0	0	0	0	9	11	17	28	40	52	59	100
	mean= 9.127 meanmm= 0.0018 stddev= 2.436 skewness= 0.361 kurtosis= 0.870 nkurtosis= 0.465																		
	%tile5= 5.778 %tile16= 6.917 %tile25= 7.364 %tile50= 8.417 %tile75= 10.951 %tile84= 12.049 %tile95= 13.390																		
D23-1200	phi	1.00	1.50	2.00	2.50	3.00	3.50	4.00	4.50	5.00	5.50	6.00	6.50	7.00	7.50	8.00	8.50	9.00	14.00
	cumpercent	0	0	0	0	0	0	0	0	0	0	1	5	11	22	33	45	52	100
	mean= 9.473 meanmm= 0.0014 stddev= 2.334 skewness= 0.343 kurtosis= 0.761 nkurtosis= 0.432																		
	%tile5= 6.500 %tile16= 7.227 %tile25= 7.636 %tile50= 8.857 %tile75= 11.396 %tile84= 12.333 %tile95= 13.479																		
D23-1300	phi	1.00	1.50	2.00	2.50	3.00	3.50	4.00	4.50	5.00	5.50	6.00	6.50	7.00	7.50	8.00	8.50	9.00	14.00
	cumpercent	0	0	0	0	0	0	0	0	0	1	2	6	16	30	44	57	65	100
	mean= 8.982 meanmm= 0.0020 stddev= 2.226 skewness= 0.470 kurtosis= 0.912 nkurtosis= 0.477																		
	%tile5= 6.375 %tile16= 7.000 %tile25= 7.321 %tile50= 8.231 %tile75= 10.429 %tile84= 11.714 %tile95= 13.286																		
D23-1400	phi	1.00	1.50	2.00	2.50	3.00	3.50	4.00	4.50	5.00	5.50	6.00	6.50	7.00	7.50	8.00	8.50	9.00	14.00
	cumpercent	0	0	0	0	0	0	0	0	0	1	4	10	17	29	41	51	58	100
	mean= 9.158 meanmm= 0.0018 stddev= 2.401 skewness= 0.382 kurtosis= 0.813 nkurtosis= 0.448																		
	%tile5= 6.083 %tile16= 6.929 %tile25= 7.333 %tile50= 8.450 %tile75= 11.024 %tile84= 12.095 %tile95= 13.405																		
D23-1450	phi	1.00	1.50	2.00	2.50	3.00	3.50	4.00	4.50	5.00	5.50	6.00	6.50	7.00	7.50	8.00	8.50	9.00	11.00
	cumpercent	0	0	0	0	0	2	4	4	7	14	23	31	40	51	59	65	70	100
	mean= 8.133 meanmm= 0.0036 stddev= 2.718 skewness= 0.350 kurtosis= 0.939 nkurtosis= 0.484																		
	%tile5= 4.667 %tile16= 5.611 %tile25= 6.125 %tile50= 7.455 %tile75= 9.833 %tile84= 11.333 %tile95= 13.167																		
D23-1475	phi	1.00	1.50	2.00	2.50	3.00	3.50	4.00	4.50	5.00	5.50	6.00	6.50	7.00	7.50	8.00	8.50	9.00	14.00
	cumpercent	0	0	0	0	3	9	17	18	26	41	55	64	72	77	81	84	86	100
	mean= 6.086 meanmm= 0.0147 stddev= 2.511 skewness= 0.294 kurtosis= 1.570 nkurtosis= 0.611																		
	%tile5= 3.167 %tile16= 3.937 %tile25= 4.937 %tile50= 5.821 %tile75= 7.300 %tile84= 8.500 %tile95= 12.214																		
D23-1510	phi	1.00	1.50	2.00	2.50	3.00	3.50	4.00	4.50	5.00	5.50	6.00	6.50	7.00	7.50	8.00	8.50	9.00	14.00
	cumpercent	0	1	4	11	25	39	49	49	49	50	51	52	56	62	68	74	78	100
	mean= 6.181 meanmm= 0.0138 stddev= 3.556 skewness= 0.315 kurtosis= 0.786 nkurtosis= 0.440																		
	%tile5= 2.071 %tile16= 2.679 %tile25= 3.000 %tile50= 5.500 %tile75= 8.625 %tile84= 10.364 %tile95= 12.864																		
D23-1530	phi	1.00	1.50	2.00	2.50	3.00	3.50	4.00	4.50	5.00	5.50	6.00	6.50	7.00	7.50	8.00	8.50	9.00	14.00
	cumpercent	0	2	16	50	74	81	84	84	85	87	89	91	93	94	95	96	96	100
	mean= 2.833 meanmm= 0.1403 stddev= 1.469 skewness= 0.610 kurtosis= 2.790 nkurtosis= 0.736																		
	%tile5= 1.607 %tile16= 2.000 %tile25= 2.132 %tile50= 2.500 %tile75= 3.071 %tile84= 4.000 %tile95= 8.000																		
D23-1850	phi	1.00	1.50	2.00	2.50	3.00	3.50	4.00	4.50	5.00	5.50	6.00	6.50	7.00	7.50	8.00	8.50	9.00	14.00
	cumpercent	0	5	34	60	77	82	84	84	85	87	89	91	92	93	94	95	96	100
	mean= 2.666 meanmm= 0.1576 stddev= 1.638 skewness= 0.617 kurtosis= 2.617 nkurtosis= 0.724																		
	%tile5= 1.500 %tile16= 1.690 %tile25= 1.845 %tile50= 2.308 %tile75= 2.941 %tile84= 4.000 %tile95= 8.500																		

D25-200

phi	1.00	1.50	2.00	2.50	3.00	3.50	4.00	4.50	5.00	5.50	6.00	6.50	7.00	7.50	8.00	8.50	9.00	14.00
cumpercent	0	0	0	0	0	1	2	3	4	5	8	13	20	29	39	48	55	100

mean= 9.193 meanmm= 0.0017 stddev= 2.581 skewness= 0.254 kurtosis= 0.825 nkurtosis= 0.452
%tile5= 5.500 %tile16= 6.714 %tile25= 7.278 %tile50= 8.643 %tile75= 11.222 %tile84= 12.222 %tile95= 13.444

D25-310

phi	1.00	1.50	2.00	2.50	3.00	3.50	4.00	4.50	5.00	5.50	6.00	6.50	7.00	7.50	8.00	8.50	9.00	11.00
cumpercent	0	0	0	0	2	3	5	6	7	8	11	19	30	44	57	67	75	100

mean= 8.281 meanmm= 0.0032 stddev= 2.486 skewness= 0.269 kurtosis= 1.656 nkurtosis= 0.624
%tile5= 4.000 %tile16= 6.312 %tile25= 6.773 %tile50= 7.731 %tile75= 9.000 %tile84= 10.800 %tile95= 13.000

D25-410

phi	1.00	1.50	2.00	2.50	3.00	3.50	4.00	4.50	5.00	5.50	6.00	6.50	7.00	7.50	8.00	8.50	9.00	14.00
cumpercent	0	1	3	7	25	45	55	55	58	62	67	71	76	81	85	88	90	100

mean= 4.792 meanmm= 0.0361 stddev= 2.683 skewness= 0.643 kurtosis= 0.972 nkurtosis= 0.493
%tile5= 2.250 %tile16= 2.750 %tile25= 3.000 %tile50= 3.750 %tile75= 6.900 %tile84= 7.875 %tile95= 11.500

D25-500

phi	1.00	1.50	2.00	2.50	3.00	3.50	4.00	4.50	5.00	5.50	6.00	6.50	7.00	7.50	8.00	8.50	9.00	14.00
cumpercent	0	1	3	8	20	34	46	47	54	65	72	78	82	86	89	91	93	100

mean= 4.933 meanmm= 0.0327 stddev= 2.351 skewness= 0.269 kurtosis= 1.098 nkurtosis= 0.523
%tile5= 2.200 %tile16= 2.833 %tile25= 3.179 %tile50= 4.714 %tile75= 6.250 %tile84= 7.250 %tile95= 10.429

D25-600

phi	1.00	1.50	2.00	2.50	3.00	3.50	4.00	4.50	5.00	5.50	6.00	6.50	7.00	7.50	8.00	8.50	9.00	14.00
cumpercent	0	0	0	2	8	15	22	23	25	30	41	52	62	71	76	81	85	100

mean= 6.285 meanmm= 0.0128 stddev= 2.778 skewness= 0.083 kurtosis= 1.354 nkurtosis= 0.575
%tile5= 2.750 %tile16= 3.571 %tile25= 5.000 %tile50= 6.409 %tile75= 7.900 %tile84= 8.875 %tile95= 12.333

D25-710

phi	1.00	1.50	2.00	2.50	3.00	3.50	4.00	4.50	5.00	5.50	6.00	6.50	7.00	7.50	8.00	8.50	9.00	14.00
cumpercent	0	0	0	3	12	21	26	27	29	36	47	58	66	73	77	81	84	100

mean= 6.120 meanmm= 0.0144 stddev= 2.933 skewness= 0.137 kurtosis= 1.046 nkurtosis= 0.511
%tile5= 2.611 %tile16= 3.222 %tile25= 3.900 %tile50= 6.136 %tile75= 7.750 %tile84= 9.000 %tile95= 12.437

D23-820

phi	1.00	1.50	2.00	2.50	3.00	3.50	4.00	4.50	5.00	5.50	6.00	6.50	7.00	7.50	8.00	8.50	9.00	14.00
cumpercent	0	0	0	1	5	11	16	17	20	29	43	53	61	68	73	77	80	100

mean= 6.783 meanmm= 0.0091 stddev= 2.977 skewness= 0.265 kurtosis= 1.344 nkurtosis= 0.573
%tile5= 3.000 %tile16= 4.000 %tile25= 5.278 %tile50= 6.350 %tile75= 8.250 %tile84= 10.000 %tile95= 12.750

D25-910

phi	1.00	1.50	2.00	2.50	3.00	3.50	4.00	4.50	5.00	5.50	6.00	6.50	7.00	7.50	8.00	8.50	9.00	14.00
cumpercent	0	0	0	3	8	13	23	24	29	44	53	62	67	72	75	78	80	100

mean= 6.494 meanmm= 0.0111 stddev= 3.110 skewness= 0.344 kurtosis= 1.211 nkurtosis= 0.548
%tile5= 2.700 %tile16= 3.650 %tile25= 4.600 %tile50= 5.833 %tile75= 8.000 %tile84= 10.000 %tile95= 12.750

D25-1020	phi	1.00	1.50	2.00	2.50	3.00	3.50	4.00	4.50	5.00	5.50	6.00	6.50	7.00	7.50	8.00	8.50	9.00	14.00
	cumpercent	0	0	3	22	42	51	61	61	64	67	71	75	79	82	84	86	88	100

mean= 4.596 meanmm= 0.0414 stddev= 2.909 skewness= 0.664 kurtosis= 1.030 nkurtosis= 0.507
%tile5= 2.053 %tile16= 2.342 %tile25= 2.575 %tile50= 3.444 %tile75= 6.500 %tile84= 8.000 %tile95= 11.917

D25-1130	phi	1.00	1.50	2.00	2.50	3.00	3.50	4.00	4.50	5.00	5.50	6.00	6.50	7.00	7.50	8.00	8.50	9.00	14.00
	cumpercent	0	0	5	28	38	49	58	59	64	71	76	80	83	85	87	89	91	100

mean= 4.348 meanmm= 0.0491 stddev= 2.650 skewness= 0.569 kurtosis= 1.091 nkurtosis= 0.522
%tile5= 2.000 %tile16= 2.239 %tile25= 2.435 %tile50= 3.556 %tile75= 5.900 %tile84= 7.250 %tile95= 11.222

D25-1200	phi	1.00	1.50	2.00	2.50	3.00	3.50	4.00	4.50	5.00	5.50	6.00	6.50	7.00	7.50	8.00	8.50	9.00	14.00
	cumpercent	0	1	16	61	77	83	88	88	89	91	93	94	95	96	97	98	99	100

mean= 2.659 meanmm= 0.1583 stddev= 1.213 skewness= 0.625 kurtosis= 2.626 nkurtosis= 0.724
%tile5= 1.633 %tile16= 2.000 %tile25= 2.100 %tile50= 2.378 %tile75= 2.937 %tile84= 3.600 %tile95= 7.000

D25-1300	phi	1.00	1.50	2.00	2.50	3.00	3.50	4.00	4.50	5.00	5.50	6.00	6.50	7.00	7.50	8.00	8.50	9.00	14.00
	cumpercent	0	1	30	66	83	88	91	91	92	93	94	95	96	97	98	98	98	100

mean= 2.379 meanmm= 0.1923 stddev= 1.082 skewness= 0.469 kurtosis= 2.375 nkurtosis= 0.704
%tile5= 1.569 %tile16= 1.759 %tile25= 1.914 %tile50= 2.278 %tile75= 2.765 %tile84= 3.100 %tile95= 6.500

D25-1450	phi	1.00	1.50	2.00	2.50	3.00	3.50	4.00	4.50	5.00	5.50	6.00	6.50	7.00	7.50	8.00	8.50	9.00	14.00
	cumpercent	0	10	63	88	96	97	98	98	98	98	98	98	98	98	98	98	98	100

mean= 1.951 meanmm= 0.2586 stddev= 0.472 skewness= 0.257 kurtosis= 1.156 nkurtosis= 0.536
%tile5= 1.250 %tile16= 1.557 %tile25= 1.642 %tile50= 1.877 %tile75= 2.240 %tile84= 2.420 %tile95= 2.937

D25-2100	phi	1.00	1.50	2.00	2.50	3.00	3.50	4.00	4.50	5.00	5.50	6.00	6.50	7.00	7.50	8.00	8.50	9.00	14.00
	cumpercent	52	88	92	93	94	94	94	94	94	95	96	97	97	97	97	97	97	100

mean= 0.905 meanmm= 0.5342 stddev= 1.103 skewness= 0.265 kurtosis= 2.641 nkurtosis= 0.725
%tile5= 0.096 %tile16= 0.308 %tile25= 0.481 %tile50= 0.962 %tile75= 1.319 %tile84= 1.444 %tile95= 5.500

D41-50	phi	1.00	1.50	2.00	2.50	3.00	3.50	4.00	4.50	5.00	5.50	6.00	6.50	7.00	7.50	8.00	8.50	9.00	14.00
	cumpercent	0	0	0	0	0	3	7	8	14	22	31	41	52	62	71	76	80	100

mean= 7.345 meanmm= 0.0062 stddev= 2.582 skewness= 0.283 kurtosis= 1.349 nkurtosis= 0.574
%tile5= 3.750 %tile16= 5.125 %tile25= 5.667 %tile50= 6.909 %tile75= 8.400 %tile84= 10.000 %tile95= 12.750

D41-100	phi	1.00	1.50	2.00	2.50	3.00	3.50	4.00	4.50	5.00	5.50	6.00	6.50	7.00	7.50	8.00	8.50	9.00	14.00
	cumpercent	0	0	0	1	2	4	8	9	16	24	32	40	49	59	68	74	78	100

mean= 7.471 meanmm= 0.0056 stddev= 2.741 skewness= 0.247 kurtosis= 1.236 nkurtosis= 0.553
%tile5= 3.625 %tile16= 5.000 %tile25= 5.562 %tile50= 7.050 %tile75= 8.625 %tile84= 10.364 %tile95= 12.864

D41-150	phi	1.00	1.50	2.00	2.50	3.00	3.50	4.00	4.50	5.00	5.50	6.00	6.50	7.00	7.50	8.00	8.50	9.00	14.00
	cumpercent	0	0	0	0	2	6	10	11	17	25	34	43	53	62	71	77	81	100

mean= 7.185 meanmm= 0.0069 stddev= 2.629 skewness= 0.230 kurtosis= 1.347 nkurtosis= 0.574
%tile5= 3.375 %tile16= 4.917 %tile25= 5.500 %tile50= 6.850 %tile75= 8.333 %tile84= 9.789 %tile95= 12.684

D41-200	phi	1.00	1.50	2.00	2.50	3.00	3.50	4.00	4.50	5.00	5.50	6.00	6.50	7.00	7.50	8.00	8.50	9.00	14.00
	cumpercent	0	4	23	34	38	43	49	50	52	55	61	68	75	81	85	88	90	100

mean= 4.730 meanmm= 0.0377 stddev= 3.026 skewness= 0.259 kurtosis= 0.833 nkurtosis= 0.454
%tile5= 1.526 %tile16= 1.816 %tile25= 2.091 %tile50= 4.500 %tile75= 7.000 %tile84= 7.875 %tile95= 11.500

D41-250	phi	1.00	1.50	2.00	2.50	3.00	3.50	4.00	4.50	5.00	5.50	6.00	6.50	7.00	7.50	8.00	8.50	9.00	14.00
	cumpercent	2	16	52	79	85	89	92	92	93	94	95	95	95	96	97	97	97	100

mean= 2.130 meanmm= 0.2285 stddev= 1.096 skewness= 0.490 kurtosis= 2.504 nkurtosis= 0.715
%tile5= 1.107 %tile16= 1.500 %tile25= 1.625 %tile50= 1.972 %tile75= 2.426 %tile84= 2.917 %tile95= 6.000

D41-300	phi	1.00	1.50	2.00	2.50	3.00	3.50	4.00	4.50	5.00	5.50	6.00	6.50	7.00	7.50	8.00	8.50	9.00	14.00
	cumpercent	1	14	46	83	88	92	95	95	95	95	95	95	95	95	95	95	95	100

mean= 2.062 meanmm= 0.2395 stddev= 0.698 skewness= 0.195 kurtosis= 1.620 nkurtosis= 0.618
%tile5= 1.154 %tile16= 1.531 %tile25= 1.672 %tile50= 2.054 %tile75= 2.392 %tile84= 2.600 %tile95= 4.000

D41-350	phi	1.00	1.50	2.00	2.50	3.00	3.50	4.00	4.50	5.00	5.50	6.00	6.50	7.00	7.50	8.00	8.50	9.00	14.00
	cumpercent	1	15	50	73	80	87	92	92	93	94	94	95	96	97	97	97	97	100

mean= 2.267 meanmm= 0.2078 stddev= 1.255 skewness= 0.566 kurtosis= 2.196 nkurtosis= 0.687
%tile5= 1.143 %tile16= 1.514 %tile25= 1.643 %tile50= 2.000 %tile75= 2.643 %tile84= 3.286 %tile95= 6.500

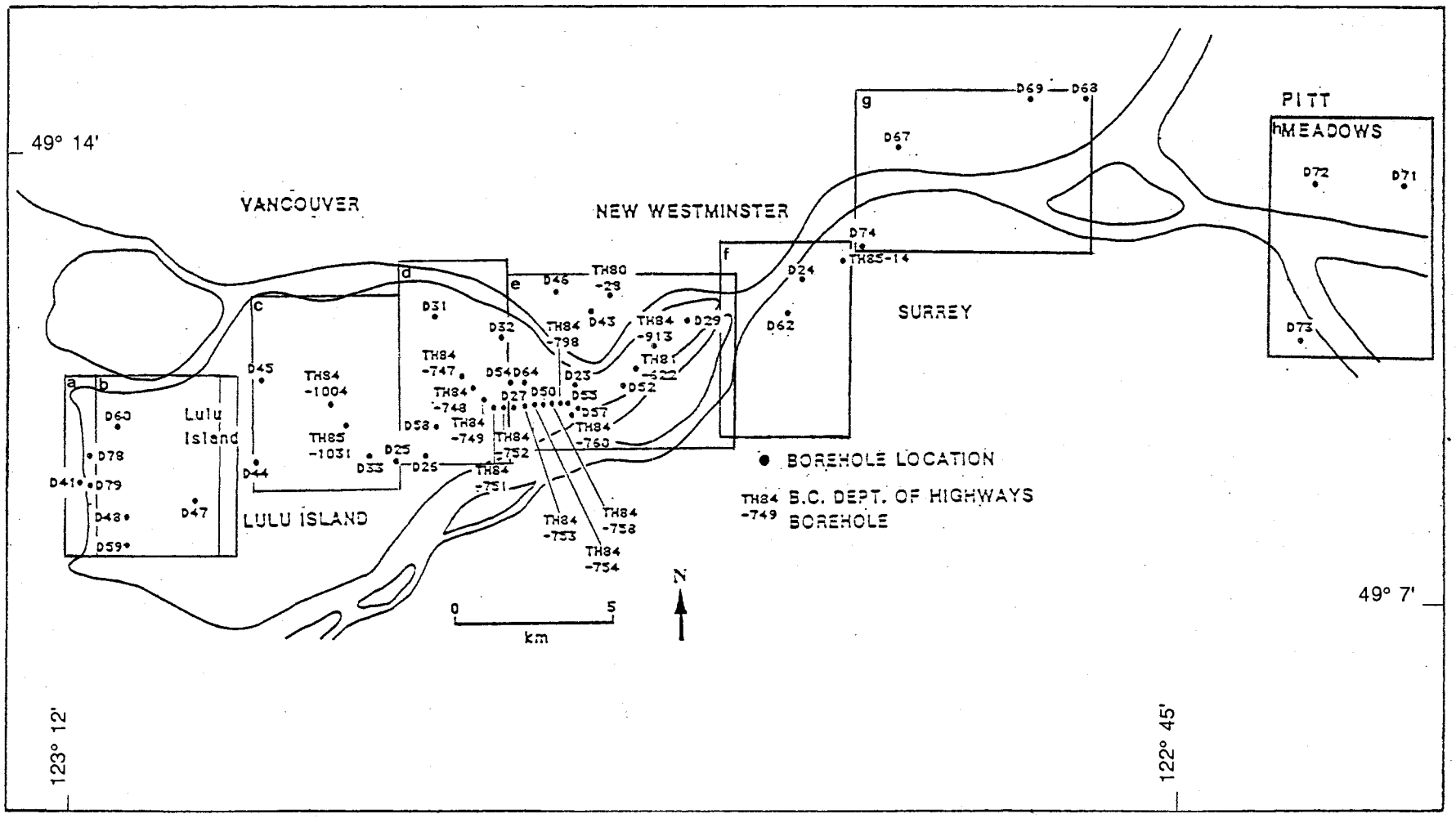

APPENDIX 2: PRECISE SITE LOCATIONS AND ELEVATIONS

Site locations are indicated on reproductions of 1: 25 000 topographic map sheets. Elevations from benchmark levelling are given in metres (ca. = estimated elevation).

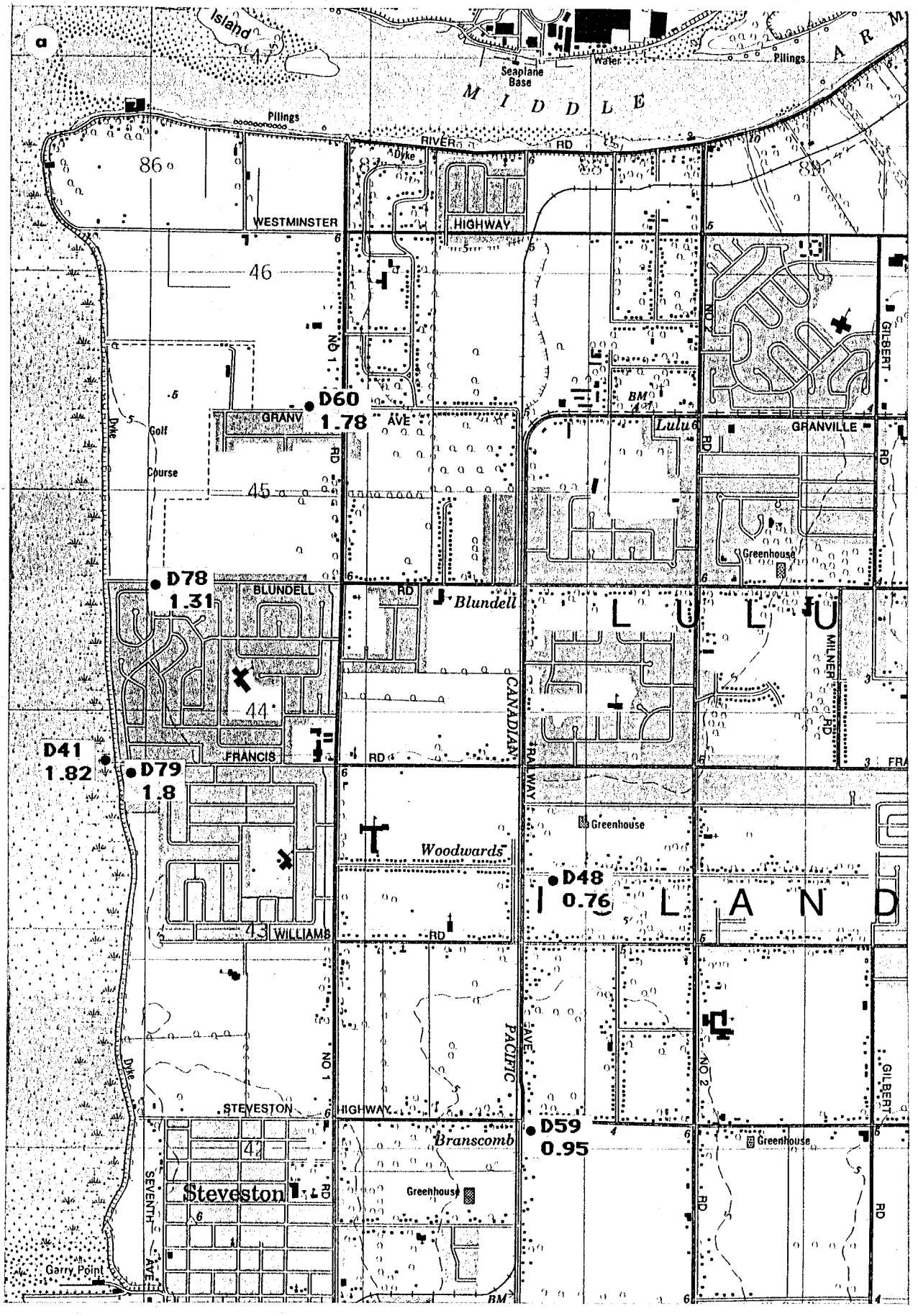
a
Island
Seaplane Base
Water
Pilings
M I D D L E A R M
Pilings
RIVER RD
Dyke
86
87
88
89
WESTMINSTER
HIGHWAY
46
NO 1
NO 2
GILBERT
D60
1.78
GRANV AVE
Golf Course
Dyke
BM
Lulu
GRANVILLE
RD
45
Greenhouse
D78
1.31
BLUNDELL
Blundell
L U L U
MILNER
44
CANADIAN
RAILWAY
D41
1.82
D79
1.8
FRANCIS
Greenhouse
Woodwards
D48
0.76
I S L A N D
43
WILLIAMS
PACIFIC
AVE
STEVESTON
HIGHWAY
D59
0.95
Branscomb
Greenhouse
42
Steveston
SEVENTH AVE
Garry Point
BM

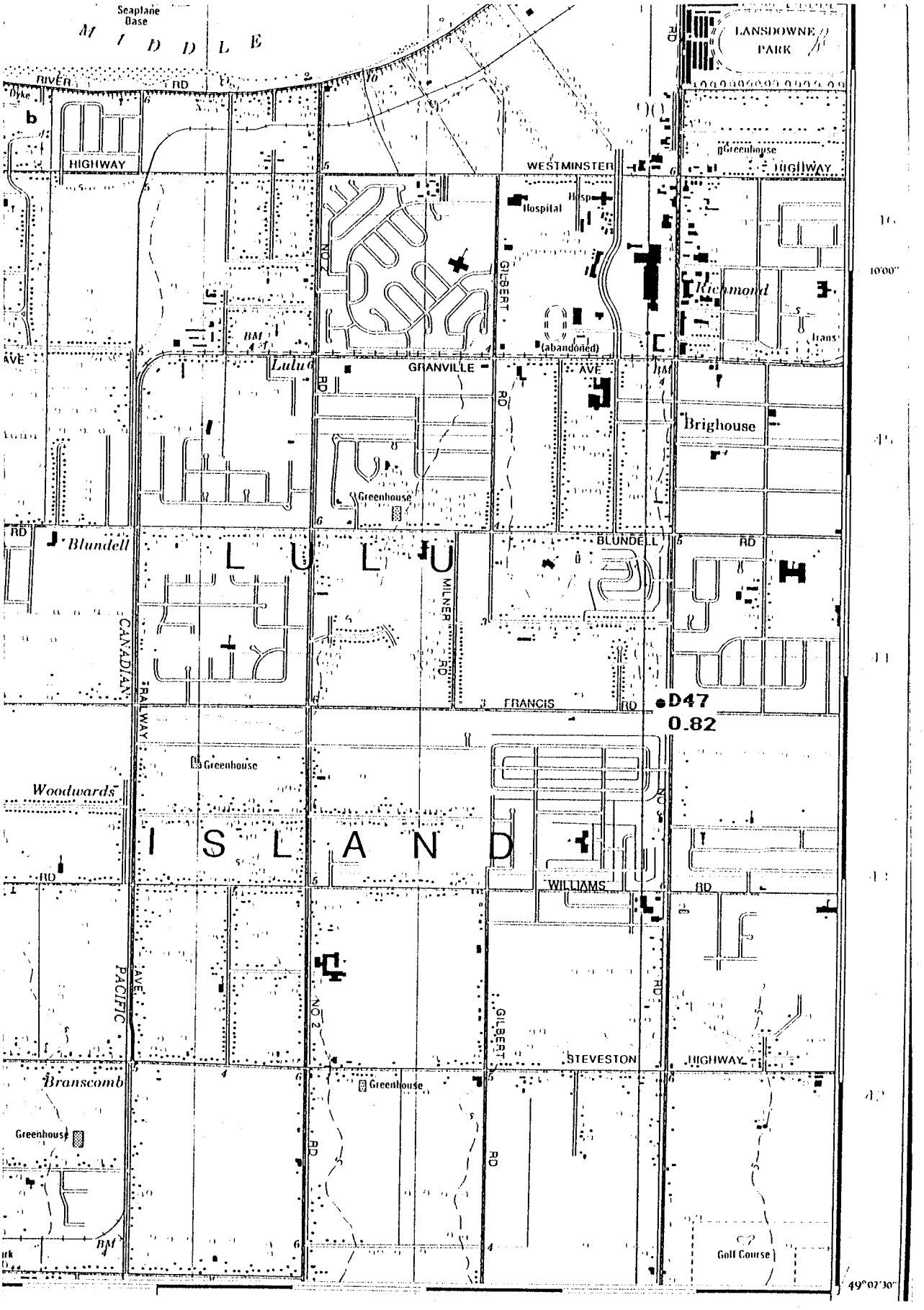
Seaplane Base
MIDDLE
RIVER RD
HIGHWAY
WESTMINSTER
LANSDOWNE PARK
Greenhouse
Hospital
NO 2
GILBERT
Richmond
(abandoned)
GRANVILLE AVE
Lulu
Brighouse
Blundell
LULU
ISLAND
MILNER RD
CANADIAN RAILWAY
BLUNDELL RD
FRANCIS RD
D47
0.82
Woodwards
WILLIAMS RD
PACIFIC AVE
STEVESTON HIGHWAY
Branscomb
Golf Course
49°07'30"

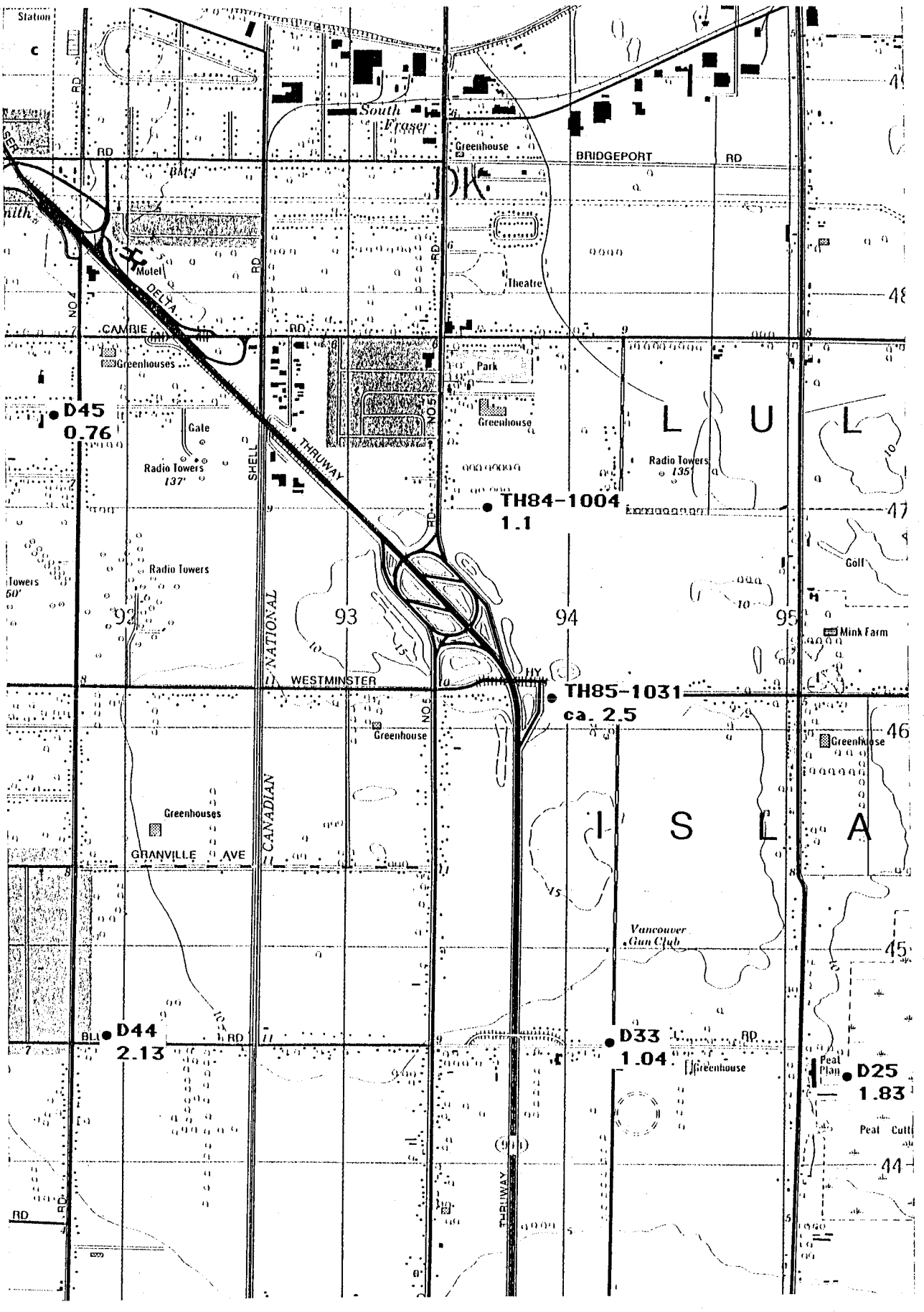
Station
South Fraser
Greenhouse
BRIDGEPORT RD
Motel
DELTA
CAMBIE RD
Greenhouses
Theatre
Park
Greenhouse
D45
0.76
Gate
Radio Towers
137'
SHELL
THRUWAY
TH84-1004
1.1
Radio Towers
135'
L U L
Golf
Mink Farm
Radio Towers
93
94
95
NATIONAL
WESTMINSTER HY
TH85-1031
ca. 2.5
Greenhouse
Greenhouses
GRANVILLE AVE
CANADIAN
I S L A
Vancouver Gun Club
D44
2.13
D33
1.04
Greenhouse
D25
1.83
Peat Plan
Peat Cutt
RD
THRUWAY

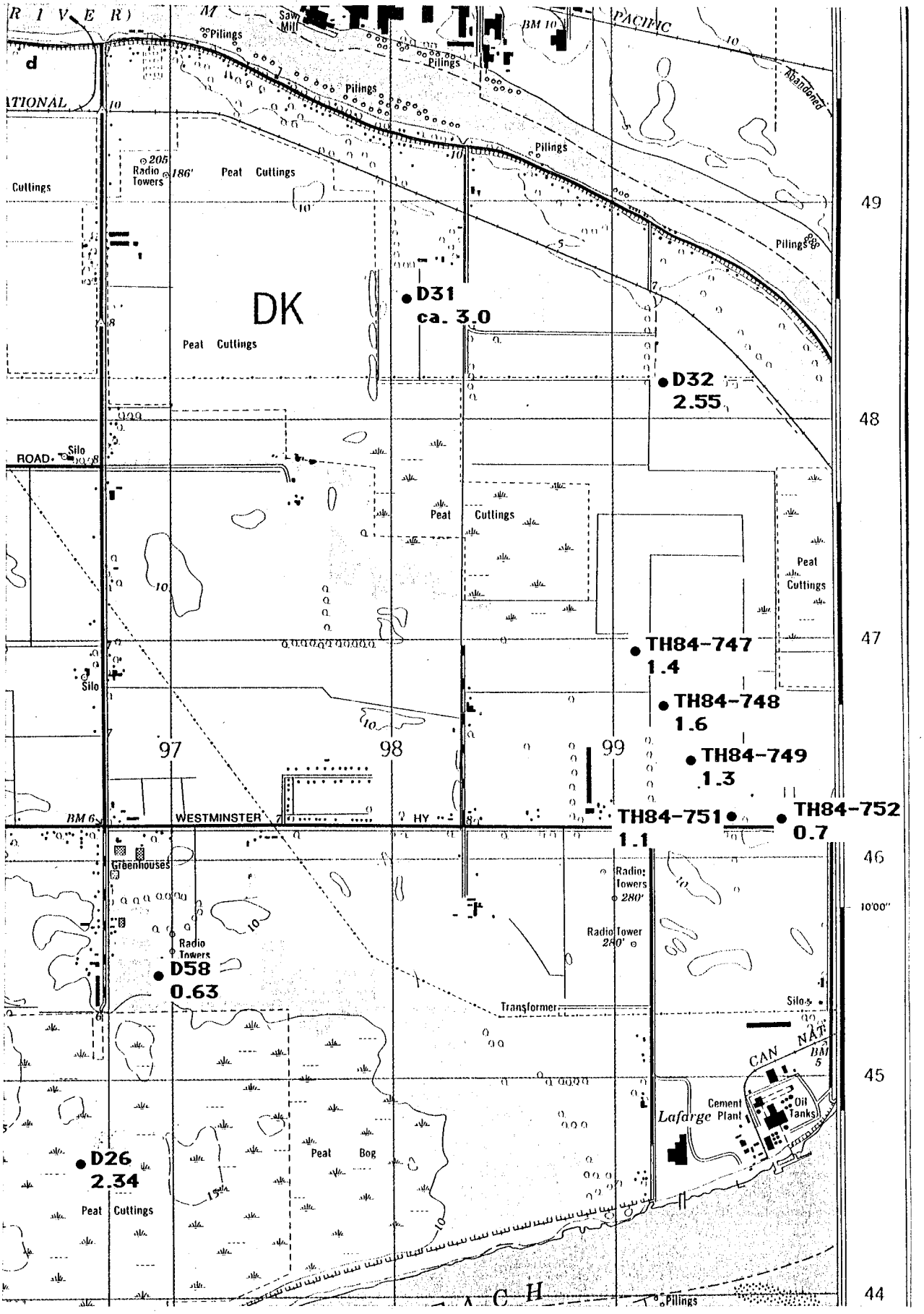
Sawmill
Pilings
BM 10
PACIFIC
Abandoned
Radio Towers
186'
Peat
Cuttings
DK
D31
ca. 3.0
D32
2.55
Silo
ROAD
TH84-747
1.4
TH84-748
1.6
TH84-749
1.3
TH84-751
1.1
TH84-752
0.7
97
98
99
BM 6
WESTMINSTER
HY
Greenhouses
Radio Towers
280'
Radio Tower
280'
D58
0.63
Transformer
CAN NAT
BM 5
Cement Plant
Lafarge
Oil Tanks
D26
2.34
Bog
C H
49
48
47
46
45
44
10'00"

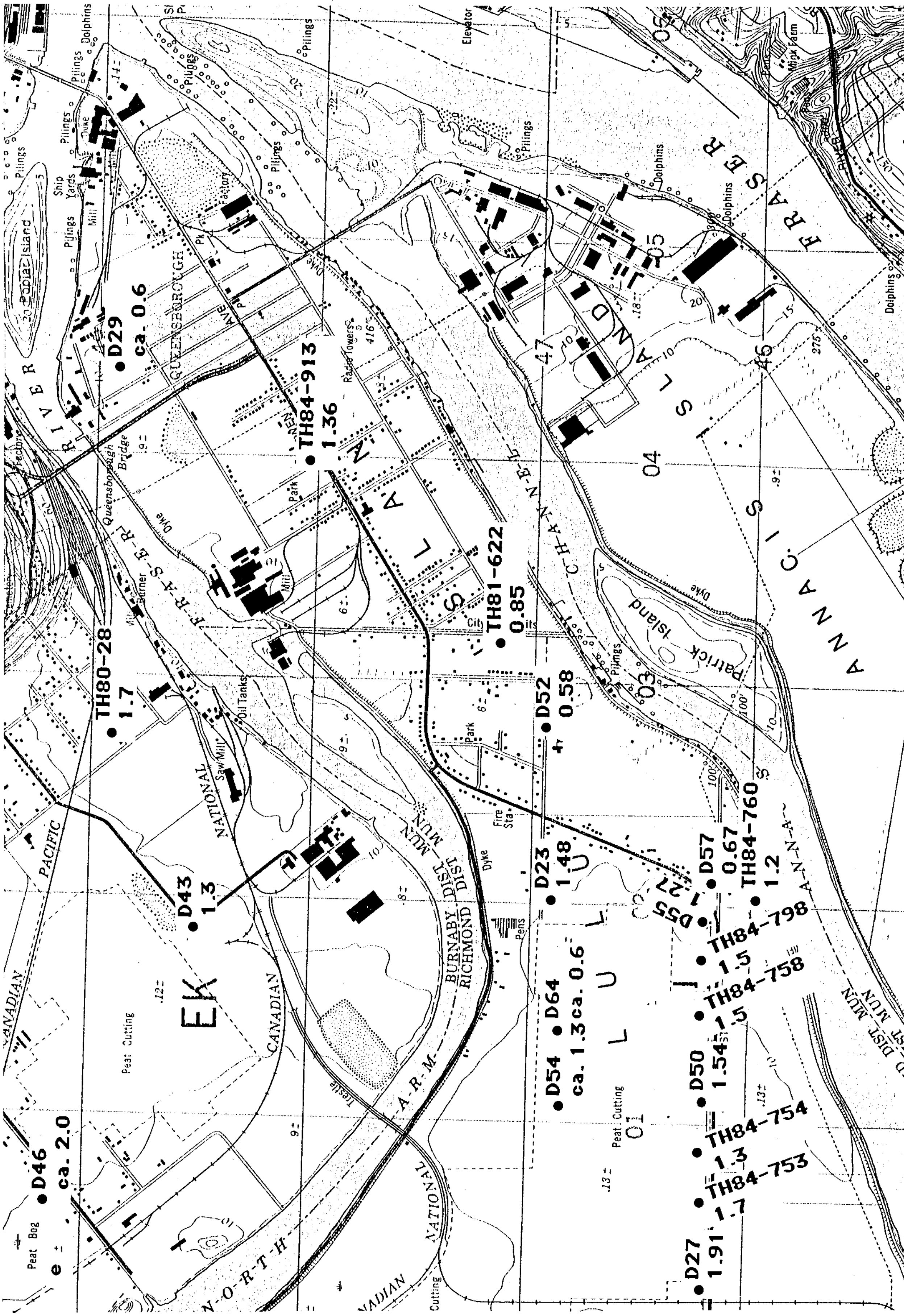
D29
ca. 0.6
TH84-913
1.36
TH81-622
0.85
TH80-28
1.7
D52
0.58
D43
1.3
D23
1.48
D57
0.67
TH84-760
1.2
D55
1.27
TH84-798
1.5
TH84-758
1.5
D54
ca. 1.3
D64
ca. 0.6
D50
1.54
TH84-754
1.3
TH84-753
1.7
D27
1.91
D46
ca. 2.0
FRASER RIVER
ANNACIS ISLAND
ANNACIS CHANNEL
LULU ISLAND
Queensborough Bridge
QUEENSBOROUGH
Patrick Island
Poplar Island
Peat Cutting
Peat Bog
NORTH ARM
BURNABY DIST MUN
RICHMOND DIST MUN
CANADIAN NATIONAL
CANADIAN PACIFIC
Dolphins
Pilings
Dyke
Oil Tanks
Saw Mill
Mill
Fire Sta
Radio Towers
Trestle
Ship Yards
Elevator

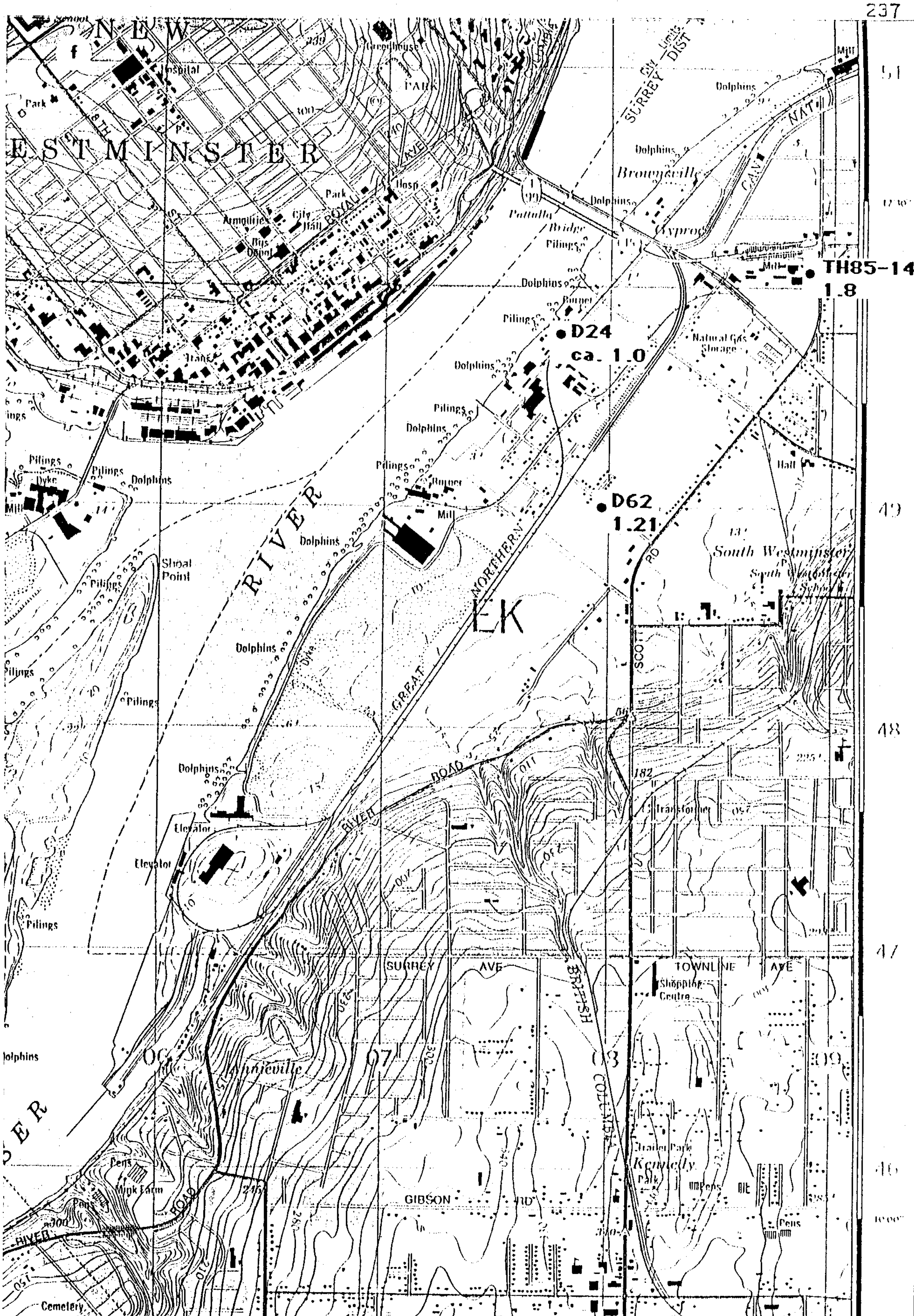
NEW
ESTMINSTER
Hospital
Park
Greenhouse
PARK
SURREY DIST
City Limits
Mill
Dolphins
Brownsville
CAN NAT
Armouries
City Hall
Bus Depot
Hosp
Park
Pattullo Bridge
Pilings
Gyproc
TH85-14
1.8
Burner
D24
ca. 1.0
Natural Gas Storage
Dolphins
Pilings
Dyke
Mill
RIVER
D62
1.21
Hall
Shoal Point
South Westminster
South Westminster School
GREAT NORTHERN
EK
SCOTT RD
Dyke
RIVER ROAD
Transformer
Elevator
SURREY AVE
TOWNLINE AVE
BRITISH COLUMBIA
Shopping Centre
Annieville
Trailer Park
Kennedy
Park
Pens
Mink Farm
GIBSON RD
ROAD
RIVER
Cemetery
47
48
49
51
46

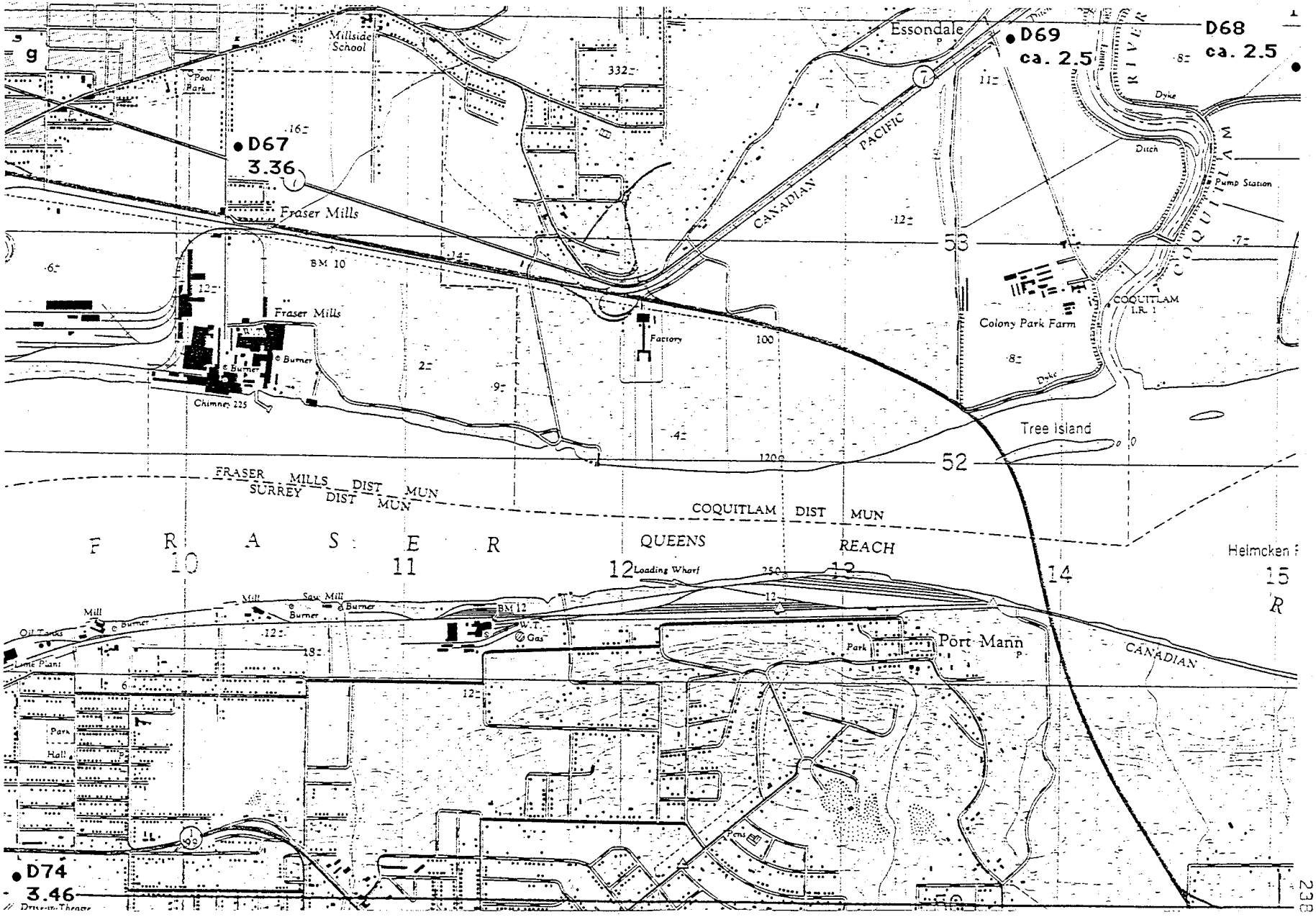
D67
3.36
D69
ca. 2.5
D68
ca. 2.5
D74
3.46
Millside School
Pool
Park
Fraser Mills
BM 10
Chimney 235
Burner
Factory
CANADIAN PACIFIC
Essondale
Dyke
Ditch
Pump Station
COQUITLAM RIVER
Colony Park Farm
COQUITLAM I.R. 1
Tree Island
FRASER MILLS DIST MUN
SURREY DIST MUN
COQUITLAM DIST MUN
F R A S E R
QUEENS REACH
10
11
12
13
14
15
Loading Wharf
Saw Mill
Mill
Oil Tanks
Lime Plant
BM 12
W.T.
Gas
Port Mann
Park
Hall
CANADIAN
Helmcken

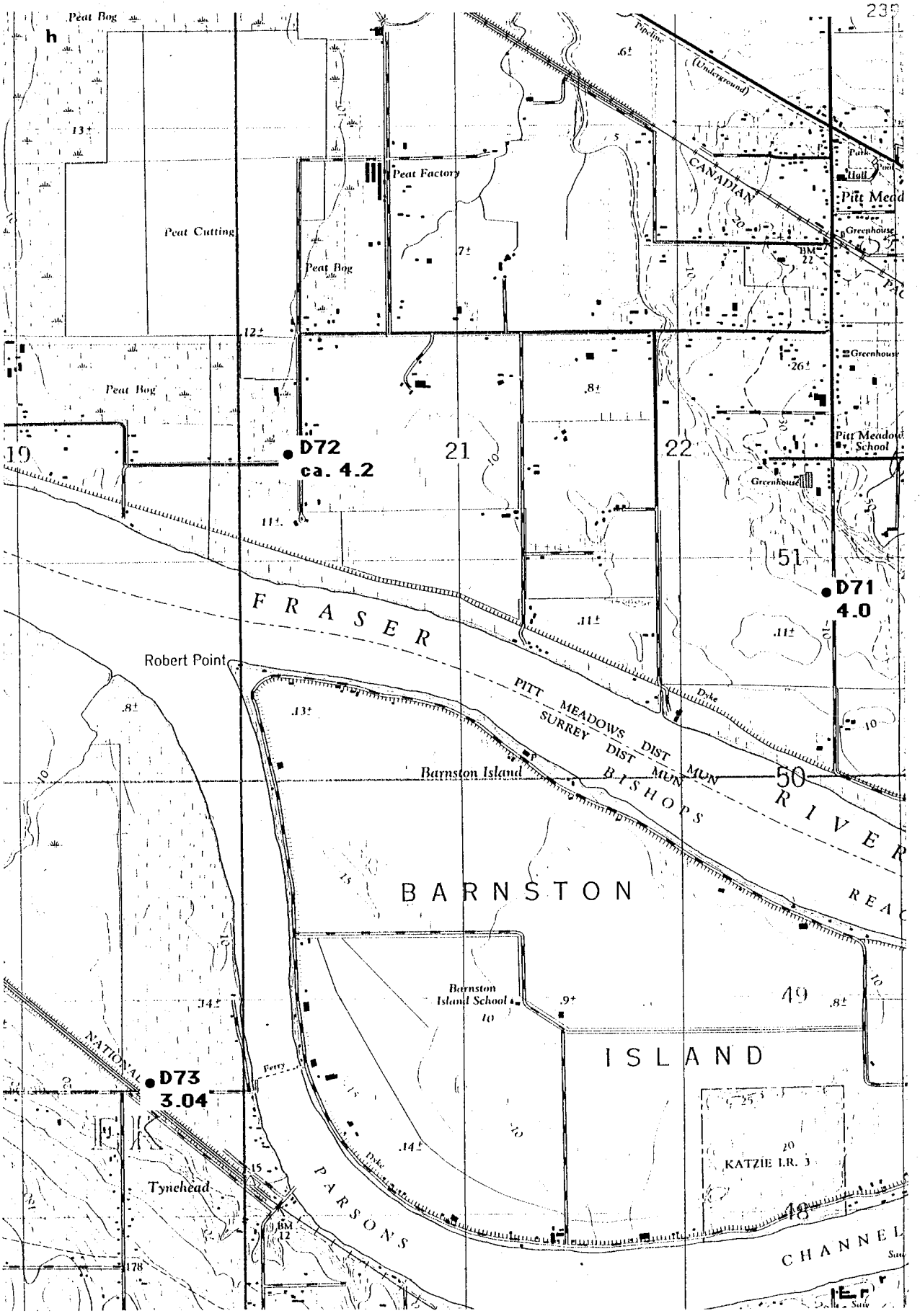
Peat Bog
Peat Factory
Peat Cutting
Peat Bog
Peat Bog
Pipeline
(Underground)
CANADIAN
Pitt Mead
Greenhouse
Greenhouse
Greenhouse
Pitt Meadow
School
D72
ca. 4.2
D71
4.0
19
21
22
51
50
FRASER
Robert Point
PITT MEADOWS DIST MUN
SURREY DIST MUN
BISHOPS
RIVER
Barnston Island
BARNSTON
ISLAND
Barnston
Island School
49
NATIONAL
D73
3.04
Ferry
Tynehead
PARSONS
KATZIE I.R. 3
CHANNEL
Dyke
Dyke

APPENDIX 3

VOLUME CALCULATIONS: FRASER DELTA

Example:

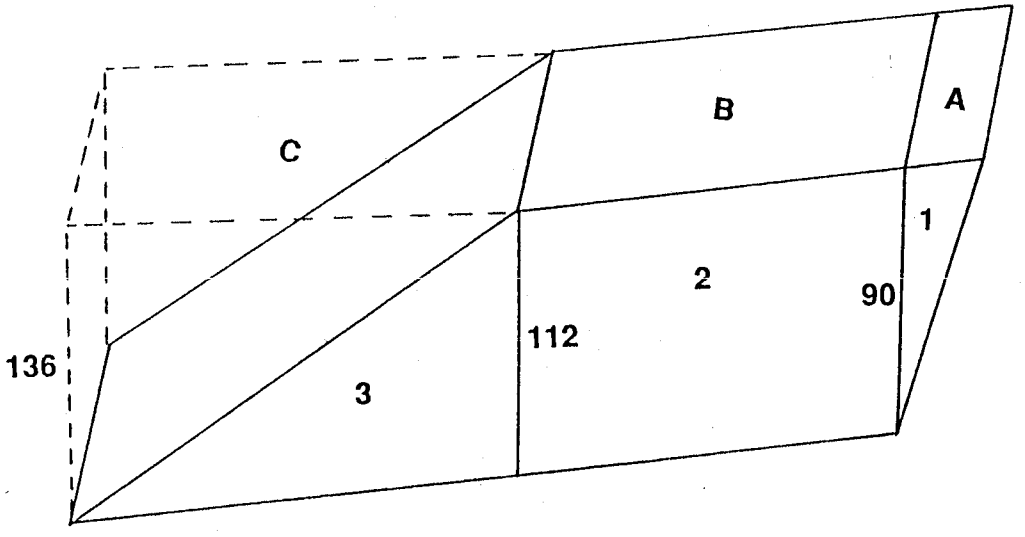

Volume 1= Area A x 90/2
Volume 2= Area B x (90+112)/2
Volume 3= Area C x (112+136)/2 - 1/2(Area C x 136)
Total volume= Volume 1 + Volume 2 + Volume 3

Note: no further growth assumed for Boundary Bay after 2250 yr BP, depth of Boundary Bay foreslope deposits estimated at 192 m. All depths and distances shown on diagrams are in metres

9000 yr BP

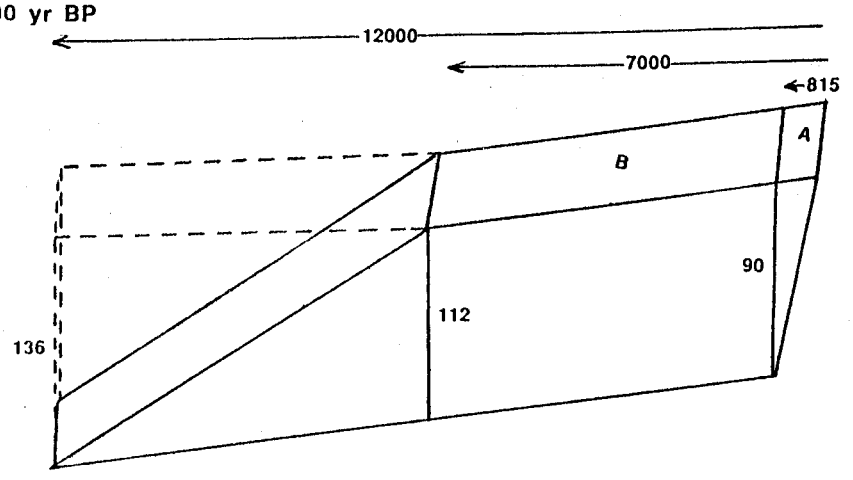

ENVIRONMENT	AREA (m^2)	MEAN DEPTH (m)	VOLUME (m^3)
TIDAL FLATS (A)	1.324×10^6	45	6×10^7
TIDAL FLATS (B)	2.675×10^7	101	2.7×10^9
FORESLOPE	7.125×10^7	124	3.99×10^9

TOTAL VOL: 6.75×10^9

9000-8000 yr BP

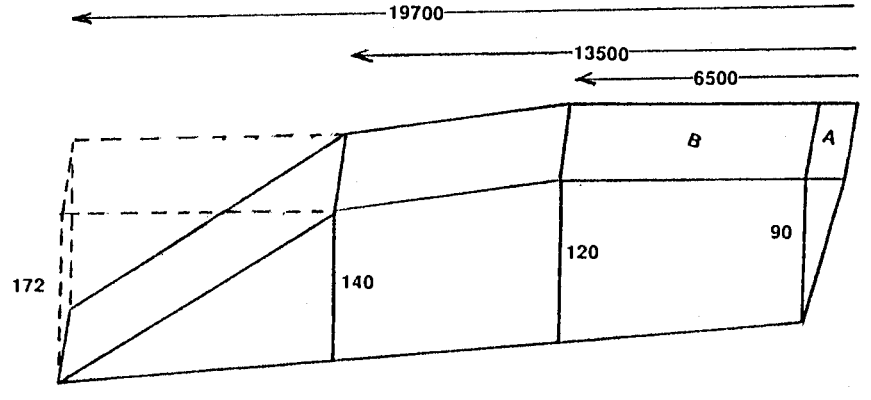

ENVIRONMENT	AREA (m^2)	MEAN DEPTH (m)	VOLUME (m^3)
TERRESTRIAL (A)	1.324×10^6	45	6×10^7
TERRESTRIAL (B)	2.2×10^7	105	2.31×10^9
TIDAL FLATS	9.8×10^7	130	1.274×10^{10}
FORESLOPE	1.674×10^8	156	1.1718×10^{10}

TOTAL VOL: 2.6828×10^{10}

Volume added, 9000-8000 yr Bp: 2.0078×10^{10}

8000-6800 yr BP

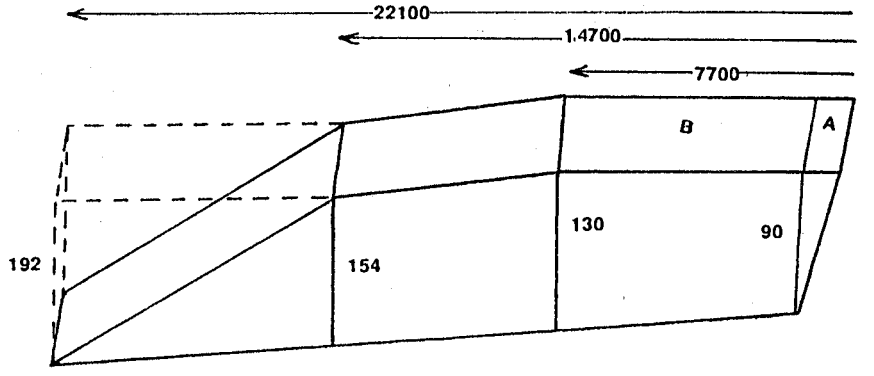

ENVIRONMENT	AREA (m^2)	MEAN DEPTH (m)	VOLUME (m^3)
TERRESTRIAL (A)	1.32×10^6	45	6×10^7
TERRESTRIAL (B)	3.45×10^7	110	3.795×10^9
TIDAL FLATS	1.4×10^8	142	1.988×10^{10}
FORESLOPE	2.886×10^8	173	2.2222×10^{10}

TOTAL VOL: 4.59572×10^{10}

Volume added, 8000-6800 yr BP: 1.91292×10^{10}

6800-6200 yr BP

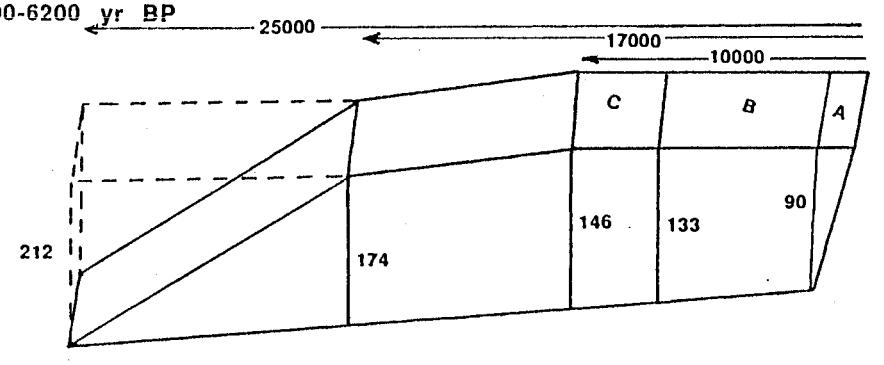

ENVIRONMENT	AREA (m^2)	MEAN DEPTH (m)	VOLUME (m^3)
TERRESTRIAL (A)	1.324×10^6	45	6×10^7
TERRESTRIAL (B)	3.45×10^7	111.5	3.84675×10^9
TERRESTRIAL (C)	2.875×10^7	139.5	4.010625×10^9
TIDAL FLATS	1.671×10^8	160	2.6736×10^{10}
FORESLOPE	3.053×10^8	193	2.65611×10^{10}

TOTAL VOL: 6.1214475×10^{10}

Volume added, 6800-6200 yr BP: 1.5257275×10^{10}

6200-5800 yr BP

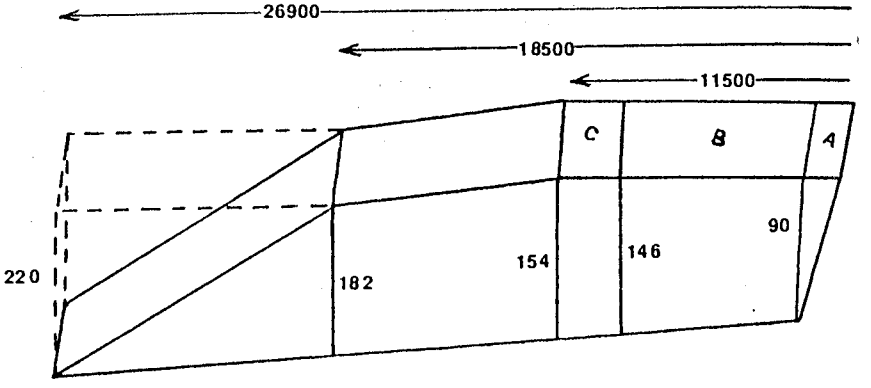

ENVIRONMENT	AREA (m^2)	MEAN DEPTH (m)	VOLUME (m^3)
TERRESTRIAL (A)	1.324×10^6	45	6×10^7
TERRESTRIAL (B)	6.25×10^7	118	7.375×10^9
TERRESTRIAL (C)	2.475×10^7	150	3.7125×10^9
TIDAL FLATS	1.8485×10^8	168	3.10548×10^{10}
FORESLOPE	3.5135×10^8	201	3.197285×10^{10}

TOTAL VOL: 7.417515×10^{10}

Volume added, 6200-5800 yr BP: 1.2960675×10^{10}

5800-4500 yr BP

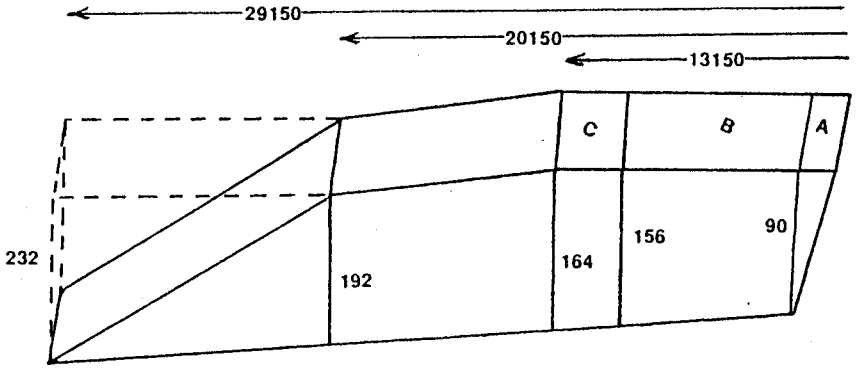

ENVIRONMENT	AREA (m^2)	MEAN DEPTH (m)	VOLUME (m^3)
TERRESTRIAL (A)	1.324×10^6	45	6×10^7
TERRESTRIAL (B)	8.725×10^7	123	1.073175×10^{10}
TERRESTRIAL (C)	3.365×10^7	160	5.384×10^9
TIDAL FLATS	2.0835×10^8	178	3.70863×10^{10}
FORESLOPE	4.0685×10^8	212	3.90576×10^{10}

TOTAL VOL: 9.231965×10^{10}

Volume added, 5800-4500 yr BP: 1.81445×10^{10}

4500-2250 yr BP

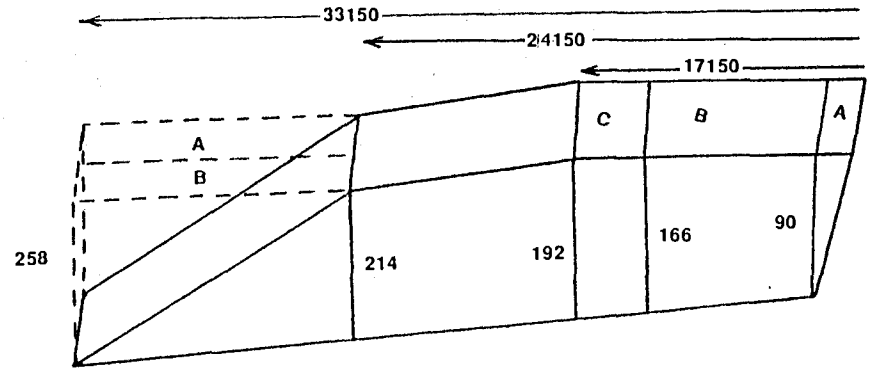

ENVIRONMENT	AREA (m^2)	MEAN DEPTH (m)	VOLUME (m^3)
TERRESTRIAL (A)	1.324×10^6	45	6×10^7
TERRESTRIAL (B)	1.209×10^8	128	1.54752×10^{10}
TERRESTRIAL (C)	1.2575×10^8	179	2.250925×10^{10}
TIDAL FLATS	2.29075×10^8	203	4.4857925×10^{10}
FORESLOPE (A)	3.24×10^8	236	3.4668×10^{10}
FORESLOPE (B) (Boundary Bay)	1.53×10^8	192	1.1628×10^{10}

TOTAL VOL: 1.2919838×10^{11}

Volume added, 4500-2250 yr BP: 3.687873×10^{10}

2250-Present

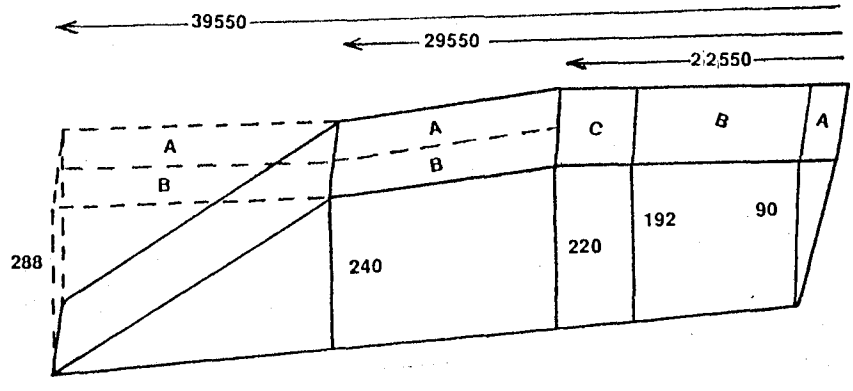

ENVIRONMENT	AREA (m^2)	MEAN DEPTH (m)	VOLUME (m^3)
TERRESTRIAL (A)	1.324×10^6	45	6×10^7
TERRESTRIAL (B)	2.4665×10^8	141	3.477765×10^{10}
TERRESTRIAL (C)	1.098×10^8	206	2.26188×10^{10}
TIDAL FLATS (A)	1.66×10^8	230	3.818×10^{10}
TIDAL FLATS (B)	6.8075×10^7	203	1.3819225×10^{10}
FORESLOPE (A)	3.5×10^8	240	4.2×10^{10}
FORESLOPE (B)	1.53×10^8	192	1.1628×10^{10}

TOTAL VOL: 1.6308368×10^{11}

Volume added, 2250-Present: 3.3885295×10^{10}

VOLUME CALCULATIONS: FRASER RIVER FLOODPLAIN

ESTIMATED GEOMETRY OF AGGRADATIONAL SEDIMENT WEDGE

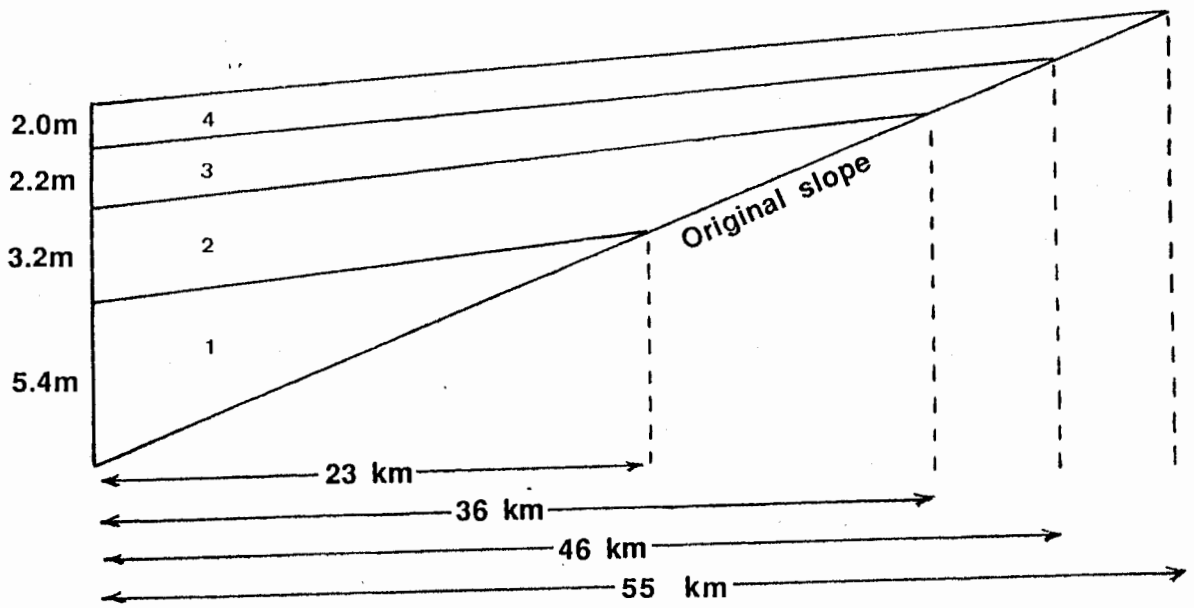

FLOODPLAIN AGGRADATION VOLUMES

PERIOD (yr BP)	DEPTH OF AGGRADATION (m)	AREA AGGRADED (m)	AGGRADATION VOLUME (m)
8000-6800	5.4	1.828X10	4.9356x10
6800-6200	3.2	2.1249x10	6.32464x10
5800-4500	2.2	2.46865x10	5.05703x10
4500-2250	2.0	3.1249x10	5.59355x10

Note: volume of segment 1 = 0.5 x 5.4 x $area_1$
volume of segment 2 = (3.2 x $area_1$) +
((0.5 x 3.2 x ($area_2$ - $area_1$))

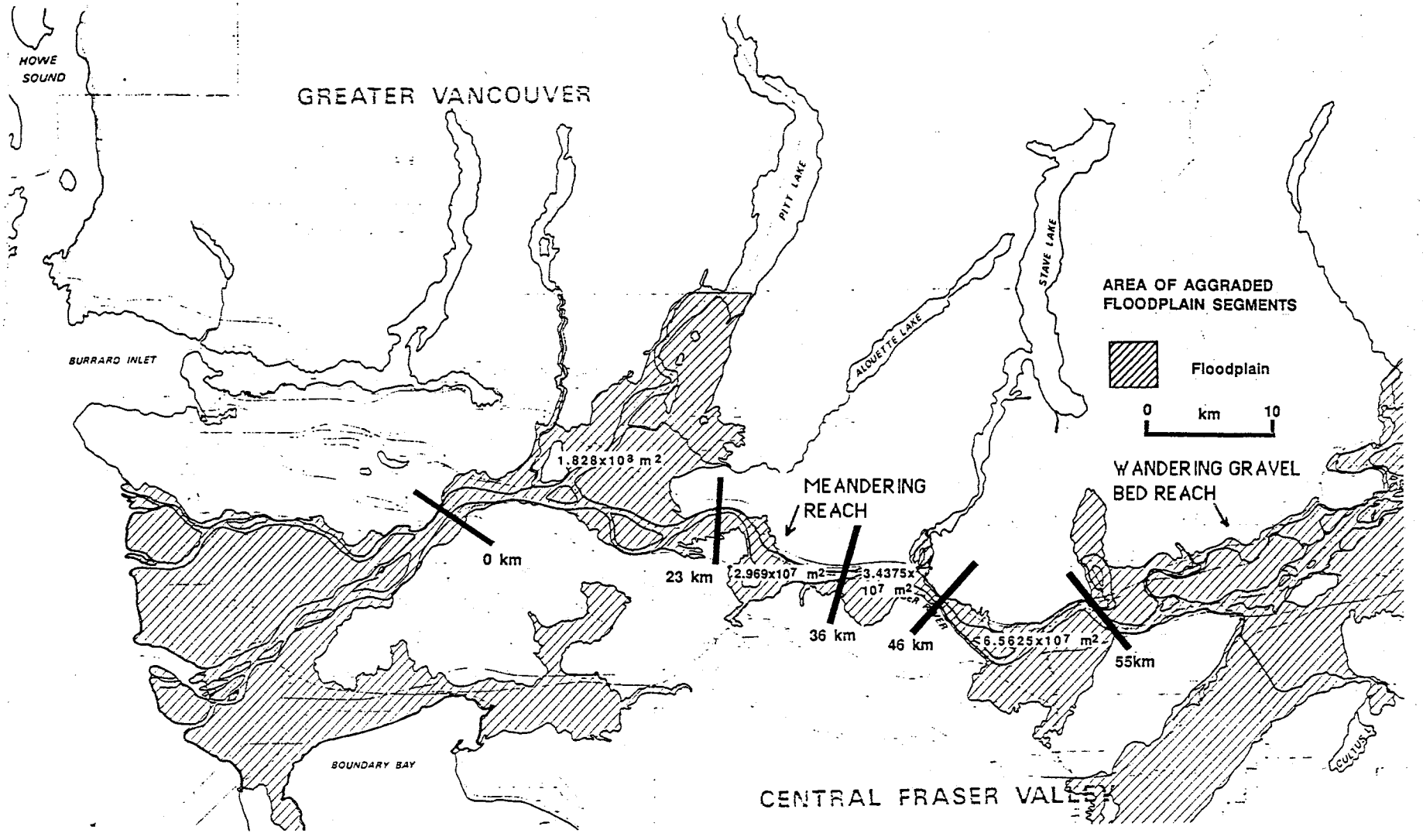
HOWE SOUND
GREATER VANCOUVER
PITT LAKE
STAVE LAKE
ALOUETTE LAKE
BURRARD INLET
AREA OF AGGRADED FLOODPLAIN SEGMENTS
Floodplain
0 km 10
1.828x10⁸ m²
MEANDERING REACH
WANDERING GRAVEL BED REACH
0 km
23 km
2.969x10⁷ m²
3.4375x 10⁷ m²
36 km
46 km
6.5625x10⁷ m²
55km
BOUNDARY BAY
CULTUS
CENTRAL FRASER VALLEY

REFERENCES

Ages, A. and Woolard, A., 1976. The tides in the Fraser River estuary: Pacific Marine Science Report 76-5, Institute of Ocean Sciences, Patricia Bay, Sidney, B.C., 100 p.

Armstrong, J.E., 1956. Surficial Geology Of Vancouver Area, British Columbia. Geological Survey of Canada, Paper 55-40, 16 p.

_____, 1957. Surficial geology of New Westminster map area, British Columbia. Geological Survey of Canada, Paper 57-5, 25 p.

_____, 1981. Post-Vashon Wisconsin glaciation, Fraser Lowland, British Columbia, Canada. Geological Survey of Canada, Bulletin 322, 34 p.

_____, 1984. Environmental and engineering applications of the surficial geology of the Fraser Lowland, British Columbia. Geological Survey of Canada, Paper 83-23, 54 p.

Armstrong, J.E., Crandell, D.R., Easterbrook, D.J. and Noble, J.B., 1965. Late Pleistocene stratigraphy and chronology in southwestern British Columbia and northwestern Washington. Geological Society of America, Bulletin, v. 76, pp. 321-330.

Armstrong, J.E. and Hicock, S.R., 1980a. Surficial geology, New Westminster, British Columbia. Geological Survey of Canada, Map 1484A.

_____, 1980b. Surfical (sic) geology, Vancouver, British Columbia. Geological Survey of Canada, Map 1486A.

Bacon, C.R., 1983. Eruptive history of Mount Mazama and Crater Lake caldera, Cascade Range, U.S.A. Journal Of Volcanology And Geothermal Research, v. 18, pp. 57-115.

Bertin, E.P., 1970. Principles And Pactices Of X-ray Spectrometric Analysis. Plenum Press, New York.

Bird, J.R., Russell, L.H., Scott, M.D. and Ambrose, W.R. 1978. Obsidian characterization with elemental analysis by proton induced gamma-ray emission. Analytical Chemistry, v. 50, No. 2082.

Blunden, R.H., 1973. Urban geology of Richmond, British Columbia. University of British Columbia, Department of Geological Sciences, Report No. 15, 13 p.

_____, 1975. Urban geology of Richmond, British Columbia - interpreting a delta landscape. University of British Columbia, Department of geological Sciences, Adventure in Earth Science Series, No. 15, 35 p.

Brune, G., 1948. Rates of sediment production in midwestern United States: U.S. Dept. Agricultural Soil Conserv. Service Tech. Pub. No. 65, 40 p.

Cant, D.J. and Walker, R.G., 1976. Development of a braided-fluvial facies model for the Devonian Battery Point Sandstone, Quebec. Canadian Journal of Earth Sciences, v. 13, pp. 102-119.

Church, M. and Ryder, J.M., 1972. Paraglacial sedimentation: a consideration of fluvial processes conditioned by glaciation. Geological Society of America, Bulletin, v. 83, pp. 3059-3072.

Clague, J.J., 1980. Late Quaternary geology and geochronology of British Columbia. Part 1: radiocarbon dates. Geological Survey of Canada, Paper 80-13, 28 p.

_____, 1981. Late Quaternary geology and geochronology of British Columbia. Part 2: summary and discussion of radiocarbon-dated Quaternary history. Geological Survey of Canada, Paper 81-35, 41 p.

_____, 1983. Glacio-isostatic effects of the Cordilleran ice sheet, British Columbia, Canada. (in) Smith, D.E. and Dawson, A.G., (eds), Shorelines and isostasy: Academic press, London, pp. 321-343.

Clague, J.J., Harper, J.R., Hebda, R.J. and Howes, D.E., 1982. Late Quaternary sea levels and crustal movements, coastal British Columbia. Canadian Journal of Earth Sciences, v. 19, pp. 597-618.

Clague, J.J. and Luternauer, J.L., 1982. Where the river meets the sea: studies of the Fraser Delta. Geos, v. 11, No. 2, pp. 8-12.

_____, 1983. Late Quaternary geology of southwestern British Columbia. Geological Association of Canada, Mineralogical Association of Canada and Canadian Geophysical Union Joint Annual Meeting (1983), Field Excursion Guidebook, Field Trip 6, 99 p.

Clague, J.J., Luternauer, J.L. and Hebda, R.J., 1983. Sedimentary environments and post-glacial history of the Fraser River delta and lower Fraser Valley, British Columbia. Canadian Journal of Earth Sciences, v. 20, pp. 1314-1326.

Cockbain, A.E., 1963. Distribution of Foraminifera in Juan De Fuca and Georgia Straits, British Columbia, Canada. Contributions from the Cushman Foundation for Formaminiferal Research. v. 14, part 2, (1963).

Coleman, J.M. and Prior, D.B., 1982. Deltaic environments, (in) Scholle, P.A. and Spearing, D.R., (eds) Sandstone Depositional Environments, AAPG Memoir 31, pp. 139-178.

Coleman, J.M. and Wright, L.D., 1971. Analysis of major river systems and their deltas: procedures and rationale: Louisiana State University, Coastal Studies Institute Tech. Report, 95, 125 p.

_____, 1973. Variability of modern river deltas. Transactions, Gulf Coast Assoc. of Geol. Soc., 23rd Annual Convention, Houston, Texas, 1973.

_____, 1975. Modern river deltas: variability of processes and sand bodies. (in) Broussard, M.L., (ed) Deltas, Models For Exploration, Houston Geol. Soc. pp. 99-149.

_____, 1977. Research techniques in deltas. Geoscience And Man v. 18, pp. 35-51.

Cormie, A.B., 1981. Chemical correlation of volcanic ashes for use as stratigraphic markers in archaeology. M.A. Thesis, Simon Fraser Uiversity, Burnaby, British Columbia, 168 p.

Cormie, A.B., Nelson, D.E. and Huntley, D.J., 1981. X-ray fluorescence analysis as a rapid method of identifying tephras discovered in archaeological sites. (in) Self, S. and Sparks, S.J., (eds) Tephra Studies, D. Reidel, Dordrecht, Holland.

Curray, J.R., 1964. Transgressions and regressions. (in) Miller, R.L., (ed) Papers In Marine Geology, (Shepard Commemorative Volume), MacMillan, co., New York, pp. 175-203.

Curtis, D.M., 1970. Miocene deltaic sedimentation, Louisiana Gulf Coast. (in) Morgan, J.P., (ed) Deltaic sedimentation, modern and ancient, Society of Economic Paleontologists and Mineralogists, special pub. 15, pp. 293-308.

De Raff, J.F.M., Reading, H.G. and Walker, R.G., 1965. Cyclic sedimentation in the Lower Westphalian of North Devon, England. Sedimentology, v. 4, p. 1-52.

Folk, R.L. and Ward, W., 1957. Brazos River bar, a study in the significance of grain size parameters. Journal of Sedimentary Petrology, v. 27, pp. 3-27.

Frazier, D.E., 1967. Recent deltaic deposits of the Mississippi delta: their development and chronology. Transactions, Gulf Coast Assoc. Geol. Socs., v. 17, pp. 287-315.

Fulton, R.J., 1971. Radiocarbon chronology of southern British Columbia. Geological Survey of Canada, Paper 71-37, 28 p.

Futyma, R.P., 1986. MICHIGRANA: The Michigan Graphing Program For Pollen Analysis, User's Manual, Department of Botany, University of Michigan.

Galloway, W.E., 1975. Process framework for describing the morphologic and stratigraphic evolution of deltaic depositional systems. (in) Broussard, M.L. (ed) Deltas, Models For Exploration, Houston Geol. Soc., pp. 88-98.

Gilbert, G.K., 1890. Lake Bonneville. United States Geological Survey, Monographs, v. 1, Washington Government Printing Office (1890).

Hebda, R.J., 1977. The paleocology of a raised bog and associated deltaic sediments of the Fraser River delta. Ph.D Thesis, University Of British Columbia, Vancouver, B.C., 202 p.

Heusser, C.J., 1973. Environmental sequence following the Fraser advance ofthe Juan de Fuca lobe, Washington. Quaternary Research, v. 3, No. 2, pp. 284-306.

Heusser, C.J., Heusser, L.E. and Peteet, D.M., 1985. Late Quaternary climatic change on the American North Pacific Coast. Nature, v. 315, No. 6019, pp. 485-487.

Hoos, L.M. and Packman, G.A., 1974. The Fraser River estuary, status of environmental knowledge to 1974. Canada Department of the Environmental, Regional Board, Pacific region, estuary working group, special estuary series, 1, 518 p.

Hutchinson, I., 1982. Vegetation-environment relations in a brackish marsh, Lulu Island, Richmond, B.C. Canadian Journal of Botany, v. 60, pp. 452-462.

Johnson, W.A., 1921. Sedimentation of the Fraser River. Geological Survey of Canada, Memoir 125, 46 p.

Kellerhals, P. and Murray, J.W., 1969. Tidal flats at Boundary Bay, Fraser River delta, British Columbia. Bul. Can. Petrol. Geol., v. 17 No. 1, pp. 67-91.

Kostaschuk, R.A., Luternauer, J.L. and Millard, T.H., 1986. Sediment transport during the 1985 freshet in the outer Main Channel of the Fraser River estuary, British Columbia. Geological Survey of Canada, Paper 86-1A, pp. 565-570.

Kostaschuk, R.A. and Luternauer, J.L., 1987. Large scale sedimentary processes in a trained high-energy, sand-rich estuary: Fraser River delta, British Columbia. Geological Survey of Canada, Paper 87-1A, pp. 727-734.

Kidd, G.J.A., 1953. Fraser River suspended sediment survey, interim report for period 1949-1952: Victoria, B.C., British Columbia Dept. of Lands and Forests, Water Rights branch, 46 p. (mimeo).

Knighton, D., 1984. Fluvial Forms And Processes. Edward Arnold.

Luternauer, J.L., 1977. Fraser Delta sedimentation, Vancouver, British Columbia. Geological Survey of Canada, Paper 77-1A, pp. 65-72.

_____ 1980. Genesis of morphological features on the western delta front of the Fraser River, British Columbia - status of knowledge. (in) McCann, S.B., (ed) Coastlines Of Canada, Geological Survey of Canada, Paper 80-10, pp. 381-396.

Luternauer, J.L. and Murray, J.W., 1973. Sedimentation on the western delta front of the Fraser River, British Columbia. Canadian Journal of Earth Sciences, v. 10, pp. 1642-1663.

Luternauer, J.L. and Finn, W.D.L., 1983. Stability of the Fraser River delta front. Canadian Geotechnical Journal, v. 20, No. 4, pp. 606-616.

Luternauer, J.L., Clague, J.J., Hamilton, T.S., Hunter, J.A., Pullan, S.E. and Roberts, M.C., 1986. Structure and stratigraphy of the southwestern Fraser River delta: a trial shallow seismic profiling and coring survey. Geological Survey of Canada, Paper 86-1B, pp. 707-714.

Mathews, W.H. and Shepard, F.P., 1962. Sedimentation of Fraser River delta, British Columbia (Includes discussion by K. Terzaghi). Amer. Assoc. Petrol. Geol., Bulletin, v. 46, pp. 1416-1443.

Mathews. W.H., Fyles, J.G. and Nasmith, H.W., 1970. Post-glacial crustal movements in southwestern British Columbia and adjacent Washington State. Canadian Journal of Earth Sciences, v. 7, pp.690-702.

Mathewes, R.W. and Westgate, J.A., 1980. Bridge River tephra: revised distribution and significance for detecting old carbon errors in radiocarbon dates of limnic sediments in southern British Columbia. Canadian Journal of Earth Sciences, v. 17, pp. 1454-1461.

McKenna, G.T. and Luternauer, J.L., 1987. First documented large failure at the Fraser River Delta front, British Columbia. Geological Survey of Canada, Paper 87-1A, pp. 919-924.

Medley, E. and Luternauer, J.L., 1976. Use of aerial photographs to map sediment distribution and to identify historical changes on a tidal flat. Geological Survey of Canada, Paper 76-1C, pp. 293-304.

Miall, A.D., 1978. Lithofacies types and vertical profile models in braided river deposits: a summary. (in) Miall, A.D. (ed) Fluvial Sedimentology, Can. Soc. Petrol. Geol. Mem., v. 5, pp. 597-604.

_____, 1984a. Deltas. (in) Walker, R.G., (ed) Facies Models, Geoscience Canada Reprint Series 1.

_____, 1984b. Principles Of Sedimentary Basin Analysis. Springer-Verlag, New York.

Middleton, G.V., 1978. Facies. (in) Fairbridge, R.W. and Bourgeois, J. (ed) Encyclopedia of Sedimentology, Stroudsberg, Pa., Dowden, Hutchinson and Ross, pp. 323-325.

Milliman, J.D., 1980. Sedimentation in the Fraser River and its estuary, southwestern British Columbia (Canada). Estuarine and Coastal Marine Science, v. 10, pp. 609-633.

Mullineaux, D.R., Waldron, H.H. and Rubin, M., 1965. Stratigraphy and chronology of late interglacial and early Vashon glacial time in the Seattle area, Washington. United States Geological Survey, Bulletin, 1194-0, 10 p.

Murray, J.W., 1973. Distribution and ecology of living benthic Foraminiferids.

Nasmith, H.W., Mathews, W.H. and Rouse, G.E., 1967. Bridge River ash and some other recent ash beds in British Columbia. Canadian Journal of Earth Sciences, v. 4, No. 1, pp. 163-170.

North, M.E.A. and Teversham, J.M., 1984. The vegetation of the floodplain of the lower Fraser, Serpentine and Nicomekl Rivers, 1859-1890. Syesis, v. 17, pp. 47-66.

Pharo, C.H. and Barnes, W.C., 1976. Distribution of surficial sediments of the central and southern Strait of Georgia, British Columbia. Canadian Journal of Earth Sciences, v. 13, pp. 684-696.

Phleger, F.B., 1967. Marsh foraminiferal patterns, Pacific coast of North America. An. Inst. Biol. Univ. Nal. Auton. Mexico, v. 38, Ser, Cienc. Del Mar Y Limnol. (1): 11-38.

Roberts, M.C., Williams, H.F.L., Luternauer, J.L. and Cameron, B.E.B., 1985. Sedimentary framework of the Fraser River delta, british Columbia: preliminary field and laboratory results. Geological Survey of Canada, Paper 85-1A, pp. 717-722.

Scott, A.J. and Fisher, W.L., 1969. Delta systems and deltaic deposition. (in) Delta Systems In The Exploration For Oil And Gas, Research Colloquium: Bur. Econ. Geol., Univ. Texas.

Scott, D.B., 1976. Quantitative studies of marsh Foraminifera patterns in Southern California and their application to Holocene stratigraphic problems. First international symposium on benthic Foraminifera of continental margins. Part A, ecology and biology, maritime sediments, special publication 1, pp. 153-170.

_____, 1977. Distribution and population dynamics of marsh-estuarine Foraminifera with applications to relocating Holocene sea levels; Dalhousie University, Halifax, unpubl. Ph.D. dissertation, 252 p.

Scott, D.B. and Medioli, F.S., 1978. Vertical zonations of marsh Foraminifera as accurate indicators of former sea levels. Nature, v. 272, pp. 528-531.

_____, 1980a. Quantitative studies of marsh Foraminifera distributions in Nova Scotia: implications for sea level studies. Cushman Foundation for Foraminiferal Research, special publication number 17, 58 p.

_____, 1980b. Living Vs. total Foraminifera populations: their relative usefulness in paleoecology. Journal of Paleoecology, v. 54, pp. 814-831.

Scott, D.B., Williamson, M.A. and Duffett, T.E., 1981. Marsh Foraminifera on Prince Edward Island: their recent distribution and application for former sea level studies. Maritime sediments and Atlantic geology, v. 17, pp. 98-1219.

Schumm, S.A., 1963. The disparity between present rates of denudation and orogeny. United States Geological Survey, Prof. Paper 454-H, 13p.

Scruton, P.C., 1960. Delta building and the deltaic sequence. (in) Shepard, F.P. et al., (eds) Recent sediments, northwest Gulf of Mexico, Am. Assoc. Petrol. Geol., Spec. Pub., pp. 82-102.

Smith, D.G., 1984. Vibracoring fluvial and deltaic sediments: tips on improving penetration and recovery. Journal of Sedimentary Petrology, v. 54, No. 2, pp. 660-663.

Smith, D.G.W. and Westgate, J.A., 1969. Electron probe technique for characterizing pyroclastic deposits. Earth And Planetary Science Letters, v. 5, pp. 313-319.

Smith, D.A., Scott, D.B. and Medioli, T.S., 1984. Marsh Foraminifera in the Bay of Fundy: modern distribution and application to sea-level determinations. Maritime Sediments And Atlantic Geology, v. 20, pp. 127-142.

SPSS Inc. 1986. SPSSX User's Guide, 2nd. ed., SPSS Inc.

Straaten, L.M.J.U., van. 1960. Some recent advances in the study of deltaic sedimentation. Liverpool Manchester Geological Journal, v. 2, pp. 411-442.

Styan, W.B., 1981. The sedimentology, petrography and geochemistry of some Fraser Delta peat deposits. M.Sc. Thesis, University Of British Columbia, Vancouver, B.C. 188 p.

Styan, W.B. and Bustin, R.M., 1984. Sedimentology of Fraser River peat deposits: a modern analogue for some deltaic coals. Special Publication of the International Association of Sedimentologists, v. 7, pp. 241-271

Swan Wooster Engineering Co., 1967. Vancouver Outer Port Study, Map I-2, Sturgeon Bank Topography, Swan Wooster Engineering Co., Vancouver.

Vail, P.R., Mitchum, R.M. and Thompson, S., 1977. Seismic stratigraphy and global changes of sea level, part 3: relative changes of sea level from coastal onlap. (in) Payton, C.E. (ed) Seismic Stratigraphy - Applications To Hydrocarbon Exploration, Am. Assoc. Petrol. Geol., Memoir 26, pp. 63-81.

Walker, R.G., 1984. (ed) Facies Models. Geoscience Canada Reprint Series 1.

Walther, J., 1894. Einleitung in die geologie als historische wissenschaft, Bd. 3, lithogenesis der gegenwart, pp. 535-1055. Fischer-Verlag, Jena.

Westgate, J.A. and Dreimanis, A., 1967. Volcanic ash layers of recent age at Banff National Park, Alberta, Canada. Canadian Journal of Earth Sciences, v. 4, pp. 155-161.

Westgate, J.A., Smith, D.G.W. and Tomlinson, M., 1970. Late Quaternary tephra layers in southwestern Canada. (in) Early Man And Environments In Northwest North America, University of Calgary Press, Calgary.

Woldseth, R., 1973. All You Ever Wanted To Know About XES, X-Ray Energy Spectrometry. Kevex Corporation, Burlingame, California.

Wright, L.D., 1978. Deltaic sediments and sedimentary structures. (in) Davis, R.A., (ed) Coastal Sedimentary Environments.

Wright, L.D. and Coleman, J.M., 1973. Variations in morphology of major river deltas as functions of ocean wave and river discharge regimes. Am. Assoc. Petrol. Geol., Bulletin, v. 57, No. 2, pp. 370-398.